Stony Brook University

Poliovirus Pathogenesis: A study of New World Monkey CD155 receptors and a new Mouse Model for Oral Pathogenesis

A Dissertation Presented

by

Shaukat Ali Khan

to

The Graduate School

in Partial Fulfillment of the

Requirements

for the Degree of

Doctor of Philosophy

in

Molecular and Cellular Biology

Immunology and Pathology

Stony Brook University

May 2008

Stony Brook University

The Graduate School

Shaukat Ali Khan

We, the dissertation committee for the above candidate for the

Doctor of Philosophy degree, hereby recommend

acceptance of this dissertation.

Eckard Wimmer – Dissertation Advisor
Distinguished Professor, Department of Molecular Genetics and Microbiology

Michael Frohman - Chairperson of Defense
Department of Molecular and Cellular Pharmacology

Jorge Benach
Department of Molecular Genetics and Microbiology

Nancy Reich
Department of Molecular Genetics and Microbiology

Carol Carter
Department of Molecular Genetics and Microbiology

This dissertation is accepted by the Graduate School

Lawrence Martin

Dean of the Graduate School

Abstract of the Dissertation

Poliovirus Pathogenesis: A study of New World Monkey CD155 receptors and a new Mouse Model for Oral Pathogenesis

by

Shaukat Ali Khan

Doctor of Philosophy

in

Molecular and Cellular Biology

Immunology and Pathology

Stony Brook University

2008

Poliovirus is a small RNA virus belonging to the genus *Enterovirus* of the family *Picornaviridae*. Poliovirus causes a unique human neurologic disease involving the destruction of motor neurons, which leads to paralysis and even death (poliomyelitis). In contrast to the Old World Monkeys (OWMs), most New World Monkeys (NWMs) are not susceptible to poliovirus (PV), regardless of the route of infection. We have investigated the molecular basis of restricted PV pathogenesis of NWMs with two kidney cell lines of NWMs, TMX (Tamarin) and NZP-60 (Marmoset), and characterized their PV receptor homologues. TMX cells were susceptible to infection by PV1 (Mahoney) and PV3 (Leon) but not by PV2 (Lansing). Binding studies to TMX cells indicated that the formation of PV/receptor complexes increases when measured first at 4°C and then at 25°C whereas PV2 did not significantly bind to TMX cells at either temperature. On the other hand, NZP-60 cells were not susceptible to infection by any of the PV serotypes. However, a low amount of PV1 bound to NZP-60 cells at 4°C but there was no increase of binding at 25°C. In contrast, both NWM cell lines supported genome replication and virion formation when transfected with viral RNAs of either serotype, an observation indicating that infection was blocked in receptor-virus interaction. To overcome the receptor block in marmoset cells, we substituted 3 amino acids in the marmoset receptor (nCD155), H80Q, N85S, and P87S, that occur in the human PV receptor, hCD155. Cells expressing the mutant receptor (L-nCD155mt) were now susceptible to infection with

PV1, which correlated with an increase in PV1 bound receptor complexes from 4°C to 25°C. L-nCD155mt cells were, however, still resistant to PV2 and PV3. These data show that an increase in the formation of PV/receptor complexes, when measured at 4°C and at 25°C correlates with, and is an indicator of, successful infection at 37°C, suggesting that the complex formed at 25°C may be an intermediate in PV uptake.

The virus infects humans by ingestion but the molecular mechanisms of oral pathogenesis are poorly understood. Except for monkeys, no animal models exist for the study of oral infection. Based on monkey studies, it has been determined that the initial step in PV infection and pathogenesis is the replication of the virus in tissues of the gastrointestinal tract, most likely in gut associated lymphoid tissues (GALT), but the precise sites of replication are not known. One difficulty with studying the early steps of PV pathogenesis is that in TgPVR21 mice, generated with human CD155 promoter and gene, CD155 is not expressed in the alimentary canal; hence, the TgPVR21 mice cannot be infected orally. Murine CD155 (mCD155; also known as Tage4), a member of the CD155/nectin family, has been accepted as the mouse orthologue of human CD155. The mCD155 does not serve as a functional PV receptor, nevertheless, the murine and human CD155 recognize same panel of ligands whenever examined: nectin-3, CD226, CD96 and vitronectin. Like human CD155, mCD155 lacks self adhesion and contributes substantially to the establishment of adheren juntions between epithelial cells. More importantly they are expressed in the GALT of human and mice in similar patterns. We describe here the generation of a transgenic mouse model in which the *mCD155* promoter controls the expression of the *CD155* coding region. The *mCD155*tg mice show CD155 expression in brain, spinal cord, kidney and liver by western blot. The CD155 expression is detected in the GALT of the 3 and 6 week old mice by immunostaining. Infection by parenteral routes of the *mCD155*tg mice with PV1 (Mahoney), results in similar clinical symptoms to the corresponding infections of TgPVR21 mice (mice transgenic with the *CD155* gene). *mCD155*tg mice, in addition, are also susceptible to oral infection in 3 week old or younger mice. Thus we have successfully generated a mouse model that expresses CD155 in the GALT and is susceptible to oral infection, a natural route of PV infection.

Dedication

To my parents, Gulab Deen Khan and Janet Khan, and my siblings, Ali, Kaneez, Liaqat, and Muneez, for their unwavering love and support.

Table of Contents

List of Figures

List of Tables

Acknowledgement

"It takes a village to raise a child."

African Proverb

This proverb aptly applies to a graduate student. The completion of this dissertation is not an achievement that I can share by myself but an accomplishment that would not have been possible without constant support and help of my peers, friends and mentors.

My deepest gratitude goes to Dr. Eckard Wimmer for taking me under his tutelage and for his constant encouragement, support, and guidance throughout my years in his lab.

Beside Dr. Wimmer in the lab, Dr. Aniko Paul has been wonderful for taking me under her wings. She has been a life saver over the years for reading multiple drafts of my papers. But most of all, for the conversations ranging from science to opera.

My sincere thanks also go to my committee members: Dr. Michael Frohman, Dr. Jorge Benach, Dr. Carol Carter and Dr. Nancy Reich. I could not have picked a better group of people to guide me through last couple of years. They have always been helpful with their insightful and thoughtful suggestions on the direction of my projects.

I am also grateful to my collaborators; Dr. Nomoto, Dr. Rossmann, Dr. Bernhardt, and Dr. Iwasaki's group for their generosity with the materials and time.

I would also like to thank Xiaozhong Peng and Hidemi Toyoda, with whom I have collaborated on different projects.

Last but not least, I would like to thank all the past and present members of the Wimmer lab. Over the years they have not just become colleagues but real good friends. Special thanks to David, Helen, Hidemi, Janaki, JoAnn, Kate, Sakina, Scott, Tatjana and Ying for keeping me sane and reminding me that I have a life outside the lab.

Chapter I

Introduction

Background

Poliovirus (PV) discovered nearly 100 years ago (Landsteiner and Popper, 1909), is an RNA virus belonging to the genus *Enterovirus* in the family *Picornaviridae.* This family includes a large number of human pathogens, including coxsackie B viruses, enterovirus 71, parechoviruses, and hepatitis A virus, which all can cause severe to life threatening diseases. They have a wide pathological spectrum, causing diseases such as meningitis, encephalitis, myocarditis, paralysis, diarrhetic and respiratory diseases. Together, all human picornaviruses can cause up to six billion human infections each year.

PV is found as three serotypes (Burnet, 1931; Paralysis, 1951). The virus replicates mainly in the gastrointestinal (GI) tract for up to 60 days post infection, often unnoticed or accompanied only by mild cold-like symptoms. Spread to the central nervous system (CNS), combined with apparent disease syndromes is relatively rare. Only at a rate of 10^{-2} for serotype 1, and 10^{-3} for serotypes 2 and 3 does PV cause neurological disease.

Although poliomyelitis, a disease caused by PV, is no longer a major public health threat, it has been associated with mankind since ancient times. This assumption is based on a well known example of a stela from the 18th Egyptian dynasty (1550-1333 B.C.), which depicts doorkeeper Ram with an atrophic right leg, possibly the consequence of an earlier childhood polio infection (Eggers, 2002). The first known clinical description of poliomyelitis is attributed to British scientist Michael Underwood, who described a disease compatible with poliomyelitis, and noted that it was an uncommon disorder afflicting chiefly children one to five years old (Eggers, 2002). In 1840, orthopedist Jacob Heine concluded that the reason for sudden flaccid paralysis of extremities should be localized in the spinal cord. This observation was confirmed by Duchenne de Boulogne who demonstrated an early loss of the faradic irritability of muscles later permanently paralyzed, in contrast to those that may recover (Eggers, 2002). First histopathological evidence of spinal cord complication in paralysis was reported in three key papers in 1870 by Charcot and Joffroy (Charcot and Joffroy, 1870), Vulpian (Vulpian, 1870), and Parrot and Joffroy (Parrot and Joffroy, 1870). These three papers corroborated Heine's assumption that the site of infection and irreversible damage

is the gray matter of the anterior horns with the loss of motor neurons, leading to paralysis.

Up to 1850, poliomyelitis outbreaks were sporadic. But in the later half of the 19th century, larger outbreaks of the disease were observed. It was keenly perceived that the outbreaks occurred primarily in late summer and early fall, with a dramatic peak in August (Eggers, 2002). Ivor Wickman made an astute observation that the disease spread through contact from person to person and large percentages of cases were nonparalytic.

Before 1905, the cause of poliomyelitis was attributed to such hypotheses as cooling, seasonal occurrence, and teething. In 1909, Landsteiner and Popper injected a spinal cord suspension of a nine year old child who had died from paralysis intraperitoneally (i.p.) into two old world monkeys (OWMs), which subsequently went on to develop paralysis and showed histopathology similar to poliomyelitis (Landsteiner and Popper, 1909). Since the suspension was filtered to remove cellular infectious agents prior to administration to the animals, Landsteiner and Popper correctly concluded that the infectious agent must be a virus. Once the etiological agent of poliomyelitis was determined and means of easy propagation was developed (Enders, Weller, and Robbins, 1949), two excellent PV vaccines were independently developed, the inactivated vaccine by Jonas Salk (Salk, 1954) and a live attenuated oral vaccine by Albert Sabin (Sabin, 1957). The advent and successes of these two vaccines led the World Health Organization (WHO), on the heel of a successful eradication of smallpox, to initiate efforts of global eradication of PV (ref. see (Wimmer, Hellen, and Cao, 1993)).

Although no longer a major public health threat in the developed world, poliomyelitis spurred huge research endeavors over several decades (1960-present times), which led to the establishment of basic virological techniques. These include virus purification protocols, crystallization of the virion, an efficient tissue culture system and plaque assay analysis (Bachrach and Schwerdt, 1952; Dulbecco and Vogt, 1954; Enders, Weller, and Robbins, 1949; Robbins, Enders, and Weller, 1950; Schaffer and Schwerdt, 1955). In addition, PV research led to the discovery of an uncapped messenger RNA (Nomoto, Lee, and Wimmer, 1976), the internal ribosome entry site (IRES) (Jang et al., 1988; Pelletier and Sonenberg, 1988), a 5'-terminal genome-linked protein (Lee et al., 1977; Nomoto et al., 1977), and a 3'-terminal poly(A) (Yogo and Wimmer, 1972). PV

was also the first animal RNA virus genome to be sequenced (Kitamura et al., 1981), which confirmed the existence of the polyprotein. PV was the first virus to be replicated *de novo* in a cell-free extract (Molla, Paul, and Wimmer, 1991), as well as to be chemically synthesized (Cello, Paul, and Wimmer, 2002).

Genome organization

The PV genome consists of a single (+) sense RNA molecule of 7441 nucleotides (Fig. 1). The viral genome can be divided into three regions: the 5' non-translated region (NTR) of 742 nt, followed by a single open reading frame (ORF), coding for a polyprotein of 2209 amino acids, and finally the polyadenylated 3' non-translated region of 70 nt (Kitamura et al., 1981).

Unlike most eukaryotic mRNAs, the PV genomic RNA does not carry a m7G cap structure essential for translational initiation of normal eukaryotic mRNA. Instead, the 5' NTR is covalently linked to VPg, a virus-encoded 22 amino acid long protein (Lee et al., 1977). The 5' NTR is composed of two secondary structures; a cloverleaf (Andino, Rieckhof, and Baltimore, 1990; Rivera, Welsh, and Maizel, 1988) and the downstream IRES. The cloverleaf has been implicated in the formation of the replication complex both during (+) strand and (-) strand RNA synthesis (Andino et al., 1993; Andino, Rieckhof, and Baltimore, 1990; Barton, O'Donnell, and Flanegan, 2001; Gamarnik and Andino, 2000; Harris et al., 1994; Herold and Andino, 2000; Parsley et al., 1997; Xiang et al., 1995), while cap-independent translation of the genome is initiated by binding of the virally modified host translation machinery to the IRES (Jang et al., 1988; Pelletier and Sonenberg, 1988).

The 247 kDa polyprotein can be subdivided into regions denoted P1, P2 and P3 (Fig. 1). The P1 region encodes for structural proteins, while P2 and P3 encode for nonstructural proteins. Following translation of the mRNA, the polyprotein is processed by virus-encoded proteinases; $2A^{pro}$, $3C^{pro}$/$3CD^{pro}$ in *cis* and in *trans*.

In contrast to the 5' NTR, there is comparatively less known about the 3' NTR. Besides containing the polyadenylated tail, it contains two stem loops and is suggested to be involved in (-) strand RNA synthesis (Rohll et al., 1995).

Cellular life cycle

Cell entry

The cellular life cycle of PV is schematically represented in Figure 2. PV entry into the cell is mediated by binding to an immunoglobulin-like cell surface protein called CD155 (Mendelsohn, Wimmer, and Racaniello, 1989) (Fig. 3). CD155 is composed of three Ig-like domains, one variable domain (V) and two constant domains (C2) (Fig. 3). Mutational analysis on the V domain of CD155 and PV1 was used to determine that CD155 inserts itself into a surface depression of the viral capsid known as the "canyon", which surrounds each of the twelve five-fold axes of the icosahedral capsid (Aoki et al., 1994; Bernhardt et al., 1994b; Colston and Racaniello, 1994; Harber et al., 1995; Liao and Racaniello, 1997). The interaction of PV with its receptor has been confirmed through structural analyses by cryo-electron microscopy (EM) (Belnap et al., 2000; He et al., 2000).

In order for virus uncoating to occur, the PV capsid, which is so stable that it is resistant to 2% SDS and pH 2, has to be destabilized. At physiological temperatures, multiple CD155 molecules trigger an irreversible conformational change in the native virion (160S particle). This conformationally altered virion (135S) is a result of externalization of the myristoylated capsid protein VP4 and of the putative N-terminal amphipathic helix of VP1 (reviewed in (Hogle, 2002)). Both of the externalized proteins are inserted into the cell membrane, allowing the particles to anchor to the membrane in a receptor-independent manner (Fricks and Hogle, 1990). The 135S particles are then internalized by a clathrin- and caveolin-independent, but actin and tyrosine kinase-dependent mechanism (Brandenburg et al., 2007). The release of the viral genome takes place only after internalization from an endocytic compartment localized within 100–200 nm of the plasma membrane (Brandenburg et al., 2007). Upon release of the RNA genome, the empty capsid (80S particle) is transported away along microtubules (Brandenburg et al., 2007).

Interestingly, CD155 has two different binding affinities to the virus (McDermott et al., 2000). The first step can be studied at 4°C and is likely electrostatic in nature. The second step occurs at physiological temperatures and leads to irreversible structural changes of the virion, resulting in the formation of an A-particle (135S) in which VP4 is absent (Hogle, 2002). Under favorable conditions of tissue culture studies, the two step process is favorable and would proceed quickly; the reaction may be much slower when

the virus encounters the receptor within a host tissue, such as a motor neuron synapse (Mueller, Wimmer, and Cello, 2005). Here, virus-receptor binding and transition to the activated state could be separated; thus, virus can be transported retrogradely through the neuron, only uncoating under favorable conditions (Mueller, Wimmer, and Cello, 2005).

Polyprotein translation and proteolytic processing

After the viral genome has been released into the cell, the 5'NTR-linked viral protein VPg is believed to be cleaved by an unknown cellular phosphodiesterase (Wimmer, 1982). Following cleavage, the genome serves as a messenger RNA that is translated into a single polyprotein by host cell ribosomes, whose proteolytic cleavage products serve as capsid precursors and replication proteins (Fig. 2) (Wimmer, Hellen, and Cao, 1993). Even though the expression of a polyprotein suggests that all viral proteins are produced at an equimolar ratio, a cascade of slow and fast proteolytic cleavages by its proteinases $2A^{pro}$ and $3C^{pro}/3CD^{pro}$ allows PV a certain degree of processing control (Fig. 1).

After translation, $2A^{pro}$ carries out a cis- cleavage of the Tyr*Gly bond at its own N-terminus to release P1 from P2-P3. The second major cleavage is the release of P3 from P2 through *cis*- cleavage by $3C^{pro}/3CD^{pro}$ (Lawson and Semler, 1992). Followed by highly ordered successive *trans*- cleavage events by $3C^{pro}/3CD^{pro}$, the non-structural proteins, 2A, 2BC, 3AB, 2B, 2C, 3A, 3B (VPg), $3C^{pro}$, $3D^{pol}$ and the capsid proteins VP0, VP1 and VP3 are released from their precursors. The last cleavage, that of VP0, occurs during assembly of the virus particle, presumably by an autocatalytic mechanism involving the encapsidating RNA, to yield VP4 and VP2 (Basavappa et al., 1994). This cleavage is referred to as a maturation cleavage because it is required for the infectivity of the virus.

In addition to polyprotein processing, $2A^{pro}$ and $3C^{pro}$ are actively involved in the inhibition of host cell functions. $2A^{pro}$ cleaves eukaryotic initiation factor 4G (eIF4G), a component of the cap recognizing complex eIF4F, thereby shutting off cap-dependent host cell translation (Krausslich et al., 1987; Sonenberg, 1987) to the benefit of the virus' own cap independent, IRES driven translation. In addition, host cell transcription is inhibited by the inactivation of transcription factor TFIIIC (Clark et al., 1991) and cleavage of the TATA box binding protein (Yalamanchili et al., 1996) by $3C^{pro}$.

RNA replication

The switch from RNA translation to replication is believed to occur with the interaction of 5' cloverleaf with the 3' poly(A), in effect circularizing the genome (Herold and Andino, 2001). This hypothesis is based on the ability of $3CD^{pro}$ to bind the cellular poly(A) binding protein (PABP), suggesting that the genome may circularize through the interaction of the 3AB/$3CD^{pro}$/PCBP2 ribonucleoprotein complex at the 5' cloverleaf and PABP associated with the 3' poly(A) (Herold and Andino, 2001). A recent hypothesis has been proposed by Semler and his group: PCBP2, through its three K-homologous (KH) domains, forms protein-protein and RNA-protein complexes with the viral translation and replication machinery. They found that 3C/3CD cleaves PCBP2 domain KH3, and the truncated PCBP2ΔKH3 is unable to function in translation but maintains its activity in viral replication; thus PCBP2, can mediate switch from viral translation to replication (Perera et al., 2007).

RNA replication occurs via a following simplified pathway:
(+) strand virion RNA → (-) strand synthesis → RF → (+) strand sybthesis → RI → (+) stand RNA, where RF is the replicative form (double strand RNA), and RI is the replicative intermediate (a (-) strand partially hybridized to numerous nascent (+) strands) (Wimmer, Hellen, and Cao, 1993).

All of the non-structural proteins are involved in some step of the genome replication, as determined by mutational and genetic studies (reviewed in (Paul, 2002)). The enzyme most directly involved in RNA synthesis, the RNA dependent RNA polymerase $3D^{pol}$, catalyzes primer dependent synthesis of both (-) and (+) strands. In addition to the elongation of the RNA chains on a template (Flanegan and Baltimore, 1977), $3D^{pol}$ also uridylylates VPg (Paul et al., 1998). VPg(3B) serves as a protein primer for both (-) and (+) strand synthesis after being uridylylated on a conserved tyrosine residue to form VPg-pU-pU. The template for the uridylylation of VPg is an internal RNA hairpin structure termed cis-replicating element (cre) in the 2C coding region (Goodfellow et al., 2000) (Fig. 1).

RNA replication takes place on rosette-like membranous structures that are induced by viral protein $2C^{ATPase}$ and $2BC^{ATPase}$ (Bienz et al., 1990; Cho et al., 1994; Teterina et al., 1997). The membranes are derived from the endoplasmic reticulum of

host cell. 3AB is thought to insert its hydrophobic domain into these membranes and recruit $3D^{pol}$ to the replication complex by means of 3AB's affinity to $3D^{pol}$ and $3CD^{pro}$.

The newly synthesized (+) strand RNA is encapsidated by an unknown mechanism. Following encapsidation maturation cleavage of VP0 in the procapsid occurs to form VP4 and VP2.

CD155: function and role in pathogenesis

The pace of progress in PV pathogenesis all but halted after the advent of successful vaccine developments by Sabin and Salk in the 1950s, whereas the study of the molecular biology of the virus had flourished through present times. Humans are the only natural hosts for PV. Of non-human primates, New World monkeys (NWM) are generally not susceptible to infection by the oral route. Susceptibility by parenteral routes is extraneous where it is not only determined by a PV serotype but also by the NWM species. On the other hand, Old World monkeys (OWM) and chimpanzees are sensitive to peroral infections in laboratory conditions. However, primate research is costly and the cases of wild type PV have dwindled due to great success with the existing PV vaccines. Mice, through affordable experimental animals, are resistant to infections owing to the lack of expression of a suitable receptor. An exception are certain strains of PV type 2 and a type 1 that, after intracerebral injection, cause paralysis and death in mice (for ref. see (Gromeier, Lu, and Wimmer, 1995)).

The PV receptor was discovered when mouse fibroblast L cells were transformed with HeLa cell DNA; the resultant cells were susceptible to PV infection (Mendelsohn, Wimmer, and Racaniello, 1989). The encoded receptor, which allowed PV susceptibility, is now referred to as CD155 (also known as PVR) (for the designation of *CD155*, see (Freistadt and Eberle, 1997)). So far, CD155 is the only cell surface protein known to serve as a PV receptor. However, homologues of CD155 have been identified in other species, such as murine CD155 (also known as Tumor antigen glycoprotein E4 (Tage4)) (Baury et al., 2001; Chadeneau, LeMoullac, and Denis, 1994; Mueller and Wimmer, 2003; Ravens et al., 2003). CD155 is a highly glycosylated 80 kDa type Ia single-pass transmembrane protein belonging to the Ig superfamily (Bernhardt et al., 1994a; Bibb, Bernhardt, and Wimmer, 1994; Koike et al., 1990; Mendelsohn, Wimmer, and Racaniello, 1989; Wimmer et al., 1994). Alternative splicing of the *CD155* primary

transcript gives rise to 4 isoforms: CD155α and δ, which are the membrane bound PV receptors, and CD155β and γ, which lack the transmembrane domain, and are thus found as secreted proteins (Baury et al., 2003; Koike et al., 1990) (Fig. 3). Both CD155α and δ, which differ only in the length of their cytoplasmic domain (Fig. 3C), carry a Tctex-1 binding motif (Mueller et al., 2002). However, only the longer C-terminal tail of CD155α has a tyrosine binding motif of the μ1B subunit, which localizes the protein to the basolateral domain of the polarized epithelial cells (Ohka et al., 2001). CD155δ is sorted to both the basolateral and apical domains of polarized cells. CD155 mRNA expression has been detected in the brain, spinal cord, leukocytes, lung, ileum, placenta, heart, skeletal muscle, kidney, liver, as assayed by Northern blot analyses, although the precise cell types involved in infection are often not known (Mueller, Wimmer, and Cello, 2005).

Recently great progress has been made in elucidating the cellular function of human CD155 and these functions have also been confirmed for murine CD155 (mCD155). CD155 has been shown to interact with the extracellular matrix protein vitronectin thereby mediating cell to matrix contacts (Lange et al., 2001; Ravens et al., 2003), in agreement with basolateral sorting of CD155α in polarized cells (Ohka et al., 2001). In addition to cell to matrix contacts, CD155 also *trans*-interacts with nectin-3, an Ig superfamily member related to CD155 (Ikeda et al., 2003; Mueller and Wimmer, 2003). This interaction is involved in the formation of cell-cell adheren junctions (Sato et al., 2004). Unlike nectins, which can form homophilic interactions, CD155 and mCD155 lack self adhesion.

CD155 expression on certain target cells can also stimulate cytotoxic activity by natural killer (NK) cells due to an interaction with DNAM-1 (CD226) and CD96 in NK cells (Bottino et al., 2003; Fuchs et al., 2004). In addition, binding of DNAM-1 on monocytes to CD155 on vascular endothelial cells promotes trans-endothelial migration of monocytes (Reymond et al., 2004).

The cytoplasmic domain of CD155α and CD155δ interact with Tctex-1, a light chain subunit of the retrograde motor complex dynein (Mueller et al., 2002). Both CD155 and Tctex-1 are expressed on neurons throughout the spinal cord (Mueller, Wimmer, and Cello, 2005). The localization of both CD155 and Tctex-1 in motor

neurons and their interaction presents a working model for retrograde transport of PV in neurons. As mentioned earlier, the binding of the CD155α cytoplasmic domain to the μ1B subunit of the clathrin adaptor complex is responsible for basolateral sorting (Ohka et al., 2001). Upon binding of CD155 to its ligands, including PV, a conserved Immunoreceptor Tyrosine based Inhibitory Motif (ITIM) is phosphorylated. This phosphorylation event leads to association with the tyrosine phosphatase SHP-2, resulting in reduced cell-matrix adhesion and increased cell migration in vitro (Oda, Ohka, and Nomoto, 2004).

Interestingly, not all tissues that express CD155, such as the liver and kidney, are sites of PV infection (Freistadt, Kaplan, and Racaniello, 1990; Koike et al., 1991; Mendelsohn, Wimmer, and Racaniello, 1989). Possible explanations of this discrepancy are as follows. First, early detection studies were done with Northern blots, which do not distinguish between different splice variants. Second, the expression of splice variants could inactivate the virus thus making the tissue resistant to infection. This could be the case in liver, where the splice variants CD155β and CD155γ are predominantly expressed (Baury et al., 2003). Alternatively, CD155 tightly bound to ligands may not be available for virus binding. Finally, interferon responses in certain tissues may be unfavorable for replication, leading to an abortive infection (Ida-Hosonuma et al., 2005).

PV pathogenesis

PV is transmitted via the fecal-oral route. The most frequent manifestation of PV infection in humans is the replication in the gastrointestinal tract and subsequent shedding of the virus in feces (Melnick, 1996; Sabin, 1956). The specific site of PV replication and cell types in which the virus initially replicates following entry into the host remains unknown. However, the virus could generally be isolated from the lymphatic tissues of the gastrointestinal tract, such as the tonsils, the Peyer's patches (PP) of the ileum and mesenteric lymph nodes (Bodian, 1956; Bodian and Horstmann, 1965; Melnick, 1996; Sabin, 1956). The incubation period usually lasts for seven to fourteen days but may vary from two to thrity-five days or even longer. Primary (minor) transient viremia occurs in most infected individuals and the virus spreads to the systemic reticuloendothelial tissue without clinical manifestations (Mueller, Wimmer, and Cello, 2005). Consequently, nearly 95% of the infections in which minor viremia develops are

asymptomatic. In 4-8% of the infected individuals, a second major viremia ensues causing symptoms that are generally associated with and may lead to false diagnosis of other viral diseases; headache, sore throat, fever, nausea and vomiting (Bodian and Horstmann, 1965; Melnick, 1996; Sabin, 1956). A fraction of those with major viremia proceed to develop symptoms of CNS involvement. Neurological symptoms are rare complications of PV infection and poliomyelitis affects less than 1% of infected individual for PV type 1 (PV1) and 0.1% for PV type 2 and 3 (PV2 and PV3) (Nathanson and Martin, 1979).

Poliomyelitis is marked by a selective destruction of motor neurons, leading to paralysis and, in severe cases, to respiratory arrest and death. The molecular mechanisms by which PV causes poliomyelitis are poorly understood, especially regarding early events of the infection and the sites and cells responsible for PV infection. Our knowledge of early events of PV pathogenesis is based mainly on experiments in primates (ref. within (Mueller, Wimmer, and Cello, 2005)). The data obtained by these early studies could be best surmised by two models presented by Bodian and Sabin.

Bodian proposed his pathogenesis model based on studies from chimpanzees and from studies of infection in humans (Fig. 4) (Bodian, 1955). After ingestion of the virus, Bodian found virus in the pieces of intestine containing Peyer's patches but not in adjacent pieces of the ileum (Bodian, 1955). From this observation he proposed that the virus initially grew in the Peyer's patches, as well as in the tonsils. After an initial spurt of replication, the virus invaded the lymphatic system and subsequently the blood stream. Once viremia occurred, the virus invaded the CNS and caused neurological complications.

Unlike the Bodian model, the Sabin model differs on the initial sites of PV replication (Fig. 4) (Sabin, 1956). In Sabin's view, the virus first replicates in the epithelium of the mucosa of the oropharynx and the lower alimentary tract. Release of the virus from the epithelium is then absorbed into the regional lymph nodes and sometimes into the bloodstream. However, the virus that reaches the blood is quickly removed by the cells of the reticuloendothelial system. From the various sites of replication in the alimentary canal and other extraneural tissues, the virus invades the corresponding sympathetic or sensory peripheral ganglia and then spreads to the CNS.

The two models of pathogenesis differ considerably, from the sites of initial replication to the route of CNS invasion. However, generation of mouse models (discussed below in detail; (Koike et al., 1991; Ren et al., 1990)), though not applicable for studies of PV oral infection, have shed light on how PV spreads to the CNS. First, the virus may directly pass from the blood into the CNS by crossing the blood brain barrier (BBB), independently of the receptor (Yang et al., 1997). Second, the virus is transported by retrograde axonal transport ascending from the spinal cord and brain (reference within (Mueller, Wimmer, and Cello, 2005)). Interestingly, both theories depend on the presence of virus in the blood (viremia). These mouse studies preclude the Sabin model of pathogenesis of the CNS, since the Sabin model does not heavily rely on viremia for CNS complications. In the Bodian model, viremia is a precondition for neurological complications.

The mouse models have been instrumental in our understanding of complications in PV infections of the CNS. They are susceptible by parenteral routes; however, unlike chimpanzees and old world monkeys, mouse models are not susceptible to infection by oral route. Hence, a detailed description of the first step in pathogenesis, replication in the alimentary canal, remains completely unknown.

Mouse models

Identification of the PV receptor facilitated the development of transgenic mice expressing the human PV receptor. These mice had not only been beneficial in the study of PV pathogenesis but also in the physiological function of the receptor itself (Mueller, Wimmer, and Cello, 2005). Since the identification of CD155, multiple transgenic mice have been constructed, where the CD155 gene or its isoforms are driven under a variety of promoters.

Susceptibility of Wild type mice to infection with PV

Most wild type strains of PV do not infect mice regardless of the route of infection, and therefore do not cause neurological disease in mice. An exception is MEF-1, a strain of PV2 which was reported to be neurovirulent when injected intracerebrally (i.c.) without prior passage in mouse brain (Schlesinger, Morgan, and Olitsky, 1943). Other PV2 strains were adapted to grow in mouse CNS, such as PV2 (Lansing) (Armstrong, 1939). In addition, a neurovirulent mouse adapted strain of PV1 [PV1(LS-

a)] was also isolated (Li and Schaeffer, 1953). Even though these strains are neurovirulent in mouse CNS, they cannot infect any cultured rodent cells unless the cells have been transformed with CD155 (Mendelsohn, Wimmer, and Racaniello, 1989). Also, the murine CD155 (mCD155; also known as Tage4) does not serve as a receptor for the mouse-adapted PV (Khan, SA, Mueller, S, Wimmer, E. unpublished data). The current hypothesis on the mode of entry of the PV1(LS-a), is that multiple mutations in the coding regions of VP1 and $2A^{pro}$ lead to instability of the virus, thereby contributing to mouse neurovirulence (Lu et al., 1994). Furthermore, a comparison of the histopathology of the wild type mice with that of the mouse-adapted strains showed diffuse encephalomyelitis that affected neuronal cell populations without discrimination, whereas in primates and CD155 tg mice the damage was restricted to motor neurons (Gromeier, Lu, and Wimmer, 1995). Therefore, wild type mice are not an animal model of poliovirus as first the route of infection is limited to i.c. infection and the disease produced is not poliomyelitis.

Susceptibility of tg mice with Human promoter and Human CD155 gene (CD155 tg mice) to PV infection

The isolation and characterization of CD155 (Koike et al., 1990; Mendelsohn, Wimmer, and Racaniello, 1989; Wimmer et al., 1994) made possible the construction of *CD155 tg* mice (Koike et al., 1991; Ren et al., 1990). These transgenic animals, when injected with PV, showed signs of paralysis similar to those of human poliomyelitis (Koike et al., 1991; Ren et al., 1990) and they have been central in the elucidation of PV spread to the CNS (Mueller, Wimmer, and Cello, 2005). Unfortunately, the scope of the studies in these tg animals is limited to events that follow the crucial step of infection by ingestion. This is because CD155 expression in CD155 tg mouse tissues does not entirely match that in human tissues (Koike, Aoki, and Nomoto, 1994). The difference is decisive in the gastrointestinal tract of the transgenic animals. Here, the human CD155 is not expressed at all, an observation explaining why none of the CD155 tg mice constructed can be infected orally (Iwasaki et al., 2002) (Fig. 5).

Susceptibility of CD155 tg mice deficient in the alpha/beta interferon receptor (CD155/*ifnar* KO mice) to PV infection

PV selectively replicates in neurons of CD155 tg mice, however, CD155 is expressed in both target and non-target tissues. CD155/*ifnar* KO were constructed to assess the role of alpha/beta interferon in tissue tropism (Ida-Hosonuma et al., 2005). The CD155/*ifnar* KO mice showed increased susceptibility to PV when compared to CD155 tg mice. After intravenous (i.v.) infection, viral antigens were found in the liver, spleen, and pancreas in addition to the CNS (Ida-Hosonuma et al., 2005). In addition, the mice were also susceptible to oral infection (Ohka et al., 2007). However, the analysis of early sites of replication after oral infection is complicated since even the non-target tissues are susceptible to infection due to a lack of IFN response.

Susceptibility of tg mice with Intestinal fatty acid binding protein promoter and CD155δ mice (TgFABP-PVR) to PV infection

Since the lack of expression in the alimentary canal was most likely responsible for susceptibility of the CD155 tg mice to PV, Racaniello's group used the promoter of the Intestinal fatty acid binding protein to express CD155δ cDNA in tg mice (TgFABP-PVR) (Zhang and Racaniello, 1997). As expected, CD155δ was expressed in enterocytes, but an analysis of PPs (Germinal centers (GC) and other cells insides the PPs) was not reported except for unpublished note that CD155δ was found on M-cells. However, these mice were not susceptible to oral infection. The failure to achieve oral infection in TgFABP-PVR mice could be related to (i) lack of CD155δ expression beyond the linings of the intestine, specifically in the GC, endothelial cells and other cells in PP and/or (ii) lack of expression of the other isoforms of CD155.

Susceptibility of tg mice with β-actin promoter and CD155δ (cPVR) to PV infection

Andino's group used the β-actin promoter to express CD155δ and found expression in most tissues analyzed, including the small intestine (Crotty et al., 2002). No analysis of the gut-associated lymphoid tissues (GALT) was included, however, oral, rectal or gastric infections were nonproductive at any dose. The cPVR mouse (Crotty et al., 2002) showed paralysis after intramuscular (i.m.) or intracerebral (i.c.) inoculation at modest doses but, astonishingly, needed a large dose for intraperitoneal (i.p.) or intravenous (i.v.) inoculation when compared to the CD155 tg mice.

Susceptibility of tg mice with CMV enhancer and β-actin promoter driving CD155α expression (CAG-PVR) to PV infection

When isoform CD155α was expressed nearly ubiquitously under the control of the CMV enhancer and β-actin promoter (CAG-promoter)(Ida-Hosonuma et al., 2002), the resulting tg mouse could not be infected orally and progression of infections to neurological complication was very rare, regardless of the dose and the route of inoculation (Ida-Hosonuma et al., 2002). However, the authors detected neutralizing antibodies against PV in the serum of surviving mice inoculated by i.p. and i.v. routes (Ida-Hosonuma et al., 2002).

Susceptibility of tg mice with Nectin-2 promoter and the CD155 gene (MPVRtg) to PV infection

Finally, Nomoto's group expressed the CD155 gene under the control of the nectin-2 promoter (Yanagiya et al., 2003). This study was initiated at a time when it was erroneously believed that the mouse mph gene (mouse PV receptor homologue; now called nectin-2) was homologous to the human CD155 gene. This, in fact, was discovered to not be the case. Nectin-2 is a novel cell adhesion molecule related to but not homologous to CD155. It belongs to the same novel Ig-like superfamily as does CD155 (Mueller et al., 2003; Takai et al., 2003). Mouse nectin-2 is normally prominently expressed in the mouse liver; thus, CD155 was also expressed strongly in that organ in the MPVRtg mice (Yanagiya et al., 2003). No analysis of CD155 expression of the GALT tissues was presented. Interestingly, PV replicated well in the liver and brain of these tg animals expressing CD155α and -δ. Oral infections of the tg animals, however, were unsuccessful at any dose.

Specific topics of this dissertation

The central theme of this dissertation revolves around the pathogenesis of PV. In Chapter II of this dissertation, I will present experiments that, in part, explain why NWM species are sporadically sensitive to PV serotypes. Unlike OWMs and chimpanzees, most NWMs are not susceptible to PV infection. In the event NWMs are sensitive, the infectivity is dependent on the species, route of infection and serotype of the virus. Since PV infection is dependent on the cellular receptor CD155, I characterized the CD155 homologs of the NWM species, Tamarin and Marmoset. In addition, I carried out

experiments to elucidate the mechanism leading to diverse phenotypes of the Tamarin and Marmoset cell lines on infection with different PV serotypes.

In Chapter III, I will describe the generation and characterization of the first immunocompetent mouse model that is sensitive to oral infection. Prior to my studies, none of the mice generated were sensitive to oral infection, unless the mice were immuno-compromised by specifically lacking alpha/beta interferon receptor. I was able to overcome this hurdle by generating a mouse model that expresses the human CD155 structural gene under the control of mouse CD155 promoter. Using this strategy I was able to generate a mouse model that is sensitive to oral infection.

Figure 1. Genomic organization and proteolytic processing of the poliovirus polyprotein. A terminal protein VPg (structure and sequence are indicated on the left) is linked covalently to the 5' NTR. The 5' NTR consists of several stem loops that form the 5' cloverleaf followed by the IRES element. The single open reading frame is translated into a polyprotein of 247 kDa that is processed by the virally encoded proteinases 2Apro (circle) and 3Cpro/3CDpro (triangles). Filled shapes indicate fast cleavages and open shapes indicate slow cleavages. The VP0 maturation cleavage is marked by a diamond. The structure and sequence of the *cre* element located in the coding sequence of protein 2C, is given on the right (modified from Mueller et. al. 2005).

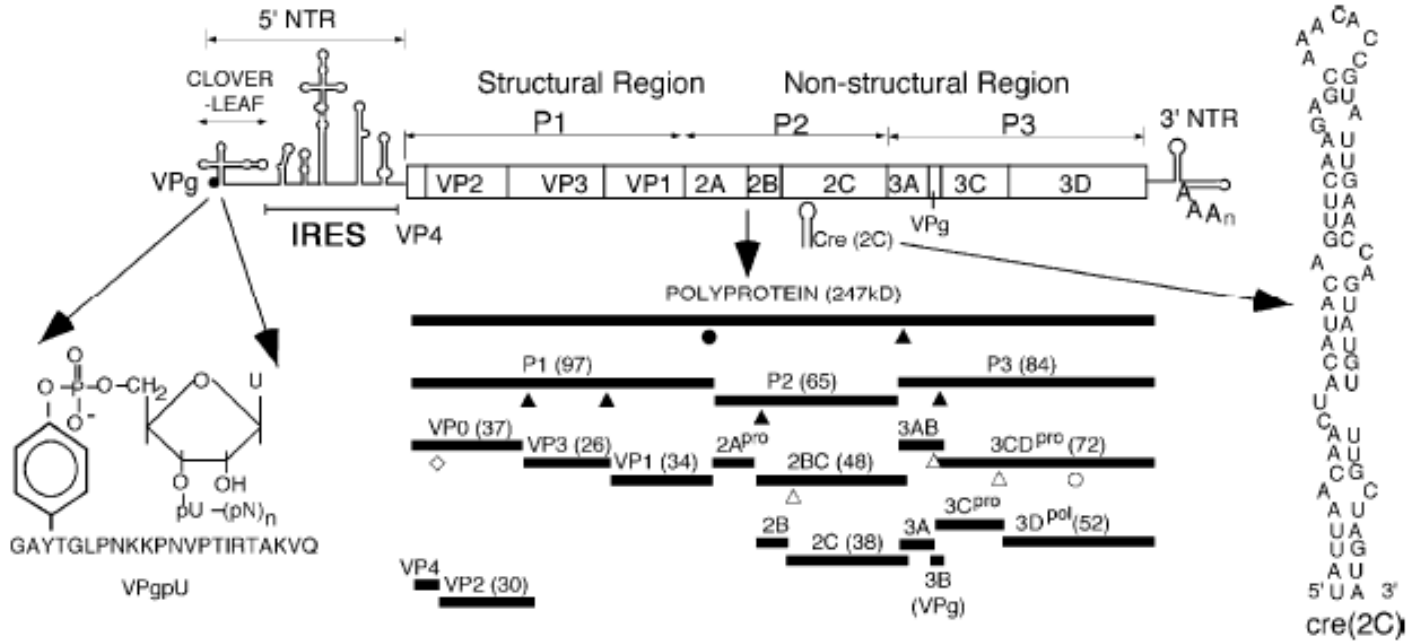
5' NTR
CLOVER
-LEAF
VPg
IRES
VP4
Structural Region
Non-structural Region
P1
P2
P3
3' NTR
VP2
VP3
VP1
2A
2B
2C
3A
3C
3D
VPg
Cre (2C)
POLYPROTEIN (247kD)
P1 (97)
P2 (65)
P3 (84)
VP0 (37)
VP3 (26)
VP1 (34)
2A^pro
2BC (48)
3AB
3CD^pro (72)
3C^pro
3D^pol (52)
2B
2C (38)
3A
3B
(VPg)
VP4
VP2 (30)
GAYTGLPNKKPNVPTIRTAKVQ
VPgpU
pU –(pN)n
cre(2C)

Figure 2. The life cycle of poliovirus. PV enters into host cells through interaction of the virus canyon with CD155 on the cell surface. The viral particles are internalized by a clathrin- and caveolin-independent, but actin and tyrosine kinase-dependent mechanism. After adsorption, the virus releases its genome into the cytoplasm. Following VPg cleavage, virion genome serves as a messenger RNA that is translated into a single polyprotein by host cell ribosomes, and whose proteolytic cleavage products serve as capsid precursors and replication proteins. RNA replication takes place on rosette-like membranous structures that are induced by viral proteins. The newly synthesized (-) strand RNA, then serves as the template to generate progeny (+) strand RNAs. The newly synthesized (+) RNA can either serve as template for protein synthesis or packaged into new virions. Virions are then released from the host cell to initiate another infection cycle.

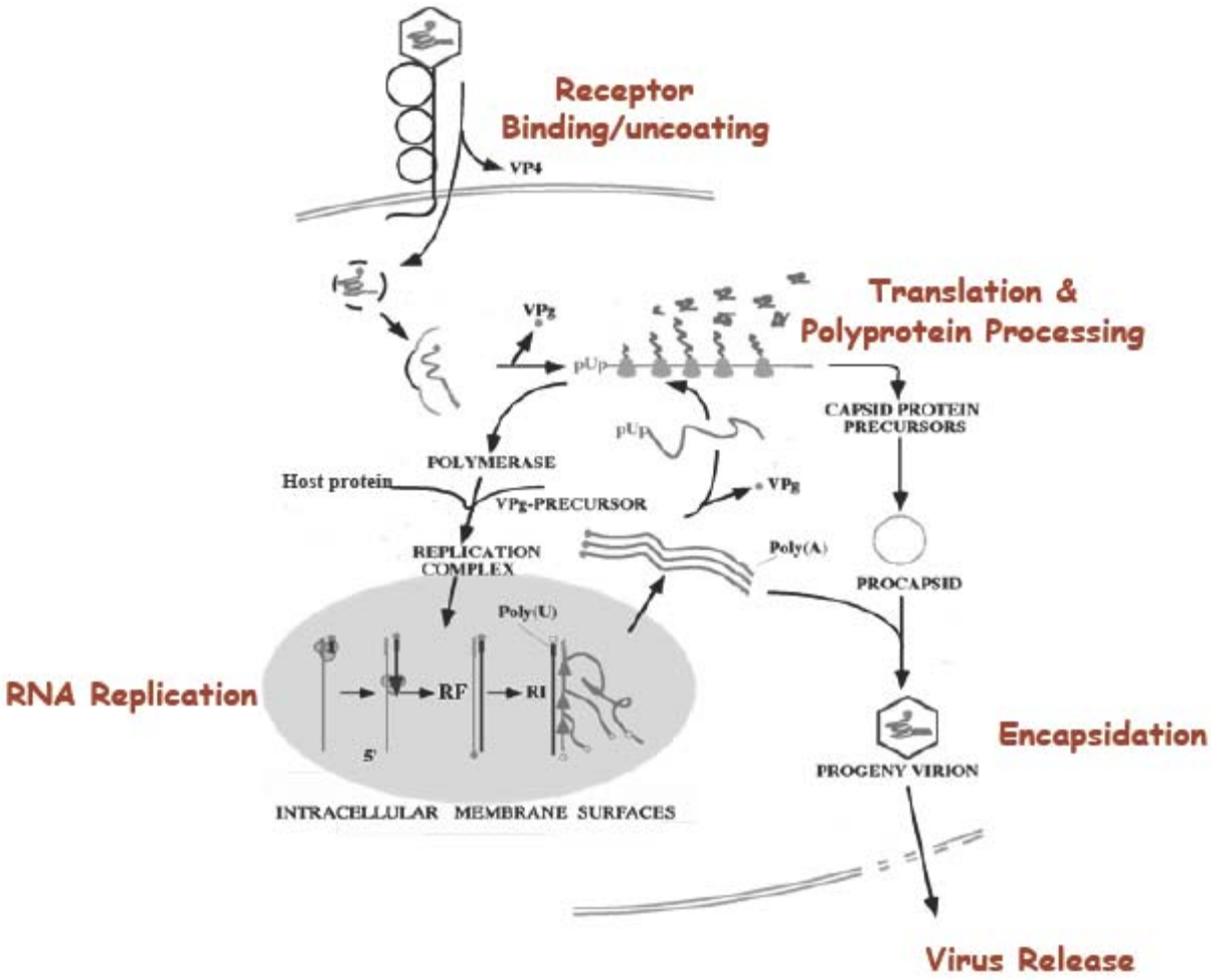
Receptor
Binding/uncoating
VP4
Translation &
Polyprotein Processing
VPg
pUp
CAPSID PROTEIN
PRECURSORS
POLYMERASE
Host protein
VPg-PRECURSOR
VPg
REPLICATION
COMPLEX
Poly(A)
PROCAPSID
Poly(U)
RNA Replication
RF
RI
5'
Encapsidation
PROGENY VIRION
INTRACELLULAR MEMBRANE SURFACES
Virus Release

Figure 3. The CD155 protein. **(A)** Three extracellular immunoglobulin-like domains (V, C2, C2) are formed by disulfide bonds (S-S). The transmembrane domain (T) and the potential extracellular glycosolation sites (diamonds) are shown. Numbers indicate the amino acid residues of each domain. **(B)** CD155 gene organization. CD155 is composed of 8 exons, where first 5 exons (green) encode for three domains, while exon 6 encodes the transmembrane (blue) and exon 7 and 8 for the cytoplasmic tail (red). **(C)** The CD155 mRNA is spliced to yield four isoforms. CD155α and δ are membrane bound and differ in the length of their cytoplasmic tail. CD155β and γ are secreted and lack the transmembrane domain.

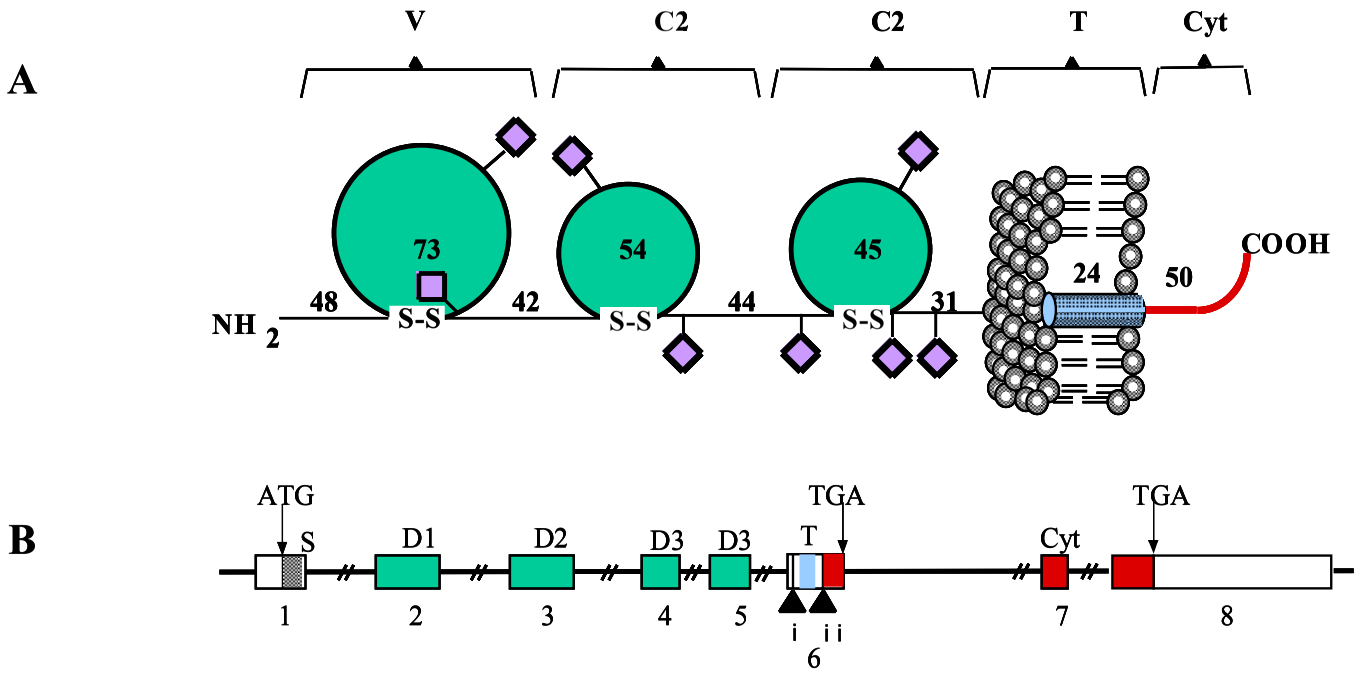
A
V
C2
C2
T
Cyt
73
54
45
NH 2
48
S-S
42
S-S
44
S-S
31
24
50
COOH
B
ATG
S
D1
D2
D3
D3
T
TGA
Cyt
TGA
1
2
3
4
5
i
ii
6
7
8
C
PVRδ
PVRα
PVRβ
PVRγ

Figure 4. The Bodian and Sabin pathogenesis model. Schematic representation of the primary sites of poliovirus replication as defined by Bodian (red text) and Sabin (blue text). Unlike Sabin model where virus initially grows in mucosa layer, in Bodian model virus initially grows in secondary lymphoid tissues. Beside discrepancy on primary site of replication the virus follows the same pathway to CNS, the exception being that according to Sabin, virus can directly infect nerve ganglia (blue text) (Bodian 1955, Sabin 1956).

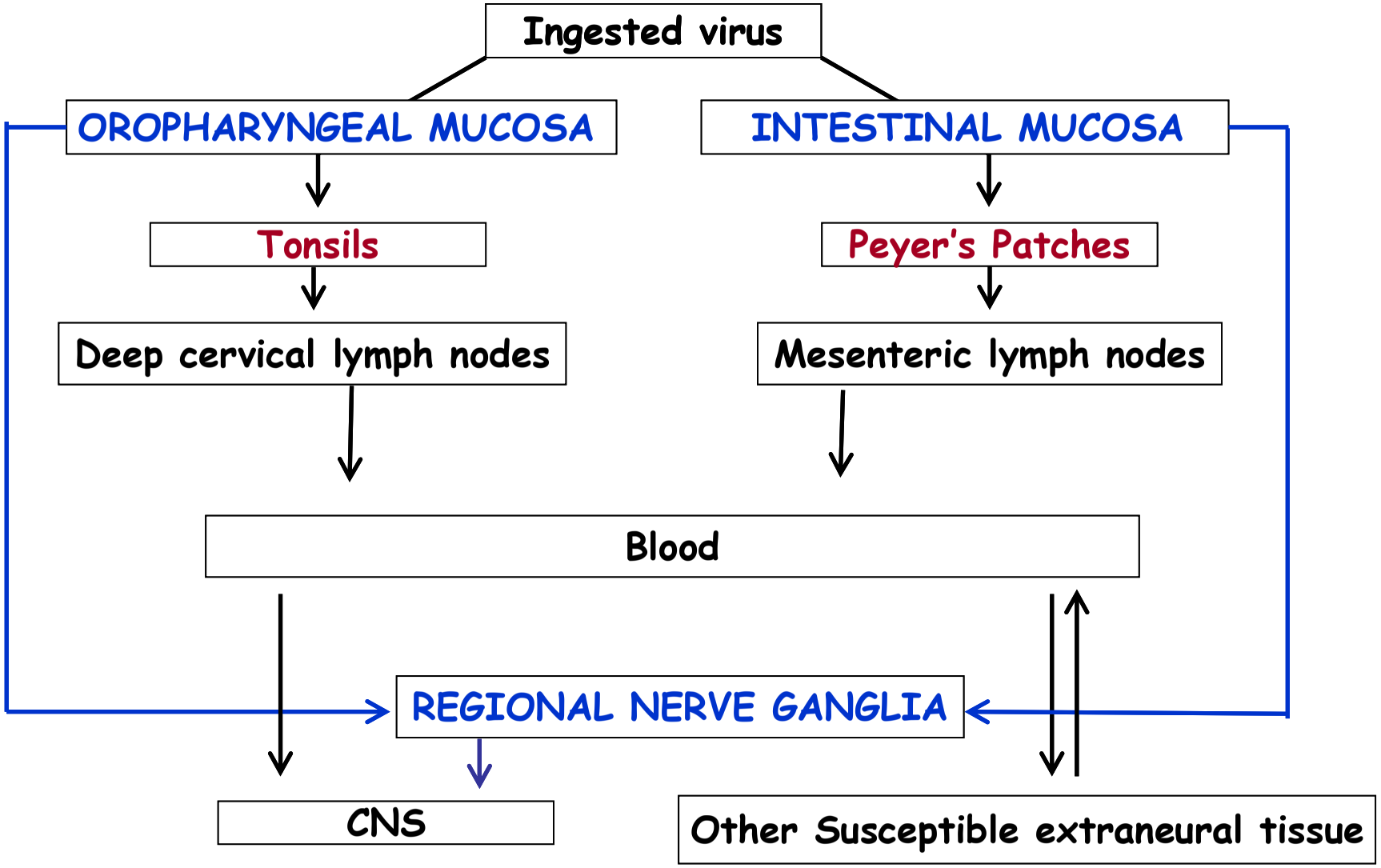
Ingested virus
OROPHARYNGEAL MUCOSA
INTESTINAL MUCOSA
Tonsils
Peyer's Patches
Deep cervical lymph nodes
Mesenteric lymph nodes
Blood
REGIONAL NERVE GANGLIA
CNS
Other Susceptible extraneural tissue

Figure 5. CD155 expression in the Peyer's patches of **(A)** human and **(B)** CD155 tg mice. CD155 was labeled with monoclonal mouse Ab D171 for human samples and rabbit polyclonal NAEZ8 for mice. White arrow in panel A shows follicle-associated epithelium. G, germinal centers; S, subepithelium dome; L, lumen. (modified from Iwasaki et. al. 2001).

A

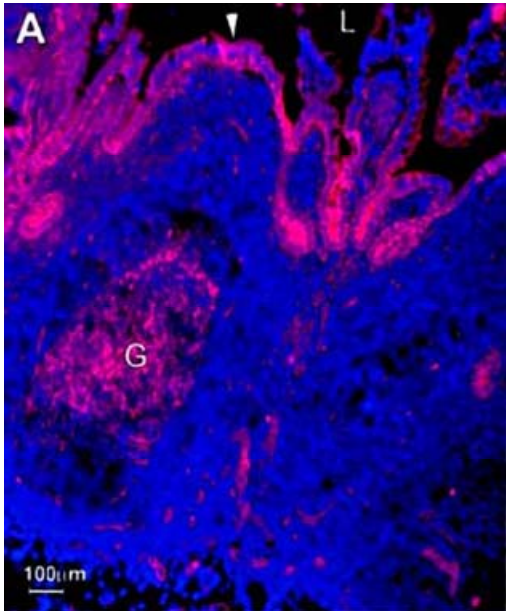

B

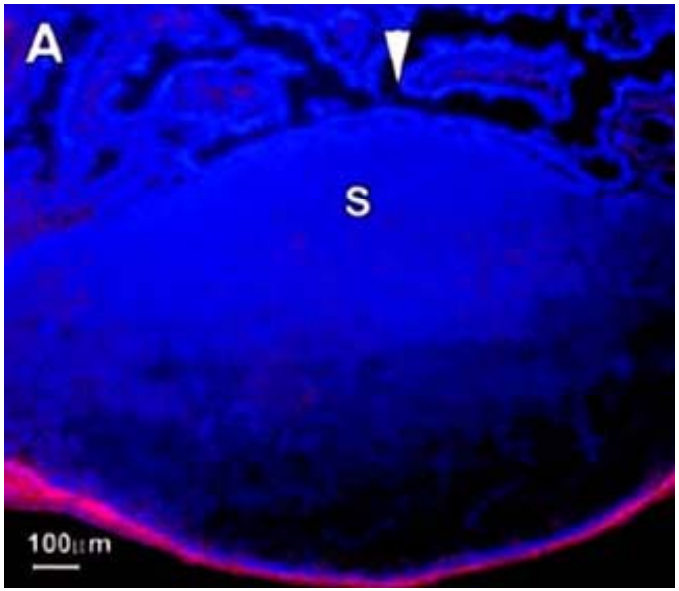

Chapter II

Characterization of the New World Monkey homologues of the Human Poliovirus receptor CD155

Background

Poliovirus (PV) is characterized by a highly restricted host and tissue tropism. Infecting by the oral-fecal route, only humans are natural hosts of PV. Disease symptoms are predominantly neurological but they are rare, depending upon the serotype (Mueller, Wimmer, and Cello, 2005). The major determinant of virus pathogenicity is the human cell surface receptor CD155 (PVR) although other factors such as interferon also plays an important role (Ida-Hosonuma et al., 2005). CD155 has been thoroughly characterized (Mueller, Wimmer, and Cello, 2005) and homologues of this protein are known to exist in primates and non-primates (Ida-Hosonuma et al., 2003). Non-human primates, such as chimpanzees and African green monkeys (AGMs), which are members of Old World Monkeys (OWMs) have been shown to be susceptible to PV infection. In the wild, however, PV infections of non-human primates are not well documented.

PV is a non-enveloped plus-stranded RNA virus, a member of the genus *Enterovirus* and in the *Picornaviridae* family. Its genome is approximately 7,500 nucleotides long, carrying a small viral protein (VPg) covalently linked to the 5' terminus and a poly(A) tail at the 3' terminus (Fig. 1A). The genome encodes a single large polyprotein, encoding structural proteins (P1) and non-structural proteins (P2 and P3). Proteolytic processing of P1, P2, and P3 by the virus-encoded proteinases $2A^{pro}$ and $3C^{pro}/3CD^{pro}$ generates the functional proteins. Sixty copies of each of the four capsid polypeptides (VP1-VP4), processed from P1, assemble to form a capsid shaped as an icosahedron with five-, three- and two-fold axes (Hogle, Chow, and Filman, 1985; Rossmann, 2002). In contrast to VP1, VP2, and VP3, the smallest capsid polypeptide, VP4, is located inside the capsid. The capsid proteins, VP1, VP2 and VP3, fold as eight stranded antiparallel β-barrels whereby the antigenic regions are hydrophilic β-turns within these structures (Hogle and Filman, 1989; Rossmann and Johnson, 1989). They give rise to three different sets of neutralization antigenic sites and, hence, the virus exists in three serotypes (types 1 – 3) (Burnet, 1931; Paralysis, 1951). A notable structural feature of the capsid is the "canyon", a depression characteristic for capsids of all entero- and rhinoviruses, which is a site of cellular receptor binding (Rossmann, 2002).

CD155, the only known cellular receptor mediating uptake of PV into cells, is a highly glycosylated single-span membrane protein (about 80 kDa) belonging to the

immunoglobulin superfamily (Fig. 2) (Koike et al., 1990; Mendelsohn, Wimmer, and Racaniello, 1989; Rieder and Wimmer, 2002). CD155 can be broadly divided into 5 domains: three extracellular Ig-like domains (one variable (V) and two constant (C) domains), a transmembrane domain, and a cytoplasmic tail (Fig. 2). The human *CD155* gene is expressed in cells in four variants (α, β, γ, δ) through alternate splicing of the CD155 transcript RNA. Two of the variants (β and γ) occur in a soluble form, while the other two variants (α and δ) are membrane bound and serve as the receptor for PV. Human CD155 (hCD155), α and δ, differ only in the length and sequence of their cytoplasmic (C-terminal) tail. Genetic and biochemical evidence have identified the V-domain of CD155 as the virus binding domain (Aoki et al., 1994; Belnap et al., 2000; Bernhardt et al., 1994; Harber et al., 1995; He et al., 2000; He et al., 2003; Morrison et al., 1994; Xing et al., 2000). Interestingly, these genetic modifications have indicated that the three PV serotypes interact with the V-domain in a slightly different manner (Harber et al., 1995), a phenomenon that I have observed also in my studies of the interaction between the human CD155 (hCD155) homologues of NWMs reported here.

CD155 is the founding member of a family of immunoglobulin molecules, whose function has generally been characterized as adhesion proteins (Ogita and Takai, 2006). Specifically, CD155 has been shown to mediate cell-to-matrix contacts by specifically binding to vitronectin (Lange et al., 2001). Moreover, it has been shown that CD155 recruits the adhesion molecule nectin-3 to cell-cell junctions through a trans-heterophilic interaction (Mueller and Wimmer, 2003). CD155 also acts as a ligand for DNAX accessory molecule-1 (DNAM-1) and this interaction results in DNAM-1-dependent enhancement of NK-mediated lysis of target cells (Bottino et al., 2003). The C-terminal domains of both membrane bound forms of hCD155, α and δ, interact with Tctex-1, a small protein of the dynein motor complex, and are involved in retrograde axonal transport of the virus-receptor complex (Mueller et al., 2002; Ohka et al., 2004). Another element found only in the C- terminal domain of hCD155α is the tyrosine containing binding motif of the μ1B subunit of the clathrin adaptor complex, which directs CD155α transport to the basolateral surface in polarized epithelial cells (Ohka et al., 2001).

Shortly after the discovery of hCD155, putative homologues were described, most of which were related to, but not homologous to hCD155 (Eberle et al., 1995; Morrison

and Racaniello, 1992; Ravens et al., 2003). The most thoroughly studied human and rodent proteins related to CD155 are called nectins (Ogita and Takai, 2006), while the rodent orthologue of CD155 has now been named as Tage4 (Baury et al., 2001; Ravens et al., 2003). Just like the nectins, however, Tage4 has no affinity to PV ((Ravens et al., 2003); Khan, S., Mueller, S. and Wimmer, E., unpublished data). The only CD155 related proteins with an affinity to PV are found in Chimpanzees, Old World Monkeys (OWMs), and New World Monkeys (NWMs). OWMs, exemplified by African Green Monkeys (AGMs) have been thoroughly studied because of their susceptibility to PV by oral infection, which is highly inefficient compared to humans (Koike et al., 1992; Sabin, 1956). AGMs posses two genes coding for three membrane-bound forms of CD155 (Koike et al., 1992). These are two splice variants, AGMα1 and AGMδ1 of the first gene and AGMα2, which is encoded by a second locus in the genome (Koike et al., 1992). Both AGMα1 and AGMα2 serve as functional PV receptors and have amino acid similarity to hCD155α of 90.2% and 86.4%, respectively (Koike et al., 1992). AGMδ1 also serves as a functional receptor of PV.

Of the monkey species, the least studied with respect to PV pathogenesis are NWMs, whose habitat is limited to the tropical forests of Central and South America. NWMs are composed of four families; *Cebidae*, *Aotidae*, *Pitheciidae,* and *Atelidae*. Unlike OWMs, early studies have indicated that NWMs cannot be infected by the oral route, and any susceptibility by injection may depend not only on the animal species but also on the PV serotype (Hsiung, Black, and Henderson, 1964). Similarly, early tissue culture studies have shown that only PV1 displayed susceptibility to capuchin monkey cells, however with no cytopathic effect (Kaplan, 1955a; Kaplan, 1955b; Kaplan and Melnick, 1955). Recently, Koike and his colleagues (Ida-Hosonuma et al., 2003) have analyzed the gene specifying the hCD155 homologue of brown capuchin monkeys (Subfamily *Cabinae,* Genus *Cebus*). They showed that the V-domain of capuchin monkey cDNA, when spliced onto the C-domain of hCD155, could promote infection of mouse L-cells that were transformed with the chimeric receptor (Ida-Hosonuma et al., 2003). Infection, however, was restricted to only one serotype (PV1) and no analyses of the mechanism of restriction have been reported (Ida-Hosonuma et al., 2003).

The aim of my studies was to examine whether the susceptibility of NWMs to

infection by different PV serotypes is due to virus-receptor interaction or to translation and replication. I have selected two kidney cell lines from tamarins (TMX) and marmosets (NZP-60) of the genera *Saguinus* and *Callithrix*, respectively, and belonging to the subfamily of *Callitrichinae* of NWMs. Marmoset cells were found to be resistant to PV infection with all PV serotypes, while tamarin cells showed sensitivity only to PV1 and PV3. These phenotypes have been observed in spite of high expression of the CD155 homologues by both NWM cells and by normal translation and replication of PV RNAs or of the PV luciferase (PV-Luc) replicon once transfected into the cells. However, I observed significant differences in the binding of PV serotype to NWM cell lines. Only PV1 is able to bind (but not infect) NZP-60 cells whereas PV2 and PV3 display no virus-receptor bound complexes on these cells. Moreover, I detected virus-receptor bound complexes with PV1 and PV3 but not PV2 on TMX cells. Generally, if the formation of virus-receptor complexes was higher at 25°C than at 4°C, the binding would lead to cellular infection at 37°C, an observation suggesting that the complex formed at 25°C may be an intermediate in the early steps of infection. When mutations were introduced into the V domain of the marmoset CD155, the mutant receptor was able to bind PV1 and also catalyze uncoating and infection. My results indicate that the restriction of PV infection of NWM cell lines is related to their receptors' ability to form initial complexes with the virus serotype in question.

MATERIALS AND METHODS

Cloning of NWMs CD155 cDNAs. Based on the conserved cDNA sequences of human and AGM CD155, primers were designed corresponding to hCD155 cDNA sequence 122-136 (5'-TGGGCGACTCCGTGA-3') and 942-977 (5'-CACCAATGCCC TAGGAGCTCGCCAGGCAGAACTGAC-3'). RT-PCR was performed on total RNA of the NWM cell lines and the 800 bp fragment was amplified and sequenced. Sequence specific primers from partial NWM CD155 cDNAs were designed and the 5' and 3' ends were amplified using the 5'/3' Race Kit (Roche). The full length CD155 cDNA was amplified using primers, TMX 5' (5'-GGCGATATCAGAGCTAGGCCGCCGCGTG-3'), TMX 3' (5'-GTTCTAGAATCCTA GGAAGAGTTGGCCAC AG-3'), NZP 5' (5'-GGCGATATCAGAGCCATGGCCGCCGCGTG-3'), and NZP 3' (5'-ACTCTAGACT GTCACCTTGTGCCCTTTGTCTG-3'). The TMX and NZP CD155 cDNA were cloned

into mammalian expression vector pcDNA 3.1 (+) (Invitrogen) using restriction sites, *EcoRV* and *XbaI*. The N-terminal signal peptide and transmembrane helix were identified in the deduced protein sequence using SignalP and TMHMM on CBS prediction server (http://www.cbs.dtu.dk/services) (Bendtsen et al., 2004; Kall, Krogh, and Sonnhammer, 2004).

Cells. HeLa R19, mouse fibroblast Ltk$^-$ cells, and stably transfected Ltk$^-$ cells with PV receptor variants were maintained in Dulbecco's modified Eagle's medium (DMEM), containing 10% fetal bovine serum (FBS) and 1% penicillin/streptomycin. Primary kidney cells from a black tailed marmoset (*callithrix argentata*) were obtained from ATCC (CRL-1924; designation NZP-60). A Tamarin (*saguinus mystax*) primary kidney cell line, designated TMX, was generously donated by Dr. S. U. Emerson and Dr. R. H. Purcell, of the National Institute of Health. TMX were maintained in DMEM containing 5% FBS, 5% bovine calf serum (BCS), and 1% penicillin/streptomycin. NZP-60 cells were maintained in 50% DMEM and 50% F-12 nutrient media containing 10% FBS and 1% penicillin/streptomycin.

Generation of stable cell lines. Ltk$^-$ mouse fibroblast were maintained in DMEM containing 10% FBS. Cells were plated 24 h before transfection on 35 mm plate. The cells were transfected with pcDNA 3.1 (+) plasmid containing NWMs CD155 variants with Lipofectamine® 2000 transfection reagent (Invitrogen). After 24 h the cells were selected in presence of Geneticin® (Invitrogen). After selection, cell pools were labeled with mouse monoclonal antibody (mAb) p286 (donated by Dr. Nomoto) at a concentration of 20 µg/ml. Each sample was washed with phosphate buffered saline solution (PBS) and then stained with FITC-conjugated goat anti-mouse IgG (BD bioscience). Labeled cells were sorted by fluorescent-activated cell sorting (FACS) VANTAGE (Beckton Dickinson). Sorted cell lines were maintained in DMEM, containing 10% FBS and 1% penicillin/streptomycin.

Preparation of purified PV serotypes and viral RNA. Polioviruses used in this study were the most commonly studied representatives of the three serotypes (Mahoney, Lansing, and Leon). It could be argued that experiments with different strains of a given serotype would show different results. I cannot exclude this possibility but I believe strain variations would not change the basic conclusions drawn from the experiments described

here. This is because structurally, all three serotypes have similar architecture (Filman et al., 1989; Hogle, Chow, and Filman, 1985; Lentz et al., 1997), the serotypes largely being defined by numerous surface changes in exposed protrusions of the virion (Minor et al., 1986). Changes to switch serotypes would be dramatic while changes to yield different strains would be subtle. I therefore assume here that my experiments of receptor/virus interaction with, say, serotype 1 PV(M) is likely to reflect experiments with different strains of the same serotype. PV1 (Mahoney), PV2 (Lansing) and PV3 (Leon) were grown in HeLa cells at 37°C and the cells were harvested after 8 h post infection. The plates were subjected to three consecutive freeze-thaw cycles and the virus titer was determined by plaque assay on HeLa cell monolayers, as previously described (Pincus et al., 1986).

To obtain viral RNA genome, the PV serotypes were additionally purified by CsCl gradient centrifugation. Viral RNA was isolated from the purified virus stocks with a 1:1 mixture of phenol and chloroform. The purified viral RNA was precipitated by the addition of 2 volumes of ethanol and resuspended in RNase free water.

One-step growth curve of PV serotypes. Cell monolayers (1 x 10^6 cells) were incubated with 10 multiplicity of infection (MOI) of virus for 30 min, at room temperature, on a rocker platform. After 30 min, cells were washed three times with PBS and incubated at 37°C in DMEM containing 2% BCS. The cells were harvested at 0, 2, 4, 6, 8, 12, 24, and 48 h post infection. The plates were subjected to three consecutive freeze-thaw cycles, and the viral titers of the supernatants were determined by plaque assay on HeLa cell monolayers, as previously described (Pincus et al., 1986).

Transfection of viral RNAs into cells. The purified viral RNA was transfected into monolayers with the TransMessenger Transfection Reagent (Qiagen). Transfected cells were incubated in DMEM, supplemented with 2% BCS at 37°C either until complete cytopathic effect (CPE) was observed or for at least 24 h post-transfection. After three rounds of freeze-thaw cycles, the lysate was clarified of cell debris by low-speed centrifugation. Virus titers were determined by plaque assay (Pincus et al., 1986).

In vitro transcription and transfection of PV luciferase (PV-Luc) replicon. The PV-Luc replicon (Fig. 1B) (Li et al., 2001) was digested with *DraI* before transcription with T7 RNA polymerase. RNA transcripts were transfected into

monolayers of various cell types in 35mm dishes by the TransMessenger Transfection Reagent (Qiagen).

Measurement of PV RNA translation and replication using luciferase replicons. After transfection with PV-Luc replicon, various cell lines were incubated at 37°C in DMEM with 2% BCS. The cells were grown with or without 2 mM guanidine hydrochloride (GnHCl). At 12 h post-transfection, the growth medium was removed from the dishes, and the cells were washed gently with 2 ml of PBS. The 35 mm dishes were lysed with 300 µl of "passive" lysis buffer (Promega). 50 µl of luciferase assay reagent (Promega) was mixed with 20 µl of lysate, and the firefly luciferase activity was measured with an Optocomp I luminometer (MGM Instruments, Inc.).

Detection of CD155 expression levels on cell surface by flow cytometry. $1x10^6$ cells in suspension were incubated for 30 min at room temperature with or without mAb p286 at a concentration of 20 µg/ml. mAb recognizes an epitope of the V-domain of hCD155 (Yanagiya et al., 2005). Each sample was washed with PBS and then stained with FITC-conjugated goat anti-mouse IgG (BD bioscience). After washing, 10^3 cells were analyzed by FACS caliber (Beckton Dickson).

Binding assay of PV serotypes. PV1, PV2, and PV3 capsid proteins were labeled with [^{35}S] methionine and the viruses were purified by CsCl gradient centrifugation as previously described (Bibb et al., 1994). $1x10^6$ cells were incubated with 10^8 PFU of labeled virus at 4ºC or 25°C for 30 min. After incubation, the virus-cell complex was pelleted by microcentrifugation and the cell pellets were washed 3 times with PBS. The amount of radioactivity of the cell pellet was quantitated with a liquid scintillation counter (Packard Tri-Carb) in counts per minute (cpm). All samples were done in triplicate.

Alteration assays. Alteration assays were performed as described previously (Fricks and Hogle, 1990). Purified [^{35}S] methionine-labeled virions (approximately 10 M.O.I) were added to cells in DMEM at a density of 5 X 10^6 cells per ml and incubated for 30 min at 25°C. The cells were washed and fresh DMEM with 2% FBS was added and cells were incubated at 37°C for 45 min. The cells were pelleted and dissolved in 0.5% Triton X-100 in PBSA (PBS containing 0.01% bovine serum albumin). The solution was layered on top of 15% to 30% sucrose gradient in PBSA. The gradients

were centrifuged for 75 min at 40,000 rpm in an SW41 rotor. Fractions were collected from the bottom and counted as described above. The gradient markers were made by heating labeled PV1 at 56°C for 10 min followed by incubation on ice for 20 min. Equal amount of heated and unheated virus were layered on the gradient.

Site-Directed Mutagenesis. The following primers were used to make mutations in the marmoset CD155 and tamarin CD155 cDNA in pcDNA 3.1 (+) vector by site directed mutagenesis kit (Stratagene): H77Q Sense (5'-CGTCTTCCACCAAACTCAG GGCCCC-3'); H77Q Antisense (5'-GGGGCCCTGAG TTTGGTGGAAGACG-3'); NZP N82YP/SYS Sense (5'-CAGGGCCCCAGCTACTCGGAGTCCGAAC-3'); NZP N82YP/SYS Antisense (5'-TCGGACTCCGAGTAGCTGGGGCCCTGAG-3'), TMX N80YL/SYS Sense (5'-CAGGGCCCCAGCTACTCGGAGTCCGA ACG-3'), and TMX N80YL/SYS Antisense (5'-TTCGGACTCCGAGTAGCTGGGCCCTG AG-3').

Nucleotide sequence accession numbers. The nucleotide sequence data for the cDNAs for marmoset CD155 (nCD155) and tamarin CD155 (tCD155) have been submitted to GenBank under accession numbers, EU277851 and EU277852, respectively.

RESULTS

Identification of CD155 homologues in NWM cell lines. To ascertain whether TMX and NZP-60 cells have a homologue of CD155, I first stained the cells with a panel of monoclonal antibodies against hCD155 of which mAb p286 bound to receptors expressed on both NWM cells with the same intensity as on Ltk^- cells over expressing hCD155 (data not shown). This result suggested that the NWM cells expressed putative homologues of hCD155 that share structural motifs. To identify this receptor, I first amplified an 800 bp fragment by PCR from a cDNA library of the NWM cell lines, using primers based on highly conserved sequences in human and AGM CD155. This 800 bp fragment was sequenced and species specific primers were used for the rapid amplification of the 5' and 3' cDNA ends (RACE) to obtain the full length cDNA sequences of tamarin CD155 (tCD155) and marmoset CD155 (nCD155) (Fig. 2).

On analysis of the cDNA sequences, I found that tCD155 has an open reading frame (ORF) of 1,167 bp, which encodes a 388 amino acid polypeptide, while the nCD155 has a slightly longer ORF of 1,200 bp, encoding a 399 amino acid polypeptide

(Fig. 2). The tCD155 and nCD155 share 74% and 75% amino acid identity, and 87% and 88% nucleotide identity, respectively, with hCD155α (Table 1). In addition to sequence similarities with hCD155, both tCD155 and nCD155 express the Ig-like structure V-C2-C2, a hallmark of the immunoglobulin superfamily, similar to hCD155 and AGM CD155 (Fig. 3). In comparison to hCD155, which has eight N-glycosylation sites, tCD155 and nCD155 have six sites, while AGMα1 has seven, AGMδ1 has six, and AGMα2 has five sites (Koike et al., 1992) (Fig. 3). The cytoplasmic tails of the tCD155 and nCD155 differ in length, however, both share a consensus sequence for the binding of Tctex-1 and the tyrosine-containing binding motif for the μ1B subunit with hCD155α (Fig. 2 and 3) (Mok, Lo, and Zhang, 2001; Ohka et al., 2001). The close relationship of the extracellular domains and the presence of consensus binding sequences in the cytoplasmic tails in all receptor molecules (Fig. 3) suggests that the NWM CD155 homologues have biological functions similar to that of hCD155. It should be noted that an examination of the NWM receptors did not reveal to us distinct isoforms or receptors expressed from gene duplications.

Susceptibility of NWM cell lines to infection with PV serotypes. Given that the NWM cell lines express a CD155 homologue, I performed one-step growth curve experiments to determine their susceptibility to infection with different PV serotypes (Fig. 4). In TMX cells, PV1 showed delayed early growth compared to that observed in HeLa cells; although by 48 h post infection, the viral titers were comparable (Fig. 4A). PV3, on the other hand, produced lower viral titers after 48 h post infection, when compared to HeLa cells (Fig. 4C). PV2 did not show growth on TMX cells exceeding the original inoculum (Fig. 4B). However there was a decrease in titer at 5 h (eclipse) followed by an increase at 12 h (Fig. 4B). Finally, NZP-60 cells were resistant to infection with all PV serotypes (Fig. 4).

Resistance of NWMs to PVs is not related to inhibition of translation or RNA replication. There are several possible explanations of the NZP-60 cells' resistance to infection with all PV serotypes and of the TMX cells' resistance to only PV2. First, resistance to infection could be due to a defect in the interaction between virus and receptor. Second, there could be an intracellular block at the stage of translation or replication. To test the latter possibility, both TMX and NZP-60 cells were transfected

with PV1, PV2 and PV3 RNA and found to produce virus titers comparable to those obtained on transfected Ltk$^-$ cells, regardless of which cell lines were used (Fig. 5A).

To study translation in the absence of replication, I used a PV-Luc replicon that contained the firefly luciferase gene instead of the P1 domain of the PV polyprotein (Fig. 1B) (Li et al., 2001). After transfection with the replicon, the cells were incubated in the presence of guanidine HCl (GnHCl), a potent inhibitor of PV RNA replication, and the luciferase activity measured 12 h post transfection. The luciferase activity obtained in cell cultures with GnHCl represents translation of the input mRNAs. In mouse Ltk$^-$ cells there was a 10 fold increase in luciferase signal when GnHCl was omitted from the culture and similar increases were also observed with the TMX and NZP-60 cells (Fig. 5B). I conclude from this observation that intracellular replication of genomic RNA of all three serotypes analyzed is not blocked. This data suggests that the resistance to infection of NWM cell lines with different PV serotypes is related to one or more of the earliest steps in the viral life cycle: receptor binding, uptake, or uncoating.

CD155 expression levels on NWM cell lines. To determine whether susceptibility of the NWM cells to PV infection is related to the surface expression of the CD155 homologues, I employed flow cytometry and mAb p286 isolated against an epitope of the V-domain of hCD155 (Yanagiya et al., 2005). By this procedure I found the signal to CD155 on TMX cells to be comparable to that on HeLa cells and two-fold higher on NZP-60 cells than on HeLa cells (Fig. 6). Considering the possibility that mAb p286 may recognize the different receptors with different affinities I cannot firmly conclude that more nCD155 is expressed on NZP-60 cells than hCD155 on HeLa cells. However, there can be no doubt that both NWM receptors are expressed on the respective monkey kidney cells and, consequently, it is unlikely that the inability of some PV strains to grow on the NWM cell lines is the result of insufficient levels of receptor molecules for interaction with PV.

Binding efficiency of PV strains to NWM cell lines. Infection by PV is initiated when the virus docks to CD155 receptor molecules at the cell surface. This interaction subsequently leads to uncoating and internalization of the viral genome (He et al., 2000). Having established that PV can translate and replicate in both TMX and NZP-60 cells, I was interested in determining the binding ability of the PV serotypes to the NWM

receptors by a receptor-excess assay. It has been shown previously that PV interacts with CD155 in two distinct steps (McDermott et al., 2000). The first step can be studied at 4°C and is probably electrostatic in nature. The second step occurs at physiological temperatures and leads to irreversible structural changes of the virion, resulting in the formation of an A-particle in which VP4 is absent (Hogle, 2002). The first step in the entry pathway is the formation of an initial binding complex, which can be isolated at below physiological temperatures. Here I have isolated this initial binding complex into two separate steps, at 4°C and at 25°C using [^{35}S]-labeled virus. At temperatures from 0°C to 25°C, the virus bound to cells can be recovered in an active form (Holland, 1962), thus I can study virus-receptor binding complexes at 25°C without forming A-particles.

On analysis of the data from the binding assays, I found PV1-receptor complexes on TMX cells at 4°C, but the amount of virus-receptor complexes increased by 4 fold at 25°C (Fig. 7A). In contrast, PV3 showed lower amount of bound complexes at 4°C compared to PV1, but the amount of bound complexes increased by 10 fold at 25°C (Fig. 7C). PV2, on the other hand, showed same amount of bound complexes on Ltk$^-$ cells at 4°C or at 25°C (Fig. 7B). PV1-receptor complexes were observed on NZP-60 cells, however without an appreciable increase in binding from 4°C to 25°C (Fig. 7A). The levels of PV2 and PV3 bound complexes on NZP-60 cells were similar to background levels on Ltk$^-$ cells at either 4°C or 25°C (Fig. 7B and 7C).

The observed increase in binding of PV1 and PV3 to tCD155 at 25°C, in comparison to 4°C, suggested to us that the increase in association of the virus to the receptor led to successful infection. This would also explain why PV1 does not infect NZP-60 cells: binding of this strain to nCD155 is very low and did not significantly increase at 25°C when compared to that at 4°C.

Conformationally altered virus particles. As noted above, the increase in the amount of virus-receptor complexes from 4°C to 25°C correlated with successful infection of TMX cells at 37°C (Figs. 3 and 7). Next I wanted to determine whether the transition from native to subviral particles can be demonstrated directly upon incubation of the NWM cells with PV. As illustrated in Fig. 8, TMX cells produced 135S particles although the conversion was inefficient under the conditions of the experiment. NZP-60 cells, on the other hand, did not yield a significant amount of subviral particles.

Mutational analysis of the V domain of the nCD155 and tCD155. Unlike TMX cells, which showed an increase in receptor bound complexes from 4°C to 25°C with PV1, NZP-60 cells did not bind a significant amount of virus and there was no appreciable change in complex formation from 4°C to 25°C. The nCD155, therefore, can bind PV1 weakly but it cannot catalyze the structural changes in the virion necessary for infection. Since the V domain of CD155 is the site of virus binding, I analyzed the V domains of human, AGM, tCD155 and nCD155 by alignment to identify potential amino acids that are involved in binding and uncoating of PV1 (Fig. 9; numbering of amino acids in the V domains of tCD155 and nCD155 will be referred to according to the numbering of hCD155). Previously, mutations of hCD155 in the C'C", C"D, DE, EF loops, and in the N-terminal part of the C" β-strand were found to affect both PV1 binding and replication (Aoki et al., 1994; Bernhardt et al., 1994; Colston and Racaniello, 1994; Harber et al., 1995; Liao and Racaniello, 1997; Morrison et al., 1994).

On analysis of the CD155 homologue alignments, I found six amino acids, Q80, S85, S87, K90, N105 and V115, that have been implicated in viral binding as determined by cryoelectron microscopy (He et al., 2003). The corresponding residues have been substituted in the loops and the β-sheet of both tCD155 and nCD155 (Fig 9). Based on previous mutagenesis studies, I can eliminate from consideration three of the six amino acid positions, K90, N105, and V115 because they did not influence binding and replication (Bernhardt et al., 1994). It has been previously shown that a K90/D mutation in hCD155 did not affect either PV binding or replication (Bernhardt et al., 1994). Therefore, the corresponding K90/E substitution found in NWM CD155 is also unlikely to affect PV binding and replication. Similarly, an N105/D substitution, which eliminates an N-glycosolation site, is also present in the AGM, a functional receptor (Fig. 9). In addition, it was shown that hCD155 lacking two N-glycosolation sites (N105/D and N120/S) had an enhanced binding affinity to the virus (Bernhardt et al., 1994). I doubt, therefore, that a change of the N105 site will significantly influence binding to the NWM receptors. Mutation of E116DE to AAA in the EF loop abolished virus binding, likely due to the loss of consecutive charged residues in this region of hCD155 (Bernhardt et al., 1994). Since a V115/A substitution does not result in charge disruption of the EF loop, I predict that this substitution would also not significantly influence binding of PV.

This leaves us with three mutations that may affect the binding of PV to the receptors nCD155 and tCD155. The amino acids Q80, S85, and S87 mutations in hCD155 have all resulted either in decrease or loss of PV1 binding (Bernhardt et al., 1994; Harber et al., 1995; Morrison et al., 1994). Therefore, I changed the corresponding amino acids in NWM receptors to H80/Q for both NWM receptors and N85YP/SYS and N85YL/SYS for nCD155 and tCD155, respectively (Fig. 9, boxed residues). The cDNAs of mutant and wild type (wt) NWM CD155 receptors were then used to create stable mouse Ltk^- cell lines expressing the proteins. As indicated earlier, mouse Ltk^- cells lack a receptor for PV and only become sensitive to infection if a functional receptor is expressed or viral RNA is transfected into the cells.

Interestingly, stably transformed mouse Ltk^- cell lines expressing a nCD155 mutant (L-nCD155mt) or a tCD155 mutant (L-tCD155mt) were competent to bring about a productive infection with significant titers of PV1 in both cell lines (Fig. 10A). However, L-nCD155mt cells were still resistant to PV2 and PV3 infections (Fig. 10B and 10C). Both L-tCD155 and L-tCD155mt cells were permissive to all three serotypes. Surprisingly, they were permissive to PV2 infection (Fig. 10B), where PV2 did not either show growth or formed virus-receptor complexes on TMX cells (Fig. 4B and 7B).

Since L-nCD155mt and L-tCD155mt cells were permissive to PV infection, I performed binding assays to ascertain the amount of virus-receptor complexes on the cells. L-nCD155mt cells showed very low amount of PV1 receptor complexes at 4°C; however, there was a 3 fold increase in binding from 4°C to 25°C (Fig. 11A). Interestingly, PV1-receptor complexes were found on NZP-60 cells, whereas there were no complexes on L-nCD155 cells (Figs. 7A and 11A). PV2 and PV3 did not form complexes on either L-nCD155 or L-nCD155mt cells. Both L-tCD155 and L-tCD155mt cells exhibited a 2 to 3 fold increase in binding to PV1 after a temperature change from 4°C to 25°C, however, L-tCD155mt cells had higher amount of PV1-receptor complexes than L-tCD155 cells at either temperature (Fig. 11A). PV2 and PV3 receptor complexes were found on both L-tCD155 cells and L-tCD155mt cells with increase in complexes from 4°C to 25°C (Fig. 11B and 11C). However, there was no difference in amount of virus-receptor complexes between the tCD155 or tCD155mt receptors.

DISCUSSION

I have identified CD155 homologues (tCD155 and nCD155) to the human poliovirus receptor (hCD155) in cells of tamarin and marmoset monkeys (TMX and NZP-60), two species of the NWMs. The proposed structures of tCD155 and nCD155 that display amino acid identities of 74% and 75%, respectively, with hCD155α place these proteins into the new Ig superfamily (Fig. 3) of which hCD155 is the founding member. In general, CD155 homologues show a high degree of sequence divergence across different species. For example, hCD155α is 90% similar to AGMα1, a member of the OWMs, but only 42% to Tage4, the rodent orthologue of CD155 (Ravens et al., 2003). Yet, Tage4 also expresses Tctex-1 and the tyrosine-containing binding motif of the μ1B subunit in its C-terminal domain, and its expression in the GI tract in rodents (Ravens et al., 2003) is very similar to that of CD155 in the human GI tract (Iwasaki et al., 2002). It is tempting to speculate that members of the new CD155 Ig family, whether of human, monkey or rodent origin, perform important and related functions for their respective organisms. This function, however, does not include affinity to PV: the interaction between PV and CD155 is not to the advantage of the host and, thus, PV binding affinity is not conserved amongst all CD155 homologues or orthologues (Mueller, Wimmer, and Cello, 2005).

Unlike the OWMs, the NWMs are not susceptible to oral infection with PV. NWMs, however, can be infected by intracerebral injection but, surprisingly, this is dependent not only upon the NWM species but also upon the PV serotype. Amongst the serotypes, PV1 is clearly favored in its ability to infect the NWM cells, tamarin and brown capuchin. PV3 can also infect tamarin cells, whereas PV2 is excluded from interaction with those NWM CD155 molecules that have been tested. These include the black tailed marmoset, tamarin and brown capuchin, all members of subfamilies of the family *Cebidae* (my studies; (Ida-Hosonuma et al., 2003; Kaplan, 1955a; Kaplan, 1955b; Kaplan and Melnick, 1955)). In their study on rapid sequence changes of the *CD155* gene during evolution, Ida-Hosonuma et al. have shown that the V-domain of the brown capuchin CD155, if exchanged for the V-domain of hCD155, can serve as receptor for PV1 only, an observation not further investigated (Ida-Hosonuma et al., 2003).

Unlike TMX cells, NZP-60 cells are resistant to all three serotypes. My experiments have clearly shown that the inability of the three PV serotypes investigated

here to infect marmoset NZP-60 cells is related to the earliest step in infection: lack of ability to form virus-receptor complexes. If the cell membrane barrier is bypassed by transfection of virion RNA, replication and virus maturation occurs just as efficiently as in mouse Ltk^- cells, a highly permissive substrate for intracellular PV replication. Fittingly, on transfection of the PV-Luc replicon, the NZP-60 cells showed significant levels of translation and replication of replicon RNA.

The resistance of NZP-60 cells to PV infection cannot be explained by a lack of nCD155 expression on these cells. Flow cytometry of the NWM cells show that expression of nCD155 on NZP-60 cells under the conditions of the experiments is nearly two-fold higher than that of hCD155 on HeLa cells or tCD155 on TMX cells. Together, these data show that the block to infection of NZP-60 cells occurs at the stage of receptor binding, a conclusion supported by binding studies of PV serotypes to these cells. I could not determine whether the nCD155 protein can alter virions since the amount of virus-receptor bound complexes was very low on the NZP-60 cells.

Previous experiments have shown that the receptor-virus interaction follows biphasic kinetics ((McDermott et al., 2000) and ref. therein). The initial binding step involving an electrostatic interaction is fully reversible and temperature independent. The second step requires near physiological temperatures for an increase in "breathing" of the virion structure, thereby exposing higher affinity binding sites (McDermott et al., 2000). This additional binding leads to irreversible structural changes of the (bound) virion and is hypothesized that, in turn, results in additional contacts with the north rim of the "canyon", leading to the uncoating of the virus (He et al., 2003; Hogle, 2002; McDermott et al., 2000). My experiments reported here are in accordance with this mechanism. They show an increase in the binding of the virions when the temperature of binding is increased from 4°C to 25°C. Interestingly, increased binding, in turn, co-varies with a productive infection, regardless of the level of virus-receptor complexes. Specifically, PV1 and PV3 both showed an increase in the amount of bound virus complexes from 4°C to 25°C and a concomitant replication in TMX cells. Moreover, the amount of receptor bound complexes to PV1 was higher than that to PV3, which correlated with higher titers of PV1 in TMX cells. In contrast, PV1 showed no growth

phenotype in NZP-60 cells and there was no appreciable increase in virus-receptor complexes from 4°C to 25°C.

Since successful infection requires structural changes of the virion associated with an increase in bound complexes from 4°C to 25°C, I assessed TMX and NZP-60 cells ability to alter virion particles after binding. In support of my infection and binding data, TMX cells converted the 160S native particles to 135S particles, whereas the NZP-60 cells were deficient in binding thus unable to alter virion particles. Therefore, I made an attempt to change the amino acid composition of the V domains of tCD155 and nCD155 by mutagenesis with the aim of affecting PV1 binding. Previous studies have shown that mutation of three amino acids in hCD155 (Q80, S85 and S87) caused a loss in viral binding and replication of PV1 (Bernhardt et al., 1994; Morrison et al., 1994). By alignment of hCD155, tCD155, and nCD155, these amino acids were predicted to be involved in virion binding if engineered into the NWM CD155. Accordingly, the mutant receptors were expressed in mouse fibroblast cells (L-tCD155mt and L-nCD155mt) and their ability for virus binding and uncoating was determined.

My data showed an increase in the formation of virus-receptor complexes as well as in viral titers for both L-tCD155mt and L-nCD155mt cells with PV1. The L-nCD155mt cells were able to support PV1 infection, although the virus-receptor complexes in L-nCD155mt cells was 55 fold lower than in HeLa cells at 4°C. However, the PV1 and nCD155mt complexes increased 3 fold from 4°C to 25°C, seemingly enough to lead to a productive infection of L-nCD155mt cells. Notably, PV1 did not show any virus-receptor complexes on L-nCD155 cells but were found on NZP-60 cells. This apparent discrepancy could be due to the lack of complexes that wt nCD155 can form in marmoset cells but not in mouse cells, thus interfering with the already weak binding of the receptor to the virus in L-nCD155 cells. The mutations engineered into tCD155 did not lead to any significant changes in infection between L-tCD155 and L-tCD155mt cells. Surprisingly, both L-tCD155 and L-tCD155mt cells were susceptible to PV2 infections whereas, TMX cells are resistant to PV2 infection. On TMX cells, I did observe an eclipse followed by growth; however, there was no difference in viral titers between 0 h and 48 h. The possibility exists that the tCD155 can probably uncoat the virus, albeit very slowly as seen by the eclipse in TMX infection with PV2 (Fig. 4B). But

on TMX cells the virus may not be able to interact as efficiently with tCD155 as it does on L-tCD155 cells; thus the discrepancy between infection on both cells. However, the mutations do not confer an increase in virus-receptor complexes with either PV2 or PV3. The mutations engineered into NWM CD155 molecules were selected based on mutagenesis studies of hCD155 and binding to PV1. Therefore, the mutations may not have significance in the binding of the other two serotypes. This would lend support to the hypothesis that there are distinct binding differences between CD155 and PV serotypes. As pointed out before, I do not believe that the differences described here are strain specific rather than serotype specific. The structures of all three PV serotypes show a high degree of similarity in architecture that is necessary for morphogenesis, stability and receptor binding of the virion. The three serotypes, on the other hand, are defined by a large number of amino acid substitutions mapping over large areas of the virion (Minor et al., 1986). This leaves little room for variability with respect to strains of a given serotype

The profound differences by which the three PV serotypes bind to CD155 receptors are surprising. To be sure, the extent of virus-receptor complex formation of the PV strains to hCD155 is very similar (Belnap et al., 2000) and so are corresponding structures of the virus/receptor complexes (Bibb et al., 1994; He et al., 2003). Originally, the differences were discovered only when mutants of hCD155 were studied (Bernhardt et al., 1994; Harber et al., 1995). For example, cell line 84, containing a mutation at P84SYS/HYSA in hCD155, is deficient in binding PV1 and Sabin 1, but not Sabin 2 or Sabin 3 (Harber et al., 1995). A hybrid PV1 virus in which the neutralizing antigenic site Ia was exchanged with that of PV2, showed an increase in virus bound complexes on cell line 84 (Harber et al., 1995). Therefore, the mutation P84SYS/HYSA in hCD155 leads to loss of binding of PV1, which can be rescued by the exchange of antigenic sites on the virus surface (Harber et al., 1995).

Like with mutant hCD155 molecules, the differences are remarkable in the binding of the three PV serotypes to the NWM CD155 receptors (my studies; (Ida-Hosonuma et al., 2003)). When Ltk^- cells were transformed with a chimeric receptor of brown capuchin/hCD155, the cells were susceptible to PV1, but not to PV2 or PV3 (Ida-Hosonuma et al., 2003). Surprisingly, there is only a difference of 4 amino acids in the V

domain of the brown capuchin and marmoset CD155 (data not shown). As mentioned, the brown capuchin/hCD155 chimera is susceptible to PV1 while marmoset cells are not susceptible. The diversity of interactions between the NWM CD155 molecules and the PV serotypes has given rise to differences in serotype susceptibility of the NWM species.

Evidence has been presented previously suggesting that C-cluster coxsackie A viruses may be the progenitors of the PVs, the critical event being a switch from the ICAM-1 receptor to the CD155 receptor (Jiang et al., 2007). This raises a possibility that a hitherto hidden polio-like virus may have evolved by adapting to one or the other NWM CD155 for proliferation. Such polio-like virus may present a reservoir that may seed PVs back into the human population once poliovirus has been eradicated globally and an anti-polio vaccination has been permanently terminated, as is the current plan of the World Health Organization.

Table 1. Sequence similarities between human CD155 and tamarin, marmoset and african green monkey CD155 homologues.

Species	Amino Acid similarity (%)	Nucleic Acid similarity (%)
Human (hCD155α)	100	100
Tamarin (tCD155)	74	87
Marmoset (nCD155)	75	88
African Green Monkey (AGMα1)	90	93

Figure 1. Structure of PV genomic RNA and PV-Luc replicon **(A)** Schematic diagram of the full-length PV genome [PV1 (Mahoney)] and **(B)** of the PV-Luc replicon. The single-stranded RNA is covalently linked to the virus-encoded protein VPg at the 5'-end of the non-translated region (5'NTR). The 5'NTR consists of two *cis*-acting domains, the cloverleaf and the internal ribosomal entry site (IRES), which are separated by a spacer region. The polyprotein (open box) consists of a structural (P1) and two nonstructural coding domains (P2 and P3), specifying the capsid and replication proteins, respectively. In the replicons the P1 domain of the polyprotein is replaced with the coding sequence of the firefly luciferase gene. The cre stem-loop is the cis acting replication element mapping to the 2CATPase coding region. The 3'-terminal non-translated region consists of a 65 nt long heteropolymeric region followed by a poly(A) tail.

A

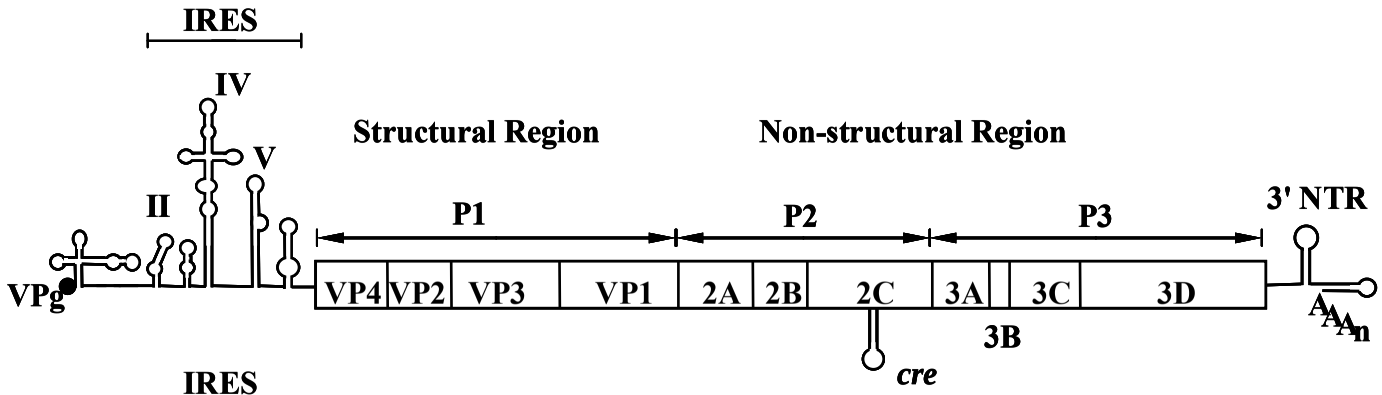
IRES
IV
V
II
VPg
Structural Region
Non-structural Region
P1
P2
P3
3' NTR
VP4
VP2
VP3
VP1
2A
2B
2C
3A
3C
3D
3B
cre
An

B

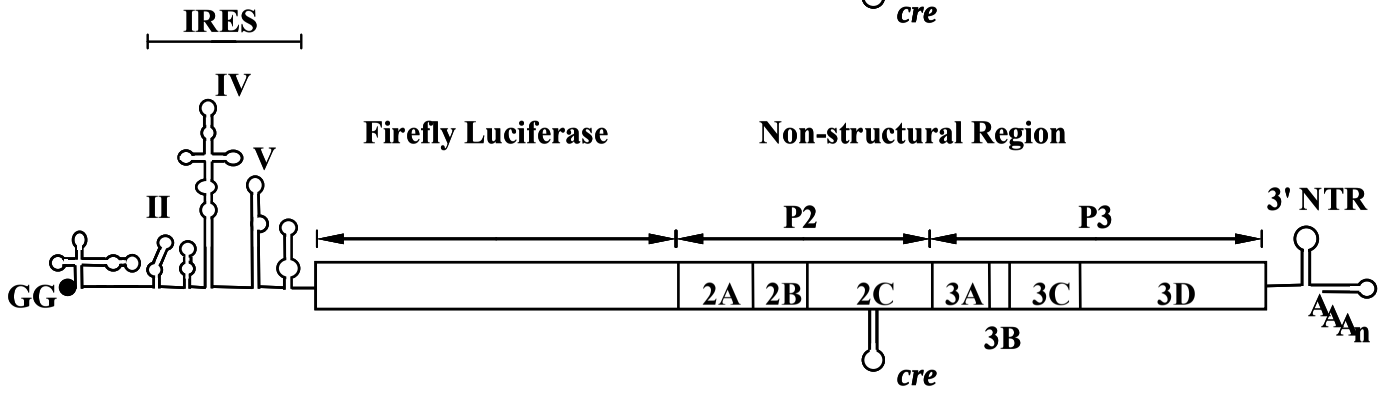
IRES
IV
V
II
GG
Firefly Luciferase
Non-structural Region
P2
P3
3' NTR
2A
2B
2C
3A
3C
3D
3B
cre
An

Figure 2. Nucleotide and deduced amino acid sequences of NWM CD155. cDNA sequences for the coding region beginning with initiator codon AUG of **(A)** tamarin CD155 (tCD155) and **(B)** marmoset CD155 (nCD155). The first and second lines depict nucleotide and deduced amino acids, respectively. Position of signal peptide *(box)*, transmembrane domain *(bold and box)*, putative N-glycosolation sites *(underlined)*, Tctex-1 *(bold)* and μ1B subunit *(bold and underlined)* are indicated.

```
atggccgccgcgtggccgctgaggcttctggctctgctggtgctgacccagtcatgcccg 60
 M  A  A  A  W  P  L  R  L  L  A  L  L  V  L  T  Q  S  C  P  20
ggaactggagacatcgtcctgaaggcgcccacccaggtgcacggcttcttgggcgactcc 120
 G  T  G  D  I  V  L  K  A  P  T  Q  V  H  G  F  L  G  D  S  40
gtgacgctgccctgccacctgaagctgcacacggaggtgacgcacgtgtcgcaggtgact 180
 V  T  L  P  C  H  L  K  L  H  T  E  V  T  H  V  S  Q  V  T  60
tggacgcggctcagtggctcacgcagcgtggccgtcttccaccatactcagggccccaac 240
 W  T  R  L  S  G  S  R  S  V  A  V  F  H  H  T  Q  G  P  N  80
tacctggagtccgaacggctggaattcgtggccgccaggctaggagcggagctgcgggat 300
 Y  L  E  S  E  R  L  E  F  V  A  A  R  L  G  A  E  L  R  D  100
gcctcgctaagggtgttcgagctgcgcgccgaggatgaaggcaactacacctgcctgttc 360
 A  S  L  R  V  F  E  L  R  A  E  D  E  G  N  Y  T  C  L  F  120
gtcatgttccctcagggcagcaggagcgccgttacctggctccgagtgttcgccaagccc 420
 V  M  F  P  Q  G  S  R  S  A  V  T  W  L  R  V  F  A  K  P  140
cagaacacagctgaggctcagaaggtccagctcaccggagagcctgtgcccgtggcccga 480
 Q  N  T  A  E  A  Q  K  V  Q  L  T  G  E  P  V  P  V  A  R  160
tgcatctccacaggggtcgcccgcctgcccgaatcacctggcactcagacctgggcggg 540
 C  I  S  T  G  G  R  P  P  A  R  I  T  W  H  S  D  L  G  G  180
atggccaatatgagccagaagccagggctcctgtctggcacagtcaccgtcaccagccac 600
 M  A  N  M  S  Q  K  P  G  L  L  S  G  T  V  T  V  T  S  H  200
tggattatggtgccctcaagccaggtggacggcaagaatgtgacctgcaaagtggagcag 660
 W  I  M  V  P  S  S  Q  V  D  G  K  N  V  T  C  K  V  E  Q  220
gagagcttcgagacgcctcagctgctggctgtgaacctcaccgtgtactatcccccagag 720
 E  S  F  E  T  P  Q  L  L  A  V  N  L  T  V  Y  Y  P  P  E  240
gtatccatttctggctatgatggcaactggtacctcggccagcctgaggccagcctgacc 780
 V  S  I  S  G  Y  D  G  N  W  Y  L  G  Q  P  E  A  S  L  T  260
tgtgatgctcgcagcaacccagagcccacaggctatgagtggagcacgaccatgggtcct 840
 C  D  A  R  S  N  P  E  P  T  G  Y  E  W  S  T  T  M  G  P  280
ctgccaccctctgctgtggcccagggcgcccagctgctcatccgtcctgtagacaagtca 900
 L  P  P  S  A  V  A  Q  G  A  Q  L  L  I  R  P  V  D  K  S  300
atcaacacgactttcatctgcaatgtcaccagttccctaggagctcgccaggcagaactg 960
 I  N  T  T  F  I  C  N  V  T  S  S  L  G  A  R  Q  A  E  L  320
actgtccaggtcaaagagggacctcccagtgaaccccaggcatgtcctggagcgtcatc 1020
 T  V  Q  V  K  E  G  P  P  S  E  P  P  G  M  S  W  S  V  I  340
Gtcgtcccgattctgggaatcctggctgttctggccatgctggggtgtgggctttatttc 1080
 V  V  P  I  L  G  I  L  A  V  L  A  M  L  G  C  G  L  Y  F  360
tatcagtccagatgttcccgtccgacggctgccagaacctcggttaataggcccgtctcc 1140
 Y  Q  S  R  C  S  R  P  T  A  A  R  T  S  V  N  R  P  V  S  380
tatgcacctgtggccaactcttcctag 1167
 Y  A  P  V  A  N  S  S  -  388
```

Figure 2. Nucleotide and deduced amino acid sequences of NWM CD155. cDNA sequences for the coding region beginning with initiator codon AUG of **(A)** tamarin CD155 (tCD155) and **(B)** marmoset CD155 (nCD155). The first and second lines depict nucleotide and deduced amino acids, respectively. Position of signal peptide *(box)*, transmembrane domain *(bold and box)*, putative N-glycosolation sites *(underlined)*, Tctex-1 *(bold)* and μ1B subunit *(bold and underlined)* are indicated.

```
atggccgccgcgtggccgctgctgctgctgctggctctgctggtgctgtcccagtcacgc 60
 M  A  A  A  W  P  L  L  L  L  L  A  L  L  V  L  S  Q  S  R  20
ccgggaaccgaagacatcgtcctgaaggcgcccacccaggtgcacggcttcttgggcgac 120
 P  G  T  E  D  I  V  L  K  A  P  T  Q  V  H  G  F  L  G  D  40
tccgtgacgctgccctgccacctgcagctgcccagcacagaggtgacgcacgtgtcgcag 180
 S  V  T  L  P  C  H  L  Q  L  P  S  T  E  V  T  H  V  S  Q  60
ctgacttggacgcggctcagtgactcacgcagcgtggccgtcttccaccatactcagggc 240
 L  T  W  T  R  L  S  D  S  R  S  V  A  V  F  H  H  T  Q  G  80
cccaactacccggagtccgaacggctggaattcgtggccgccagactaggggcggaactg 300
 P  N  Y  P  E  S  E  R  L  E  F  V  A  A  R  L  G  A  E  L  100
cgggatgcctcgctgagggtgttcgagctgcgcgccgaggatgaaggcaactacacctgc 360
 R  D  A  S  L  R  V  F  E  L  R  A  E  D  E  G  N  Y  T  C  120
ctgttcgtcatgttcccccagggcagcaggagcgcggttacctggctccgagtgttcgcc 420
 L  F  V  M  F  P  Q  G  S  R  S  A  V  T  W  L  R  V  F  A  140
aagccccaaaacacagctgaggctcagaaggtccagctcaccggagagcctgtgcccgtg 480
 K  P  Q  N  T  A  E  A  Q  K  V  Q  L  T  G  E  P  V  P  V  160
gcccgatgtgtctccacagagggtcgcccgcctgcccgaatcacctggcactcagacctg 540
 A  R  C  V  S  T  E  G  R  P  P  A  R  I  T  W  H  S  D  L  180
ggcgggatggccaatacgagccaggagccagggctcctgtctggcacagtcactgtcacc 600
 G  G  M  A  N  T  S  Q  E  P  G  L  L  S  G  T  V  T  V  T  200
agcctctggattttggtgccctcaagccaggtggatggcaagaatgtgacctgcaaagtg 660
 S  L  W  I  L  V  P  S  S  Q  V  D  G  K  N  V  T  C  K  V  220
gagcaggagagcttcgagacgcctcagctgctggctgtgaacctcaccgtgtactatccc 720
 E  Q  E  S  F  E  T  P  Q  L  L  A  V  N  L  T  V  Y  Y  P  240
ccagaggtatccatttctggctatgatggcaactggtacctcggccagactgaggccagc 780
 P  E  V  S  I  S  G  Y  D  G  N  W  Y  L  G  Q  T  E  A  S  260
ctgacctgcgatgctcgcagcaacccagagcccacaggctatgagtggagcacgaccatg 840
 L  T  C  D  A  R  S  N  P  E  P  T  G  Y  E  W  S  T  T  M  280
ggtcctctgccaccctctgctatggcccagggcgcccagctcctcatccatcctgtggac 900
 G  P  L  P  P  S  A  M  A  Q  G  A  Q  L  L  I  H  P  V  D  300
aagttaatcaacacgactttcatctgcaacgtcaccagtgccctaggagctcgccaggca 960
 K  L  I  N  T  T  F  I  C  N  V  T  S  A  L  G  A  R  Q  A  320
gaactgactgtccaggtcaaagagggacctcccagtgaacccccaggcatgtccaggaac 1020
 E  L  T  V  Q  V  K  E  G  P  P  S  E  P  P  G  M  S  R  N  340
aacatcctcctgattctgggacccctgggggttgttctggccctgctgggagttgggctt 1080
 N  I  L  L  I  L  G  P  L  G  V  V  L  A  L  L  G  V  G  L  360
tatttctgttggtccagatgttcccgtccgacagctgccagcacctcggttaataggccc 1140
 Y  F  C  W  S  R  C  S  R  P  T  A  A  S  T  S  V  N  R  P  380
gtctcctatgcgcctgtggccaactctttcgaggatccacagacaaagggcacaaggtga 1200
 V  S  Y  A  P  V  A  N  S  F  E  D  P  Q  T  K  G  T  R  -  399
```

Figure 3. The predicted structure of CD155 homologues. Schematic diagram of the CD155 structures of human (hCD155α), AGM CD155 (AGMα1), tamarin (tCD155), and marmoset (nCD155). Three extracellular immunoglobulin-like domains (*circles*) are formed by disulfide bonds. The transmembrane domain and the C-terminus are shown with binding domains for Tctex-1 *(empty box*) and μ1B subunit *(shaded box)*. The predicted N-glycosolation sites are shown on immunoglobulin domains (*squares*), as well as the number of amino acids that compose each domain. hCD155 is produced in four different splice variants (α, β, γ, δ) that differ in the presence of the transmembrane domain and the length of the C-terminal domain. AGM CD155 occurs in two splice variants AGMα1 and AGMδ1, and AGMα2 is encoded by a second gene.

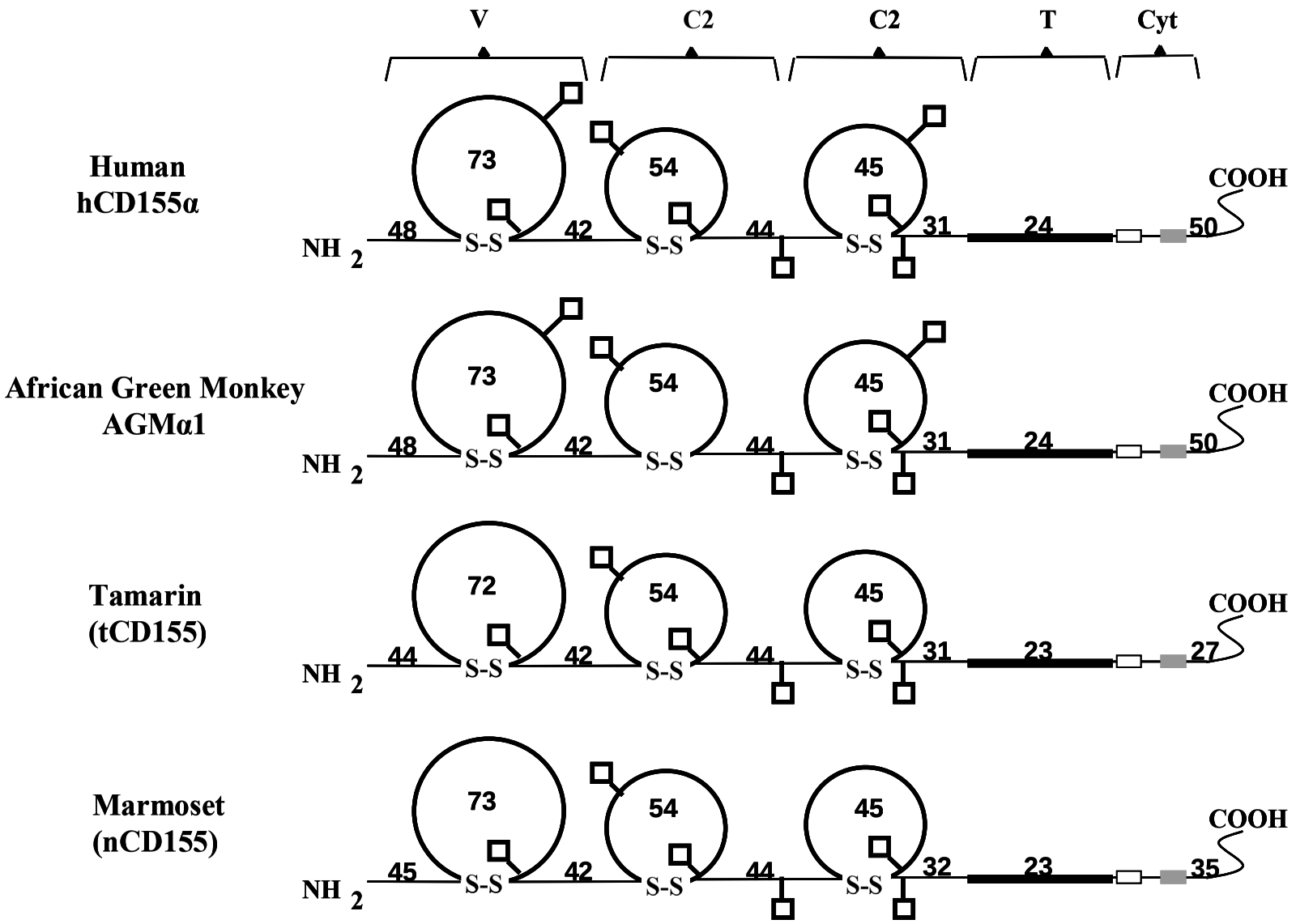
V
C2
C2
T
Cyt
Human
hCD155α
African Green Monkey
AGMα1
Tamarin
(tCD155)
Marmoset
(nCD155)
NH 2
COOH
S-S
73
54
45
72
48
42
44
31
24
50
23
27
45
32
35

Figure 4. One step growth curves of PV serotypes on various cell lines. One-step growth curve in mouse (Ltk-), human (HeLa), marmoset (NZP-60) and tamarin (TMX) cells were carried out as described in Materials and Methods. **(A)** PV1, **(B)** PV2, and **(C)** PV3. Each point represents the mean of virus titers from three experiments.

A

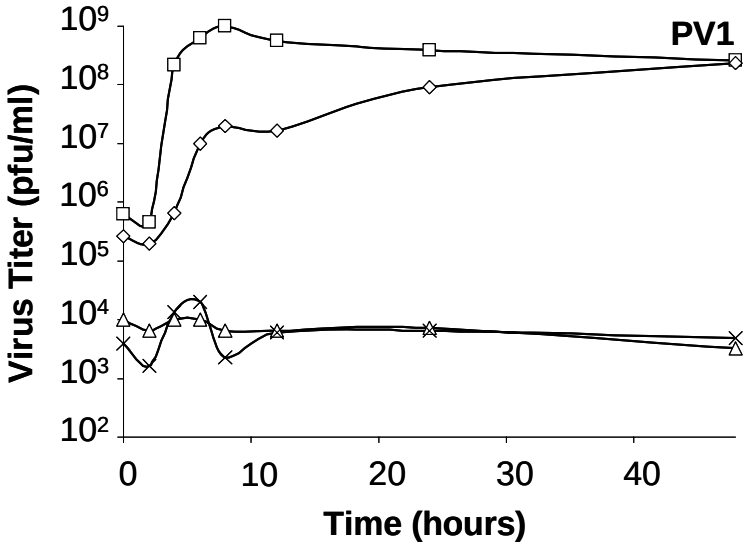
PV1
Virus Titer (pfu/ml)
10^9
10^8
10^7
10^6
10^5
10^4
10^3
10^2
0
10
20
30
40
Time (hours)

B

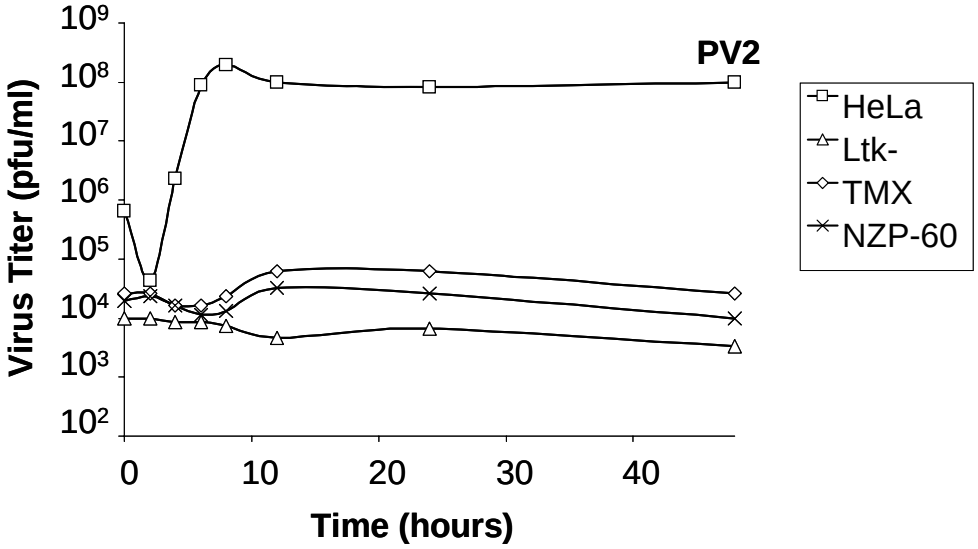
PV2
Virus Titer (pfu/ml)
10^9
10^8
10^7
10^6
10^5
10^4
10^3
10^2
0
10
20
30
40
Time (hours)
HeLa
Ltk-
TMX
NZP-60

C

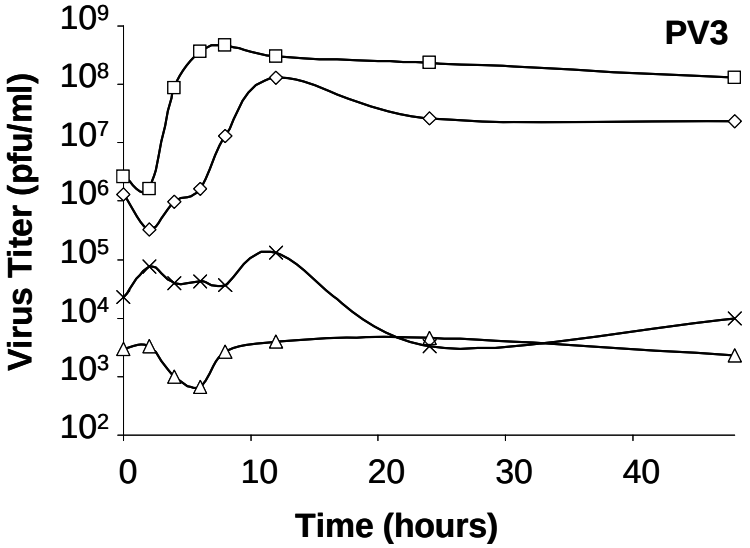
PV3
Virus Titer (pfu/ml)
10^9
10^8
10^7
10^6
10^5
10^4
10^3
10^2
0
10
20
30
40
Time (hours)

Figure 5. Translation and Replication of PV RNA and PV-Luc replicon in different cell lines. **(A)** Virus titers of PV1(Mahoney), PV2 (Lansing) and PV3 (Leon) in marmoset (NZP-60), tamarin (TMX) and mouse (Ltk-) cells after transfection of PV1 RNA as described in Materials and Methods. **(B)** Firefly luciferase activity of PV-Luc replicons. Transfection of PV-Luc replicon RNAs into various cell lines, with or without 2mM GnHCl, and the measurement of luciferase activity are described in Materials and Methods.

A

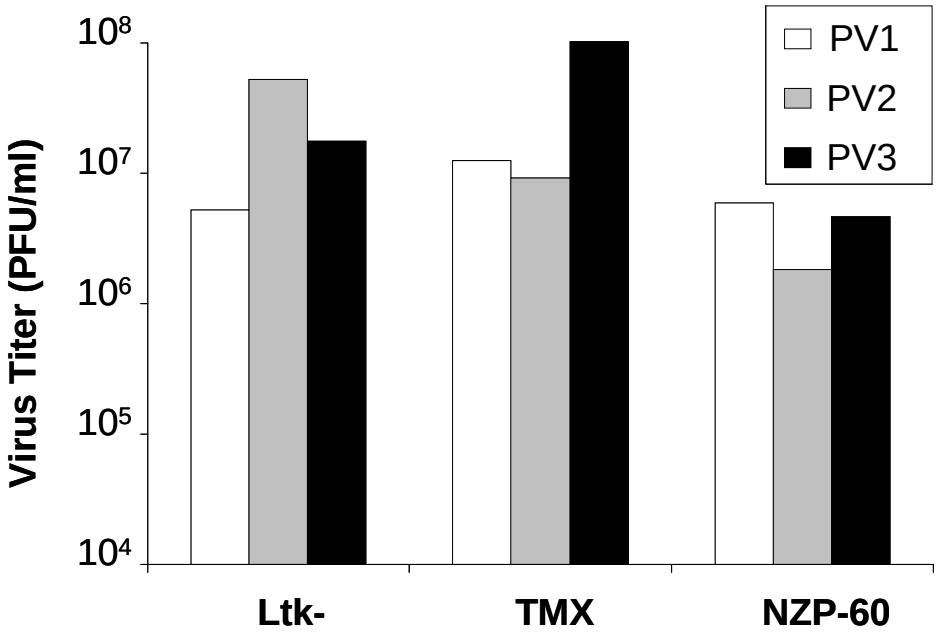
Virus Titer (PFU/ml)
10^8
10^7
10^6
10^5
10^4
PV1
PV2
PV3
Ltk-
TMX
NZP-60

B

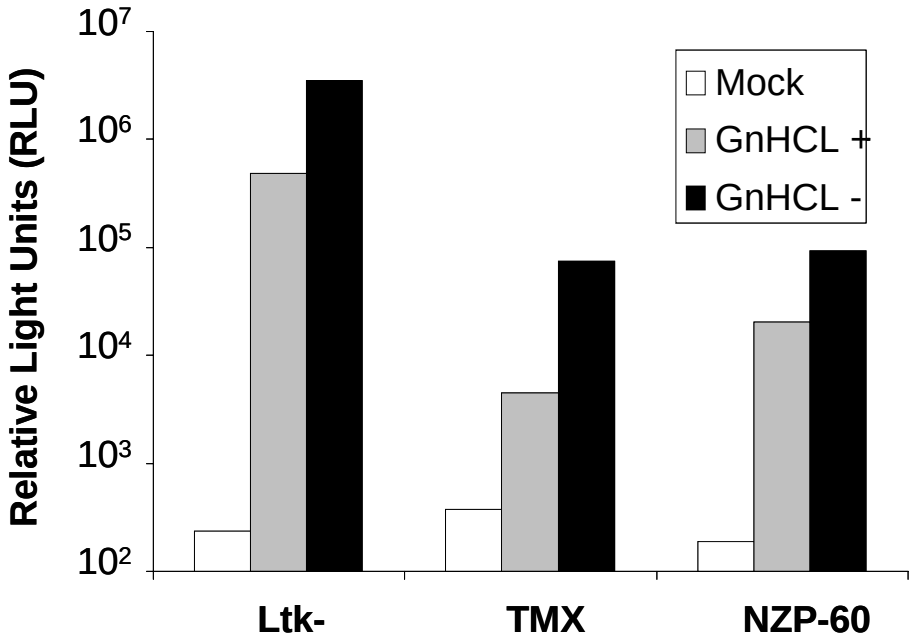
Relative Light Units (RLU)
10^7
10^6
10^5
10^4
10^3
10^2
Mock
GnHCL +
GnHCL -
Ltk-
TMX
NZP-60

Figure 6. Analysis of the expression levels of CD155 on cell surface by flow cytometry. The CD155 expression levels on the surface of human (HeLa), mouse (Ltk-), tamarin (TMX), and marmoset (NZP-60) cell lines was determined by flow cytometry using mAb p286 and secondary Ab anti-mouse FITC, as described in Materials and Methods. The data is expressed in arbitrary units.

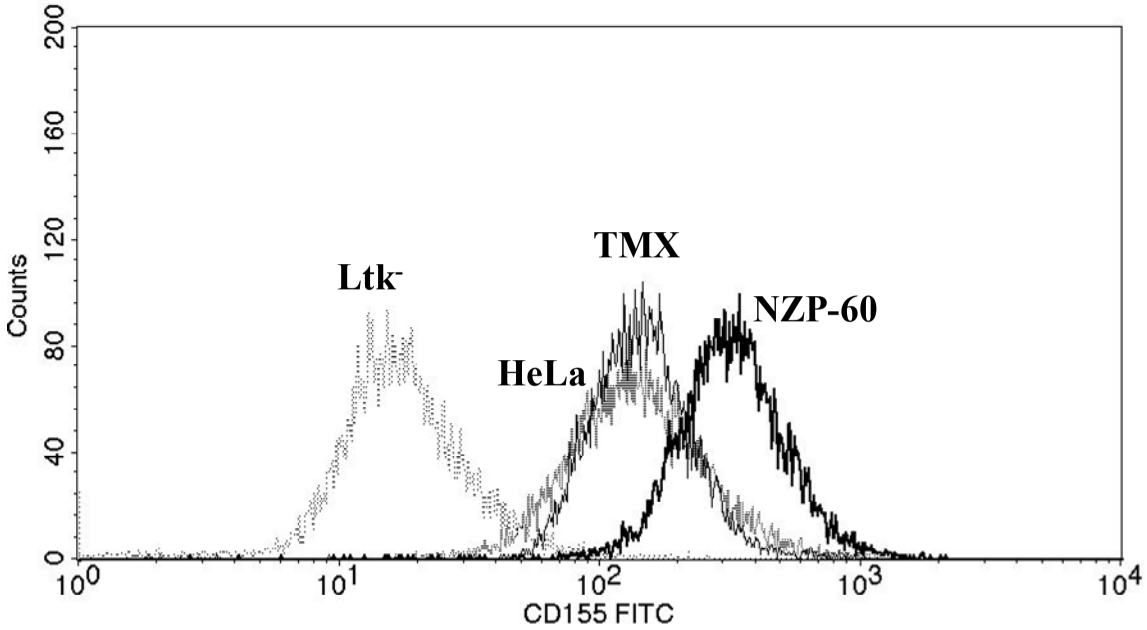

	Ltk-	HeLa	TMX	NZP-60
Mean Fluorescence *	27.92	155.92	159.07	332.71

*Mean fluorescence was determined by counting 10^6 cells.

Figure 7. Binding assay of PV strains to various cell lines. The binding of 108 PFU [35S] labeled **(A)** PV1, **(B)** PV2, and **(C)** PV3 to 106 cells of human (HeLa), tamarin (TMX), marmoset (NZP-60) and mouse (Ltk-) was measured as described in Materials and Methods. The values are an average of three experiments.

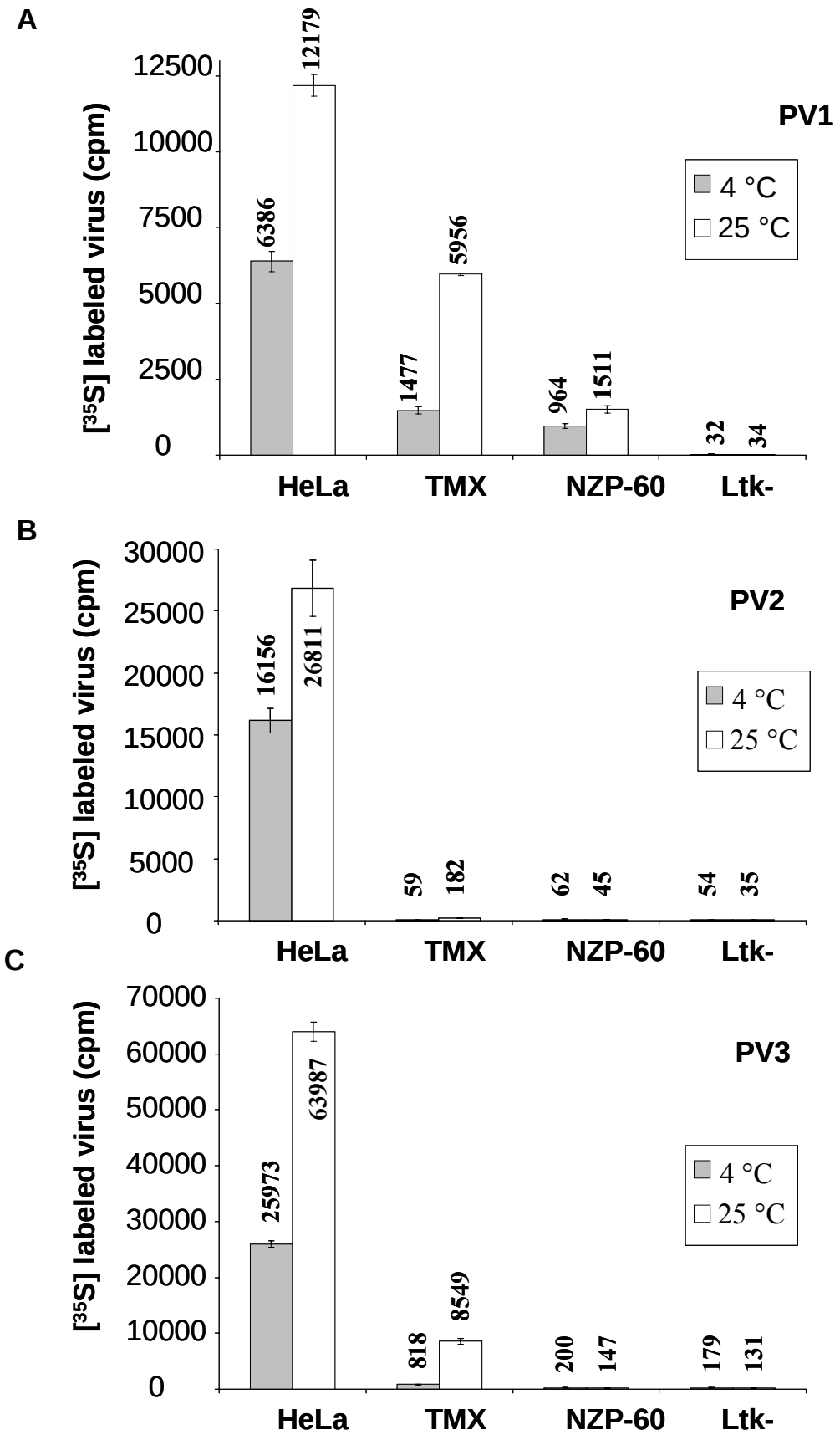
A
PV1
[35S] labeled virus (cpm)
12500
10000
7500
5000
2500
0
6386
12179
1477
5956
964
1511
32
34
4 °C
25 °C
HeLa
TMX
NZP-60
Ltk-
B
PV2
[35S] labeled virus (cpm)
30000
25000
20000
15000
10000
5000
0
16156
26811
59
182
62
45
54
35
4 °C
25 °C
HeLa
TMX
NZP-60
Ltk-
C
PV3
[35S] labeled virus (cpm)
70000
60000
50000
40000
30000
20000
10000
0
25973
63987
818
8549
200
147
179
131
4 °C
25 °C
HeLa
TMX
NZP-60
Ltk-

Figure 8. Sucrose density gradient fractionation of extracts of [35S] methionine-labeled infected cells. Purified native virions were attached to the cells at 25°C and incubated at 37°C for 45 min before lysis. The lysates were laid on a sucrose gradient and the gradients were fractionated from the bottom. Unheated and heated labeled virions were used as controls.

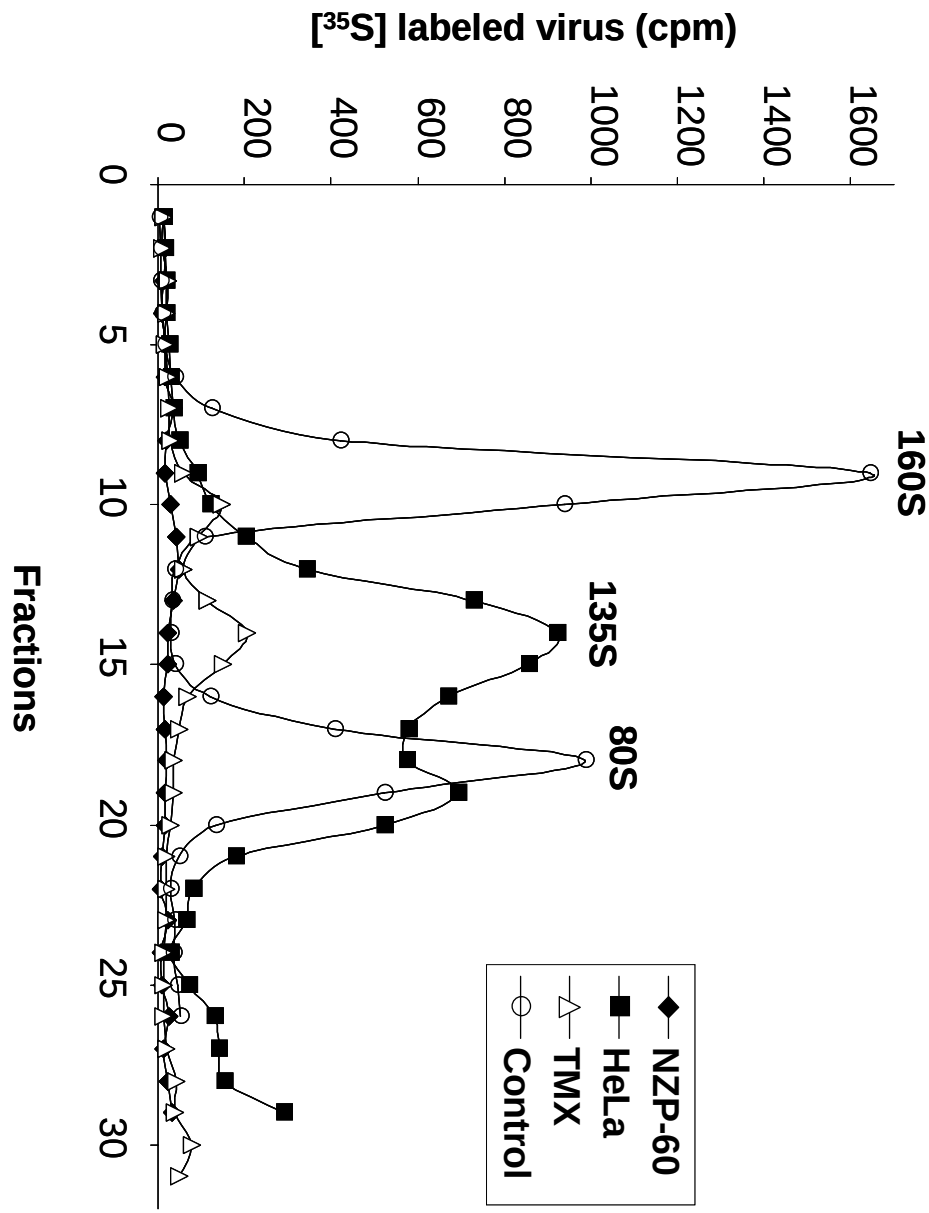
[35S] labeled virus (cpm)
1600
1400
1200
1000
800
600
400
200
0
0
5
10
15
20
25
30
Fractions
160S
135S
80S
NZP-60
HeLa
TMX
Control

Figure 9. Amino acid alignment of the V domain of CD155 homologues. Amino acid alignment of the V domains of human (hCD155), African green monkey (AGMα1 and AGMα2), tamarin (tCD155) and marmoset (nCD155) proteins. Residues identified for binding all three PV strains are shown in bold, residues identified in binding two serotypes are shown in shaded bold, and residues identified binding in only one serotype are shown in grey. The arrows indicate the β-strands of the V domain. Residues implicated in binding to PV by previous mutational analyses are marked with an X (Bernhardt et. al. 1994; Harber et. al. 1995) and a + (Aoki et al., 1994; Colston and Racaniello, 1994; Liao and Racaniello, 1997; Morrison et al., 1994). in the lines above the residue numbers. The boxed residues donate amino acids mutated for this study. The numbering of amino acids corresponds to V domains of hCD155 (Figure modified from He et. al. 2003).

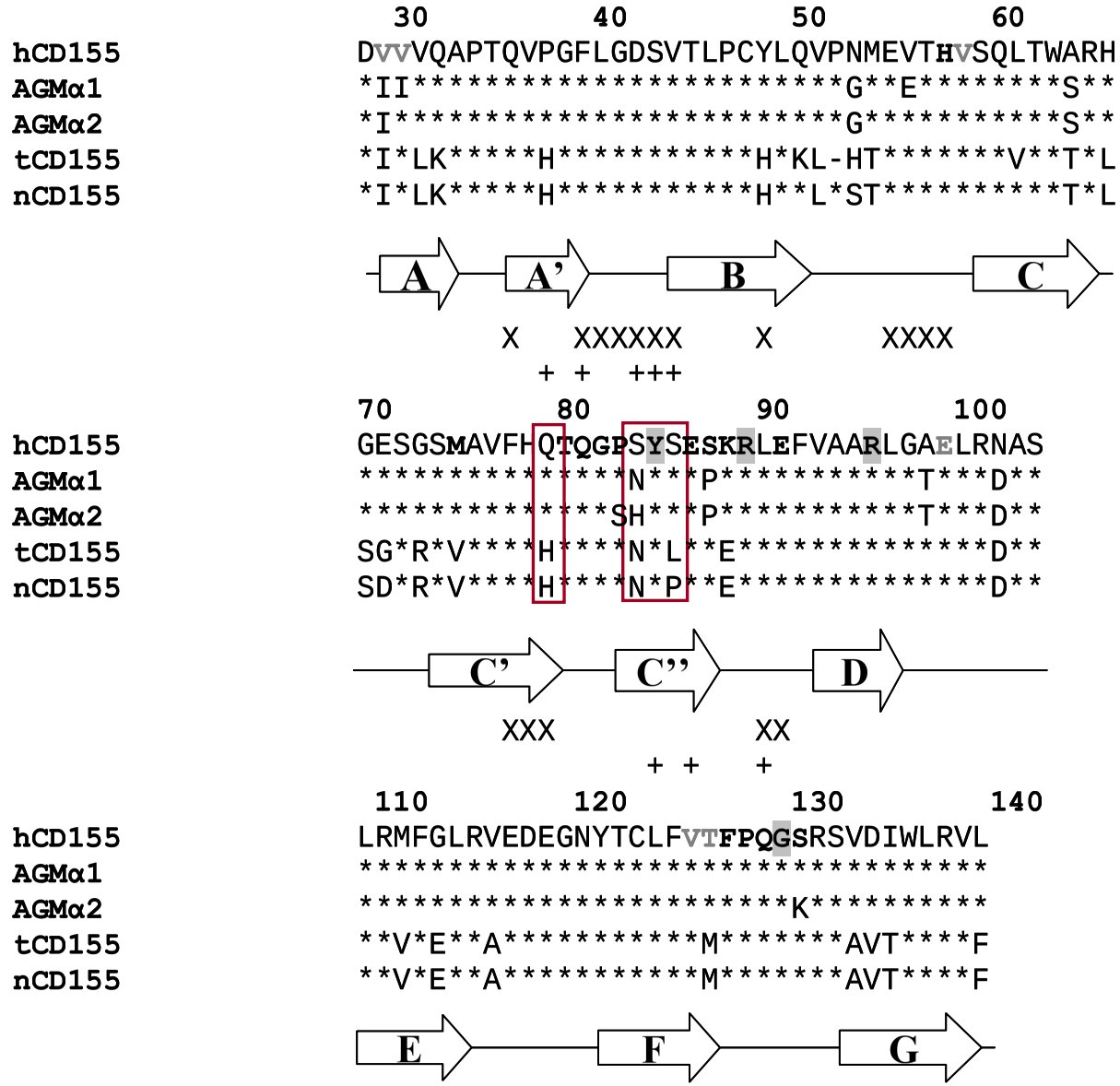
30 40 50 60
hCD155 DVVVQAPTQVPGFLGDSVTLPCYLQVPNMEVTHVSQLTWARH
AGMα1 *II**********G**E*******S**
AGMα2 *I**********G**********S**
tCD155 *I*LK*****H**********H*KL-HT******V**T*L
nCD155 *I*LK*****H**********H**L*ST**********T*L
A A' B C
X XXXXXX X XXXX
+ + +++
70 80 90 100
hCD155 GESGSMAVFHQTQGPSYSESKRLEFVAARLGAELRNAS
AGMα1 **********N***P**********T***D**
AGMα2 **********SH***P**********T***D**
tCD155 SG*R*V****H****N*L**E**********D**
nCD155 SD*R*V****H****N*P**E**********D**
C' C'' D
XXX XX
+ + +
110 120 130 140
hCD155 LRMFGLRVEDEGNYTCLFVTFPQGSRSVDIWLRVL
AGMα1 **********
AGMα2 **********K**********
tCD155 **V*E**A**********M******AVT****F
nCD155 **V*E**A**********M******AVT****F
E F G

Figure 10. Infection of stably transfected Ltk- cell lines with PV serotypes. Viral titers of PV serotypes growing in Ltk- cells stably expressing human CD155 (L-hCD155), marmoset CD155 (L-nCD155), mutant nCD155 (L-nCD155mt), tamarin CD155 (L-tCD155) and mutant tCD155 (L-tCD155mt) was determined at 0 h and 48 h. **(A)** PV1 **(B)** PV2 **(C)** PV3.

A

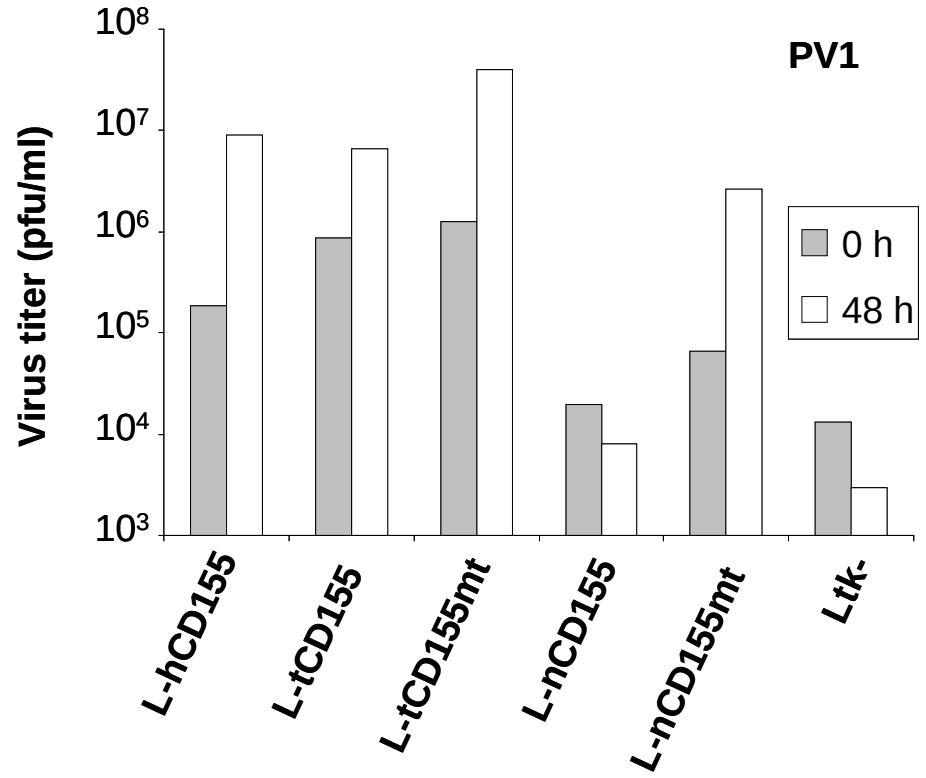
PV1
Virus titer (pfu/ml)
10^8
10^7
10^6
10^5
10^4
10^3
0 h
48 h
L-hCD155
L-tCD155
L-tCD155mt
L-nCD155
L-nCD155mt
Ltk-

B

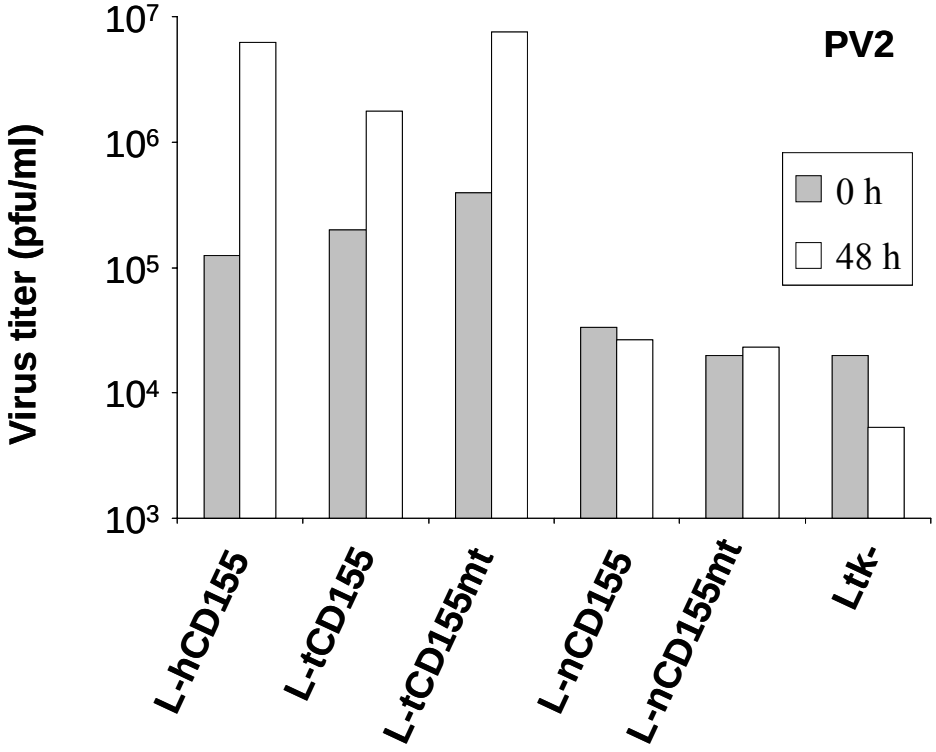
PV2
Virus titer (pfu/ml)
10^7
10^6
10^5
10^4
10^3
0 h
48 h
L-hCD155
L-tCD155
L-tCD155mt
L-nCD155
L-nCD155mt
Ltk-

Figure 10. Infection of stably transfected Ltk- cell lines with PV serotypes. Viral titers of PV serotypes growing in Ltk- cells stably expressing human CD155 (L-hCD155), marmoset CD155 (L-nCD155), mutant nCD155 (L-nCD155mt), tamarin CD155 (L-tCD155) and mutant tCD155 (L-tCD155mt) was determined at 0 h and 48 h. **(A)** PV1 **(B)** PV2 **(C)** PV3.

C

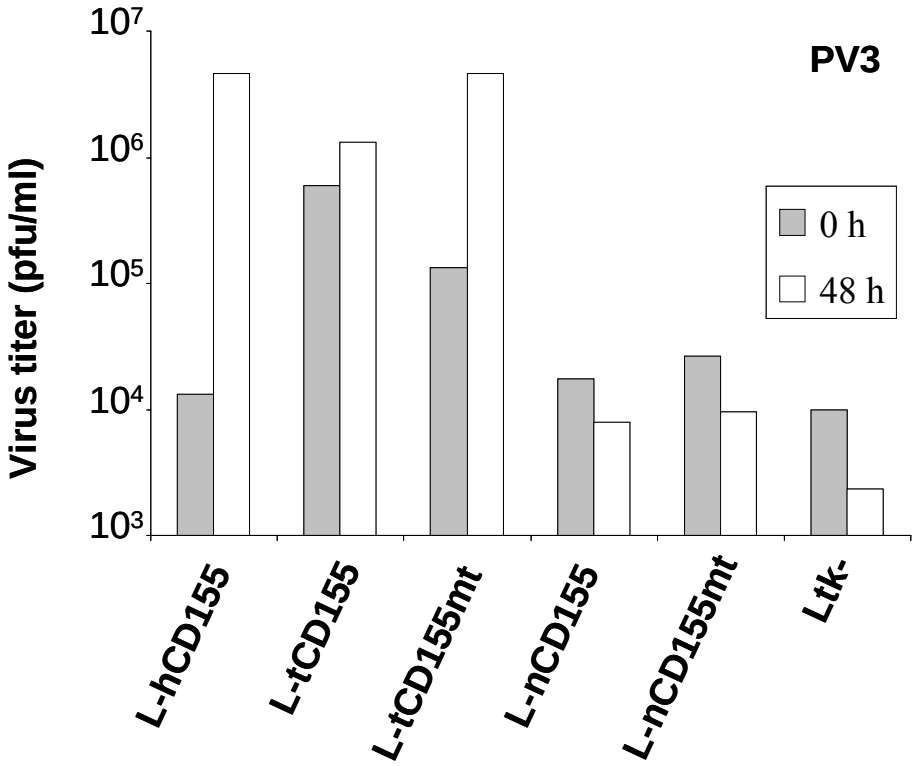
PV3
Virus titer (pfu/ml)
10^7
10^6
10^5
10^4
10^3
0 h
48 h
L-hCD155
L-tCD155
L-tCD155mt
L-nCD155
L-nCD155mt
Ltk-

Figure 11. Virus binding assay on stably transfected Ltk- cell lines. The binding of [35S] labeled virus was measured on Ltk- cells stably expressing human CD155 (L-hCD155), marmoset CD155 (L-nCD155), mutant nCD155 (L-nCD155mt), tamarin CD155 (L-tCD155) and mutant tCD155 (L-tCD155mt) as described in Materials and Methods. **(A)** PV1 **(B)** PV2 **(C)** PV3.

A

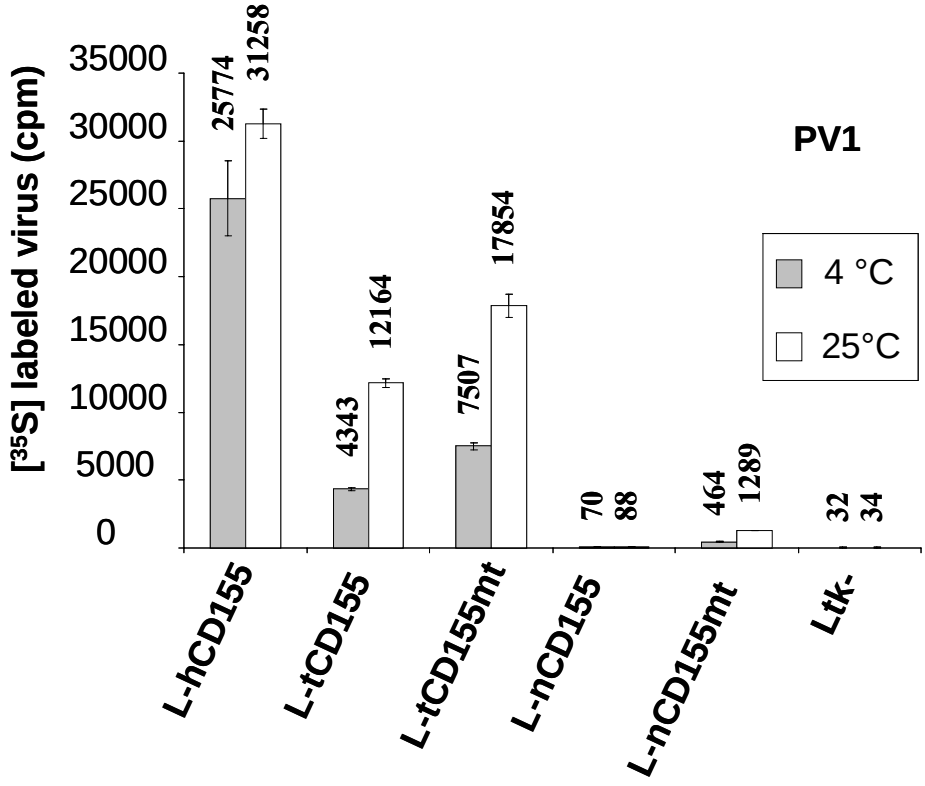
PV1
[35S] labeled virus (cpm)
35000
30000
25000
20000
15000
10000
5000
0
25774
31258
4343
12164
7507
17854
70
88
464
1289
32
34
4 °C
25°C
L-hCD155
L-tCD155
L-tCD155mt
L-nCD155
L-nCD155mt
Ltk-

B

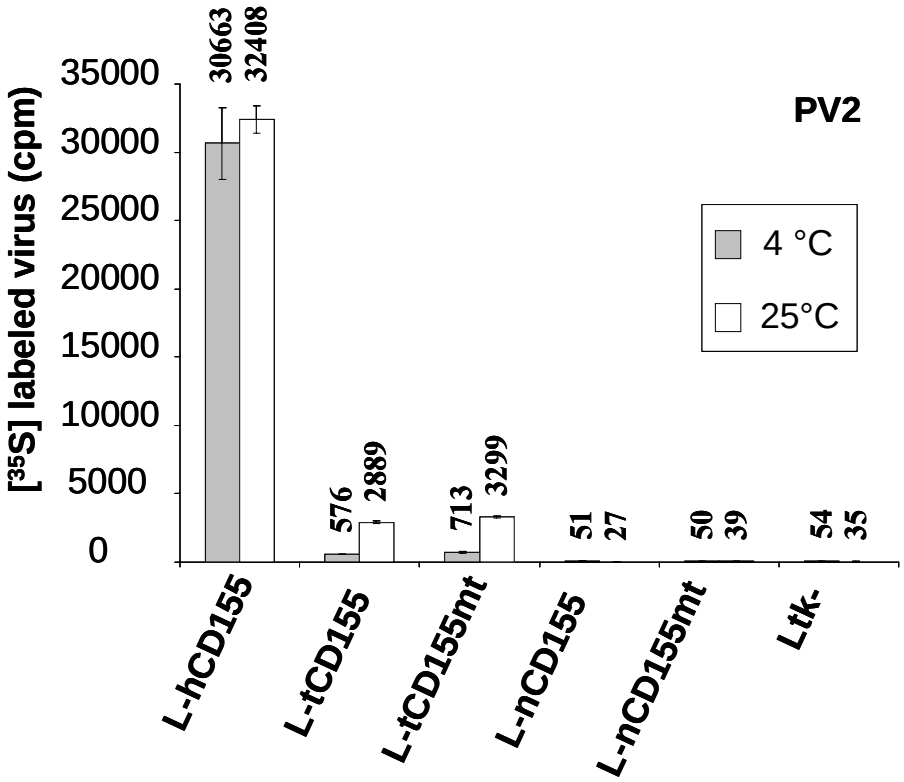
PV2
[35S] labeled virus (cpm)
35000
30000
25000
20000
15000
10000
5000
0
30663
32408
576
2889
713
3299
51
27
50
39
54
35
4 °C
25°C
L-hCD155
L-tCD155
L-tCD155mt
L-nCD155
L-nCD155mt
Ltk-

Figure 11. Virus binding assay on stably transfected Ltk- cell lines. The binding of [35S] labeled virus was measured on Ltk- cells stably expressing human CD155 (L-hCD155), marmoset CD155 (L-nCD155), mutant nCD155 (L-nCD155mt), tamarin CD155 (L-tCD155) and mutant tCD155 (L-tCD155mt) as described in Materials and Methods. **(A)** PV1 **(B)** PV2 **(C)** PV3.

C

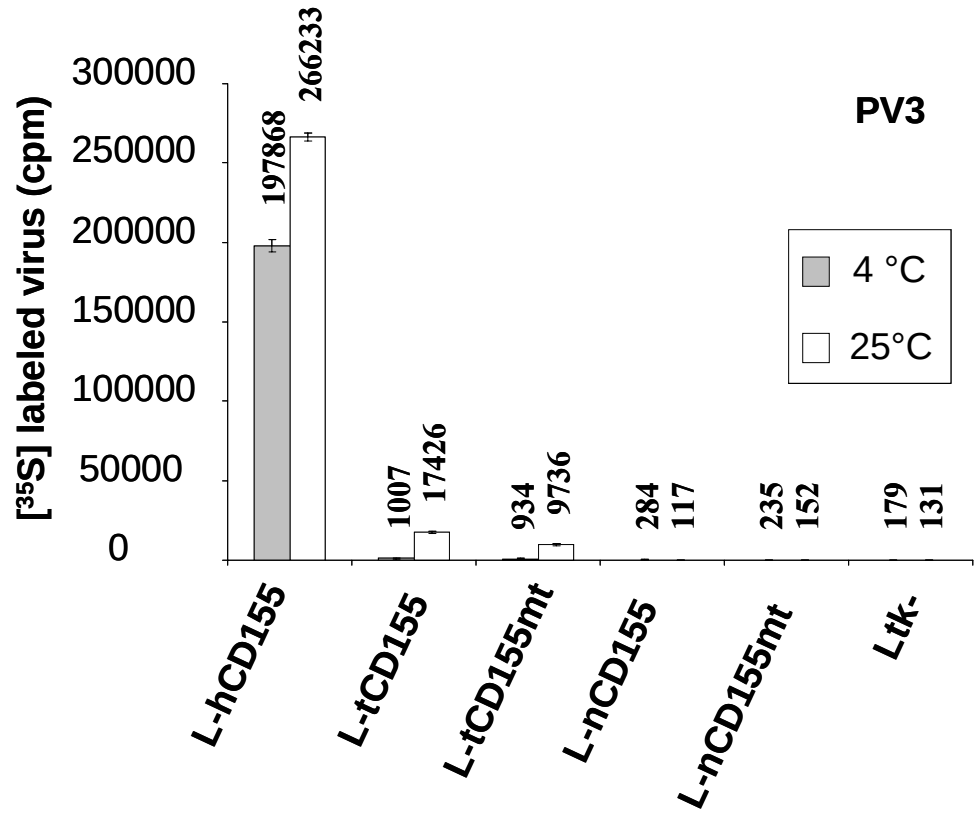
PV3
[35S] labeled virus (cpm)
300000
250000
200000
150000
100000
50000
0
197868
266233
1007
17426
934
9736
284
117
235
152
179
131
4 °C
25°C
L-hCD155
L-tCD155
L-tCD155mt
L-nCD155
L-nCD155mt
Ltk-

Chapter III

Transgenic mouse expressing human CD155 under the control of the murine CD155 promoter as a model for oral pathogenesis of poliovirus

Background

The molecular mechanisms by which poliovirus (PV) causes a neurological disease, poliomyelitis, are poorly understood. This lack of knowledge is not surprising considering the multitude of events preceding the viral disease that include entry into the host, primary sites of replication, spread through the host, cell and tissue tropism, secondary sites of replication, cell injury, immune response, and clearance (Tyler and Fields, 1990). Our understanding of these events is limited to entry of the virus by ingestion and the clearance of infection by predominantly humoral immune response. All other stages in PV pathogenesis remain largely obscure (Minor, 1997) despite the fact that PV is one of the most thoroughly investigated viruses of all times.

PV discovered nearly 100 years ago (Landsteiner and Popper, 1909), is an RNA virus belonging to the genus *Enterovirus* of the family *Picornaviridae*. This family includes a large number of human pathogens, such as coxsackie B viruses, enterovirus 71, parechoviruses, and hepatitis A virus, all of which can cause severe and even life threatening diseases. Poliovirus causes a neurological disease known as poliomyelitis, which leads to destruction of motor neurons and eventually to paralysis of the limbs and in some cases even death. Together all human picornaviruses cause up to six billion human infections each year.

In order to understand the mechanisms by which PV causes disease, various animal models have been developed. In 1908, Landsteiner and Popper intraperitoneally injected a monkey with a suspension of spinal cord tissue obtained from a child who had died from complications stemming from a paralytic disease (Landsteiner and Popper, 1909). The infected monkeys developed symptoms and histopathology similar to humans affected with poliomyelitis, thus the first animal model of PV was established. In addition to non-human primate models, non-transgenic (tg) mice have also been used to study poliomyelitis. Certain PV serotype 2 strains have been shown to cause neurological disease in non-tg mice, when virus was inoculated via an intracerebral (i.c.) route. However, histopathological analysis of the infected mice showed that the virus affected all neuronal cell populations without discrimination, whereas in primates and humans, the neurological damage is restricted to spinal cord motor neurons (Gromeier, Lu, and Wimmer, 1995). The lack of tissue tropism, limitation of infections by certain

strains and most importantly infection by only i.c. route eliminates the non-tg mouse model for the study of poliovirus pathogenesis. The discovery of the PV receptor, CD155 (Mendelsohn, Wimmer, and Racaniello, 1989), eventually led to the generation of tg mice. These mice are susceptible to infection by parenteral routes and show neuronal histopathology similar to primates. However, none of these mice are sensitive to oral infection (Crotty et al., 2002; Ida-Hosonuma et al., 2002; Koike et al., 1991; Ren et al., 1990; Yanagiya et al., 2003; Zhang and Racaniello, 1997), with the exception of a tg mouse recently generated that, in addition to expressing of the human CD155 receptor, also lacks the alpha/beta interferon receptor (Ida-Hosonuma et al., 2005; Ohka et al., 2007).

The host range of PV, restricted to humans and primates, is primarily determined by the cellular receptor, CD155 (also known as PVR) (for the designation of CD155, see (Freistadt and Eberle, 1997)). So far, CD155 is the only cell surface protein known to serve as a PV receptor. It is a highly glycosylated 80 kDa type Ia single-pass transmembrane protein belonging to the Ig (Immunoglobulin) superfamily (Bernhardt et al., 1994; Bibb, Bernhardt, and Wimmer, 1994; Koike et al., 1990; Mendelsohn, Wimmer, and Racaniello, 1989; Wimmer et al., 1994). The isolation and characterization of human CD155 (hCD155) (Koike et al., 1990; Mendelsohn, Wimmer, and Racaniello, 1989; Wimmer et al., 1994) enabled the construction of the first CD155 tg mice. These mice were generated by expressing human CD155 under the control of the human CD155 promoter (Koike et al., 1991; Ren et al., 1990). However, these mice were resistant to oral infection which is the primary route of infection in humans. The inability of these mice to be infected orally was hypothesized to be due to a difference in expression of CD155 in the tissues of the alimentary tract of murine and humans (Iwasaki et al., 2002; Koike, Aoki, and Nomoto, 1994). CD155 is expressed in gut-associated lymphoid tissues (GALT), specifically on human follicle associated epithelium (FAE), microfold (M) cells and in germinal centers (GC) of the Peyer's patches (PP) (Iwasaki et al., 2002). TgPVR21 mice, a strain of the CD155 tg mouse generated by Koike et al. (Koike et al., 1991), do not express CD155 on any cells in the alimentary tract. The lack of receptor on the cells of the alimentary tract, the site of virus entry, explains the insusceptibility of these mice to oral infection. There were several attempts to express CD155 in the

alimentary tract by expressing CD155 under the control of diverse promoters, such as the β-actin promoter, intestinal fatty acid binding protein (IFABP) promoter, specific for intestinal enterocytes, and finally the nectin-2 promoter, which was wrongly assumed to be a CD155 homologue (Crotty et al., 2002; Ida-Hosonuma et al., 2002; Yanagiya et al., 2003; Zhang and Racaniello, 1997). Unfortunately none of these attempts were able to yield a mouse model that was sensitive to oral infection. Interestingly, an innate immune response in virus pathogenesis was observed. When TgPVR21 mice were backcrossed with interferon alpha/beta receptor knockout mice (TgPVR21/*ifnar* KO), they were now susceptible to oral infection (Ida-Hosonuma et al., 2005; Ohka et al., 2007). In primates and TgPVR21 mice, virus replication has been restricted to small intestine and CNS tissues, whereas in TgPVR21/*ifnar* KO mice virus is isolated from all tissues. Lack of tissue tropism makes these mice a poor model for the study of early events in poliovirus pathogenesis.

To overcome the lack of expression of CD155 in the GALT, I expressed CD155 under the control of the promoter of a mouse orthologue of CD155 (mCD155). mCD155 (also known as Tage4) was discovered as a prominent cell surface protein expressed in rat colon and mammary carcinoma cells and later identified in mice as well (Chadeneau, LeMoullac, and Denis, 1994; Ravens et al., 2003). mCD155 and hCD155 have a conserved gene structure and both localize to the syngeneic chromosome in mice (Baury et al., 2001). Although mCD155 shares only 42% amino acid similarity with human hCD155, all critical protein domains are conserved in both proteins, such as the Tctex-1 binding motif, and the tyrosine containing binding motif of the μ1B subunit within the cytoplasmic tail. Both mCD155 and hCD155 lack self-adhesion and heterophilically *trans*-interact with nectin-3, a member of the nectin family, and vitronectin (Ikeda et al., 2003; Mueller and Wimmer, 2003; Ravens et al., 2003). hCD155/mCD155 expression on certain target cells can also stimulate cytotoxic activity by natural killer cells by interaction with DNAM-1 (CD226) and CD96 on NK cells (Bottino et al., 2003; Fuchs et al., 2004; Seth et al., 2007). Most importantly, hCD155 and mCD155, respectively, are expressed in the alimentary tract of humans and mice in a similar pattern (Iwasaki et al., 2002; Ravens et al., 2003). They are expressed on enterocytes, the FAE, M cells and in the GCs of the PPs.

The aim of these studies was to generate a new transgenic mouse model (mCD155tg) in which CD155 is expressed in the alimentary tract. I was successful in expressing CD155 in the alimentary tract but only 3 week old or younger mice were susceptible to oral infection. After oral inoculation, viral replication was detected in the upper small intestine followed by onset of viremia and finally replication in brain and spinal cord. The course of pathogenesis of the virus from replication in small intestine followed by onset of viremia and lastly CNS complications mirrors pathogenesis of humans and non-human primates. Thus I have successfully generated an oral mouse model of poliomyelitis.

Materials and Methods

Cells and Viruses. HeLa R19 and mouse Ltk$^-$ cells were maintained in Dulbecco's modified Eagle's medium (DMEM) containing 10% fetal bovine serum (FBS) and 1% penicillin/streptomycin.

The virulent PV1 (Mahoney) strain was grown on HeLa R19 cells and was employed in this study.

Plasmid construction. The mCD155 promoter was amplified from clone CAAA01210663 (Ravens et al., 2003) by PCR using forward primer (5' CACCTAAGGCT AGCCCAAACTCTCTCAC 3') and reverse primer (5' GAGCCATAAGCTTCCGGTCCG ATCCAG 3'). The underlined positions denote NheI and HindIII restriction sites introduced for ease of cloning. Using NheI and HindIII restriction sites, the 2.5 kb mCD155 promoter was cloned into the multiple cloning site of pGL3-Basic, a promoter-less Luciferase expression vector (clone 1-1). Clone 1-1 was treated with XbaI and HindIII to generate a 914 bp promoter fragment and with BglII and HindIII to generate a 406 bp fragment. The promoter fragments were then ligated into the pGL3-Basic using NheI and HindIII for the 914 bp fragment and BglII and HindIII for 406 bp fragment to generate clone 1-2 and clone 1-3, respectively. As a positive control for luciferase activity, the cytomegalovirus (CMV) promoter was also cloned into pGL3-Basic vector, giving rise to pGL3-CMV.

Cosmid generation. The 800 bp sequence containing Exon 1 of the CD155 gene using the forward primer (5' AGCAAAGCTTATGGCCCGAGCCATGG 3') and the reverse primer (5' GGTCAGAGGGGTTCTAGAGTCAAGTGTC 3') was amplified

from pTL-HC5 (Koike et al., 1990), where underlined sequences denote HindIII and XbaI cleavage sites. The PCR product and clone 1-1 were treated with HindIII and XbaI and the products were ligated giving rise to clone 1-3, containing mCD155 promoter and Exon 1 of CD155. Site Directed mutagenesis was then used to restore the mCD155 sequence upstream of ATG, in process destroying the HindIII site introduced to ligate the mCD155 promoter and the Exon 1 of CD155 gene (clone 1-4). The primers for the Site Directed mutagenesis were Sense primer (5' TGGATCGGACCGGAACCACATGGCCCGAGCCATG 3') and Antisense primer (5' CATGGCTCGGGCCATGTGGTTCCGGTCCGATCCA 3'). Through PCR the mCD155 promoter and Exon 1 of CD155 fragment was amplified using the forward primer (5' CTTACGGATCCTAGCCCAAACTCTC 3') and the reverse primer (5' CTGCTAGCTTATGGCCTGGGTATG 3'). The underlined sequences represent BamHI and NheI restriction sites. The PCR product was then inserted into SuperCos-1 vector (clone 2-1). Clone 2-1 was constructed by ligating SuperCOS1 vector treated with BamHI and XbaI and PCR product with BamHI and NheI. Clone 3-1 was constructed by cutting the cos sequence of the SuperCOS-1 vector with BamHI and XbaI, which then was ligated into the pCDNA 3.1(+) vector.

A PinAI/ApaI digested clone 2-1 (including the mCD155 promoter and exon 1), a AgeI/NheI digested pTL-HC5 (containing the CD155 structural gene), and the NheI/SphI digested clone 3-1 (containing the cos sequence) were ligated and packaged by using Gigapack® III XL Packaging Extract (Stratagene). *Escherichia coli* JM109 cells were infected with the phage particles carrying the cosmid clone of mhCD155 fusion gene.

Transfection of plasmids into Ltk$^-$ cells. Mouse Ltk$^-$ cells were transfected using Lipofectamine™ (Invitrogen). The transfection procedure was followed as described by the manufacturer. In brief, 1 µg of plasmid was diluted in 100 µl of Opti-MEM® (Invitrogen). In another tube, 6 µl of Lipofectamine™ was diluted to 100 µl of Opti-MEM®. Both tubes were mixed and incubated at room temperature for 30 min. After incubation, 800 µl of Opti-MEM® was added to the tubes to bring the final volume to 1 ml. Ltk$^-$ cells in a 35 mm dish, that were approximately 70% confluent, were washed once with Phosphate buffered saline (PBS) and then the Lipofectamine™ solution was

added to the cells. The cells were incubated for 6 hours at 37° C, after which time the medium was removed and replaced with fresh medium and 10% FBS.

Luciferase activity. All transfected cells were harvested 36 h after transfection. The cells were washed gently with 2 ml of PBS and lysed with 300 μl of "passive" lysis buffer (Promega). 50 μl of luciferase assay reagent (Promega) was mixed with 20 μl of lysate, and the firefly luciferase activity was measured with an Optocomp I luminometer (MGM Instruments, Inc.).

Virus growth. Cell monolayers (1 x 10^6 cells) were incubated with 10 multiplicity of infection (MOI) of virus for 30 min at room temperature on a rocker platform. After 30 min, cells were washed three times with PBS and incubated at 37°C in DMEM containing 2% bovine calf serum (BCS). The cells were harvested at 0 h and 24 h post infection. The plates were subjected to three consecutive freeze-thaw cycles, and the viral titers of the supernatants were determined by plaque assay on HeLa cell monolayers, as previously described (Pincus et al., 1986).

Analysis of CD155 isoforms. The L-mhCD155 cells, Ltk^- cells transfected with fusion cosmid mhCD155, were assayed for their ability to express *CD155* isoforms. The total RNA was purified by TRIZOL reagent (Invitrogen) and RT-PCR was carried out by the SuperScript™ II First-Strand Synthesis System for RT-PCR (Invitrogen). The cDNA was then amplified by forward primer (5' TCCTGTGGACAAACCAATCAACAC 3') and reverse primer (5' GAGGCGCTGGCATGCTCTGT 3') as described by Baury et al. (Baury et al., 2003) (Fig. 5A). As mentioned previously, the splicing sites of *CD155* isoforms differ in Exon 6, giving rise to two membrane associated proteins, *CD155*α and *CD155*δ, and two secreted isoforms, *CD155*β and *CD155*γ. The primers are designed to correspond to sequences in exon 5 and exon 7, thus I can determine the expression of three isoforms, *CD155*α, *CD155*β and *CD155*γ. Since *CD155*δ terminates in intron 6 it cannot be amplified using these primers.

Generation of transgenic mice. The mhCD155 cosmid was linearized with NotI to remove all exogenous bacterial vector sequences (Fig. 6). The linearized DNA was introduced into pronuclei of Taconic ICR mouse zygotes. Mice were screened for the transgene by PCR to amplify ca. 600 bp within the intron 5 and exon 6 with forward primer (5' CTTGTCTCTGCTTTTCGTTA 3') and reverse primer (5'

CAGCACAGAGCCCGTAG TAG 3'). As a result, one line of transgenic mice, mCD155tg, was established. The transgenic line was maintained in the heterozygous stage.

TgPVR21 mice (Koike et al., 1991) were maintained at homozygous stage. Taconic ICR mouse line was used as a control.

All mice used had been maintained under specific-pathogen-free conditions and were treated in strict compliance with guidelines established by the Stony Brook University.

Western Blot Analysis. The brain, spinal cord, liver and small intestine from tg mice and non-tg mice were homogenized in a motor driven homogenizer with solution A (250 mM sucrose, 1mM EDTA [pH 7.2], 20 mM Tris-HCl [pH 7.5], and COMPLETE™ protease inhibitor cocktail tablet [Roche]) to prepare 10% emulsions. The crude extracts were centrifuged at 43,000 rpm for 2 h at 4°C in a Beckman TLA-100.3 rotor, and the pellet was suspended in solution A containing 1% Nonident P-40 at 4°C for 1 h. This suspension was centrifuged again at 43,000 rpm for 2 h at 4°C as described above. The amount of protein in the supernatant was estimated by using the Bio-Rad protein assay kit. 50 μg of protein was run on a 12.5% polyacrylamide gel in a buffer containing 0.1% sodium dodecyl sulfate (SDS) and then transferred onto a Nitrocellulose membrane. The membrane was probed first with rabbit anti-CD155 polyclonal antibody (Iwasaki et al., 2002) and then with Alexa Fluor 680 goat anti-rabbit IgG (Invitrogen), and visualized by using SuperSignal® West Pico Chemiluminescent Substrate (Pierce) in accordance with the manufacturer's instruction.

Immunostaining of cells. The plasmids were transfected into the mouse Ltk^- cells by the Lipofectamine™ procedure as described above. After a 36 h incubation period cells were fixed and incubated with primary mouse monoclonal antibody 18.1, specific for *CD155*. The cells were subsequently incubated with secondary horse reddish peroxidase (HRP) antibody and developed with the Vector® VIP substrate kit (Vector Labs, California) and visualized under the microscope.

Multiple-color immunofluorescence staining of tissues. To examine the distribution of CD155 expression, frozen sections of the small intestine, Peyer's patches (PP), and kidney were stained using CD155 and CD23 antibodies by a procedure similar

to that described by (Iwasaki and Kelsall, 2000) with minor modifications. In brief, 6–8-μm frozen tissue sections on glass slides were fixed in cold acetone and blocked with TNB buffer (NEN Life Science Products) containing 5% normal donkey serum. The sections were further treated with the avidin/biotin kit (Vector Laboratories) to block endogenous biotin. Endogenous peroxidase activity was quenched with 1% H_2O_2 for 10 min, and purified polyclonal rabbit antiserum CD155 (Iwasaki et al., 2002) was added for 1.5 h at room temperature. Slides were washed and incubated with biotin conjugated donkey $F(ab')^2$ anti–rabbit IgG (Jackson Immunoresearch Laboratories) for 30 min, followed by incubation with streptavidin–horseradish peroxidase conjugate (Zymed Laboratories). The antigens were detected with either tetramethylrhodamine-tyramide or fluorescein isothiocyanate–tyramide (NEN Life Science Products), according to manufacturer's instructions. In the case of double-labeling on the same section, the sections were treated with 2% H_2O_2 for 10 min, followed by blocking with avidin-biotin and incubation with 100 mg/ml mouse IgG (Sigma-Aldrich) for 20 min and, finally, with F(ab')2 goat antimouse IgG (Jackson Immunoresearch Laboratories) for 20 min. The second primary antibody anti-CD23 (eBioscience) was then added to the sections for 1.5 h. At the end of the staining, slides were washed and incubated with 4',6-diamidino-2 phenylindole (DAPI) for nuclear staining (Molecular Probes). Slides were mounted with Fluoromount G (Southern Biotechnology Associates) and were analyzed with a Leitz Orthoplan 2 fluorescence microscope or by confocal microscopy with a Zeiss LSM510 confocal microscope.

Administration of PV. Intramuscular (i.m.) administration was carried out as 100 μl injections into the thigh of the right hind leg using 27 ½ gauge syringe. Intraperitoneal (i.p.) administrations were done as 100 μl injections using an Insulin syringe. Before intracerebral (i.c.) administrations were carried out, animals were anaesthesized with a solution of Ketamine (10 mg/ml) and xylazine (0.2 mg/ml) in saline. i.c. injections were administered as 30 μl injections into the mid-brain using a 27 ½ gauge syringe. Intravenous (i.v.) inoculations administrations were done as 100 μl tail vein injections using a 27 ½ gauge syringe after warming the mice for 20 min under a heating lamp.

In 1 week old mice, 100 µl of virus was administered orally by depositing the inoculum into the mouth using a gavage needle. In 3 week old mice, the virus was administered orally using a water bottle. The mice were given 4 ml of virus solution in DMEM within 24 h using the water bottle. The time point for starting the administration was taken as time zero. For administration of viral titers in excess of 6 X 10^9 PFU, the virus was administered in two doses of equal amount over two days.

All mice were observed and scored twice daily for at least 28 days for signs or symptoms of disease: abnormal gait, lethargy, ruffled fur, arched back, paresia, flaccid paralysis and death (Cello, Paul, and Wimmer, 2002; Gromeier and Wimmer, 1998). In parallel, I also infected TgPVR21 mice. I determined mouse lethal dose 50% (LD_{50}) for all routes of infection by the method of Reed and Muench (Cello, Paul, and Wimmer, 2002).

Recovery of virus from tissues. For determination of the titer of virus in the tissues, the mice inoculated with the virus were anesthetized and whole blood was recovered from the right ventricle. Immediately, the mice were perfused with saline through the left ventricle, and the tissues were excised. The tissues were homogenized in DMEM to prepare 10% emulsions. The 10% emulsions were freeze-thawed three times. The homogenates were centrifuged to remove any debris, and the supernatant containing the virus was subjected to a plaque assay as described previously (Pincus et al., 1986).

The feces were collected on the day of tissue harvest. For every volume of feces, 10 volumes of PBS and 1 volume of chloroform was added. The solution was mixed by vortex, and debris was pelleted at 1800 g for 10 min in a Sorvall® SL-50T rotor. The supernatant was collected and virus titers were determined by plaque assay (Pincus et al., 1986).

Results

Characterization of the mCD155 promoter. I first examined the mCD155 promoters' ability to induce luciferase expression in the promoter-less vector, pGL3-Basic. On transfection of the vector containing mCD155 promoter into Ltk^- cells, I saw an increase in the luciferase activity comparable to the vector containing the CMV promoter (Fig. 1B). In Ltk^- cells, the mCD155 promoter (2500 bp) showed more than a 10-fold higher relative luciferase activity than the promoter-less pGL3-Basic vector (Fig.

1B). Subsequently, insertion of the 914 bp and 406 bp fragments of mCD155 promoter (Fig. 1A) also showed more than 10-fold higher relative luciferase activity than the pGL3-Basic vector (Fig. 1B). The ability of the mCD155 fragments to drive luciferase expression in the promoter-less vector indicates that there is promoter activity in these fragments.

Characterization of L-mhCD155 cell line. The fusion cosmid, mhCD155 (mCD155 promoter and hCD155 structural gene), was transfected into Ltk^- cells to determine cosmids ability to express CD155 and its isoforms. The expression of CD155 on the surface of L-mhCD155 cells was assessed by immunostaining. CD155 expression was observed on L-mhCD155 cells (Fig. 2B). The cells were also susceptible to PV1 infection (Fig. 3).

Generation of CD155 isoforms was confirmed in the L-mhCD155 cells by RT-PCR. I detected CD155α, CD155β and CD155γ bands similar to as observed in HeLa cells (Fig. 4B). These results indicate that hCD155 is expressed under the control of mCD155 promoter and isoforms of hCD155 are generated.

Generation of mCD155tg mice. To generate a mouse model that can be infected orally, it is essential to have a similar expression profile of CD155 in tissues in mice as is observed in humans. The CD155 tg mouse lines constructed so far have not shown CD155 expression profiles similar to that of humans. These CD155 tg mouse lines have used different promoters to express the CD155 gene or its isoforms (Crotty et al., 2002; Koike et al., 1991; Ren et al., 1990; Yanagiya et al., 2003; Zhang and Racaniello, 1997). Even though these tg mouse lines were not susceptible to oral infection, they have been beneficial in outlining the course of the disease after viremia.

Because the mouse orthologue of hCD155, mCD155 has an expression profile similar to humans (Baury et al., 2001; Ravens et al., 2003), we constructed a fusion gene cosmid containing a mCD155 promoter and the human CD155 coding region in order to generate a tg mouse, which has a CD155 protein distribution similar to mCD155. The generation of the fusion gene is described in Materials and Methods and a schematic diagram is illustrated in Fig. 5. This fusion gene carries a 2.5 kbp upstream sequence of mCD155 and a 30 kbp sequence of the CD155 coding region. The new tg line is referred to as mCD155tg.

Detection of CD155 in tissues by Western blotting. I examined the expression of CD155 in the brain, kidney, liver and small intestine by Western blot analysis (Fig. 7). A ca. 70kDa band was observed in the brain, while slightly higher bands were observed in the kidney and the liver samples (Fig. 6). The molecular mass of membrane bound hCD155, α and δ, are calculated to be 45 and 43 kDa, respectively (Koike et al., 1990). However, there are eight potential N-glycosolation sites in the extracellular domain of CD155, and depending on the degree of glycosolation they migrate to positions of molecular masses of 70 to 80 kDa. This is also true for mCD155. In previous studies, higher molecular weight forms in tissues have been seen, such as in the liver of MPVRTg25 mice, constructed with nectin-2 promoter and hCD155 structural gene (Yanagiya et al., 2003). The expression of CD155 in the small intestine was too low to be detected by western blot. Surprisingly, Bernhardt group also was not able to detect mCD155 expression of the small intestine in mice by western blot, however, Maier et. al. can detect mCD155 expression by flow cytometry and immunostaining of the cells in small intestine (Maier et al., 2007; Ravens et al., 2003).

Expression of CD155 in the GALT of tg mice. To detect CD155 expression in the small intestine using immunofluorescence, I stained PP's of 6 week old mice. The tissue was also stained with CD23 antibodies to detect naïve B cells and follicular dendritic cells (FDC). The naïve B cells are usually found in the light zone of the GC's and in the subepithelial dome (SED) where they co-localize with FDC. In the PP's of the 6 week old mice, I detected staining for CD155 in the tunica muscularis and the GALT (Fig. 7B). The expression profile of CD155 in tg mice is slightly different then detected for CD155 and mCD155 in humans and mice, respectively (Iwasaki et al., 2002; Ravens et al., 2003). In humans and mice, strong expression was seen in the GC's and on the enterocytes (Iwasaki et al., 2002; Ravens et al., 2003). Here I do not see expression of the receptor on the enterocytes and very weak expression in the GC, however, stronger expression is seen in SED and in the interfollicular T cell regions.

The expression of CD155 in the kidney of the mCD155tg mice was similar to that of TgPVR21 mice, the receptor was only expressed in the glomeruli of the kidney (Fig. 7D, (Iwasaki et al., 2002)).

Susceptibility of mCD155 tg mice to PV infection by parenteral routes. I tested the ability of the mice to be infected by i.c, i.m, i.v, and i.p routes. The mice were susceptible to infection by all parenteral routes (Table 1). The mCD155tg mice were at least ten fold more susceptible to poliomyelitis with i.c infection than with other routes. For i.m infection, paralysis was consistently seen initially in the leg that was inoculated. All routes of infection eventually led to paralysis and death as observed previously with the TgPVR21 mice (Koike, Aoki, and Nomoto, 1994).

Comparatively, mCD155tg mice were more susceptible to infection then the TgPVR21 mice. The mCD155tg mice were 1000 fold more susceptible to infection by i.p., 100 fold more susceptible by i.v., and 10 fold more susceptible by i.m. route than TgPVR21 (Table 1).

Oral susceptibility of the mCD155 tg mice to PV. Next, I determined susceptibility to oral infection. To eliminate the possibility that the gastric tube might damage epithelia in the esophagus, the virus was administered via a water bottle. 6 week old mice were found to be insensitive to oral infection; however, the 3 week old or younger mice were susceptible to oral infection (Table 2). Interestingly, there was no difference in susceptibility by oral infection in 1 week old mCD155tg and TgPVR21 mice (Table 2). These mCD155tg mice showed the same signs of paralysis as seen in adult mice (Fig. 8) and I was always able to isolate virus from the brain of the infected mice (data not shown), so the cause of paralysis is specific to poliovirus infection. Unlike mice younger than 3 weeks old, I was only able to obtain 100% lethal dose for 3 week old mCD155tg mice but not the TgPVR21 mice (Table 2). When 8 X 10^9 pfu of virus was administered, 100% of the mCD155tg mice showed paralysis and died within 8 days, while 20% of the TgPVR21 mice died (Fig. 9).

Time course of PV replication in tissues after oral infection. To assess the ability of PV to replicate in different tissues after oral administration, the titers of the virus in the feces, upper small intestine, lower small intestine, blood, spinal cord and brain were determined at 1, 2, 3, and 4 days after administration of first dose of virus (Fig. 11). The mice were inoculated with 8 X 10^9 pfu of virus in the course of two days.

The viral titers detected in the upper small intestine of mCD155tg mice were higher than those in TgPVR21 mice after administration of inoculum (Fig. 10A).

However, there was no appreciable difference in viral titers between mCD155tg and TgPVR21 mice in the lower small intestine during the course of the study (Fig. 10B). The virus initially appeared in the blood on the third day (Fig. 10C). The time of detection for virus in the blood corresponded with appearance of the virus in the brain (Fig. 10D). However, virus was not detected in the spinal cord until the fourth day (Fig. 10E). The viral titers in the feces were higher during first 2 days of infection, corresponding to administration of inoculum, however, the titers decreased in both mice after day 2 (Fig. 10F). Appearance of high titers of virus in feces of both tg mice on days 1 and 2 indicate that the mice were successfully inoculated orally.

The data indicates that the mCD155tg mice express CD155 in the alimentary tract and are more sensitive to infection by parenteral routes than previously generated TgPVR21 mice. In addition, 3 weeks old or younger mCD155tg mice are susceptible to oral infection and follow a course of disease similar to as observed in humans and non-human primates.

Discussion

One of the hurdles of successful eradication of poliovirus has been the ability of oral poliovirus vaccines (OPV) to recombine with enteroviruses, giving arise to circulating vaccine-derived PVs (cVDPV), which have led to recent outbreaks in areas free of wt PV (2007; Kew et al., 2005). Coupled with OPV's tendency for recombination and identification of immuno-deficient persons that can secrete virus for years without symptoms has severely undermined global eradication strategy. Therefore, a new strategy is needed to limit cVDPV from taking off and causing renewed outbreaks of poliomyelitis (Mueller, Wimmer, and Cello, 2005).

For successful strategies to be implemented, it is essential to understand early events of PV pathogenesis, thereby facilitating the development of either a new polio vaccine or anti-polio drugs for the control of cVDPV's in pre- and post- polio vaccination outbreaks. Oral infection is the natural route of PV infection in humans; however, early steps in PV pathogenesis in the gut are not well characterized, which may hold the key to a successful control of post-polio vaccination outbreaks. Therefore, a mouse model susceptible to oral infection would be useful in understanding these early events.

Previous attempts at generating orally susceptible mouse models have been unsuccessful due to a lack of receptor expression on the susceptible cells in the alimentary tract (Iwasaki et al., 2002; Zhang and Racaniello, 1997). However, I was able to confer oral susceptibility to TgPVR21 mice, when they were backcrossed with mice deficient in alpha/beta interferon receptors (Ohka et al., 2007). Unfortunately, these immuno-compromised mice did not show the tissue tropism typically associated with PV infections (Ida-Hosonuma et al., 2005; Ohka et al., 2007), thus they are not suitable for studying the early events in pathogenesis. Here I describe the generation of an immunocompetent transgenic mouse line, mCD155tg, expressing the hCD155 gene under the control of the mCD155 promoter.

On characterization of CD155 expression profile by western blot, I saw expression of the receptor in brain, spinal cord, kidney and liver. In TgPVR21 mice, no detectable expression has been observed in liver by western blot (Yanagiya et al., 2003); however, expression is observed in the liver of mCD155tg mice (Fig. 6). CD155 expression was too low in the small intestine to be detected by western blot, a phenomenon I have also observed with detection of mCD155 in the small intestine tissues (Gunter Bernhardt, personal communication). However, I was able to detect CD155 expression on the PP's by immunostaining. The expression profile of CD155 in mCD155tg was different than that observed for humans and mice. The striking difference being that in mCD155tg mice expression is detected in SED and interfollicular region, while no expression is observed on the enterocytes. Meanwhile, the expression of CD155 was limited to GC's and the enterocytes of both humans and mice (Iwasaki et al., 2002; Ravens et al., 2003). Interestingly, in mCD155 knockout mice, CD155 expression is still visible on the enterocytes (Maier, Mk. and Bernhardt, G. unpublished data). Hence, the expression of CD155 on enterocytes of the PP's may be an artifact in mice and humans.

Like TgPVR21 mice, the mCD155tg mice were also susceptible to infection by all parenteral routes. Beside's i.c. route, the mCD155tg mice were significantly more susceptible to poliomyelitis than in TgPVR21 mice (Table 1). In addition to increased susceptibility by parenteral routes, the 3 week old or younger mice were also susceptible to oral infection (Table 2). Surprisingly, both mCD155tg and TgPVR21 mice showed

similar susceptibility to oral infection in 1 week old mice; however, the susceptibility decreased dramatically in 3 weeks old TgPVR21 mice, with complete absence of susceptibility in adult mice.

In the present study, I was able to identify the upper small intestine of the mCD155tg mice as a site of early viral growth. The viral titers in the upper small intestine during administration of the inoculum in mCD155tg and TgPVR21 mice are equivalent; however, the titers in mCD155tg remain high while decreasing in TgPVR21 mice after inoculations (Fig. 10A). There is no difference in viral titers in the lower small intestine of both mice (Fig. 10B). By day 3, I can detect viremia and concurrently appearance of the virus in the brain (Fig. 10D and 10E). The virus was eventually detected in the spinal cord on day 4 (Fig. 10E). This result and previous observations indicate that the primary route of invasion of the CNS is through the blood brain barrier (BBB) not retrograde transport of the virus from muscles. Most importantly, the pathogenesis of the virus in mCD155tg mice is similar to as observed in humans and non-human primates; growth in the upper small intestine, followed by viremia and lastly replication in the central nervous system tissues.

The oral susceptibility to infection of 3 weeks old or younger TgPVR21 mice and 6 weeks old TgPVR21/*ifnar KO* mice is intriguing considering there was no detectable CD155 expression by immunostaining in these mice (Iwasaki et al., 2002; Yanagiya et al., 2003). The discrepancy could be due to a very low and intermittent expression of CD155 in the GALT of the TgPVR21 mice. There was no age dependent difference in expression of CD155 in the mCD155, since expression of CD155 was detected in at 3 week and 6 week of age (data not shown). Besides expression of the receptor in the GALT, I believe that the "closure" of the intestinal barrier coupled with innate immunity also plays a role in the oral pathogenesis of the virus. It has been previously reported that the intestinal epithelium of the neonatal mice is capable of non-selectively absorbing a wide variety of albumins, including egg, porcine, rabbit, bovine and humans (Lecce, 1972). When the mice reach an age of 16 to 18 days old, the "closure" of the intestinal epithelium occurs to non-selective absorption of antibody and albumins (Loria et al., 1976). This closure coincides with the decrease in susceptibility of TgPVR21 mice to oral infection. For 3 week old mice, TgPVR21 susceptibility has been reduced to 20%

lethality compared to 100% lethal infection of mCD155tg mice for the same dose of viral inoculum. While even the mCD155tg mice showed decrease in approximately 1000 fold susceptibility to oral infection in 3 week old than the 1 week old mice.

The occurrence of high viral titers in the upper small intestine after oral administration indicates either that there is no paucity of viral receptors on the mucosal cells in both mice or the virus uptake in the small intestine is receptor independent. However, the viral titers in the upper small intestine sharply drop on day 3 and 4 for the TgPVR21 mice. Indicating that virus penetrates but fails to replicate in the cells due to poor receptor expression on susceptible cells and subsequently clearance of the virus. The TgPVR21/*ifnar* KO mice lack the clearance function and tissue tropism, thus the virus can replicate in the small intestine cells. In mCD155tg mice, I believe CD155 is expressed on the susceptible cells of the upper small intestine, thus initiating viral replication and evading immune clearance in 3 week old mice. I believe 1 week old mice lack efficient clearance function thus are highly susceptible to infection, as seen by similar LD_{50} dose by the both mice. Therefore, combination of intestinal barrier and clearance function renders the mice more resistant to infection in the 3 weeks old mice.

The mechanism of oral infection of mice with PV becomes a little clearer from the studies presented here and from previous work on TgPVR21/*ifnar KO* tg mice (Ohka et al., 2007). Successful oral infection of mice requires overcoming viral viability in the stomach (Ohka et al., 2007). In the present study, I observed uptake of the virus in both 3 weeks old mice, whereas efficient viral uptake in adult mice requires neutralization of the acidic environment of the stomach. After inoculation of the virus, the second barrier lies in the expression of CD155 on the susceptible cells for successful replication in the upper small intestine. In absence of receptor on susceptible cells, the virus is efficiently cleared, as seen in the upper small intestine of TgPVR21 mice. Lack of viral clearance response in turn would allow replication of the virus even in the non-susceptible cells (Ohka et al., 2007). I have been able to overcome these two barriers in 3 weeks old mCD155tg mice resulting in there susceptibility to oral infection. While in the adult mice, combination of viral viability in the stomach and efficiency of viral clearance renders these mice unsusceptible t infection.

The high susceptibility to infection by i.c. route compared to oral route is consistent with Sabin's theory that animals at lower position on the evolutionary ladder, such as mice, are less susceptible to oral infection and more susceptible to infection by CNS then in humans (Sabin, 1956). In spite of lack of oral infection in adult mice, 3 weeks old mCD155tg mice still offer us an opportunity to identify susceptible cells in the GALT and mechanism of virus dissemination in the blood. In addition, this model presents us with a new experimental model to study efficacy of drugs in blocking oral PV pathogenesis and also recombination of OPVs.

Table 1: PLD_{50} of PV infections by parenteral routes in mice.

	TgTage4-CD155tg (PFU)	TgPVR21(PFU)
Intracerebral (i.c)	$10^{1.8}$	10^{2}
Intraperitoneal (i.p)	$10^{2.8}$	$10^{5.7}$
Intramuscular (i.m)	$10^{3.2}$	$10^{4.2}$
Intravenous (i.v)	10^{3}	$10^{5.2}$

Table 2: PLD_{50} of PV infections by oral route in mice.

Age (weeks)	Tage4-CD155tg (PFU)	TgPVR21 (PFU)
***1**	$10^{6.2}$	$10^{6.2}$
[+]3	$10^{9.5}$	[#]u.d
[+]6	u.d	u.d

*1 week old mice were administered virus by mouth using an oral gavage.
[+]3 and 6 week old mice were administered virus by a water bottle.
[#]unable to detect

Figure 1. Activity of mCD155 promoter (A) Schematic diagram of the mCD155 promoter in pGL3-Basic vector. (B) Luciferace activity of the mCD155 promoter. Ltk- cells were transfected with 1 μg of pGL3-CMV, pGL3-mCD155 (2500 bp), pGL3-mCD155 (914 bp), pGL3-mCD155 (406 bp) and pGL3-Basic. The lysates were assayed for luciferase activities using the luciferase assay system. The results are shown as relative luciferase activity of three different experiments carried out in triplicate.

A

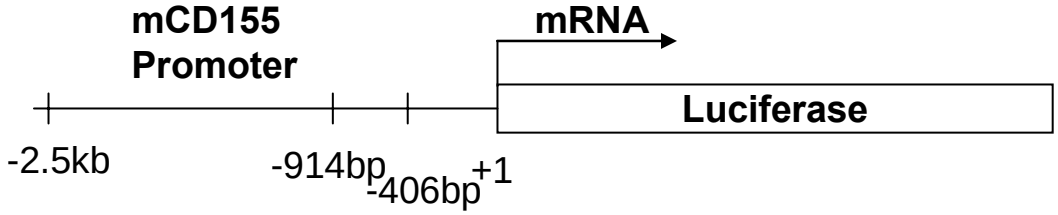
mCD155
Promoter
mRNA
Luciferase
-2.5kb
-914bp
-406bp
+1

B

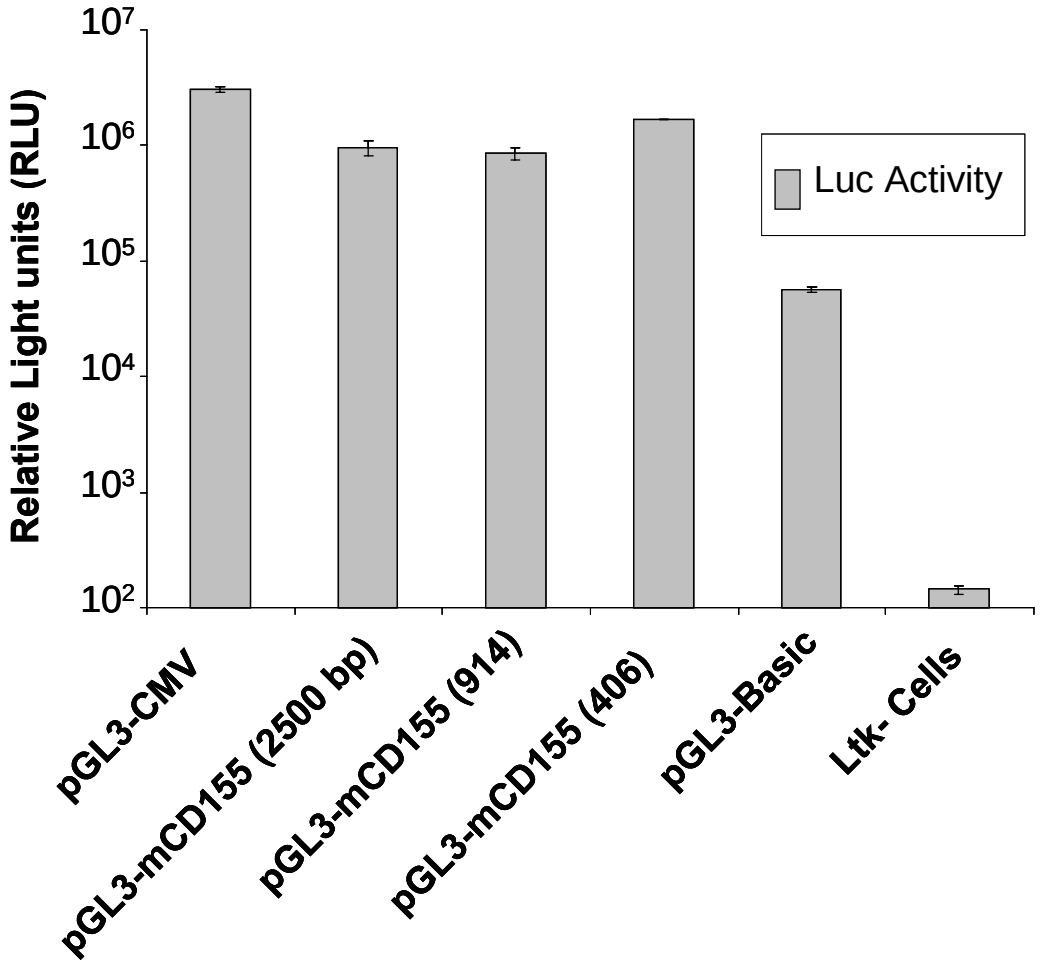
Relative Light units (RLU)
10^7
10^6
10^5
10^4
10^3
10^2
Luc Activity
pGL3-CMV
pGL3-mCD155 (2500 bp)
pGL3-mCD155 (914)
pGL3-mCD155 (406)
pGL3-Basic
Ltk- Cells

Figure 2. Expression of CD155 in mouse Ltk$^-$ cells under the control of the m*CD155* promoter. **(A)** Untransfected Ltk$^-$ cells **(B)** Ltk$^-$ cells transfected with chimeric cosmid mhCD155 (mouse promoter and human CD155 gene) **(C)** Ltk$^-$ cells transfected with HC5 (human CD155 promoter and gene). Bars 100μm (A and B); 25μm (A' and B'). Incubated with mAB 18.1 and developed with Vector® VIP substrate kit.

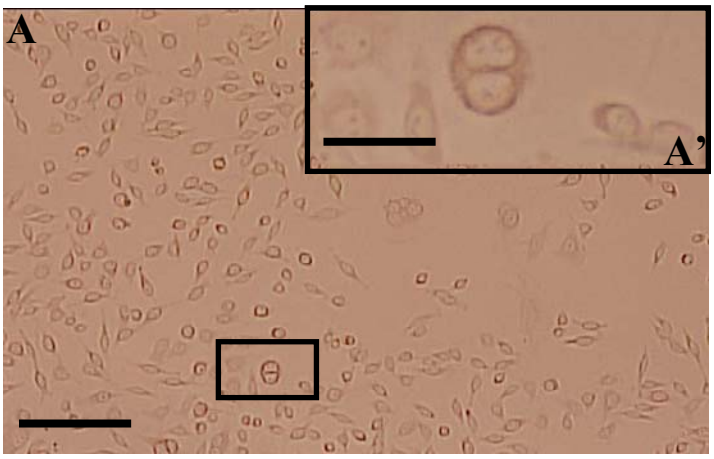
A
A’

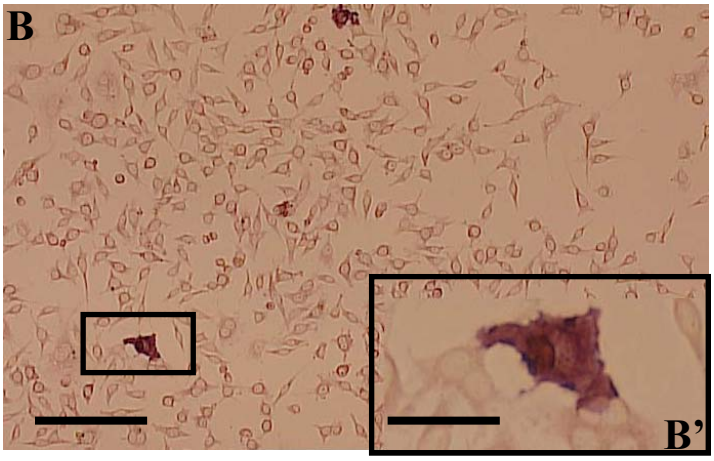
B
B’

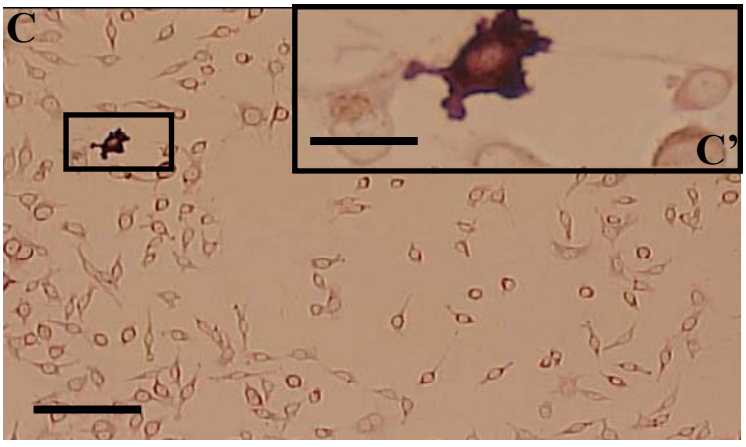
C
C’

Figure 3. Infection of cell lines with PV1. Viral titer of PV1 growing in L-mhCD155 (Ltk- cells stably expressing human CD155 under the control of mCD155 promoter), HeLa cells and Ltk- cells was determined at 0 h and 24 h.

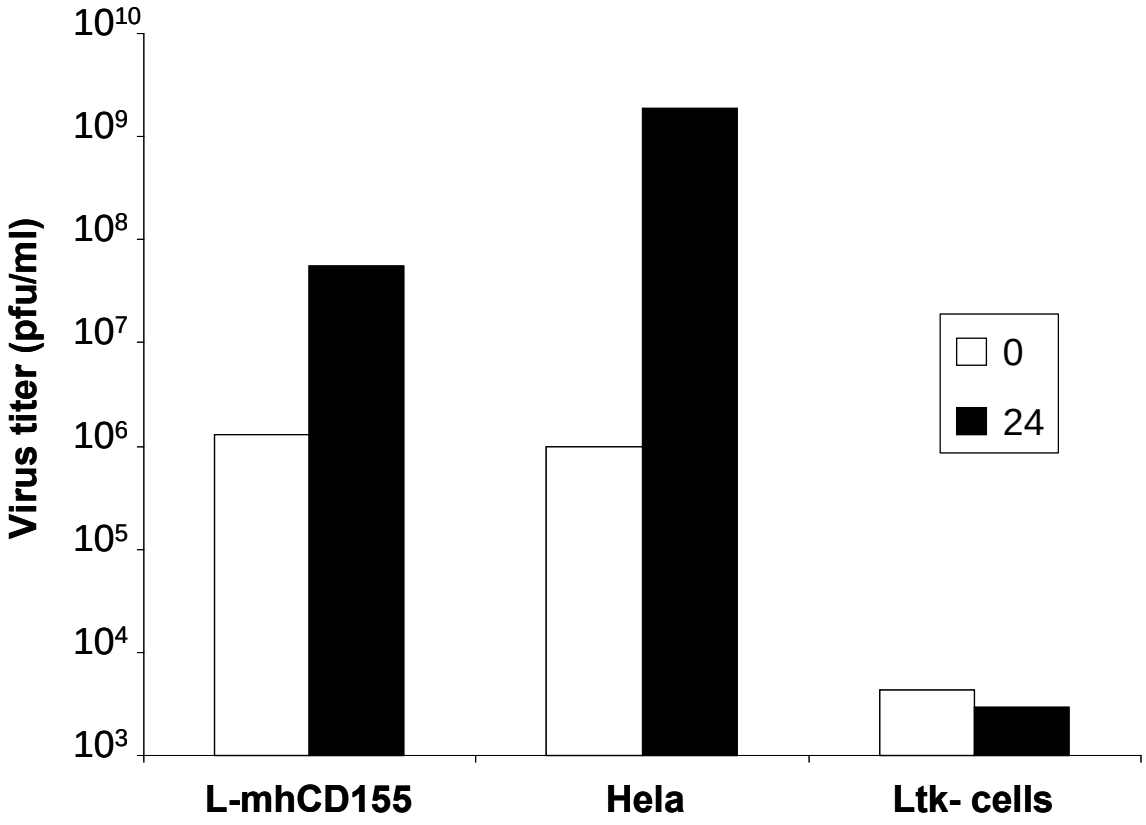
Virus titer (pfu/ml)
10^10
10^9
10^8
10^7
10^6
10^5
10^4
10^3
0
24
L-mhCD155
Hela
Ltk- cells

Figure 4. RT-PCR analysis of CD155 isoform expression in L-mhCD155 cells. **(A)** Schematic representation of the different CD155 transcript variants. Positions of the oligonucleotide primers used for RT-PCR amplifications. Oligonucleotides primers CD5 and CD15 are located in exon 5 and exon 7. Open triangles indicate the initiation codon. Closed triangles indicate stop codons. (modified from (Baury et al., 2003)) **(B)** Agarose gel showing the three major CD155 transcripts from 2 clones of Ltk- cells transfected with chimeric cosmid and HeLa cells.

A

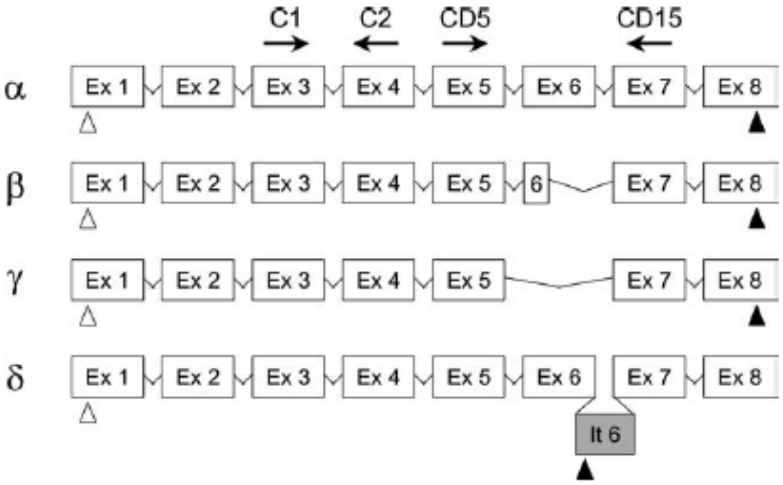
C1
C2
CD5
CD15
α
Ex 1
Ex 2
Ex 3
Ex 4
Ex 5
Ex 6
Ex 7
Ex 8
β
6
γ
δ
It 6

B

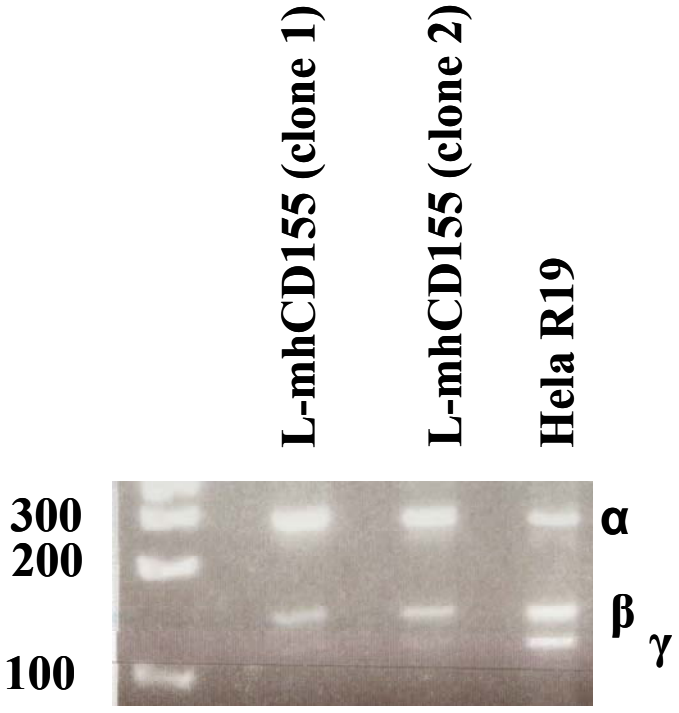
L-mhCD155 (clone 1)
L-mhCD155 (clone 2)
Hela R19
300
200
100
α
β
γ

Figure 5. Schematic design of the construction of a cosmid carrying the fusion gene of the mCD155 promoter and the human CD155 coding region.

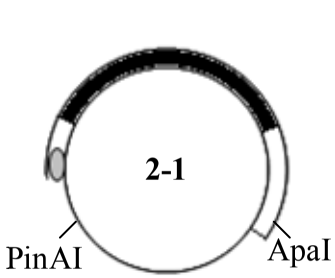

mCD155
promoter and
hCD155 Exon 1

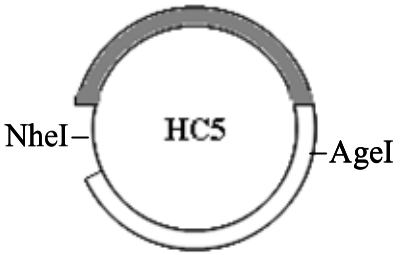

hCD155
promoter and
structural gene

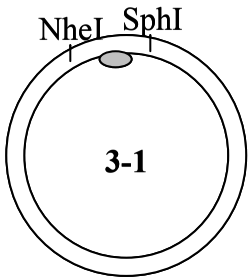

Cos sequence

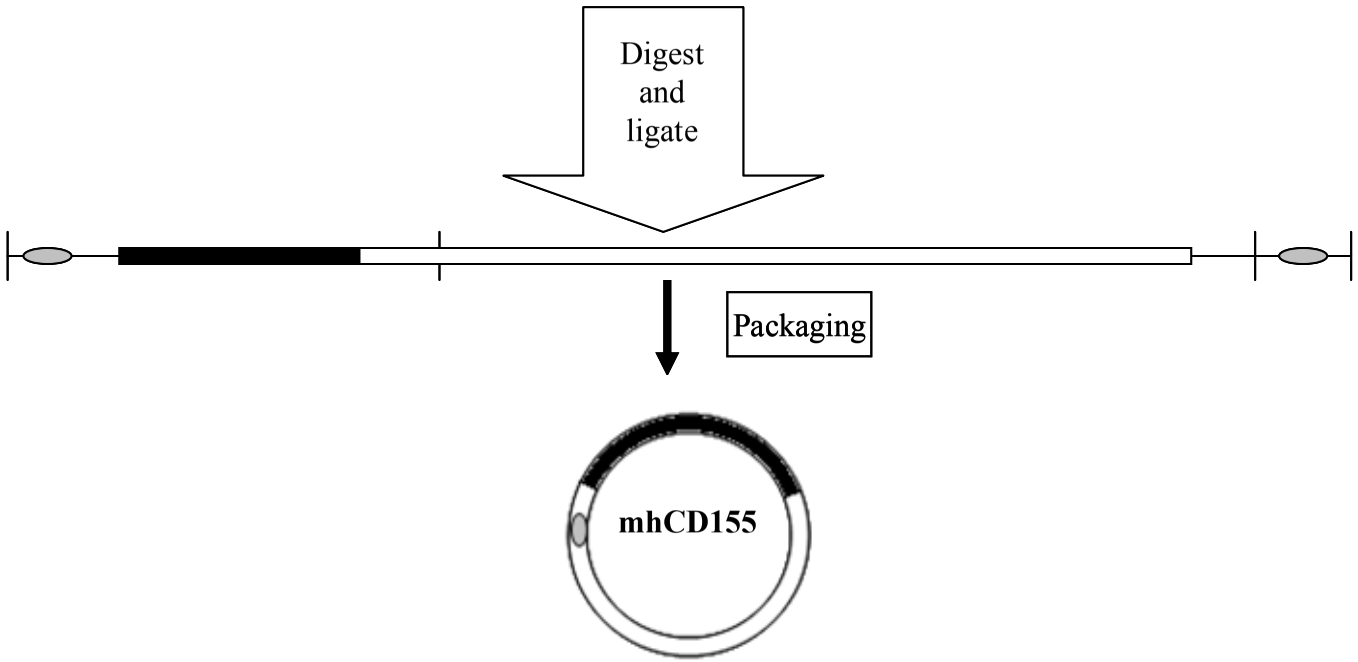

Figure 6. Detection of CD155 expression in mCD155tg mouse tissues. Western blot analysis of CD155 in ICR (lane 1), TgPVR21 (lane 2), and mCD155tg (lane 3-6) mice. Membrane fractions of various tissues were prepared, and CD155 in these fractions was detected as described in Materials and Methods.

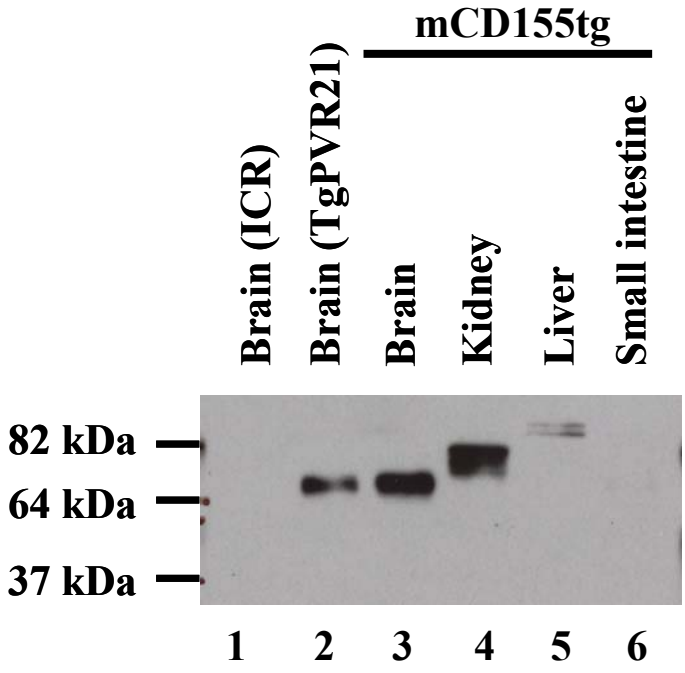
mCD155tg
Brain (ICR)
Brain (TgPVR21)
Brain
Kidney
Liver
Small intestine
82 kDa
64 kDa
37 kDa
1
2
3
4
5
6

Figure 7. Expression of CD155 in the PP's of mCD155tg mice. PP's **(A and B)** and kidneys **(C and D)** were collected from 6 week old mCD155tg mice**.** Tissue sections were stained with affinity-purified rabbit polyclonal antiserum against CD155 (*red*) and CD23 (*green*). Nucleus was stained with DAPI (*blue*). Control slides **(A and C)** were stained with just secondary antibodies. L, lumen.

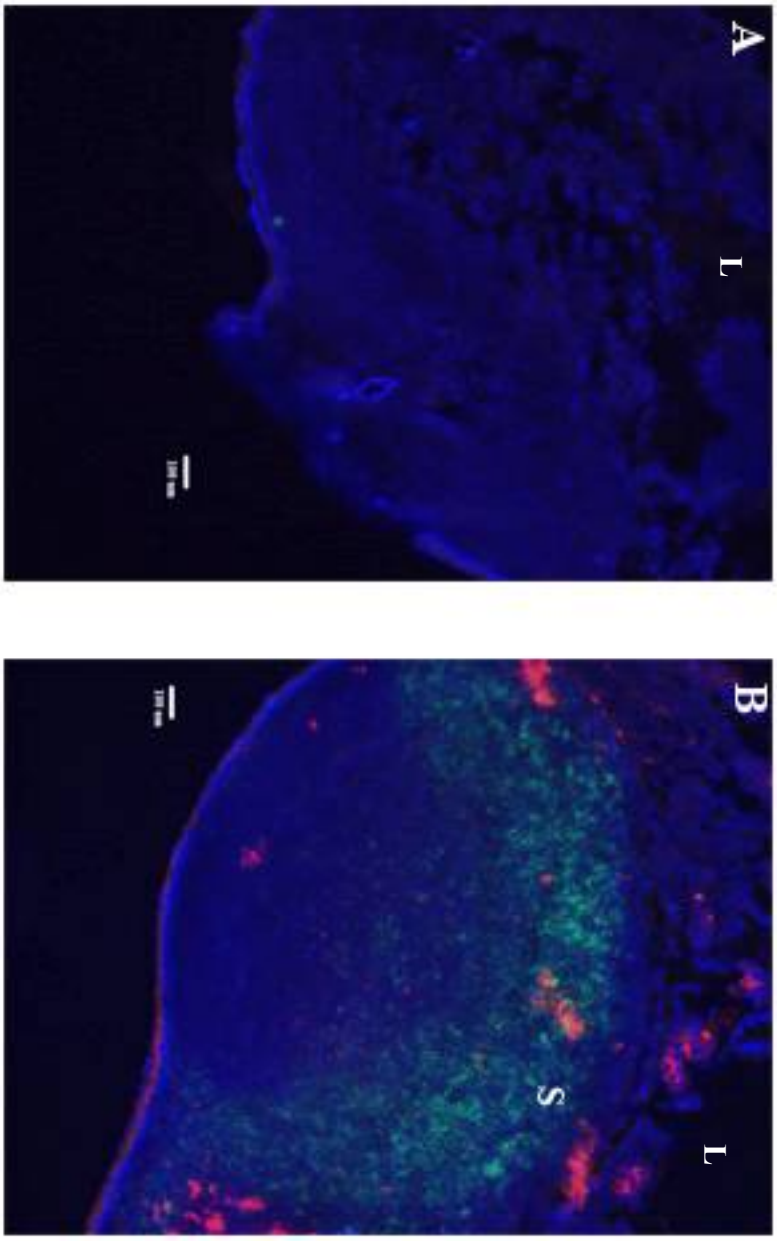
A
L
B
S
L

Figure 7. Expression of CD155 in the PP's of mCD155tg mice. PP's **(A and B)** and kidneys **(C and D)** were collected from 6 week old mCD155tg mice**.** Tissue sections were stained with affinity-purified rabbit polyclonal antiserum against CD155 (*red*) and CD23 (*green*). Nucleus was stained with DAPI (*blue*). Control slides **(A and C)** were stained with just secondary antibodies. L, lumen.

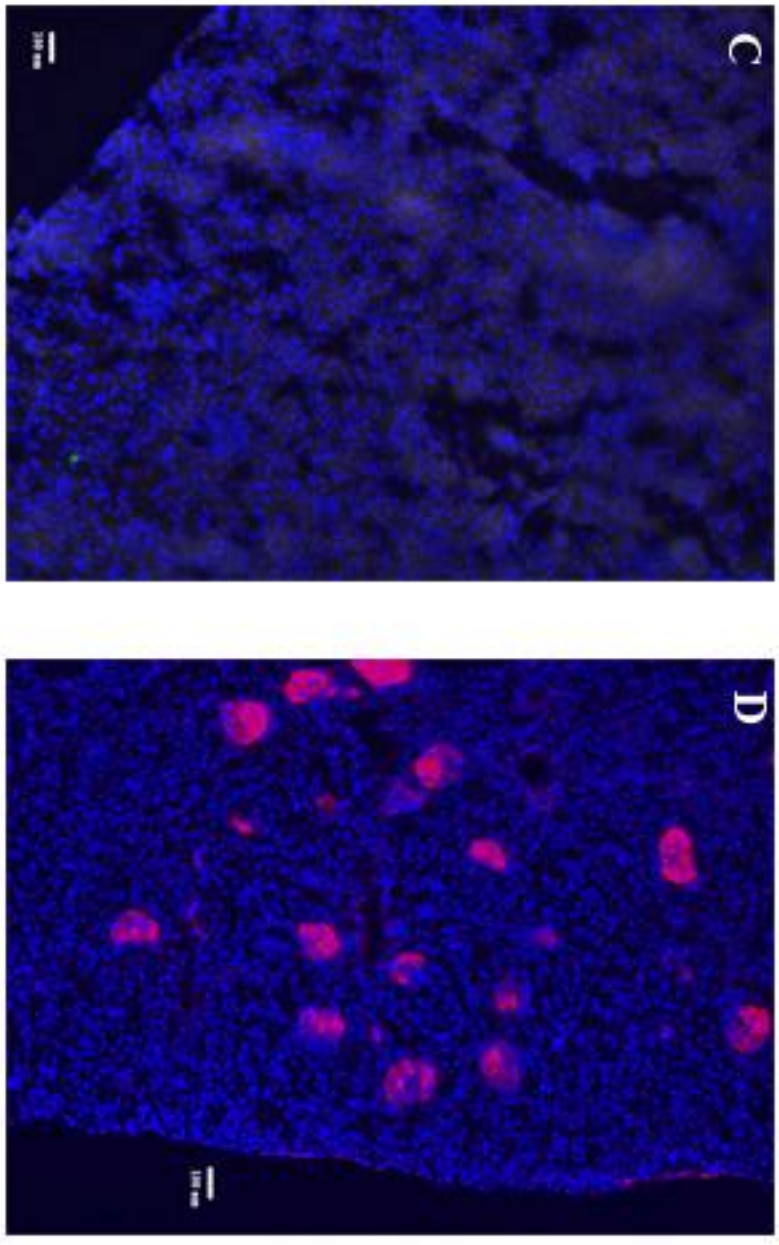
C
D

Figure 8. Infection of mice with PV by the oral route. A representative picture of complete flaccid paralysis caused by PV1 infection in a 10 day old mouse is shown. The mouse on left hand-side of the figure is a non-tg ICR control mouse.

Figure 9. Survival rates of mice after oral administration of PV. 3 weeks old mCD155tg (solid triangles) and TgPVR21 (solid squares) mice were orally administered 4 X 10^9 PFU/4 ml of PV1(M) on Day 0 and Day 1. Ten mice were observed per group.

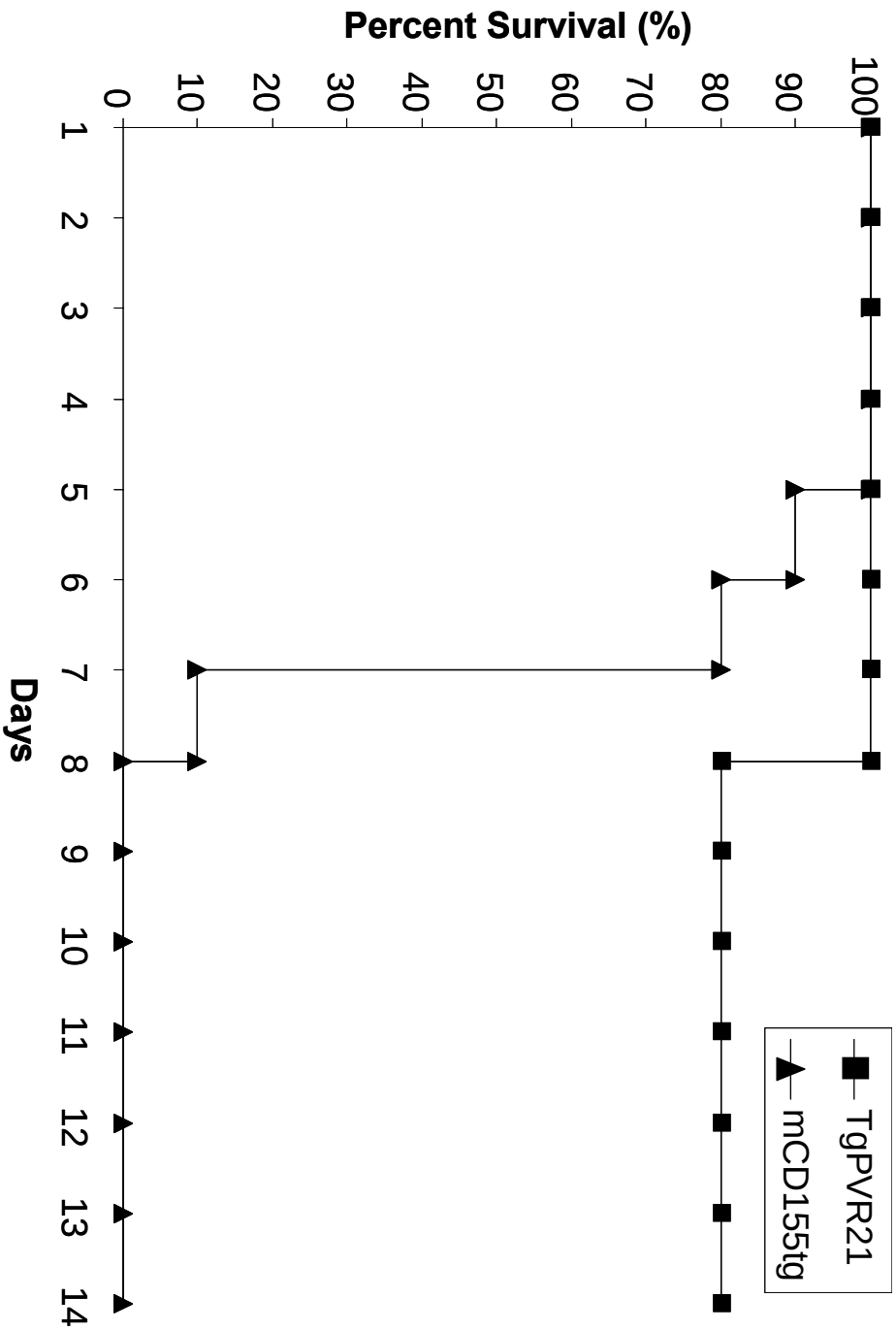
Percent Survival (%)
100
90
80
70
60
50
40
30
20
10
0
Days
1
2
3
4
5
6
7
8
9
10
11
12
13
14
TgPVR21
mCD155tg

Figure 10. Titers of PV recovered in tissues after oral administration of PV. Virus was extracted from tissues of mCD155tg (open squares) and TgPVR21 (open circles) mice. Mice were orally administered 4 X 10^9 PFU/4 ml of PV1(M) on Day 0 and Day 1 (arrows). After first administration of the virus inoculum (Day 0), the tissues were extracted on 1, 2, 3, and 4 days. The vertical axis shows the amount of PV detected in tissues (PFU/100 mg) or blood (PFU/ml) by the plaque assay (Materials and Methods). Each open square (Tage4-CD155tg) and open circle (TgPVR21) indicates one mouse. The bars indicate average amount of virus detected in mCD155tg (black bars) and TgPVR21 (white bars) mice. **(A)** Upper small intestine **(B)** Lower small intestine **(C)** Blood **(D)** Brain **(E)** Spinal Cord **(F)** Feces

A

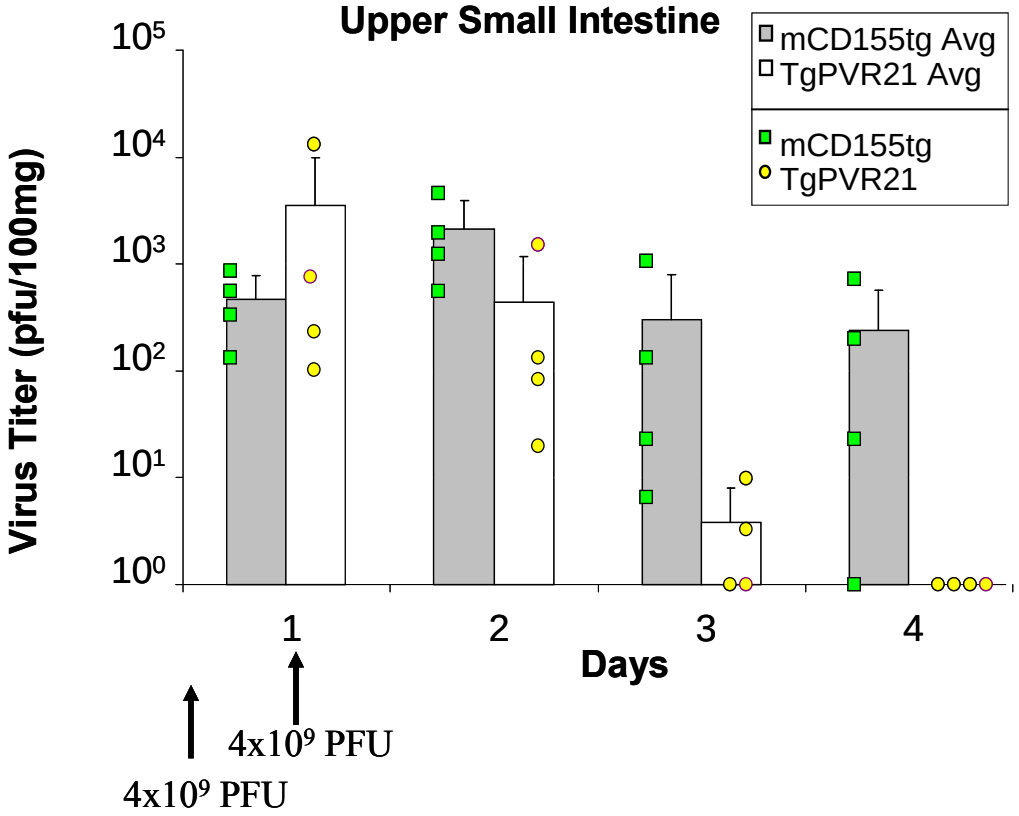
Upper Small Intestine
mCD155tg Avg
TgPVR21 Avg
mCD155tg
TgPVR21
Virus Titer (pfu/100mg)
10⁵
10⁴
10³
10²
10¹
10⁰
1
2
3
4
Days
4x10⁹ PFU
4x10⁹ PFU

B

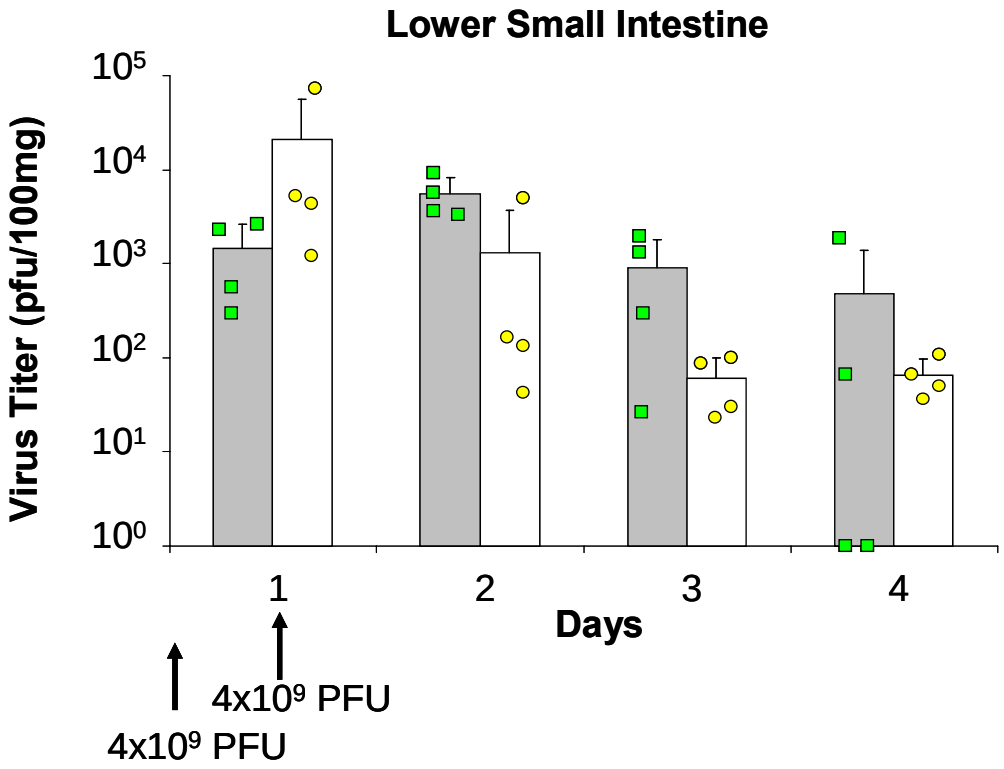
Lower Small Intestine
Virus Titer (pfu/100mg)
10⁵
10⁴
10³
10²
10¹
10⁰
1
2
3
4
Days
4x10⁹ PFU
4x10⁹ PFU

Figure 10. Titers of PV recovered in tissues after oral administration of PV. Virus was extracted from tissues of mCD155tg (open squares) and TgPVR21 (open circles) mice. Mice were orally administered 4 X 10^9 PFU/4 ml of PV1(M) on Day 0 and Day 1 (arrows). After first administration of the virus inoculum (Day 0), the tissues were extracted on 1, 2, 3, and 4 days. The vertical axis shows the amount of PV detected in tissues (PFU/100 mg) or blood (PFU/ml) by the plaque assay (Materials and Methods). Each open square (Tage4-CD155tg) and open circle (TgPVR21) indicates one mouse. The bars indicate average amount of virus detected in mCD155tg (black bars) and TgPVR21 (white bars) mice. **(A)** Upper small intestine **(B)** Lower small intestine **(C)** Blood **(D)** Brain **(E)** Spinal Cord **(F)** Feces

C

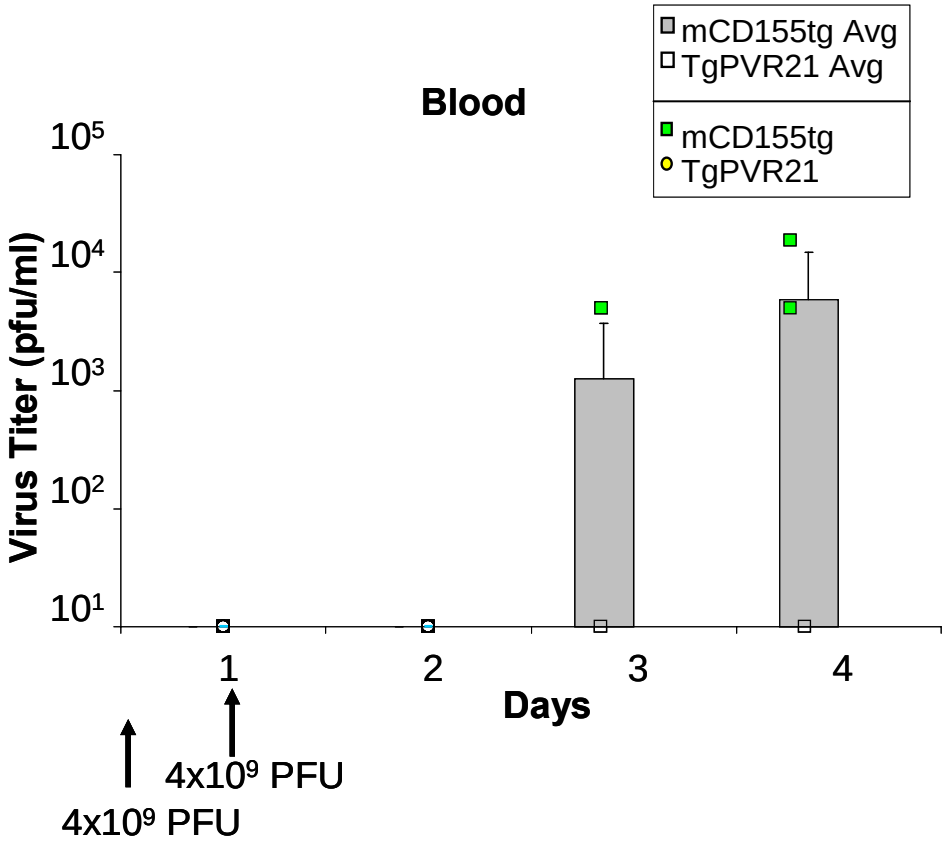
mCD155tg Avg
TgPVR21 Avg
mCD155tg
TgPVR21
Blood
Virus Titer (pfu/ml)
10^5
10^4
10^3
10^2
10^1
1
2
3
4
Days
4x10^9 PFU
4x10^9 PFU

D

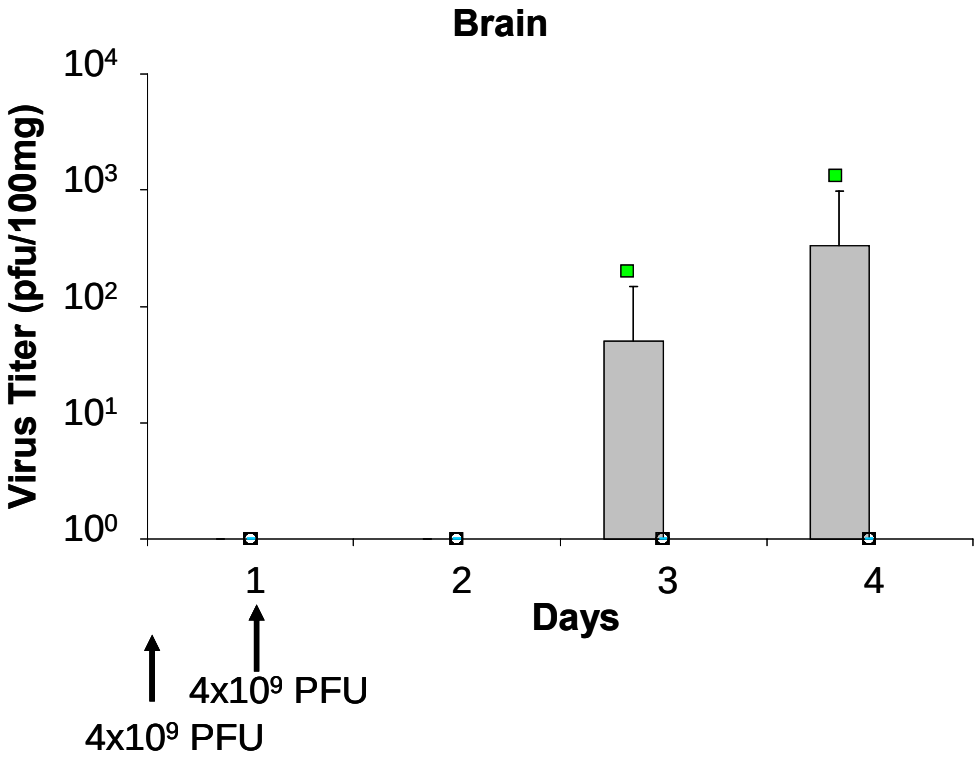
Brain
Virus Titer (pfu/100mg)
10^4
10^3
10^2
10^1
10^0
1
2
3
4
Days
4x10^9 PFU
4x10^9 PFU

Figure 10. Titers of PV recovered in tissues after oral administration of PV. Virus was extracted from tissues of mCD155tg (open squares) and TgPVR21 (open circles) mice. Mice were orally administered 4 X 10^9 PFU/4 ml of PV1(M) on Day 0 and Day 1 (arrows). After first administration of the virus inoculum (Day 0), the tissues were extracted on 1, 2, 3, and 4 days. The vertical axis shows the amount of PV detected in tissues (PFU/100 mg) or blood (PFU/ml) by the plaque assay (Materials and Methods). Each open square (Tage4-CD155tg) and open circle (TgPVR21) indicates one mouse. The bars indicate average amount of virus detected in mCD155tg (black bars) and TgPVR21 (white bars) mice. **(A)** Upper small intestine **(B)** Lower small intestine **(C)** Blood **(D)** Brain **(E)** Spinal Cord **(F)** Feces

E

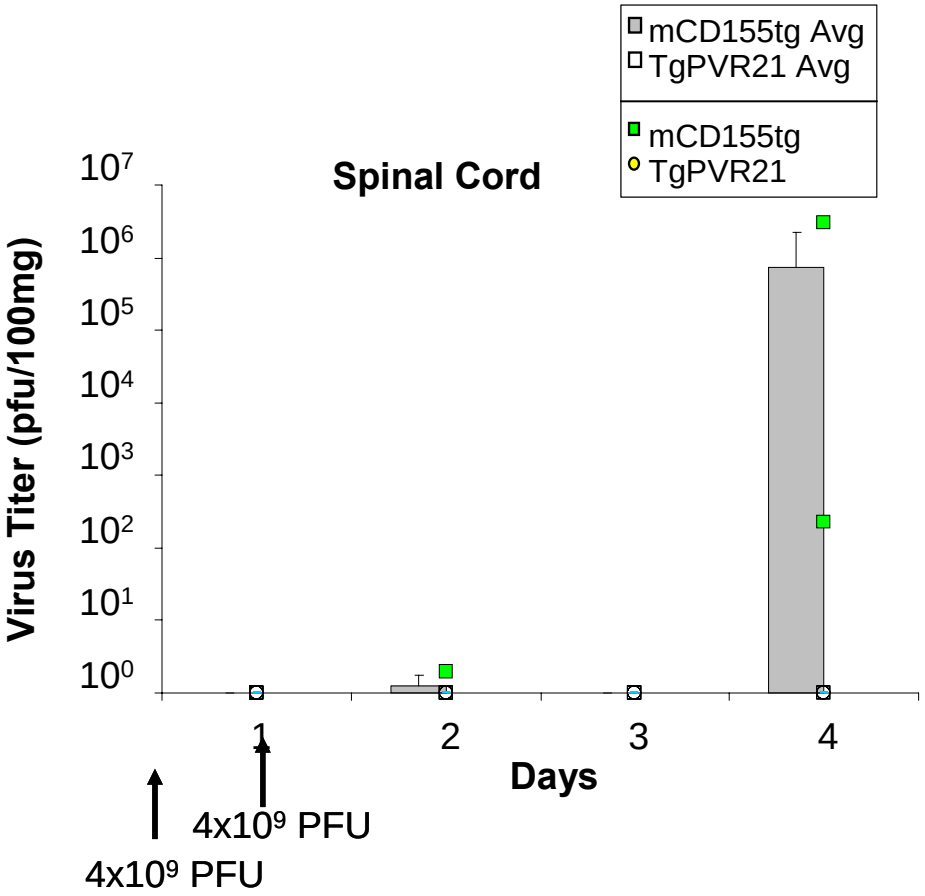
mCD155tg Avg
TgPVR21 Avg
mCD155tg
TgPVR21
Spinal Cord
Virus Titer (pfu/100mg)
10^7
10^6
10^5
10^4
10^3
10^2
10^1
10^0
1
2
3
4
Days
4x10^9 PFU
4x10^9 PFU

F

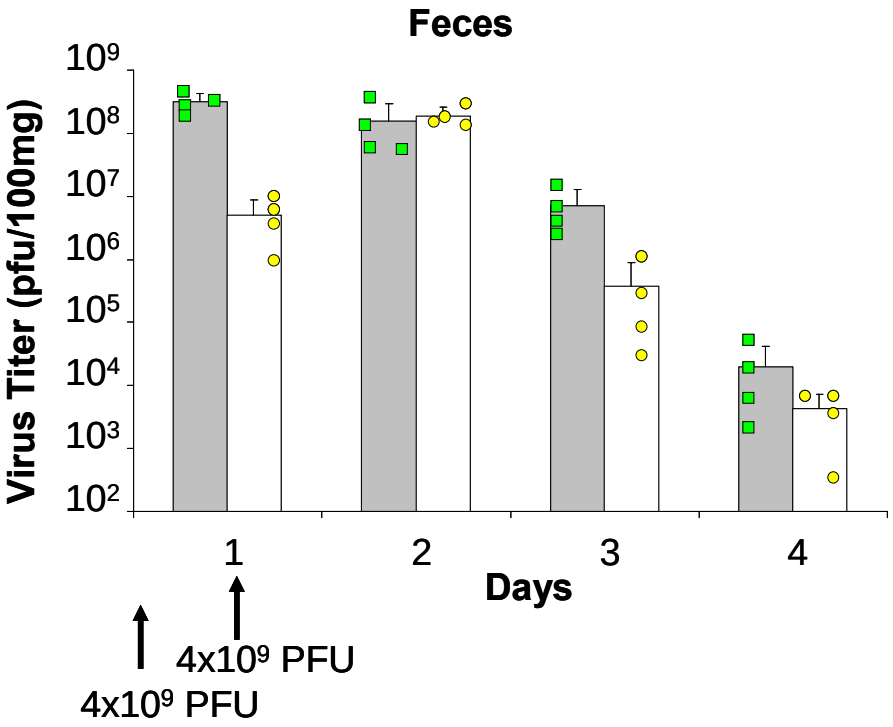
Feces
Virus Titer (pfu/100mg)
10^9
10^8
10^7
10^6
10^5
10^4
10^3
10^2
1
2
3
4
Days
4x10^9 PFU
4x10^9 PFU

Chapter IV

Summary and Discussion

The purpose of my studies was to elucidate the susceptibility of new world monkey (NWM) species to infection with poliovirus (PV) serotypes and to generate a mouse model sensitive to oral infection. Both of these topics deal with the early events of PV pathogenesis: the interaction of the virus with the receptor and the uptake of the virus into the alimentary tract.

CD155 molecule of NWMs and its interaction with polioviruses

NWMs can be infected by intracerebral injection but, surprisingly, this is dependent not only upon the NWM species but also upon the PV serotype. I found this phenomenon intriguing and decided to elucidate the mechanism of this phenotype at the molecular level. I obtained two different cell lines, TMX and NZP-60, belonging to tamarin and marmoset monkeys, respectively. In these two cell lines I saw quite a diverse phenotype, even though both monkeys' CD155 proteins shared a high amino acid similarity. Nevertheless, the TMX cells were susceptible to PV1 and PV3 infection, whereas NZP-60 cells were resistant to all three serotypes (Chapter II-Fig. 4). This observation is surprising because both NWM cell lines express CD155 on the cell surface and the genomes of all PV serotypes, replicate efficiently when transfected into these cells (Chapter III-Fig. 5 and 6). When I carried out binding assays to determine the amount of virus-receptor complexes formed on these cells, I observed a trend. There was an increase in the amount of virus-receptor complexes from 4°C to 25°C that corresponded with the successful infection of the cells (Chapter II-Fig. 4 and 7). Therefore, the lack of infection is due to the lack of virus-receptor interaction, and not due to either the availability of the receptor on the cell surface (Chapter II-Fig. 6) or the ability of PV genomes transfected into the NWM cells to replicate and produce infectious virus (Chapter II-Fig. 5A).

It has been shown previously that human CD155 interacts with all serotypes with similar binding affinities (Bibb et al., 1994). However, the amount of PV1 bound complexes on TMX cells is greater than that of PV3 and PV2 (Chapter II-Fig. 7). For unknown reasons, the rapid amino acid change of the CD155 receptor of the tamarin cell line over evolution has preserved the binding to PV1 and, to some extent, to PV3. In contrast, marmoset cells showed virus-receptor complexes for only PV1, but the binding

did not lead to successful infection, since there was no increase in bound complexes at higher temperatures.

Since the loss of binding to PV serotypes was speculated due to amino acid variation in V domain, we decided to introduce three amino acid replacements into the C'-C"-D face of the NWM CD155 V domain thereby hopefully rendering the transfected mouse Ltk^- cells susceptible to PV infection (Chapter II-Fig. 9). Based on the crystal structure of PV and cryo-EM studies of PV/hCD155 complexes, the hCD155 V domain interacts with the south wall of PV's canyon. When corresponding mutations were introduced into the marmoset receptor, nCD155, I observed that the cells were now susceptible to only PV1 infection. Fittingly binding of the mutant receptor, nCD155mt, to PV1 also increased when the temperature was increased from 4°C to 25°C (Chapter II-Fig. 10 and 11).

Our understanding of the virus-receptor interactions are based on genetic, crystallographic, and cryo-EM studies (Aoki et al., 1994; Belnap et al., 2000; Bernhardt et al., 1994; Colston and Racaniello, 1994; Harber et al., 1995; He et al., 2000; He et al., 2003; Hogle, 2002; Liao and Racaniello, 1997; Morrison et al., 1994). From these studies, it has been determined that the receptor-virus interaction follows biphasic kinetics (McDermott et al., 2000), and ref. therein). The initial virus-receptor binding step involves electrostatic interactions between the C'-C''-D' face of the receptor and the south wall of the virion canyon. This interaction is fully reversible and temperature independent. The second step occurs near physiological temperatures due to "breathing" of the virion structure, which exposes higher affinity binding sites (McDermott et al., 2000). The breathing of the virion leads to the translocation of a portion of VP1 to the capsid surface and then to the release of the internal capsid protein VP4 to so called A particles. This binding step, therefore, leads to irreversible structural changes of the (bound) virion. It is hypothesized that during this process additional contacts with the north wall of the canyon in addition to the south wall of the canyon are established, leading eventually to the uncoating of the virus in the endosomal compartment of the cell (He et al., 2003; Hogle, 2002; McDermott et al., 2000).

Crystallographic and cryo-EM studies have been important in elucidating the electrostatic interactions of the virus and the receptor. Based on these studies, it has been

concluded that the CD155 binding sites and orientation in the viral canyon of the three serotypes is similar and consequently, that all three serotypes use a similar mechanism for cell entry (He et al., 2003). Cryo-EM studies show that the closest contacts between CD155 and the virus are with the south wall and the east end of the canyon, most likely important for receptor recognition (Fig. 1), whereas the residues on the north wall of the canyon make relatively distant contacts (Fig. 1) (He et al., 2003). The receptor interaction with the north side of the canyon is hypothesized to be important for the release of the virion pocket factor (Rossmann, 2002). The pocket factor is a small fatty acid or hydrophobic compound with a polar head group derived from cellular components that binds within the capsid protein VP1 β-barrel and stabilizes the virion (Rossmann, 2002). The interaction of the receptor with the south wall, east end and the north wall of the canyon in turn leads to destabilization of the virus and uncoating (He et al., 2003)

This model of uncoating is supported by data observed for a CD155 mutant (Q130G, G131D) that is unable to interact with PV1 and PV2 but can bind to PV3. However, the binding of this CD155 mutant to PV3 does not lead to viral infection, presumably because it cannot initiate uncoating (Harber et al., 1995). These two mutated residues in CD155 lie in the FG loop (Chapter II-Fig. 9). The FG loop of CD155 is hypothesized to interact with the north wall of the canyon (He et al., 2003). These mutations in CD155 destroyed binding to PV1 and PV2, whereas in PV3 the binding was not affected because of the formation of a salt bridge between the Asp131 mutation in CD155 and Lys1168 of VP1, thus preserving binding (He et al., 2003). However, the CD155 mutant cannot initiate uncoating due to the inability of the Gly introduced at position 130 to affect release of the pocket factor and destabilizing the virion, which viral stability which is required for uncoating (He et al., 2003).

Even though the CD155 mutant (Q130G, G131D) fits the proposed model, the model does not explain the phenotype of other CD155 mutants that show serotype specific binding (Bernhardt et al., 1994; Harber et al., 1995). For example, cell line 84 expressing CD155 mutant (P84SYS/HYSA) is deficient in binding PV1 and Sabin 1, but not Sabin 2 or Sabin 3 (Harber et al., 1995). Here, the mutations lie on the C'-C"-D face of CD155 (Chapter II Fig-9), which makes contacts with the south wall of the canyon. A hybrid PV1 virus, in which the neutralizing antigenic site Ia was exchanged with that of

PV2, showed an increase in virus bound complexes on cell line 84 (Harber et al., 1995). Here, the mutation P84SYS/HYSA in hCD155 leads to a loss of binding of PV1, which can be rescued by the exchange of neutralization antigenic epitopes on the virus surface (Harber et al., 1995). This mutation shows that the neutralization epitopes in antigenic site 1 on the surface of the virus around the canyon (Fig. 1A) are actively involved in the uncoating of the virus.

This study also suggests that some of the antigenic sites play a role in the uncoating of the virus. Even though the mutations introduced in nCD155 are expected to interact with the south wall, which would have implied an increase in binding for all serotypes, the experimental data showed that the mutations only affect PV1 binding and subsequent permissivity to infection. Due to the nature of the cryo-EM method, we can only see a snapshot of the electrostatic binding at low temperature, however, I believe that at higher temperatures, the receptor may not only interact with the north wall, but may also interact with one or more antigenic sites.

The mechanism of this interaction is still unclear. Mutations found to affect serotype binding are found on the C'-C"-D face of nCD155, which interacts with the south wall. However the capsid is not a static structure, at higher temperatures the virus structure "breathes". This fluidity of the virus can play a part in modulating the interaction between the virus and the receptor, thereby allowing the antigenic sites to play a role in the destabilization of the virus and subsequent uncoating.

Construction of mCD155tg mice and its utility to study poliovirus oral infection

In addition to understanding the viral-receptor interactions of the NWM receptor, I was also interested in generating a mouse model that can be infected orally. One of the biggest drawbacks of previous mouse models has been that they cannot be infected orally. The TgPVR21 mice were generated with a cosmid containing the human CD155 promoter and gene (Koike et al., 1991). These mice were shown to lack expression of CD155 in the alimentary tract (Iwasaki et al., 2002). Since the human promoter was regulating CD155 protein expression, it was hypothesized that the human promoter may not be able to confer tissue distribution in mice as seen in humans particularly in the gastrointestinal tract. Therefore, several groups generated transgenic mice expressing

CD155 under different promoters. Two groups generated mice expressing CD155 under the control of the β-actin promoter (Crotty et al., 2002; Ida-Hosonuma et al., 2002). Even though these mice expressed CD155 in every tissue, surprisingly, they were slightly more resistant to infection by the parenteral routes than the TgPVR21 mice (Table 1) (Crotty et al., 2002; Ida-Hosonuma et al., 2002). Similarly, there was an attempt to express CD155 in the gastrointestinal tract by driving expression under the promoter of the intestinal fatty acid binding protein (IFABP). Even though these mice expressed CD155 on enterocytes, they were still not susceptible to oral infection, most likely due to a lack of expression in the gut-associated lymphoid tissues (GALT) (Zhang and Racaniello, 1997). Yanagiya et al. then proceeded to generate a mouse model with the promoter of *nectin-2*, a gene formerly believed to be the mouse homologue of human CD155. However, these mice were also not susceptible to oral infection, even though CD155 expression in the small intestine was detectable by Western blot analysis (Yanagiya et al., 2003). The possible reason for lack of oral infection in these mice could be due to a difference in the tissue distribution of nectin-2 and CD155.

In an attempt to study the effect of innate immunity during PV infection, Ida-Hosonuma et al. generated a TgPVR21/*ifnar KO* mice lacking the interferon alpha/beta receptor (Ida-Hosonuma et al., 2005). These mice lacked the tissue tropism associated with poliovirus infection, but were susceptible to oral infection (Ohka et al., 2007). However, these mice are a poor model for the study of early events of poliovirus infection, since they lack tissue tropism.

Therefore, I have generated a new mouse model mCD155tg, that expresses human CD155 under the control of the murine CD155 (mCD155) promoter. Human and mouse CD155 proteins do not share high amino acid similarity, but they perform similar cellular functions in the respective organisms (Ravens et al., 2003), and most importantly show similar tissue distribution (Iwasaki et al., 2002; Ravens et al., 2003). The mCD155tg mice were found to express CD155 in the GALT and were also susceptible to oral infection, albeit only in 3 week old or younger mice. I was also able to discern that the mCD155tg mice were more sensitive by intraperitoneal (i.p.), intramuscular (i.m.) and intravenous (i.v.) routes than the previously generated tg mice (Table 1).

Most importantly, the mCD155tg mice were susceptible to oral infection. However, the susceptibility was dependent on the age of the mice, where 1 week old were more susceptible than 3 week old mice with the eventual loss of susceptibility in adult mice (Chapter II-Table 2). Interestingly, I found that even the TgPVR21 mice were susceptible to oral infection depending on the age of the newborn animals. 1 week old TgPVR21 mice showed similar susceptibility as mCD155tg mice, while the susceptibility of 3 weeks old TgPVR21 was significantly lower than found for mCD155tg mice (Chapter III-Table 2). In addition, the 6 weeks old TgPVR21/*ifnar KO* mice, which lack interferon α/β receptor, are also susceptible to oral infection. This observation was quite intriguing since no detectable amount of receptor has been found in the alimentary tract of TgPVR21 mice either by western blot or immunostaining. This suggests the possibility that the germinal centers (GC) in TgPVR21 mice may express the receptor but at a very low level.

I saw viral growth in the upper small intestine of the mCD155tg mice. The viral titers in the upper small intestine after administration of inoculum in mCD155tg and TgPVR21 mice were equivalent; however, the titers decreased after 2 days in TgPVR21 mice whereas in the small intestine of mCD155tg mice, the viral titers remained high until the end of the study (Chapter III-Fig. 11A). This result implies that both mCD155tg and TgPVR21 mice can trap virus in the upper small intestine, however, replication only occurs in the upper small intestine of the mCD155tg mice, as observed by significantly increased viral titers in mCD155tg mice compared to that in TgPVR21 mice. In mCD155tg mice, the replication of the virus in the small intestine is followed by viremia, and then by the appearance in the central nervous system (CNS). The pathogenesis of virus in mCD155tg mice is similar to what is observed in humans and non-human primates: growth in the upper small intestine, followed by viremia and lastly replication in the CNS.

Besides expression of the receptor in the GALT, I believe that the "closure" of the intestinal barrier coupled with innate immunity also plays a role in the oral pathogenesis of the virus. The occurrence of high viral titers in the upper small intestine after oral administration indicates either that there is no paucity of viral receptors on the mucosal cells in both mice, or that the virus uptake in the small intestine is receptor independent.

However, the viral titers in the upper small intestine sharply drop on day 3 and 4 for the TgPVR21 mice, indicating that virus penetrates but fails to replicate in the cells post infection due to poor receptor expression on susceptible cells and subsequent clearance of the virus. In mCD155tg mice, I believe CD155 is expressed on the susceptible cells of the upper small intestine, thus initiating viral replication and evading immune clearance. The closure of the small intestine coincides with the change in mitotic activity of the small intestine (Loria et al., 1976). Identical susceptibility of 1 week old TgPVR21 mice and mCD155tg mice could be a result of differential expression of CD155 in neonate TgPVR21 mice. However, 6 weeks old TgPVR21/*ifnar KO* mice are susceptible to infection. Therefore, CD155 expression is not age-dependent on the cells of the small intestine of TgPVR21 mice. Similarly, I observed expression of CD155 in 3 week old and 6 week old mCD155tg mice. Another possibility is the clearance function in the mice; 1 week old mice are inefficient in clearing the virus and are thus highly susceptible. However, combination of intestinal barrier and clearance function renders the mice more resistant to infection. I have observed this for even 3 week old mCD155tg mice, which require 1000 fold more virus to be susceptible to infection than the 1 week old mice. The clearance function would in turn also explain the susceptibility of TgPVR21/*ifnar KO* mice and lack of tissue tropism.

The mCD155 transgenic mouse model gives us an opportunity to study early pathogenesis of poliovirus, particularly the localization of early sites of viral replication. Aside from studying early pathogenesis of PV, this model could be used to study colon carcinomas. Since mCD155 has been shown to be overexpressed on induced colon carcinomas, I think induction of carcinomas in this mouse model would result in overexpression of CD155 (Chadeneau, LeMoullac, and Denis, 1994). This induction of CD155 would allow us to initiate studies similar to treatment of neuroblastoma with poliovirus in our lab (Toyoda et al., 2007).

Table 1. PLD_{50} of CD155 transgenic mice

Route	mCD155tg (pfu)	TgPVR21 (pfu)	PVRtg/ IFNR KO[1] (pfu)	cPV R[2]	TgFABP-PVR[3]	CAG-PVR[4]
Intracerebral (i.c)	$10^{1.8}$	10^{2}	$10^{0.8}$	*$10^{6.6}$	>10^{7}	u.d
Intramuscular (i.m)	$10^{2.8}$	$10^{5.7}$	#n.d	$10^{5.3}$	+u.d	u.d
Intraperitoneal (i.p)	$10^{3.2}$	$10^{4.2}$	$10^{1.2}$	10^{8}	u.d	u.d
Intravenous (i.v)	10^{3}	$10^{5.2}$	$10^{1.7}$	$10^{8.3}$	u.d	u.d

[1]Ida-hosonuma et al. 2005; [2]Crotty, S et al. 2002; [3]Zhang, S et al. 1997; [4]Ida-hosonuma et al. 2002
*only saw paralysis
#not determined
+unable to detect

Figure 1. The structure of a poliovirion and the model of CD155 V domain interaction with the virus canyon. **(A)** A complete capsid structure of PV1 (M) molecular surface. One of the 12 pentameric subunits of the capsid and its five constituent triangular pseudoprotomeric subunits are illustrated. The 5X and 3X labels indicate the locations of the fivefold and the threefold axes of this pentamer. The twofold axes occur at the intersection of the three adjacent pentamers. The central pseudoprotomer illustrates the subunit geometry of VP1, VP2, and VP3 (ii). The biologically relevant protomer (to viral assembly) is pear-shaped and consists of VP1, VP2, and VP3(i). The internal VP4 protein is not visible on the surface. The canyon's north wall (A), south wall (C), and bottom (B) are indicated. The major poliovirus antigenic sites are labeled Ia, Ib, II, and III on an adjacent pseudoprotomer. **(B)** The Cα backbone of CD155 D1 is shown in black. The orientation of the canyon is marked as north, south, and east. At the right is an explanation of the north and south notation used to describe the canyon topology (modified from Harber et al. 1995 and He et. al. 2003).

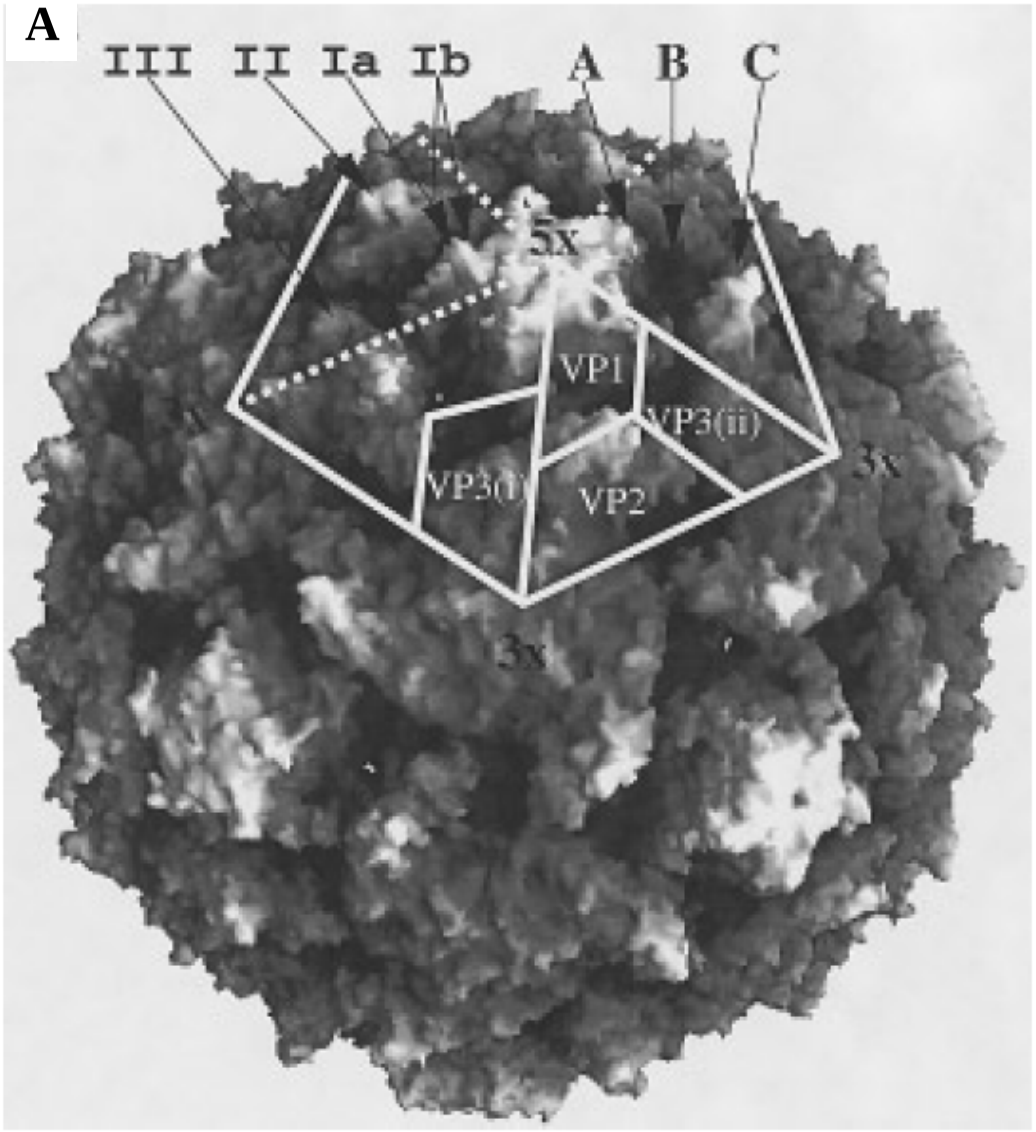
A
III
II
Ia
Ib
A
B
C
5X
VP1
VP3(ii)
VP3(i)
VP2
3X
3X

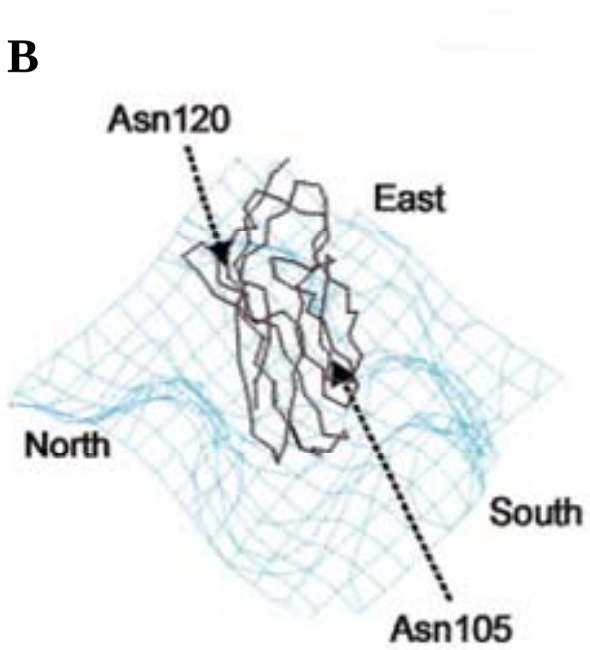
B
Asn120
East
North
South
Asn105

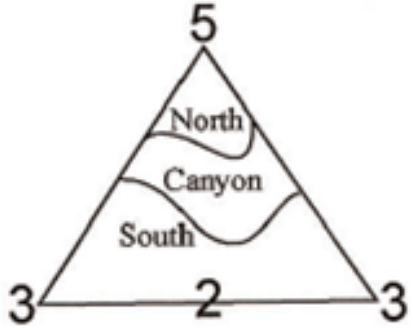
5
North
Canyon
South
3
2
3

REFERENCES

(2007). Update on vaccine-derived polioviruses--worldwide, January 2006-August 2007. *MMWR Morb Mortal Wkly Rep* **56**(38)**,** 996-1001.

Andino, R., Rieckhof, G. E., Achacoso, P. L., and Baltimore, D. (1993). Poliovirus RNA synthesis utilizes an RNP complex formed around the 5'-end of viral RNA. *Embo J* **12**(9)**,** 3587-98.

Andino, R., Rieckhof, G. E., and Baltimore, D. (1990). A functional ribonucleoprotein complex forms around the 5' end of poliovirus RNA. *Cell* **63**(2)**,** 369-80.

Aoki, J., Koike, S., Ise, I., Sato-Yoshida, Y., and Nomoto, A. (1994). Amino acid residues on human poliovirus receptor involved in interaction with poliovirus. *J. Biol. Chem.* **269,** 8431-8439.

Armstrong, C. (1939). Successful transfer of the Lansing strain of poliomyelitis virus from the cotton rat to the white mouse. *Public Health Report* **54,** 2302-2305.

Bachrach, H. L., and Schwerdt, C. E. (1952). Purification studies on Lansing poliomyelitis virus: pH stability, CNS extraction and butanol purification experiments. *J Immunol* **69**(5)**,** 551-61.

Barton, D. J., O'Donnell, B. J., and Flanegan, J. B. (2001). 5' cloverleaf in poliovirus RNA is a cis-acting replication element required for negative-strand synthesis. *Embo J* **20**(6)**,** 1439-48.

Basavappa, R., Syed, R., Flore, O., Icenogle, J. P., Filman, D. J., and Hogle, J. M. (1994). Role and mechanism of the maturation cleavage of VP0 in poliovirus assembly: structure of the empty capsid assembly intermediate at 2.9 A resolution. *Protein Sci* **3**(10)**,** 1651-69.

Baury, B., Geraghty, R. J., Masson, D., Lustenberger, P., Spear, P. G., and Denis, M. G. (2001). Organization of the rat Tage4 gene and herpesvirus entry activity of the encoded protein. *Gene* **265**(1-2)**,** 185-94.

Baury, B., Masson, D., McDermott, B. M., Jr., Jarry, A., Blottiere, H. M., Blanchardie, P., Laboisse, C. L., Lustenberger, P., Racaniello, V. R., and Denis, M. G. (2003). Identification of secreted CD155 isoforms. *Biochem Biophys Res Commun* **309**(1)**,** 175-82.

Belnap, D. M., McDermott, B. M., Jr., Filman, D. J., Cheng, N., Trus, B. L., Zuccola, H. J., Racaniello, V. R., Hogle, J. M., and Steven, A. C. (2000). Three-dimensional structure of poliovirus receptor bound to poliovirus. *Proc.Natl. Acad. Sci. U. S. A.* **97,** 73-78.

Bendtsen, J. D., Nielsen, H., von Heijne, G., and Brunak, S. (2004). Improved prediction of signal peptides: SignalP 3.0. *J Mol Biol* **340**(4)**,** 783-95.

Bernhardt, G., Bibb, J. A., Bradley, J., and Wimmer, E. (1994a). Molecular characterization of the cellular receptor for poliovirus. *Virology* **199,** 105-113.

Bernhardt, G., Harber, J., Zibert, A., deCrombrugghe, M., and Wimmer, E. (1994b). The poliovirus receptor: identification of domains and amino acid residues critical for virus binding. *Virology* **203**(2)**,** 344-356.

Bibb, J. A., Bernhardt, G., and Wimmer, E. (1994). Cleavage site of the signal sequence of the poliovirus receptor. *J. Gen. Virol.* **75,** 1875-1881.

Bibb, J. A., Witherell, G., Bernhardt, G., and Wimmer, E. (1994). Interaction of poliovirus with its cell surface binding site. *Virology* **201,** 107-115.

Bienz, K., Egger, D., Troxler, M., and Pasamontes, L. (1990). Structural organization of poliovirus RNA replication is mediated by viral proteins of the P2 genomic region. *J Virol* **64**(3)**,** 1156-63.

Bodian, D. (1955). Emerging concept of poliomyelitis infection. *Science* **122,** 105-108.

Bodian, D. (1956). Poliovirus in chimpanzee tissues after virus feeding. *Am. J. Hyg.* **64,** 181-197.

Bodian, D., and Horstmann, D. M. (1965). Polioviruses. 4 ed. *In* "Viral and Rickettsial Infections of Man" (F. Horsfall, and I. Tamm, Eds.), pp. 430-473. Lippincott, Philadelphia.

Bottino, C., Castriconi, R., Pende, D., Rivera, P., Nanni, M., Carnemolla, B., Cantoni, C., Grassi, J., Marcenaro, S., Reymond, N., Vitale, M., Moretta, L., Lopez, M., and Moretta, A. (2003). Identification of PVR (CD155) and Nectin-2 (CD112) as cell surface ligands for the human DNAM-1 (CD226) activating molecule. *J Exp Med* **198**(4)**,** 557-67.

Brandenburg, B., Lee, L. Y., Lakadamyali, M., Rust, M. J., Zhuang, X., and Hogle, J. M. (2007). Imaging Poliovirus Entry in Live Cells. *PLoS Biol* **5**(7)**,** e183.

Burnet, F. M., Macnamara, J. (1931). Immunological differences between strains of poliomyelitic virus. *Br. J. Exp. Pathol.* **12,** 57-61

Cello, J., Paul, A. V., and Wimmer, E. (2002). Chemical synthesis of poliovirus cDNA: generation of infectious virus in the absence of natural template. *Science* **297**(5583)**,** 1016-1018.

Chadeneau, C., LeMoullac, B., and Denis, M. G. (1994). A novel member of the immunoglobulin gene superfamily expressed in rat carcinoma cell lines. *J Biol Chem* **269**(22)**,** 15601-5.

Charcot, J., and Joffroy, A. (1870). Cas de paralysie infantile spinale avec lesions ds cornes anterieures de la substancegrise de la moelle epiniere. *Ach. Physiol. Norm. Pathol.* **3,** 134-152.

Cho, M. W., Teterina, N., Egger, D., Bienz, K., and Ehrenfeld, E. (1994). Membrane rearrangement and vesicle induction by recombinant poliovirus 2C and 2BC in human cells. *Virology* **202**(1)**,** 129-45.

Clark, M. E., Hammerle, T., Wimmer, E., and Dasgupta, A. (1991). Poliovirus proteinase 3C converts an active form of transcription factor IIIC to an inactive form: a mechanism for inhibition of host cell polymerase III transcription by poliovirus. *Embo J* **10**(10)**,** 2941-7.

Colston, E., and Racaniello, V. R. (1994). Soluble receptor-resistant poliovirus mutants identify surface and internal capsid residues that control interaction with the cell receptor. *Embo J* **13**(24)**,** 5855-62.

Crotty, S., Hix, L., Sigal, L. J., and Andino, R. (2002). Poliovirus pathogenesis in a new poliovirus receptor transgenic mouse model: age-dependent paralysis and a mucosal route of infection. *J Gen Virol* **83**(Pt 7)**,** 1707-20.

Dulbecco, R., and Vogt, M. (1954). Plaque formation and isolation of pure lines with poliomyelitis viruses. *J Exp Med* **99**(2)**,** 167-82.

Eberle, F., Dubreuil, P., Mattei, M. G., Devilard, E., and Lopez, M. (1995). The human PRR2 gene, related to the human poliovirus receptor gene (PVR), is the true homolog of the murine MPH gene. *Gene* **159**(2)**,** 267-272.

Eggers, H. (2002). History of Poliomyelitis and Poliomyelitis Research. *In* "Molecular biology of picornaviruses." (B. L. Semler, and E. Wimmer, Eds.), pp. 3-14. ASM Press, Washington, D.C.

Enders, J. F., Weller, T. H., and Robbins, F. C. (1949). Cultivation of the Lansing Strain of Poliomyelitis Virus in Cultures of Various Human Embryonic Tissues. *Science* **109**(2822)**,** 85-87.

Filman, D. J., Syed, R., Chow, M., Macadam, A. J., Minor, P. D., and Hogle, J. M. (1989). Structural factors that control conformational transitions and serotype specificity in type 3 poliovirus. *Embo J* **8**(5)**,** 1567-79.

Flanegan, J. B., and Baltimore, D. (1977). Poliovirus-specific primer-dependent RNA polymerase able to copy poly(A). *Proc Natl Acad Sci U S A* **74**(9)**,** 3677-80.

(1997). CD155 (poliovirus receptor). Worshop Panel Report.VI. International Worshop and Conference on Human Leukocyte Differentiation Antigens. Garland, Cambridge. pp 1075-1077. Freistadt, M. S., and Eberle, K. E.

Freistadt, M. S., Kaplan, G., and Racaniello, V. R. (1990). Heterogeneous expression of poliovirus receptor-related proteins in human cells and tissues. *Mol Cell Biol* **10**(11)**,** 5700-6.

Fricks, C. E., and Hogle, J. M. (1990). Cell-induced conformational change in poliovirus: externalization of the amino terminus of VP1 is responsible for liposome binding. *J Virol* **64**(5)**,** 1934-45.

Fuchs, A., Cella, M., Giurisato, E., Shaw, A. S., and Colonna, M. (2004). Cutting edge: CD96 (tactile) promotes NK cell-target cell adhesion by interacting with the poliovirus receptor (CD155). *J Immunol* **172**(7)**,** 3994-8.

Gamarnik, A. V., and Andino, R. (2000). Interactions of viral protein 3CD and poly(rC) binding protein with the 5' untranslated region of the poliovirus genome. *J Virol* **74**(5)**,** 2219-26.

Goodfellow, I., Chaudhry, Y., Richardson, A., Meredith, J., Almond, J. W., Barclay, W., and Evans, D. J. (2000). Identification of a cis-acting replication element within the poliovirus coding region. *J Virol* **74**(10)**,** 4590-600.

Gromeier, M., Lu, H. H., and Wimmer, E. (1995). Mouse neuropathogenic poliovirus strains cause damage in the central nervous system distinct from poliomyelitis. *Microb Pathog* **18**(4)**,** 253-67.

Gromeier, M., and Wimmer, E. (1998). Mechanism of injury-provoked poliomyelitis. *J. Virol.* **73,** 5056-5060.

Harber, J., Bernhardt, G., Lu, H. H., Sgro, J. Y., and Wimmer, E. (1995). Canyon rim residues, including antigenic determinants, modulate serotype-specific binding of polioviruses to mutants of the poliovirus receptor. *Virology* **214**(2)**,** 559-570.

Harris, K. S., Xiang, W., Alexander, L., Lane, W. S., Paul, A. V., and Wimmer, E. (1994). Interaction of poliovirus polypeptide 3CDpro with the 5' and 3' termini of the poliovirus genome. Identification of viral and cellular cofactors needed for efficient binding. *J Biol Chem* **269**(43)**,** 27004-14.

He, Y., Bowman, V. D., Mueller, S., Bator, C. M., Bella, J., Peng, X., Baker, T. S., Wimmer, E., Kuhn, R. J., and Rossmann, M. G. (2000). Interaction of the poliovirus receptor with poliovirus. *Proc. Natl. Acad. Sci. U. S. A.* **97**(1)**,** 79-84.

He, Y., Mueller, S., Chipman, P. R., Bator, C. M., Peng, X., Bowman, V. D., Mukhopadhyay, S., Wimmer, E., Kuhn, R. J., and Rossmann, M. G. (2003). Complexes of poliovirus serotypes with their common cellular receptor, CD155. *J Virol* **77**(8)**,** 4827-35.

Herold, J., and Andino, R. (2000). Poliovirus requires a precise 5' end for efficient positive-strand RNA synthesis. *J Virol* **74**(14)**,** 6394-400.

Herold, J., and Andino, R. (2001). Poliovirus RNA replication requires genome circularization through a protein-protein bridge. *Mol Cell* **7**(3)**,** 581-91.

Hogle, J. M. (2002). Poliovirus cell entry: common structural themes in viral cell entry pathways. *Annu Rev Microbiol* **56,** 677-702.

Hogle, J. M., Chow, M., and Filman, D. J. (1985). Three-dimensional structure of poliovirus at 2.9 A resolution. *Science* **229**(4720)**,** 1358-65.

Hogle, J. M., and Filman, D. J. (1989). The antigenic structure of poliovirus. *Philos Trans R Soc Lond B Biol Sci* **323**(1217)**,** 467-78.

Holland, J. J. (1962). Irreversible eclipse of poliovirus by HeLa cells. *Virology* **16,** 163-76.

Hsiung, G. D., Black, F. L., and Henderson, J. R. (1964). Susceptibility of primates to viruses in relation to taxonomic classification. *In* "Evolutionary and genetic biology of primates." (Buettener-Janusch, Ed.), Vol. vol II., pp. 1-23. Academic Press, New York.

Ida-Hosonuma, M., Iwasaki, T., Taya, C., Sato, Y., Li, J., Nagata, N., Yonekawa, H., and Koike, S. (2002). Comparison of neuropathogenicity of poliovirus in two transgenic mouse strains expressing human poliovirus receptor with different distribution patterns. *J Gen Virol* **83**(Pt 5)**,** 1095-105.

Ida-Hosonuma, M., Iwasaki, T., Yoshikawa, T., Nagata, N., Sato, Y., Sata, T., Yoneyama, M., Fujita, T., Taya, C., Yonekawa, H., and Koike, S. (2005). The alpha/beta interferon response controls tissue tropism and pathogenicity of poliovirus. *J Virol* **79**(7)**,** 4460-9.

Ida-Hosonuma, M., Sasaki, Y., Toyoda, H., Nomoto, A., Gotoh, O., Yonekawa, H., and Koike, S. (2003). Host range of poliovirus is restricted to simians because of a rapid sequence change of the poliovirus receptor gene during evolution. *Arch. Virol.* **148**(1)**,** 29-44.

Ikeda, W., Kakunaga, S., Itoh, S., Shingai, T., Takekuni, K., Satoh, K., Inoue, Y., Hamaguchi, A., Morimoto, K., Takeuchi, M., Imai, T., and Takai, Y. (2003). Tage4/Nectin-like molecule-5 heterophilically trans-interacts with cell adhesion molecule Nectin-3 and enhances cell migration. *J Biol Chem* **278**(30)**,** 28167-72.

Iwasaki, A., and Kelsall, B. L. (2000). Localization of distinct Peyer's patch dendritic cell subsets and their recruitment by chemokines macrophage inflammatory protein (MIP)-3alpha, MIP-3beta, and secondary lymphoid organ chemokine. *J. Exp. Med.* **191**(8)**,** 1381-94.

Iwasaki, A., Welker, R., Mueller, S., Linehan, M., Nomoto, A., and Wimmer, E. (2002). Immunofluorescence analysis of poliovirus receptor expression in Peyer's patches of humans, primates, and CD155 transgenic mice: implications for poliovirus infection. *J. Infect. Dis.* **186**(5)**,** 585-92.

Jang, S. K., Krausslich, H. G., Nicklin, M. J., Duke, G. M., Palmenberg, A. C., and Wimmer, E. (1988). A segment of the 5' nontranslated region of

encephalomyocarditis virus RNA directs internal entry of ribosomes during in vitro translation. *J Virol* **62**(8)**,** 2636-43.

Jiang, P., Faase, J. A., Toyoda, H., Paul, A., Wimmer, E., and Gorbalenya, A. E. (2007). Evidence for emergence of diverse polioviruses from C-cluster coxsackie A viruses and implications for global poliovirus eradication. *Proc Natl Acad Sci U S A* **104**(22)**,** 9457-62.

Kall, L., Krogh, A., and Sonnhammer, E. L. (2004). A combined transmembrane topology and signal peptide prediction method. *J Mol Biol* **338**(5)**,** 1027-36.

Kaplan, A. S. (1955a). Comparison of susceptible and resistant cells to infection with poliomyelitis virus. *Ann. N. Y. Acad. Sci.* **61**(4)**,** 830-9.

Kaplan, A. S. (1955b). The susceptibility of monkey kidney cells to poliovirus in vivo and in vitro. *Virology* **1**(4)**,** 377-92.

Kaplan, A. S., and Melnick, J. L. (1955). Multiplication of virulent poliovirus in capuchin monkey kidney cultures without microscopically observed cytopathogenicity. *Proc Soc Exp Biol Med* **90**(3)**,** 562-5.

Kew, O. M., Sutter, R. W., de Gourville, E. M., Dowdle, W. R., and Pallansch, M. A. (2005). Vaccine-derived polioviruses and the endgame strategy for global polio eradication. *Annu Rev Microbiol* **59,** 587-635.

Kitamura, N., Semler, B. L., Rothberg, P. G., Larsen, G. R., Adler, C. J., Dorner, A. J., Emini, E. A., Hanecak, R., Lee, J. J., van der Werf, S., Anderson, C. W., and Wimmer, E. (1981). Primary structure, gene organization and polypeptide expression of poliovirus RNA. *Nature* **291**(5816)**,** 547-53.

Koike, S., Aoki, J., and Nomoto, A. (1994). Transgenic mouse for the study of poliovirus pathogenicity. *In* "Cellular receptors for animal viruses" (E. Wimmer, Ed.), pp. 463-480. Cold Spring Harbor Laboratory Press, Cold Spring Harbor.

Koike, S., Horie, H., Ise, I., Okitsu, A., Yoshida, M., Iizuka, N., Takeuchi, K., Takegami, T., and A., N. (1990). The poliovirus receptor protein is produced both as membrane-bound and secreted forms. *EMBO J.* **9,** 3217-3224.

Koike, S., Ise, I., Sato, Y., Yonekawa, H., Gotoh, O., and Nomoto, A. (1992). A second gene for the African green monkey poliovirus receptor that has no putative N-

glycosylation site in the functional N-terminal immunoglobulin-like domain. *J. Virol.* **66**(12)**,** 7059-7066.

Koike, S., Taya, C., Kurata, T., Abe, S., Ise, I., Yonekawa, H., and Nomoto, A. (1991). Transgenic mice susceptible to poliovirus. *Proc. Natl. Acad. Sci. U. S. A.* **88**(3)**,** 951-955.

Krausslich, H. G., Nicklin, M. J., Toyoda, H., Etchison, D., and Wimmer, E. (1987). Poliovirus proteinase 2A induces cleavage of eucaryotic initiation factor 4F polypeptide p220. *J Virol* **61**(9)**,** 2711-8.

Landsteiner, K., and Popper, E. (1909). Ubertragung der Poliomyelitis acuta auf Affen. *Z. ImmunnitatsForsch Orig.* **2,** 377-390.

Lange, R., Peng, X., Wimmer, E., Lipp, M., and Bernhardt, G. (2001). The poliovirus receptor CD155 mediates cell-to-matrix contacts by specifically binding to vitronectin. *Virology* **285**(2)**,** 218-227.

Lawson, M. A., and Semler, B. L. (1992). Alternate poliovirus nonstructural protein processing cascades generated by primary sites of 3C proteinase cleavage. *Virology* **191**(1)**,** 309-20.

Lecce, J. G. (1972). Selective absorption of macromolecules into intestinal epithelium and blood by neonatal mice. *J Nutr* **102**(1)**,** 69-75.

Lee, Y. F., Nomoto, A., Detjen, B. M., and Wimmer, E. (1977). A protein covalently linked to poliovirus genome RNA. *Proc Natl Acad Sci U S A* **74**(1)**,** 59-63.

Lentz, K. N., Smith, A. D., Geisler, S. C., Cox, S., Buontempo, P., Skelton, A., DeMartino, J., Rozhon, E., Schwartz, J., Girijavallabhan, V., O'Connell, J., and Arnold, E. (1997). Structure of poliovirus type 2 Lansing complexed with antiviral agent SCH48973: comparison of the structural and biological properties of three poliovirus serotypes. *Structure* **5**(7)**,** 961-78.

Li, C. P., and Schaeffer, M. (1953). Adaptation of type I poliomyelitis virus to mice. *Proc Soc Exp Biol Med* **82**(3)**,** 477-81.

Li, X., Lu, H. H., Mueller, S., and Wimmer, E. (2001). The C-terminal residues of poliovirus proteinase 2A(pro) are critical for viral RNA replication but not for cis- or trans-proteolytic cleavage. *J Gen Virol* **82**(Pt 2)**,** 397-408.

Liao, S., and Racaniello, V. (1997). Allele-specific adaptation of poliovirus VP1 B-C loop variants to mutant cell receptors. *J. Virol.* **71**(12)**,** 9770-9777.

Loria, R. M., Shadoff, N., Kibrick, S., and Broitman, S. (1976). Maturation of intestinal defenses against peroral infection with group B coxsackievirus in mice. *Infect Immun* **13**(5)**,** 1397-401.

Lu, H. H., Yang, C. F., Murdin, A. D., Klein, M. H., Harber, J. J., Kew, O. M., and Wimmer, E. (1994). Mouse neurovirulence determinants of poliovirus type 1 strain LS-a map to the coding regions of capsid protein VP1 and proteinase 2Apro. *J Virol* **68**(11)**,** 7507-15.

Maier, M. K., Seth, S., Czeloth, N., Qiu, Q., Ravens, I., Kremmer, E., Ebel, M., Muller, W., Pabst, O., Forster, R., and Bernhardt, G. (2007). The adhesion receptor CD155 determines the magnitude of humoral immune responses against orally ingested antigens. *Eur J Immunol* **37**(8)**,** 2214-25.

McDermott, B. M., Jr., Rux, A. H., Eisenberg, R. J., Cohen, G. H., and Racaniello, V. R. (2000). Two distinct binding affinities of poliovirus for its cellular receptor. *J. Biol. Chem.* **275,** 23089-23096.

Melnick, J. L. (1996). Current status of poliovirus infections. *Clin Microbiol Rev* **9**(3)**,** 293-300.

Mendelsohn, C. L., Wimmer, E., and Racaniello, V. R. (1989). Cellular receptor for poliovirus: molecular cloning, nucleotide sequence, and expression of a new member of the immunoglobulin superfamily. *Cell* **56**(5)**,** 855-865.

Minor, P. (1997). Poliovirus. *In* "Viral pathogenesis" (N. Nathanson, Ed.), pp. 555-574. Lippincott-Raven, Philadelphia.

Minor, P. D., Ferguson, M., Evans, D. M., Almond, J. W., and Icenogle, J. P. (1986). Antigenic structure of polioviruses of serotypes 1, 2 and 3. *J Gen Virol* **67 (Pt 7),** 1283-91.

Mok, Y. K., Lo, K. W., and Zhang, M. (2001). Structure of Tctex-1 and its interaction with cytoplasmic dynein intermediate chain. *J Biol Chem* **276**(17)**,** 14067-74.

Molla, A., Paul, A. V., and Wimmer, E. (1991). Cell-free, de novo synthesis of poliovirus. *Science* **254**(5038)**,** 1647-51.

Morrison, M. E., He, Y. J., Wien, M. W., Hogle, J. M., and Racaniello, V. R. (1994). Homolog-scanning mutagenesis reveals poliovirus receptor residues important for virus binding and replication. *J Virol* **68**(4)**,** 2578-88.

Morrison, M. E., and Racaniello, V. R. (1992). Molecular cloning and expression of a murine homolog of the poliovirus receptor gene. *J. Virol.* **66,** 2807-2813.

Mueller, S., Cao, X., Welker, R., and Wimmer, E. (2002). Interaction of the poliovirus receptor CD155 with the dynein light chain Tctex-1 and its implication for poliovirus pathogenesis. *J. Biol. Chem.* **277**(10)**,** 7897-904.

Mueller, S., Rosenquist, T. A., Takai, Y., Broson, R. A., and Wimmer, E. (2003). Loss of nectin-2 at Sertoli-spermatid junctions leads to male infertility and correlates with severe spematozoan head and midpiece malformation, impaired binding to the zona pellucida, and oocyte penetration. *Biol. Reprod.* **69**(4)**,** 1330-1340.

Mueller, S., and Wimmer, E. (2003). Recruitment of nectin-3 to cell-cell junctions through *trans*-heterophilic interaction with CD155, a vitronectin and poliovirus receptor that localizes to $\alpha_v\beta_3$ integrin-containing membrane microdomains. *J. Biol. Chem.* **278**(33)**,** 31251-31260.

Mueller, S., Wimmer, E., and Cello, J. (2005). Poliovirus and poliomyelitis: A tale of guts, brains, and an accidental event. *Virus Res* **111**(2)**,** 175-93.

Nathanson, N., and Martin, J. R. (1979). The epidemiology of poliomyelitis: enigmas surrounding its appearance, epidemicity, and disappearance. *Am J Epidemiol* **110**(6)**,** 672-92.

Nomoto, A., Detjen, B., Pozzatti, R., and Wimmer, E. (1977). The location of the polio genome protein in viral RNAs and its implication for RNA synthesis. *Nature* **268**(5617)**,** 208-13.

Nomoto, A., Lee, Y. F., and Wimmer, E. (1976). The 5' end of poliovirus mRNA is not capped with m7G(5')ppp(5')Np. *Proc Natl Acad Sci U S A* **73**(2)**,** 375-80.

Oda, T., Ohka, S., and Nomoto, A. (2004). Ligand stimulation of CD155alpha inhibits cell adhesion and enhances cell migration in fibroblasts. *Biochem Biophys Res Commun* **319**(4)**,** 1253-64.

Ogita, H., and Takai, Y. (2006). Nectins and nectin-like molecules: roles in cell adhesion, polarization, movement, and proliferation. *IUBMB Life* **58**(5-6)**,** 334-43.

Ohka, S., Igarashi, H., Nagata, N., Sakai, M., Koike, S., Nochi, T., Kiyono, H., and Nomoto, A. (2007). Establishment of a poliovirus oral infection system in human poliovirus receptor-expressing transgenic mice that are deficient in alpha/beta interferon receptor. *J Virol* **81**(15)**,** 7902-12.

Ohka, S., Matsuda, N., Tohyama, K., Oda, T., Morikawa, M., Kuge, S., and Nomoto, A. (2004). Receptor (CD155)-dependent endocytosis of poliovirus and retrograde axonal transport of the endosome. *J Virol* **78**(13)**,** 7186-98.

Ohka, S., Ohno, H., Tohyama, K., and Nomoto, A. (2001). Basolateral sorting of human poliovirus receptor alpha involves an interaction with the mu1B subunit of the clathrin adaptor complex in polarized epithelial cells. *Biochem. Biophys. Res. Commun.* **287**(4)**,** 941-948.

Paralysis, T. C. o. T. o. t. N. F. f. I. (1951). Immunologic classification of poliomyelitis viruses. *Am. J. Hyg.* **54,** 191-274.

Parrot, J., and Joffroy, A. (1870). Note sur un cas de paralysie infantile. *Ach. Physiol. Norm. Pathol.* **3,** 309-316.

Parsley, T. B., Towner, J. S., Blyn, L. B., Ehrenfeld, E., and Semler, B. L. (1997). Poly (rC) binding protein 2 forms a ternary complex with the 5'-terminal sequences of poliovirus RNA and the viral 3CD proteinase. *Rna* **3**(10)**,** 1124-34.

Paul, A. (2002). Possible Unifying Mechanism of Picornavirus Genome Replication. *In* "Molecular Biology of Picornaviruses" (B. L. Semler, Wimmer, E., Ed.), pp. 227-246. ASM Press, Washington, DC.

Paul, A. V., van Boom, J. H., Filippov, D., and Wimmer, E. (1998). Protein-primed RNA synthesis by purified poliovirus RNA polymerase. *Nature* **393**(6682)**,** 280-4.

Pelletier, J., and Sonenberg, N. (1988). Internal initiation of translation of eukaryotic mRNA directed by a sequence derived from poliovirus RNA. *Nature* **334**(6180)**,** 320-5.

Perera, R., Daijogo, S., Walter, B. L., Nguyen, J. H., and Semler, B. L. (2007). Cellular protein modification by poliovirus: the two faces of poly(rC)-binding protein. *J Virol* **81**(17)**,** 8919-32.

Pincus, S. E., Diamond, D. C., Emini, E. A., and Wimmer, E. (1986). Guanidine-selected mutants of poliovirus: Mapping of point mutations to polypeptide 2C. *J. Virol.* **57,** 638-646.

Ravens, I., Seth, S., Forster, R., and Bernhardt, G. (2003). Characterization and identification of Tage4 as the murine orthologue of human poliovirus receptor/CD155. *Biochem Biophys Res Commun* **312**(4)**,** 1364-71.

Ren, R., Costantini, F., Gorgacz, E. J., Lee, J. J., and Racaniello, V. R. (1990). Transgenic mice expressing a human poliovirus receptor: a new model for poliomyelitis. *Cell* **63,** 353-362.

Reymond, N., Imbert, A. M., Devilard, E., Fabre, S., Chabannon, C., Xerri, L., Farnarier, C., Cantoni, C., Bottino, C., Moretta, A., Dubreuil, P., and Lopez, M. (2004). DNAM-1 and PVR regulate monocyte migration through endothelial junctions. *J Exp Med* **199**(10)**,** 1331-41.

Rieder, E., and Wimmer, E. (2002). Cellular receptors of picornaviruses: An overview. *In* "Molecular biology of picornaviruses." (B. L. Semler, and E. Wimmer, Eds.), pp. 61-70. ASM Press, Washington, D.C.

Rivera, V. M., Welsh, J. D., and Maizel, J. V., Jr. (1988). Comparative sequence analysis of the 5' noncoding region of the enteroviruses and rhinoviruses. *Virology* **165**(1)**,** 42-50.

Robbins, F. C., Enders, J. F., and Weller, T. H. (1950). The effect of poliomyelitis virus upon cells in tissue cultures. *J Clin Invest* **29**(6)**,** 841.

Rohll, J. B., Moon, D. H., Evans, D. J., and Almond, J. W. (1995). The 3' untranslated region of picornavirus RNA: features required for efficient genome replication. *J Virol* **69**(12)**,** 7835-44.

Rossmann, M. G. (2002). Picornavirus Structure Overview. *In* "Molecular Biology of Picornaviruses" (B. L. Semler, Wimmer, E., Ed.), pp. 27-38. ASM Press, Washington, DC.

Rossmann, M. G., and Johnson, J. E. (1989). Icosahedral RNA virus structure. *Annu Rev Biochem* **58,** 533-73.

Sabin, A. B. (1956). Pathogenesis of poliomyelitis; reappraisal in the light of new data. *Science* **123**(3209)**,** 1151-7.

Sabin, A. B. (1957). Properties and behavior of orally administered attenuated poliovirus vaccine. *J Am Med Assoc* **164**(11)**,** 1216-23.

Salk, J. E. (1954). [Study of non-pathogenic poliomyelitis vaccines.]. *Minerva Med* **45**(97)**,** 1502-3.

Sato, T., Irie, K., Ooshio, T., Ikeda, W., and Takai, Y. (2004). Involvement of heterophilic trans-interaction of Necl-5/Tage4/PVR/CD155 with nectin-3 in formation of nectin- and cadherin-based adherens junctions. *Genes Cells* **9**(9)**,** 791-9.

Schaffer, F. L., and Schwerdt, C. E. (1955). Crystallization of Purified Mef-1 Poliomyelitis Virus Particles. *Proc Natl Acad Sci U S A* **41**(12)**,** 1020-3.

Schlesinger, R. W., Morgan, I. M., and Olitsky, P. K. (1943). Transmission to Rodents of Lansing Type Poliomyelitis Virus Originating in the Middle East. *Science* **98**(2551)**,** 452-454.

Seth, S., Maier, M. K., Qiu, Q., Ravens, I., Kremmer, E., Forster, R., and Bernhardt, G. (2007). The murine pan T cell marker CD96 is an adhesion receptor for CD155 and nectin-1. *Biochem Biophys Res Commun* **364**(4)**,** 959-65.

Sonenberg, N. (1987). Regulation of translation by poliovirus. *Adv Virus Res* **33,** 175-204.

Takai, Y., Irie, K., Shimizu, K., Sakisaka, T., and Ikeda, W. (2003). Nectins and nectin-like molecules: roles in cell adhesion, migration, and polarization. *Cancer Sci* **94**(8)**,** 655-67.

Teterina, N. L., Gorbalenya, A. E., Egger, D., Bienz, K., and Ehrenfeld, E. (1997). Poliovirus 2C protein determinants of membrane binding and rearrangements in mammalian cells. *J Virol* **71**(12)**,** 8962-72.

Toyoda, H., Yin, J., Mueller, S., Wimmer, E., and Cello, J. (2007). Oncolytic treatment and cure of neuroblastoma by a novel attenuated poliovirus in a novel poliovirus-susceptible animal model. *Cancer Res* **67**(6)**,** 2857-64.

Tyler, K. L., and Fields, B. N. (1990). Pathogenesis of viral infections. *In* "Virology" (B. N. F. a. D. M. Knipe, Ed.), Vol. 1, pp. 191-239. 2 vols. Raven Press, New York.

Vulpian, A. (1870). Cas d;atrophie musculaire graisseuse datant de l'enfance. Lesions des cornes anterieures de la substance grise de la moelle epiniere. *Arch. Physiol. Norm. Pathol.* **3,** 316-325.

Wimmer, E. (1982). Genome-linked proteins of viruses. *Cell* **28**(2)**,** 199-201.

Wimmer, E., Harber, J. J., Bibb, J. A., Gromeier, M., Lu, H.-H., and Bernhardt, G. (1994). Poliovirus Receptors. *In* "Cellular receptors for animal viruses" (E. Wimmer, Ed.), pp. 101-127. Cold Spring Harbor Laboratory, Cold Spring Harbor.

Wimmer, E., Hellen, C. U. T., and Cao, X. M. (1993). Genetics of poliovirus. *Ann. Rev. Genet.* **27,** 353-436.

Xiang, W., Harris, K. S., Alexander, L., and Wimmer, E. (1995). Interaction between the 5'-terminal cloverleaf and 3AB/3CDpro of poliovirus is essential for RNA replication. *J Virol* **69**(6)**,** 3658-67.

Xing, L., Tjarnlund, K., Lindqvist, B., Kaplan, G. G., Feigelstock, D., Cheng, R. H., and Casasnovas, J. M. (2000). Distinct cellular receptor interactions in poliovirus and rhinoviruses. *Embo. J.* **19,** 1207-1216.

Yalamanchili, P., Harris, K., Wimmer, E., and Dasgupta, A. (1996). Inhibition of basal transcription by poliovirus: a virus- encoded protease (3Cpro) inhibits formation of TBP-TATA box complex in vitro. *J Virol* **70**(5)**,** 2922-9.

Yanagiya, A., Jia, Q., Ohka, S., Horie, H., and Nomoto, A. (2005). Blockade of the Poliovirus-Induced Cytopathic Effect in Neural Cells by Monoclonal Antibody against Poliovirus or the Human Poliovirus Receptor. *J Virol* **79**(3)**,** 1523-32.

Yanagiya, A., Ohka, S., Hashida, N., Okamura, M., Taya, C., Kamoshita, N., Iwasaki, K., Sasaki, Y., Yonekawa, H., and Nomoto, A. (2003). Tissue-specific replicating capacity of a chimeric poliovirus that carries the internal ribosome entry site of hepatitis C virus in a new mouse model transgenic for the human poliovirus receptor. *J Virol* **77**(19)**,** 10479-10487.

Yang, W. X., Terasaki, T., Shiroki, K., Ohka, S., Aoki, J., Tanabe, S., Nomura, T., Terada, E., Sugiyama, Y., and Nomoto, A. (1997). Efficient delivery of circulating poliovirus to the central nervous system independently of poliovirus receptor. *Virology* **229**(2)**,** 421-428.

Yogo, Y., and Wimmer, E. (1972). Polyadenylic acid at the 3'-terminus of poliovirus RNA. *Proc Natl Acad Sci U S A* **69**(7)**,** 1877-82.

Zhang, S., and Racaniello, V. R. (1997). Expression of the poliovirus receptor in intestinal epithelial cells is not sufficient to permit poliovirus replication in the mouse gut. *J. Virol.* **71**(7)**,** 4915-4920.

Appendix A

Characterization of the New World Monkey homologues of the Human Poliovirus receptor CD155

Shaukat Khan, Xiaozhong Peng, Jiang Yin, Ping Zhang and Eckard Wimmer

(Accepted for publication in Journal of Virology)

Characterization of the New World Monkey homologues of the Human Poliovirus receptor CD155

Shaukat Khan[1], Xiaozhong Peng[1Ψ], Jiang Yin[1§], Ping Zhang[2] and Eckard Wimmer[1*]

[1]*Department of Molecular Genetics and Microbiology, Stony Brook University, Stony Brook, NY 11794*

[2]*Department of Biological Sciences, Purdue University, West Lafayette, IN 47907*

*Corresponding author. Mailing address: Department of Molecular Genetics and Microbiology, Life Science Building Room 213, Stony Brook University, Stony Brook, NY 11794-5222. Phone: (631) 632-8787. Fax: (631) 632-8891, Email: ewimmer@ms.sunysb.edu.

[Ψ]Current address: The National Laboratory of Medical Molecular Biology, Institute of Basic Medical Sciences, Chinese Academy of Medical Sciences and Peking Union Medical College, Beijing, China.

[§]Current address: Department of Biochemistry, University of Alberta, Edmonton, Canada T6G 2H7

Word Number: 281 (Abstract), 6, 416 (Full text)

In contrast to the Old World Monkeys (OWMs), most New World Monkeys (NWMs) are not susceptible to poliovirus (PV), regardless of the route of infection. We have investigated the molecular basis of restricted PV pathogenesis of NWMs with two kidney cell lines of NWMs, TMX (Tamarin) and NZP-60 (Marmoset), and characterized their PV receptor homologues. TMX cells were susceptible to infection by PV1 (Mahoney) and PV3 (Leon) but not by PV2 (Lansing). Binding studies to TMX cells indicated that the formation of PV/receptor complexes increases when measured first at 4°C and then at 25°C whereas PV2 did not significantly bind to TMX cells at either temperature. On the other hand, NZP-60 cells were not susceptible to infection by any of the PV serotypes. However, a low amount of PV1 bound to NZP-60 cells at 4°C but there was no increase of binding at 25°C. In contrast, both NWM cell lines supported genome replication and virion formation when transfected with viral RNAs of either serotype, an observation indicating that infection was blocked in receptor-virus interaction. To overcome the receptor block, we substituted 3 amino acids in the marmoset receptor (nCD155), H80Q, N85S, and P87S, found in the human PV receptor, hCD155. Cells expressing the mutant receptor (L-nCD155mt) were now susceptible to infection with PV1, which correlated with an increase in PV1 bound receptor complexes from 4°C to 25°C. L-nCD155mt cells were, however, still resistant to PV2 and PV3. These data show that an increase in the formation of PV/receptor complexes, when measured at 4°C and at 25°C correlates with, and is an indicator of, successful infection at 37°C, suggesting that the complex formed at 25°C may be an intermediate in PV uptake.

Poliovirus (PV) is characterized by a highly restricted host and tissue tropism. Infecting by the oral-fecal route, only humans are natural hosts of PV. Disease symptoms are predominantly neurological but they are rare, depending upon the serotype (43). The major determinant of virus pathogenicity is the human cell surface receptor CD155 (PVR) although other factors such as interferon also plays an important role (21). CD155 has been thoroughly characterized (43) and homologues of this protein are known to exist in primates and non-primates (22). Non-human primates, such as chimpanzees and African green monkeys (AGMs), which are members of Old World Monkeys (OWMs)

have been shown to be susceptible to PV infection. In the wild, however, PV infections of non-human primates are not well documented.

PV is a non-enveloped plus-stranded RNA virus, a member of the genus *Enterovirus* and in the *Picornaviridae* family. Its genome is approximately 7,500 nucleotides long, carrying a small viral protein (VPg) covalently linked to the 5' terminus and a poly(A) tail at the 3' terminus. The genome encodes a single large polyprotein, encoding structural proteins (P1) and non-structural proteins (P2 and P3). Proteolytic processing of P1, P2, and P3 by the virus-encoded proteinases $2A^{pro}$ and $3C^{pro}/3CD^{pro}$ generates the functional proteins. Sixty copies of each of the four capsid polypeptides (VP1-VP4), processed from P1, assemble to form a capsid shaped as an icosahedron with five-, three- and two-fold axes (17, 51). In contrast to VP1, VP2, and VP3, the smallest capsid polypeptide, VP4, is located inside the capsid. The capsid proteins, VP1, VP2 and VP3, fold as eight stranded antiparallel β-barrels whereby the antigenic regions are hydrophilic β-turns within these structures (18, 52). They give rise to three different sets of neutralization antigenic sites and, hence, the virus exists in three serotypes (types 1 – 3) (8, 47). A notable structural feature of the capsid is the "canyon", a depression characteristic for capsids of all entero- and rhinoviruses, which is a site of cellular receptor binding (51).

CD155, the only known cellular receptor mediating uptake of PV into cells, is a highly glycosylated single-span membrane protein (about 80 kDa) belonging to the immunoglobulin superfamily (29, 36, 50). CD155 can be broadly divided into 5 domains: three extracellular Ig-like domains (one variable (V) and two constant (C) domains), a transmembrane domain, and a cytoplasmic tail (Fig. 1). The human *CD155* gene is expressed in cells in four variants (α, β, γ, δ) through alternate splicing of the CD155 transcript RNA. Two of the variants (β and γ) occur in a soluble form, while the other two variants (α and δ) are membrane bound and serve as the receptor for PV. Human CD155 (hCD155), α and δ, differ only in the length and sequence of their cytoplasmic (C-terminal) tail. Genetic and biochemical evidence have identified the V-domain of CD155 as the virus binding domain (1, 3, 5, 13-15, 39, 54). Interestingly, these genetic modifications have indicated that the three PV serotypes interact with the V-domain in a slightly different manner (13), a phenomenon that we have observed also

in our studies of the interaction between the hCD155 homologues of NWMs reported here.

CD155 is the founding member of a family of immunoglobulin molecules, whose function has generally been characterized as adhesion proteins (44). Specifically, CD155 has been shown to mediate cell-to-matrix contacts by specifically binding to vitronectin (31). Moreover, it has been shown that CD155 recruits the adhesion molecule nectin-3 to cell-cell junctions through a trans-heterophilic interaction (42). CD155 also acts as a ligand for DNAX accessory molecule-1 (DNAM-1) and this interaction results in DNAM-1-dependent enhancement of NK-mediated lysis of target cells (7). The C-terminal domains of both membrane bound forms of hCD155, α and δ, interact with Tctex-1, a small protein of the dynein motor complex, and are involved in retrograde axonal transport of the virus-receptor complex (41, 45). Another element found only in the C- terminal domain of hCD155α is the tyrosine containing binding motif of the μ1B subunit of the clathrin adaptor complex, which directs CD155α transport to the basolateral surface in polarized epithelial cells (46).

Shortly after the discovery of hCD155, putative homologues were described, most of which were related to, but not homologous to hCD155 (10, 40, 49). The most thoroughly studied human and rodent proteins related to CD155 are called nectins (44), while the rodent orthologue of CD155 has now been named as Tage4 (2, 49). Just like the nectins, however, Tage4 has no affinity to PV ((49); Khan, S., Mueller, S. and Wimmer, E., unpublished data). The only CD155 related proteins with an affinity to PV are found in Chimpanzees, OWMs, and NWMs. OWMs, exemplified by AGMs have been thoroughly studied because of their susceptibility to PV by oral infection, which is highly inefficient compared to humans (30, 53). AGMs posses two genes coding for three membrane-bound forms of CD155 (30). These are two splice variants, AGMα1 and AGMδ1, as well as AGMα2, which is encoded by a second locus in the genome (30). Both AGMα1 and AGMα2 serve as functional PV receptors and have amino acid similarity to hCD155α of 90.2% and 86.4%, respectively (30).

Of the monkey species, the least studied with respect to PV pathogenesis are NWMs, whose habitat is limited to the tropical forests of Central and South America. NWMs are composed of four families; *Cebidae*, *Aotidae*, *Pitheciidae,* and *Atelidae*.

Unlike OWMs, early studies have indicated that NWMs cannot be infected by the oral route, and any susceptibility by injection may depend not only on the animal species but also on the PV serotype (20). Similarly, early tissue culture studies have shown that only PV1 displayed susceptibility to capuchin monkey cells, however with no cytopathic effect (26-28). Recently, Koike and his colleagues have analyzed the gene specifying the hCD155 homologue of brown capuchin monkeys (Subfamily *Cabinae,* Genus *Cebus*). They showed that the V-domain of capuchin monkey cDNA, when spliced onto the C-domain of hCD155, could promote infection of mouse L-cells that were transformed with the chimeric receptor (22). Infection, however, was restricted to only one serotype (PV1) and no analyses of the mechanism of restriction have been reported (22).

The aim of our studies was to examine whether the susceptibility of NWMs to infection by different PV serotypes is due to virus-receptor interaction or to translation and replication. We have selected two kidney cell lines from tamarins (TMX) and marmosets (NZP-60) of the genera *Saguinus* and *Callithrix*, respectively, and belonging to the subfamily of *Callitrichinae* of NWMs. Marmoset cells were found to be resistant to PV infection with all PV serotypes, while tamarin cells showed sensitivity only to PV1 and PV3. These phenotypes have been observed in spite of high expression of the CD155 homologues by both NWM cells and by normal translation and replication of PV RNAs or of the PV luciferase (PV-Luc) replicon once transfected into the cells. However, we have observed significant differences in the binding of PV serotypes to NWM cell lines. Only PV1 is able to bind (but not infect) NZP-60 cells whereas PV2 and PV3 display no virus-receptor bound complexes on these cells. Moreover, we detected virus-receptor bound complexes with PV1 and PV3 but not PV2 on TMX cells. Generally, if the formation of virus-receptor complexes was higher at 25°C than at 4°C, the binding would lead to cellular infection at 37°C, an observation suggesting that the complex formed at 25°C may be an intermediate in the early steps of infection. When mutations were introduced into the V domain of the marmoset CD155, the mutant receptor was able to bind PV1 and also catalyze uncoating and infection. Our results indicate that the restriction of PV infection of NWM cell lines is related to their receptors' ability to form initial complexes with the virus serotype in question.

MATERIALS AND METHODS

Cloning of NWMs CD155 cDNAs. Based on the conserved cDNA sequences of human and AGM CD155, primers were designed corresponding to hCD155 cDNA sequence 122-136 (5'-TGGGCGACTCCGTGA-3') and 942-977 (5'-CACCAATGCCC TAGGAGCTCGCCAGGCAGAACTGAC-3'). RT-PCR was performed on total RNA of the NWM cell lines and the 800 bp fragment was amplified and sequenced. Sequence specific primers from partial NWM CD155 cDNAs were designed and the 5' and 3' ends were amplified using the 5'/3' Race Kit (Roche). The full length CD155 cDNA was amplified using primers, TMX 5' (5'-GGCGATATCAGAGCTAGGCCGCCGCGTG-3'), TMX 3' (5'-GTTCTAGAATCCTA GGAAGAGTTGGCCAC AG-3'), NZP 5' (5'-GGCGATATCAGAGCCATGGCCGCCGCGTG-3'), and NZP 3' (5'-ACTCTAGACT GTCACCTTGTGCCCTTTGTCTG-3'). The TMX and NZP CD155 cDNA were cloned into mammalian expression vector pcDNA 3.1 (+) (Invitrogen) using restriction sites, *EcoRV* and *XbaI*. The N-terminal signal peptide and transmembrane helix were identified in the deduced protein sequence using SignalP and TMHMM on CBS prediction server (http://www.cbs.dtu.dk/services) (4, 25).

Cells. HeLa R19, mouse fibroblast Ltk^- cells, and stably transfected Ltk^- cells with PV receptor variants were maintained in Dulbecco's modified Eagle's medium (DMEM), containing 10% fetal bovine serum (FBS) and 1% penicillin/streptomycin. Primary kidney cells from a black tailed marmoset (*callithrix argentata*) were obtained from ATCC (CRL-1924; designation NZP-60). A Tamarin (*saguinus mystax*) primary kidney cell line, designated TMX, was generously donated by Dr. S. U. Emerson and Dr. R. H. Purcell, of the National Institute of Health. TMX were maintained in DMEM containing 5% FBS, 5% bovine calf serum (BCS), and 1% penicillin/streptomycin. NZP-60 cells were maintained in 50% DMEM and 50% F-12 nutrient media containing 10% FBS and 1% penicillin/streptomycin.

Generation of stable cell lines. Ltk^- mouse fibroblast were maintained in DMEM containing 10% FBS. Cells were plated 24 h before transfection on 35 mm plate. The cells were transfected with pcDNA 3.1 (+) plasmid containing NWMs CD155 variants with Lipofectamine® 2000 transfection reagent (Invitrogen). After 24 h the cells were selected in presence of Geneticin® (Invitrogen). After selection, cell pools were labeled with mouse monoclonal antibody (mAb) p286 (donated by Dr. Nomoto) at a

concentration of 20 μg/ml. Each sample was washed with phosphate buffered saline solution (PBS) and then stained with FITC-conjugated goat anti-mouse IgG (BD bioscience). Labeled cells were sorted by fluorescent-activated cell sorting (FACS) VANTAGE (Beckton Dickinson). Sorted cell lines were maintained in DMEM, containing 10% FBS and 1% penicillin/streptomycin.

Preparation of purified PV serotypes and viral RNA. Polioviruses used in this study were the most commonly studied representatives of the three serotypes (Mahoney, Lansing, and Leon). It could be argued that experiments with different strains of a given serotype would show different results. We cannot exclude this possibility but we believe strain variations would not change the basic conclusions drawn from the experiments described here. This is because structurally, all three serotypes have similar architecture (11, 17, 32), the serotypes largely being defined by numerous surface changes in exposed protrusions of the virion (37). Changes to switch serotypes would be dramatic while changes to yield different strains would be subtle. We therefore assume here that our experiments of receptor/virus interaction with, say, serotype 1 PV(M) is likely to reflect experiments with different strains of the same serotype. PV1 (Mahoney), PV2 (Lansing) and PV3 (Leon) were grown in HeLa cells at 37°C and the cells were harvested after 8 h post infection. The plates were subjected to three consecutive freeze-thaw cycles and the virus titer was determined by plaque assay on HeLa cell monolayers, as previously described (48).

To obtain viral RNA genome, the PV serotypes were additionally purified by CsCl gradient centrifugation. Viral RNA was isolated from the purified virus stocks with a 1:1 mixture of phenol and chloroform. The purified viral RNA was precipitated by the addition of 2 volumes of ethanol and resuspended in RNase free water.

One-step growth curve of PV serotypes. Cell monolayers (1×10^6 cells) were incubated with 10 multiplicity of infection (MOI) of virus for 30 min, at room temperature, on a rocker platform. After 30 min, cells were washed three times with PBS and incubated at 37°C in DMEM containing 2% BCS. The cells were harvested at 0, 2, 4, 6, 8, 12, 24, and 48 h post infection. The plates were subjected to three consecutive freeze-thaw cycles, and the viral titers of the supernatants were determined by plaque assay on HeLa cell monolayers, as previously described (48).

Transfection of viral RNAs into cells. The purified viral RNA was transfected into monolayers with the TransMessenger Transfection Reagent (Qiagen). Transfected cells were incubated in DMEM, supplemented with 2% BCS at 37°C either until complete cytopathic effect (CPE) was observed or for at least 24 h post-transfection. After three rounds of freeze-thaw cycles, the lysate was clarified of cell debris by low-speed centrifugation. Virus titers were determined by plaque assay (48).

In vitro transcription and transfection of PV luciferase (PV-Luc) replicon. The PV-Luc replicon (33) was digested with *DraI* before transcription with T7 RNA polymerase. RNA transcripts were transfected into monolayers of various cell types in 35mm dishes by the TransMessenger Transfection Reagent (Qiagen).

Measurement of PV RNA translation and replication using luciferase replicons. After transfection with PV-Luc replicon, various cell lines were incubated at 37°C in DMEM with 2% BCS. The cells were grown with or without 2 mM guanidine hydrochloride (GnHCl). At 12 h post-transfection, the growth medium was removed from the dishes, and the cells were washed gently with 2 ml of PBS. The 35 mm dishes were lysed with 300 µl of "passive" lysis buffer (Promega). 50 µl of luciferase assay reagent (Promega) was mixed with 20 µl of lysate, and the firefly luciferase activity was measured with an Optocomp I luminometer (MGM Instruments, Inc.).

Detection of CD155 expression levels on cell surface by flow cytometry. $1x10^6$ cells in suspension were incubated for 30 min at room temperature with or without mAb p286 at a concentration of 20 µg/ml. mAb recognizes an epitope of the V-domain of hCD155 (55). Each sample was washed with PBS and then stained with FITC-conjugated goat anti-mouse IgG (BD bioscience). After washing, 10^3 cells were analyzed by FACS caliber (Beckton Dickson).

Binding assay of PV serotypes. PV1, PV2, and PV3 capsid proteins were labeled with [^{35}S] methionine and the viruses were purified by CsCl gradient centrifugation as previously described (6). $1x10^6$ cells were incubated with 10^8 PFU of labeled virus at 4ºC or 25°C for 30 min. After incubation, the virus-cell complex was pelleted by microcentrifugation and the cell pellets were washed 3 times with PBS. The amount of radioactivity of the cell pellet was quantitated with a liquid scintillation

counter (Packard Tri-Carb) in counts per minute (cpm). All samples were done in triplicate.

Alteration assays. Alteration assays were performed as described previously (12). Purified [^{35}S] methionine-labeled virions (approximately 10 M.O.I) were added to cells in DMEM at a density of 5 X 10^6 cells per ml and incubated for 30 min at 25°C. The cells were washed and fresh DMEM with 2% FBS was added and cells were incubated at 37°C for 45 min. The cells were pelleted and dissolved in 0.5% Triton X-100 in PBSA (PBS containing 0.01% bovine serum albumin). The solution was layered on top of 15% to 30% sucrose gradient in PBSA. The gradients were centrifuged for 75 min at 40,000 rpm in an SW41 rotor. Fractions were collected from the bottom and counted as described above. The gradient markers were made by heating labeled PV1 at 56°C for 10 min followed by incubation on ice for 20 min. Equal amount of heated and unheated virus were layered on the gradient.

Site-Directed Mutagenesis. The following primers were used to make mutations in the marmoset CD155 and tamarin CD155 cDNA in pcDNA 3.1 (+) vector by site directed mutagenesis kit (Stratagene): H77Q Sense (5'-CGTCTTCCACCAAACTCAG GGCCCC-3'); H77Q Antisense (5'-GGGGCCCTGAG TTTGGTGGAAGACG-3'); NZP N82YP/SYS Sense (5'-CAGGGCCCCAGCTACTCGGAGTCCGAAC-3'); NZP N82YP/SYS Antisense (5'-TCGGACTCCGAGTAGCTGGGGCCCTGAG-3'), TMX N80YL/SYS Sense (5'-CAGGGCCCCAGCTACTCGGAGTCCGA ACG-3'), and TMX N80YL/SYS Antisense (5'-TTCGGACTCCGAGTAGCTGGGCCCTG AG-3').

Nucleotide sequence accession numbers. The nucleotide sequence data for the cDNAs for marmoset CD155 (nCD155) and tamarin CD155 (tCD155) have been submitted to GenBank under accession numbers, EU277851 and EU277852, respectively.

RESULTS

Identification of CD155 homologues in NWM cell lines. To ascertain whether TMX and NZP-60 cells have a homologue of CD155, we first stained the cells with a panel of monoclonal antibodies against hCD155 of which mAb p286 bound to receptors expressed on both NWM cells with the same intensity as on Ltk$^-$ cells over expressing hCD155 (data not shown). This result suggested that the NWM cells expressed putative

homologues of hCD155 that share structural motifs. To identify this receptor, we first amplified an 800 bp fragment by PCR from a cDNA library of the NWM cell lines, using primers based on highly conserved sequences in human and AGM CD155. This 800 bp fragment was sequenced and species specific primers were used for the rapid amplification of the 5' and 3' cDNA ends (RACE) to obtain the full length cDNA sequences of tamarin CD155 (tCD155) and marmoset CD155 (nCD155).

On analysis of the cDNA sequences, we found that tCD155 has an open reading frame (ORF) of 1,167 bp, which encodes a 388 amino acid polypeptide, while the nCD155 has a slightly longer ORF of 1,200 bp, encoding a 399 amino acid polypeptide (Fig. 1). The tCD155 and nCD155 share 74% and 75% amino acid identity, and 87% and 88% nucleotide identity, respectively, with hCD155α (data not shown). In addition to sequence similarities with hCD155, both tCD155 and nCD155 express the Ig-like structure V-C2-C2, a hallmark of the immunoglobulin superfamily, similar to hCD155 and AGM CD155 (Fig. 1). In comparison to hCD155, which has eight N-glycosylation sites, tCD155 and nCD155 have six sites, while AGMα1 has seven, AGMδ1 has six, and AGMα2 has five sites (30) (Fig. 1). The cytoplasmic tails of the tCD155 and nCD155 differ in length, however, both share a consensus sequence for the binding of Tctex-1 and the tyrosine-containing binding motif for the μ1B subunit with hCD155α (Fig. 1) (38, 46). The close relationship of the extracellular domains and the presence of consensus binding sequences in the cytoplasmic tails in all receptor molecules (Fig. 1) suggest that the NWM CD155 homologues have biological functions similar to that of hCD155. It should be noted that an examination of the NWM receptors did not reveal to us distinct isoforms or receptors expressed from gene duplications.

Susceptibility of NWM cell lines to infection with PV serotypes. Given that the NWM cell lines express a CD155 homologue, we performed one-step growth curve experiments to determine their susceptibility to infection with different PV serotypes (Fig. 2). In TMX cells, PV1 showed delayed early growth compared to that observed in HeLa cells; although by 48 h post infection, the viral titers were comparable (Fig. 2A). PV3, on the other hand, produced lower viral titers after 48 h post infection, when compared to HeLa cells (Fig. 2C). PV2 did not show growth on TMX cells, however there was a decrease in titer at 5 h followed by an increase at 12 h (Fig. 2B).

304 Nevertheless the titer of the virus at incubation and after 48 h was similar on the cells
305 (Fig. 2B). Finally, NZP-60 cells were resistant to infection with all PV serotypes (Fig. 2).
306 **Resistance of NWMs to PVs is not related to inhibition of translation or RNA**
307 **replication.** There are several possible explanations of the NZP-60 cells' resistance to
308 infection with all PV serotypes and of the TMX cells' resistance to only PV2. First,
309 resistance to infection could be due to a defect in the interaction between virus and
310 receptor. Second, there could be an intracellular block at the stage of translation or
311 replication. To test the latter possibility, both TMX and NZP-60 cells were transfected
312 with PV1, PV2 and PV3 RNA and found to produce virus titers comparable to those
313 obtained on transfected Ltk$^-$ cells, regardless of which cell lines were used (Fig. 3A).
314 To study translation in the absence of replication, we used a PV-Luc replicon that
315 contained the firefly luciferase gene instead of the P1 domain of the PV polyprotein (33).
316 After transfection with the replicon, the cells were incubated in the presence of guanidine
317 HCl (GnHCl), a potent inhibitor of PV RNA replication, and the luciferase activity
318 measured 12 h post transfection. The luciferase activity obtained in cell cultures with
319 GnHCl represents translation of the input mRNAs. In mouse Ltk$^-$ cells there was a 10
320 fold increase in luciferase signal when GnHCl was omitted from the culture and similar
321 increases were also observed with the TMX and NZP-60 cells (Fig. 3B). We conclude
322 from this observation that intracellular replication of genomic RNA of all three serotypes
323 analyzed is not blocked. This data suggests that the resistance to infection of NWM cell
324 lines with different PV serotypes is related to one or more of the earliest steps in the viral
325 life cycle: receptor binding, uptake, or uncoating.
326 **CD155 expression levels on NWM cell lines.** To determine whether
327 susceptibility of the NWM cells to PV infection is related to the surface expression of the
328 CD155 homologues, we employed flow cytometry and mAb p286 isolated against an
329 epitope of the V-domain of hCD155 (55). By this procedure we found the signal to
330 CD155 on TMX cells to be comparable to that on HeLa cells and two-fold higher on
331 NZP-60 cells than on HeLa cells (Fig. 4). Considering the possibility that mAb p286
332 may recognize the different receptors with different affinities we cannot firmly conclude
333 that more nCD155 is expressed on NZP-60 cells than hCD155 on HeLa cells. However,
334 there can be no doubt that both NWM receptors are expressed on the respective monkey

kidney cells and, consequently, it is unlikely that that the inability of some PV strains to grow on the NWM cell lines is the result of insufficient levels of receptor molecules for interaction with PV.

Binding efficiency of PV strains to NWM cell lines. Infection by PV is initiated when the virus docks to CD155 receptor molecules at the cell surface. This interaction subsequently leads to uncoating and internalization of the viral genome (14). Having established that PV can translate and replicate in both TMX and NZP-60 cells, we were interested in determining the binding ability of the PV serotypes to the NWM receptors by a receptor-excess assay. It has been shown previously that PV interacts with CD155 in two distinct steps (35). The first step can be studied at 4°C and is probably electrostatic in nature. The second step occurs at physiological temperatures and leads to irreversible structural changes of the virion, resulting in the formation of an A-particle in which VP4 is absent (16). The first step in the entry pathway is the formation of an initial binding complex, which can be isolated at below physiological temperatures. Here we have isolated this initial binding complex into two separate steps, at 4°C and at 25°C using [^{35}S]-labeled virus. At temperatures from 0°C to 25°C, the virus bound to cells can be recovered in an active form (19), thus we can study virus-receptor binding complexes at 25°C without forming A-particles.

On analysis of the data from the binding assays, we found PV1-receptor complexes on TMX cells at 4°C, but the amount of virus-receptor complexes increased by 4 fold at 25°C (Fig. 5A). In contrast, PV3 showed lower amount of bound complexes at 4°C compared to PV1, but the amount of bound complexes increased by 10 fold at 25°C (Fig. 5C). PV2, on the other hand, showed same amount of bound complexes as Ltk$^-$ cells at 4°C or at 25°C (Fig. 5B). PV1-receptor complexes were observed on NZP-60 cells, however without an appreciable increase in binding from 4°C to 25°C (Fig. 5A). The levels of PV2 and PV3 bound complexes on NZP-60 cells were similar to background levels on Ltk$^-$ cells at either 4°C or 25°C (Fig. 5B and 5C).

The observed increase in binding of PV1 and PV3 to tCD155 at 25°C, in comparison to 4°C, suggested to us that the increase in association of the virus to the receptor led to successful infection. This would also explain why PV1 does not infect

NZP-60 cells: binding of this strain to nCD155 is very low and did not significantly increase at 25°C when compared to that at 4°C.

Conformationally altered virus particles. As noted above, the increase in the amount of virus-receptor complexes from 4°C to 25°C correlated with successful infection of TMX cells at 37°C (Figs. 2 and 5). Next we wanted to determine whether the transition from native to subviral particles can be demonstrated directly upon incubation of the NWM cells with PV. As illustrated in Fig. 6, TMX cells produced 135S particles although the conversion was inefficient under the conditions of the experiment. NZP-60 cells, on the other hand, did not yield a significant amount of subviral particles.

Mutational analysis of the V domain of the nCD155 and tCD155. Unlike TMX cells, which showed an increase in receptor bound complexes from 4°C to 25°C with PV1, NZP-60 cells did not bind a significant amount of virus and there was no appreciable change in complex formation from 4°C to 25°C. The nCD155, therefore, can bind PV1 weakly but it cannot catalyze the structural changes in the virion necessary for infection. Since the V domain of CD155 is the site of virus binding, we analyzed the V domains of human, AGM, tCD155 and nCD155 by alignment to identify potential amino acids that are involved in binding and uncoating of PV1 (Fig. 7; numbering of amino acids in the V domains of tCD155 and nCD155 will be referred to according to the numbering of hCD155). Previously, mutations of hCD155 in the C'C", C"D, DE, EF loops, and in the N-terminal part of the C" β-strand were found to affect both PV1 binding and replication (1, 5, 9, 13, 34, 39).

On analysis of the CD155 homologue alignments, we found six amino acids, Q80, S85, S87, K90, N105 and V115, that have been implicated in viral binding as determined by cryoelectron microscopy (15). The corresponding residues have been substituted in the loops and the β-sheet of both tCD155 and nCD155 (Fig 7). Based on previous mutagenesis studies, we can eliminate from consideration three of the six amino acid positions, K90, N105, and V115 because they did not influence binding and replication (5). It has been previously shown that a K90/D mutation in hCD155 did not affect either PV binding or replication (5). Therefore, the corresponding K90/E substitution found in NWM CD155 is also unlikely to affect PV binding and replication. Similarly, an N105/D substitution, which eliminates an N-glycosolation site, is also present in the AGMα1, a

functional receptor (Fig. 7). In addition, it was shown that hCD155 lacking two N-glycosolation sites (N105/D and N120/S) had an enhanced binding affinity to the virus (5). We doubt, therefore, that a change of the N105 site will significantly influence binding to the NWM receptors. Mutation of E116DE to AAA in the EF loop abolished virus binding, likely due to the loss of consecutive charged residues in this region of hCD155 (5). Since a V115/A substitution does not result in charge disruption of the EF loop, we predict that this substitution would also not significantly influence binding of PV.

This leaves us with three mutations that may affect the binding of PV to the receptors nCD155 and tCD155. The amino acids Q80, S85, and S87 mutations in hCD155 have all resulted either in decrease or loss of PV1 binding (5, 13, 39). Therefore, we changed the corresponding amino acids in NWM receptors to H80/Q for both NWM receptors and N85YP/SYS and N85YL/SYS for nCD155 and tCD155, respectively (Fig. 7, boxed residues). The cDNAs of mutant and wild type (wt) NWM CD155 receptors were then used to create stable mouse Ltk$^-$ cell lines expressing the proteins. As indicated earlier, mouse Ltk$^-$ cells lack a receptor for PV and only become sensitive to infection if a functional receptor is expressed or viral RNA is transfected into the cells. Interestingly, stably transformed mouse Ltk$^-$ cell lines expressing a nCD155 mutant (L-nCD155mt) or a tCD155 mutant (L-tCD155mt) were competent to bring about a productive infection with significant titers of PV1 in both cell lines (Fig. 8A).

Since L-nCD155mt and L-tCD155mt cells were permissive to PV1 infection, we performed binding assays on the cells to ascertain the amount of virus-receptor complexes. L-nCD155mt cells showed very low amount of PV1 receptor complexes at 4°C; however, there was a 3 fold increase in binding from 4°C to 25°C (Fig. 8B). Interestingly, PV1-receptor complexes were found on NZP-60 cells, whereas there were no complexes on L-nCD155 cells (Figs. 5A and 8B). Both L-tCD155 and L-tCD155mt cells exhibited a 2 to 3 fold increase in binding to PV1 after a temperature change from 4°C to 25°C, however, L-tCD155mt cells had higher amount of PV1-receptor complexes than L-tCD155 cells at both temperatures (Fig. 8B). Although L-nCD155mt cells bound PV1 with concomitant infection, neither PV2 nor PV3 bound to or caused infection of these cells (data not shown).

DISCUSSION

We have identified CD155 homologues (tCD155 and nCD155) to the human poliovirus receptor (hCD155) in cells of tamarin and marmoset monkeys (TMX and NZP-60), two species of the NWMs. The proposed structures of tCD155 and nCD155 that display amino acid identities of 74% and 75%, respectively, with hCD155α place these proteins into the new Ig superfamily (Fig. 1) of which hCD155 is the founding member. In general, CD155 homologues show a high degree of sequence divergence across different species. For example, hCD155α is 90% similar to AGMα1, a member of the OWMs, but only 38% to Tage4, the rodent orthologue of CD155 (49). Yet, Tage4 also expresses Tctex-1 and the tyrosine-containing binding motif of the μ1B subunit in its C-terminal domain, and its expression in the GI tract in rodents (49) is very similar to that of CD155 in the human GI tract (23). It is tempting to speculate that members of the new CD155 Ig family, whether of human, monkey or rodent origin, perform important and related functions for their respective organisms. This function, however, does not include affinity to PV: the interaction between PV and CD155 is not to the advantage of the host and, thus, PV binding affinity is not conserved amongst all CD155 homologues or orthologues (43).

Unlike the OWMs, the NWMs are not susceptible to oral infection with PV. NWMs, however, can be infected by intracerebral injection but, surprisingly, this is dependent not only upon the NWM species but also upon the PV serotype. Amongst the serotypes, PV1 is clearly favored in its ability to infect the NWM cells, tamarin and brown capuchin. PV3 can also infect tamarin cells, whereas PV2 is excluded from interaction with those NWM CD155 molecules that have been tested. These include the black tailed marmoset, tamarin and brown capuchin, all members of subfamilies of the family *Cebidae* (our studies; (22, 26-28)). In their study on rapid sequence changes of the *CD155* gene during evolution, Ida-Hosonuma et al. have shown that the V-domain of the brown capuchin CD155, if exchanged for the V-domain of hCD155, can serve as receptor for PV1 only, an observation not further investigated (22).

Unlike TMX cells, NZP-60 cells are resistant to all three serotypes. Our experiments have clearly shown that the inability of the three PV serotypes investigated here to infect marmoset NZP-60 cells is related to the earliest step in infection: lack of

ability to form virus-receptor complexes. If the cell membrane barrier is bypassed by transfection of virion RNA, replication and virus maturation occurs just as efficiently as in mouse Ltk$^-$ cells, a highly permissive substrate for intracellular PV replication. Fittingly, on transfection of the PV-Luc replicon, the NZP-60 cells showed significant levels of translation and replication of replicon RNA.

The resistance of NZP-60 cells to PV infection cannot be explained by a lack of nCD155 expression on these cells. Flow cytometry of the NWM cells show that expression of nCD155 on NZP-60 cells under the conditions of the experiments is nearly two-fold higher than that of hCD155 on HeLa cells or tCD155 on TMX cells. Together, these data show that the block to infection of NZP-60 cells occurs at the stage of receptor binding, a conclusion supported by binding studies of PV serotypes to these cells. We cannot determine whether the nCD155 protein can alter virions since the amount of virus-receptor bound complexes was very low on the NZP-60 cells.

Previous experiments have shown that the receptor-virus interaction follows biphasic kinetics ((35) and ref. therein). The initial binding step involving an electrostatic interaction is fully reversible and temperature independent. The second step requires near physiological temperatures for an increase in "breathing" of the virion structure, thereby exposing higher affinity binding sites (35). This additional binding leads to irreversible structural changes of the (bound) virion and is hypothesized that, in turn, results in additional contacts with the north rim of the "canyon", leading to the uncoating of the virus (15, 16, 35). Our experiments reported here are in accordance with this mechanism. They show an increase in the binding of the virions when the temperature of binding is increased from 4°C to 25°C. Interestingly, increased binding, in turn, co-varies with a productive infection, regardless of the level of virus-receptor complexes. Specifically, PV1 and PV3 both showed an increase in the amount of bound virus complexes from 4°C to 25°C and a concomitant replication in TMX cells. Moreover, the amount of receptor bound complexes to PV1 was higher than that to PV3, which correlated with higher titers of PV1 in TMX cells. In contrast, PV1 showed no growth phenotype in NZP-60 cells and there was no appreciable increase in virus-receptor complexes from 4°C to 25°C.

Since successful infection requires structural changes of the virion associated with an increase in bound complexes from 4°C to 25°C, we assessed TMX and NZP-60 cells ability to alter virion particles after binding. In support of our infection and binding data, TMX cells converted the 160S native particles to 135S particles, whereas the NZP-60 cells were deficient in binding thus unable to alter virion particles. Therefore, we made an attempt to change the amino acid composition of the V domains of tCD155 and nCD155 by mutagenesis with the aim of affecting PV1 binding. Previous studies have shown that mutation of three amino acids in hCD155 (Q80, S85 and S87) caused a loss in viral binding and replication of PV1 (5, 39). By alignment of hCD155, tCD155, and nCD155, these amino acids were predicted to be involved in virion binding if engineered into the NWM CD155. Accordingly, the mutant receptors were expressed in mouse fibroblast cells (L-tCD155mt and L-nCD155mt) and their ability for virus binding and uncoating was determined.

Our data showed an increase in the formation of virus-receptor complexes as well as in viral titers for both L-tCD155mt and L-nCD155mt cells with PV1. The L-nCD155mt cells were able to support PV1 infection, although the virus-receptor complexes in L-nCD155mt cells was 55 fold lower than in HeLa cells at 4°C. However, the PV1 and nCD155mt complexes increased 3 fold from 4°C to 25°C, seemingly enough to lead to a productive infection of L-nCD155mt cells. Notably, PV1 did not show any virus-receptor complexes on L-nCD155 cells, whereas virus-receptor complexes were found on NZP-60 cells. This apparent discrepancy could be due to the lack of complexes that wt nCD155 can form in marmoset cells but not in mouse cells, thus interfering with the already weak binding of the receptor to the virus in L-nCD155 cells. This may also explain why L-nCD155mt cells did not bind and could not be infected with PV2 or PV3 (data not shown). However, the mutations engineered into NWM CD155 molecules were selected based on mutagenesis studies of hCD155 and binding to PV1. Therefore, the mutations may not have significantly increased the binding of the other two serotypes. This would lend support to the hypothesis that there are distinct binding differences between CD155 and PV serotypes. As pointed out before, we do not believe that the differences described here are strain specific rather than serotype specific. The structures of all three PV serotypes show a high degree in architecture that is necessary for

519 morphogenesis, stability and receptor binding of the virion. The three serotypes, on the
520 other hand, are defined by a large number of amino acid substitutions mapping over large
521 areas of the virion (37). This leaves little room for variability with respect to strains of a
522 given serotype

523 The profound differences by which the three PV serotypes bind to CD155
524 receptors are surprising. To be sure, the extent of virus-receptor complex formation of the
525 PV strains to hCD155 is very similar (3) and so are corresponding structures of the
526 virus/receptor complexes (6, 15). Originally, the differences were discovered only when
527 mutants of hCD155 were studied (5, 13). For example, cell line 84, containing a
528 mutation at P84SYS/HYSA in hCD155, is deficient in binding PV1 and Sabin 1, but not
529 Sabin 2 or Sabin 3 (13). A hybrid PV1 virus in which the neutralizing antigenic site Ia
530 was exchanged with that of PV2, showed an increase in virus bound complexes on cell
531 line 84 (13). Therefore, the mutation P84SYS/HYSA in hCD155 leads to loss of binding
532 of PV1, which can be rescued by the exchange of antigenic sites on the virus surface (13).

533 Like with mutant hCD155 molecules, the differences are remarkable in the
534 binding of the three PV serotypes to the NWM CD155 receptors (our studies; (22)).
535 When Ltk^- cells were transformed with a chimeric receptor of brown capuchin/hCD155,
536 the cells were susceptible to PV1, but not to PV2 or PV3 (22). Surprisingly, there are
537 only a difference of 4 amino acids in the V domain of the brown capuchin and marmoset
538 CD155 (data not shown). As mentioned, brown capuchin/hCD155 chimera is susceptible
539 to PV1 while marmoset cells are not susceptible. The diversity of interactions between
540 the NWM CD155 molecules and the PV serotypes has given rise to differences in
541 serotype susceptibility of the NWM species.

542 Evidence has been presented previously suggesting that C-cluster coxsackie A
543 viruses may be the progenitors of the PVs, the critical event being a switch from the
544 ICAM-1 receptor to the CD155 receptor (24). This raises a possibility that a hitherto
545 hidden polio-like virus may have evolved by adapting to one or the other NWM CD155
546 for proliferation. Such polio-like virus may present a reservoir that may seed PVs back
547 into the human population once poliovirus has been eradicated globally and an anti-polio
548 vaccination has been permanently terminated, as is the current plan of the World Health
549 Organization.

ACKNOWLEDGEMENTS

We thank Aniko Paul, Hidemi Toyoda, Jeronimo Cello, and Steffen Mueller for technical suggestions and for help in preparation of this manuscript.

This research was supported by NIH grant AI39486. S.K. was supported by National Research Service Award T32 AI007539.

REFERENCES

1. **Aoki, J., S. Koike, I. Ise, Y. Sato-Yoshida, and A. Nomoto.** 1994. Amino acid residues on human poliovirus receptor involved in interaction with poliovirus. J. Biol. Chem. **269:**8431-8439.
2. **Baury, B., R. J. Geraghty, D. Masson, P. Lustenberger, P. G. Spear, and M. G. Denis.** 2001. Organization of the rat Tage4 gene and herpesvirus entry activity of the encoded protein. Gene **265:**185-94.
3. **Belnap, D. M., B. M. McDermott, Jr., D. J. Filman, N. Cheng, B. L. Trus, H. J. Zuccola, V. R. Racaniello, J. M. Hogle, and A. C. Steven.** 2000. Three-dimensional structure of poliovirus receptor bound to poliovirus. Proc.Natl. Acad. Sci. U. S. A. **97:**73-78.
4. **Bendtsen, J. D., H. Nielsen, G. von Heijne, and S. Brunak.** 2004. Improved prediction of signal peptides: SignalP 3.0. J. Mol. Biol. **340:**783-95.
5. **Bernhardt, G., J. Harber, A. Zibert, M. deCrombrugghe, and E. Wimmer.** 1994. The poliovirus receptor: identification of domains and amino acid residues critical for virus binding. Virology **203:**344-356.
6. **Bibb, J. A., G. Witherell, G. Bernhardt, and E. Wimmer.** 1994. Interaction of poliovirus with its cell surface binding site. Virology **201:**107-115.
7. **Bottino, C., R. Castriconi, D. Pende, P. Rivera, M. Nanni, B. Carnemolla, C. Cantoni, J. Grassi, S. Marcenaro, N. Reymond, M. Vitale, L. Moretta, M. Lopez, and A. Moretta.** 2003. Identification of PVR (CD155) and Nectin-2 (CD112) as cell surface ligands for the human DNAM-1 (CD226) activating molecule. J. Exp. Med. **198:**557-67.
8. **Burnet, F. M., Macnamara, J.** 1931. Immunological differences between strains of poliomyelitic virus. Br. J. Exp. Pathol. **12:**57-61.

9. **Colston, E., and V. R. Racaniello.** 1994. Soluble receptor-resistant poliovirus mutants identify surface and internal capsid residues that control interaction with the cell receptor. Embo. J. **13:**5855-62.
10. **Eberle, F., P. Dubreuil, M. G. Mattei, E. Devilard, and M. Lopez.** 1995. The human PRR2 gene, related to the human poliovirus receptor gene (PVR), is the true homolog of the murine MPH gene. Gene **159:**267-272.
11. **Filman, D. J., R. Syed, M. Chow, A. J. Macadam, P. D. Minor, and J. M. Hogle.** 1989. Structural factors that control conformational transitions and serotype specificity in type 3 poliovirus. Embo. J. **8:**1567-79.
12. **Fricks, C. E., and J. M. Hogle.** 1990. Cell-induced conformational change in poliovirus: externalization of the amino terminus of VP1 is responsible for liposome binding. J. Virol. **64:**1934-45.
13. **Harber, J., G. Bernhardt, H. H. Lu, J. Y. Sgro, and E. Wimmer.** 1995. Canyon rim residues, including antigenic determinants, modulate serotype-specific binding of polioviruses to mutants of the poliovirus receptor. Virology **214:**559-570.
14. **He, Y., V. D. Bowman, S. Mueller, C. M. Bator, J. Bella, X. Peng, T. S. Baker, E. Wimmer, R. J. Kuhn, and M. G. Rossmann.** 2000. Interaction of the poliovirus receptor with poliovirus. Proc. Natl. Acad. Sci. U. S. A. **97:**79-84.
15. **He, Y., S. Mueller, P. R. Chipman, C. M. Bator, X. Peng, V. D. Bowman, S. Mukhopadhyay, E. Wimmer, R. J. Kuhn, and M. G. Rossmann.** 2003. Complexes of poliovirus serotypes with their common cellular receptor, CD155. J. Virol. **77:**4827-35.
16. **Hogle, J. M.** 2002. Poliovirus cell entry: common structural themes in viral cell entry pathways. Annu. Rev. Microbiol. **56:**677-702.
17. **Hogle, J. M., M. Chow, and D. J. Filman.** 1985. Three-dimensional structure of poliovirus at 2.9 A resolution. Science **229:**1358-65.
18. **Hogle, J. M., and D. J. Filman.** 1989. The antigenic structure of poliovirus. Philos. Trans. R. Soc. Lond. B. Biol. Sci. **323:**467-78.
19. **Holland, J. J.** 1962. Irreversible eclipse of poliovirus by HeLa cells. Virology **16:**163-76.

20. **Hsiung, G. D., F. L. Black, and J. R. Henderson.** 1964. Susceptibility of primates to viruses in relation to taxonomic classification., p. 1-23. *In* Buettener-Janusch (ed.), Evolutionary and genetic biology of primates., vol. vol II. Academic Press, New York.

21. **Ida-Hosonuma, M., T. Iwasaki, T. Yoshikawa, N. Nagata, Y. Sato, T. Sata, M. Yoneyama, T. Fujita, C. Taya, H. Yonekawa, and S. Koike.** 2005. The alpha/beta interferon response controls tissue tropism and pathogenicity of poliovirus. J. Virol. **79:**4460-9.

22. **Ida-Hosonuma, M., Y. Sasaki, H. Toyoda, A. Nomoto, O. Gotoh, H. Yonekawa, and S. Koike.** 2003. Host range of poliovirus is restricted to simians because of a rapid sequence change of the poliovirus receptor gene during evolution. Arch. Virol. **148:**29-44.

23. **Iwasaki, A., R. Welker, S. Mueller, M. Linehan, A. Nomoto, and E. Wimmer.** 2002. Immunofluorescence analysis of poliovirus receptor expression in Peyer's patches of humans, primates, and CD155 transgenic mice: implications for poliovirus infection. J. Infect. Dis. **186:**585-92.

24. **Jiang, P., J. A. Faase, H. Toyoda, A. Paul, E. Wimmer, and A. E. Gorbalenya.** 2007. Evidence for emergence of diverse polioviruses from C-cluster coxsackie A viruses and implications for global poliovirus eradication. Proc. Natl. Acad. Sci. U. S. A. **104:**9457-62.

25. **Kall, L., A. Krogh, and E. L. Sonnhammer.** 2004. A combined transmembrane topology and signal peptide prediction method. J. Mol. Biol. **338:**1027-36.

26. **Kaplan, A. S.** 1955. Comparison of susceptible and resistant cells to infection with poliomyelitis virus. Ann. N. Y. Acad. Sci. **61:**830-9.

27. **Kaplan, A. S.** 1955. The susceptibility of monkey kidney cells to poliovirus in vivo and in vitro. Virology **1:**377-92.

28. **Kaplan, A. S., and J. L. Melnick.** 1955. Multiplication of virulent poliovirus in capuchin monkey kidney cultures without microscopically observed cytopathogenicity. Proc. Soc. Exp. Biol. Med. **90:**562-5.

29. **Koike, S., H. Horie, I. Ise, A. Okitsu, M. Yoshida, N. Iizuka, K. Takeuchi, T. Takegami, and N. A.** 1990. The poliovirus receptor protein is produced both as membrane-bound and secreted forms. EMBO. J. **9:**3217-3224.

30. **Koike, S., I. Ise, Y. Sato, H. Yonekawa, O. Gotoh, and A. Nomoto.** 1992. A second gene for the African green monkey poliovirus receptor that has no putative N-glycosylation site in the functional N-terminal immunoglobulin-like domain. J. Virol. **66:**7059-7066.

31. **Lange, R., X. Peng, E. Wimmer, M. Lipp, and G. Bernhardt.** 2001. The poliovirus receptor CD155 mediates cell-to-matrix contacts by specifically binding to vitronectin. Virology **285:**218-227.

32. **Lentz, K. N., A. D. Smith, S. C. Geisler, S. Cox, P. Buontempo, A. Skelton, J. DeMartino, E. Rozhon, J. Schwartz, V. Girijavallabhan, J. O'Connell, and E. Arnold.** 1997. Structure of poliovirus type 2 Lansing complexed with antiviral agent SCH48973: comparison of the structural and biological properties of three poliovirus serotypes. Structure **5:**961-78.

33. **Li, X., H. H. Lu, S. Mueller, and E. Wimmer.** 2001. The C-terminal residues of poliovirus proteinase 2A(pro) are critical for viral RNA replication but not for cis- or trans-proteolytic cleavage. J. Gen. Virol. **82:**397-408.

34. **Liao, S., and V. Racaniello.** 1997. Allele-specific adaptation of poliovirus VP1 B-C loop variants to mutant cell receptors. J. Virol. **71:**9770-9777.

35. **McDermott, B. M., Jr., A. H. Rux, R. J. Eisenberg, G. H. Cohen, and V. R. Racaniello.** 2000. Two distinct binding affinities of poliovirus for its cellular receptor. J. Biol. Chem. **275:**23089-23096.

36. **Mendelsohn, C. L., E. Wimmer, and V. R. Racaniello.** 1989. Cellular receptor for poliovirus: molecular cloning, nucleotide sequence, and expression of a new member of the immunoglobulin superfamily. Cell **56:**855-865.

37. **Minor, P. D., M. Ferguson, D. M. Evans, J. W. Almond, and J. P. Icenogle.** 1986. Antigenic structure of polioviruses of serotypes 1, 2 and 3. J. Gen. Virol. **67 (Pt 7):**1283-91.

38. **Mok, Y. K., K. W. Lo, and M. Zhang.** 2001. Structure of Tctex-1 and its interaction with cytoplasmic dynein intermediate chain. J. Biol. Chem. **276:**14067-74.

39. **Morrison, M. E., Y. J. He, M. W. Wien, J. M. Hogle, and V. R. Racaniello.** 1994. Homolog-scanning mutagenesis reveals poliovirus receptor residues important for virus binding and replication. J. Virol. **68:**2578-88.

40. **Morrison, M. E., and V. R. Racaniello.** 1992. Molecular cloning and expression of a murine homolog of the poliovirus receptor gene. J. Virol. **66:**2807-2813.

41. **Mueller, S., X. Cao, R. Welker, and E. Wimmer.** 2002. Interaction of the poliovirus receptor CD155 with the dynein light chain Tctex-1 and its implication for poliovirus pathogenesis. J. Biol. Chem. **277:**7897-904.

42. **Mueller, S., and E. Wimmer.** 2003. Recruitment of nectin-3 to cell-cell junctions through *trans*-heterophilic interaction with CD155, a vitronectin and poliovirus receptor that localizes to $\alpha_v\beta_3$ integrin-containing membrane microdomains. J. Biol. Chem. **278:**31251-31260.

43. **Mueller, S., E. Wimmer, and J. Cello.** 2005. Poliovirus and poliomyelitis: A tale of guts, brains, and an accidental event. Virus Res. **111:**175-93.

44. **Ogita, H., and Y. Takai.** 2006. Nectins and nectin-like molecules: roles in cell adhesion, polarization, movement, and proliferation. IUBMB Life **58:**334-43.

45. **Ohka, S., N. Matsuda, K. Tohyama, T. Oda, M. Morikawa, S. Kuge, and A. Nomoto.** 2004. Receptor (CD155)-dependent endocytosis of poliovirus and retrograde axonal transport of the endosome. J. Virol. **78:**7186-98.

46. **Ohka, S., H. Ohno, K. Tohyama, and A. Nomoto.** 2001. Basolateral sorting of human poliovirus receptor alpha involves an interaction with the mu1B subunit of the clathrin adaptor complex in polarized epithelial cells. Biochem. Biophys. Res. Commun. **287:**941-948.

47. **Paralysis, T. C. o. T. o. t. N. F. f. I.** 1951. Immunologic classification of poliomyelitis viruses. Am. J. Hyg. **54:**191-274.

48. **Pincus, S. E., D. C. Diamond, E. A. Emini, and E. Wimmer.** 1986. Guanidine-selected mutants of poliovirus: Mapping of point mutations to polypeptide 2C. J. Virol. **57:**638-646.

49. **Ravens, I., S. Seth, R. Forster, and G. Bernhardt.** 2003. Characterization and identification of Tage4 as the murine orthologue of human poliovirus receptor/CD155. Biochem. Biophys. Res. Commun. **312:**1364-71.

50. **Rieder, E., and E. Wimmer.** 2002. Cellular receptors of picornaviruses: An overview., p. 61-70. *In* B. L. Semler and E. Wimmer (ed.), Molecular biology of picornaviruses. ASM Press, Washington, D.C.

51. **Rossmann, M. G.** 2002. Picornavirus Structure Overview, p. 27-38. *In* B. L. Semler, Wimmer, E. (ed.), Molecular Biology of Picornaviruses. ASM Press, Washington, DC.

52. **Rossmann, M. G., and J. E. Johnson.** 1989. Icosahedral RNA virus structure. Annu. Rev. Biochem. **58:**533-73.

53. **Sabin, A. B.** 1956. Pathogenesis of poliomyelitis; reappraisal in the light of new data. Science **123:**1151-7.

54. **Xing, L., K. Tjarnlund, B. Lindqvist, G. G. Kaplan, D. Feigelstock, R. H. Cheng, and J. M. Casasnovas.** 2000. Distinct cellular receptor interactions in poliovirus and rhinoviruses. Embo. J. **19:**1207-1216.

55. **Yanagiya, A., Q. Jia, S. Ohka, H. Horie, and A. Nomoto.** 2005. Blockade of the Poliovirus-Induced Cytopathic Effect in Neural Cells by Monoclonal Antibody against Poliovirus or the Human Poliovirus Receptor. J. Virol. **79:**1523-32.

FIGURE LEGENDS

FIG. 1. The predicted structure of CD155 homologues. Schematic diagram of the CD155 structures of human (hCD155α), AGM CD155 (AGMα1), tamarin (tCD155), and of marmoset (nCD155). Three extracellular immunoglobulin-like domains (*circles*) are formed by disulfide bonds. The transmembrane domain and the C-terminus are shown with binding domains for Tctex-1 *(empty box*) and μ1B subunit *(shaded box).* The predicted N-glycosolation sites are shown on immunoglobulin domains (*squares*), as well as the number of amino acids that compose each domain. hCD155 is produced in four different splice variants (α, β, γ, δ) that differ in the presence of the transmembrane domain and the length of the C-terminal domain. AGM CD155 occurs in two splice variants AGMα1 and AGMδ1, and AGMα2 is encoded by a second gene.

FIG. 2. One step growth curves of PV strains on various cell lines. One-step growth curve in mouse (Ltk^-), human (HeLa), marmoset (NZP-60) and tamarin (TMX) cells were carried out as described in Materials and Methods. (A) PV1, (B) PV2, and (C) PV3. Each point represents the mean of virus titers from three experiments.

FIG. 3. Translation and replication of PV RNA and of PV-Luc replicon in different cell lines. (A) Virus titers of PV1(Mahoney), PV2(Lansing) and PV3(Leon) in marmoset (NZP-60), tamarin (TMX) and mouse (Ltk^-) cells after transfection of RNA as described in Materials and Methods. (B) Firefly luciferase activity of PV-Luc replicons. Transfection of PV-Luc replicon RNAs into various cell lines, with or without 2mM GnHCl, and the measurement of luciferase activity are described in Materials and Methods.

FIG. 4. Analysis of the expression levels of CD155 on cell surface by flow cytometry. The CD155 expression levels on the surface of human (HeLa), mouse (Ltk-), tamarin (TMX), and marmoset (NZP-60) cell lines was determined by flow cytometry using mAb p286 and secondary Ab anti-mouse FITC, as described in Materials and Methods. The data is expressed in arbitrary units.

FIG. 5. Binding assay of PV strains to various cell lines. The binding of 10^8 PFU [^{35}S] labeled (A) PV1, (B) PV2, and (C) PV3 to 10^6 cells of human (HeLa), tamarin (TMX), marmoset (NZP-60) and mouse (Ltk^-) was measured as described in Materials and Methods. The values are an average of three experiments.

FIG. 6. Sucrose density gradient fractionation of extracts of [^{35}S] methionine-labeled infected cells. Purified native virions were attached to the cells at 25°C and incubated at 37°C for 45 min before lysis. The lysates were laid on a sucrose gradient and the gradients were fractionated from the bottom. Unheated and heated labeled virions were used as controls.

FIG. 7. Amino acid alignment of the V domain of CD155 homologues. Amino acid alignment of the V domains of human (hCD155), African green monkey (AGMα1 and AGMα2), tamarin (tCD155) and marmoset (nCD155) proteins. Residues identified for binding all three PV strains are shown in bold, residues identified in binding two serotypes are shown in shaded bold, and residues identified binding in only one serotype are shown in grey. The arrows indicate the β-strands of the V domain. Residues

762 implicated in binding to PV by previous mutational analyses are marked with an X (5,
763 13) and a + (9, 29, 34, 39) in the lines above the residue numbers. The boxed residues
764 donate amino acids mutated for this study. The numbering of amino acids corresponds to
765 V domains of hCD155 (Figure modified from (15)).
766 **Fig. 8.** Infection and virus binding of stably transfected Ltk$^-$ cell lines. (A) Viral titers of
767 PV1 growing in Ltk$^-$ cells stably expressing human CD155 (L-hCD155), marmoset
768 CD155 (L-nCD155), mutant nCD155 (L-nCD155mt), tamarin CD155 (L-tCD155) and
769 mutant tCD155 (L-tCD155mt) was determined at 0 h and 24 h. (B) The binding of [^{35}S]
770 labeled PV1 was measured as described in Materials and Methods.

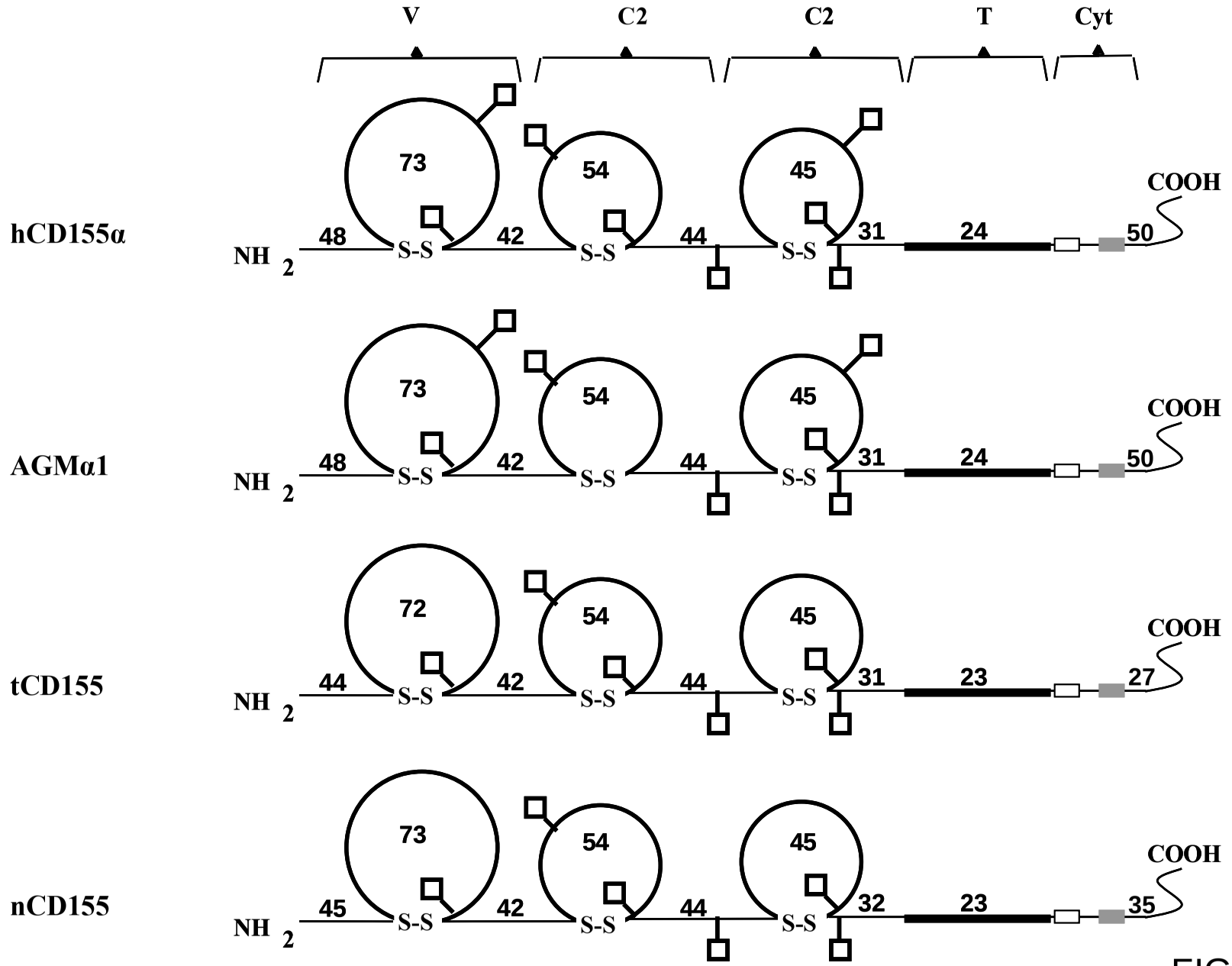
V
C2
C2
T
Cyt
hCD155α
AGMα1
tCD155
nCD155
NH 2
S-S
COOH
73
54
45
48
42
44
31
24
50
72
23
27
32
35

FIG. 1

174

771

A

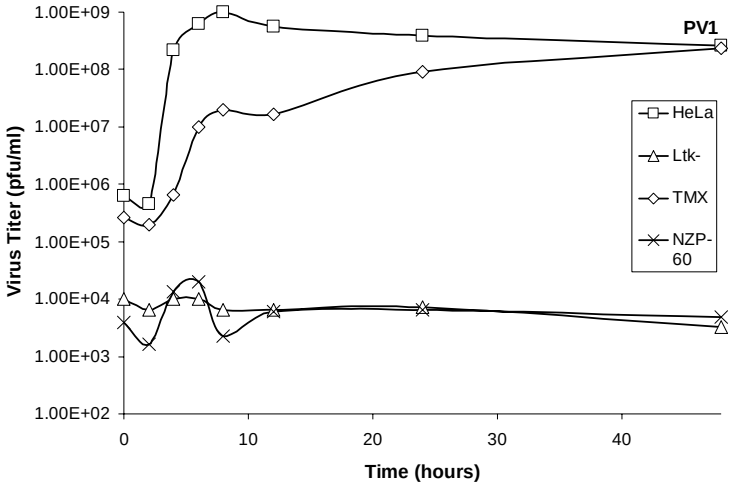
PV1
Virus Titer (pfu/ml)
1.00E+09
1.00E+08
1.00E+07
1.00E+06
1.00E+05
1.00E+04
1.00E+03
1.00E+02
0
10
20
30
40
Time (hours)
HeLa
Ltk-
TMX
NZP-60

B

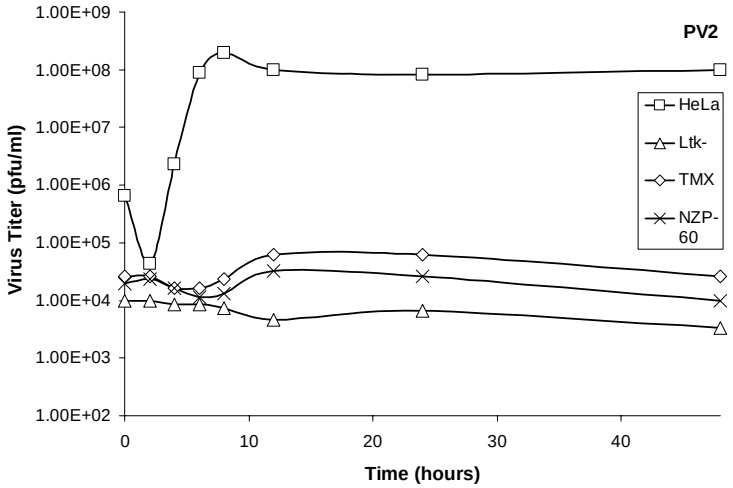
PV2
Virus Titer (pfu/ml)
1.00E+09
1.00E+08
1.00E+07
1.00E+06
1.00E+05
1.00E+04
1.00E+03
1.00E+02
0
10
20
30
40
Time (hours)
HeLa
Ltk-
TMX
NZP-60

C

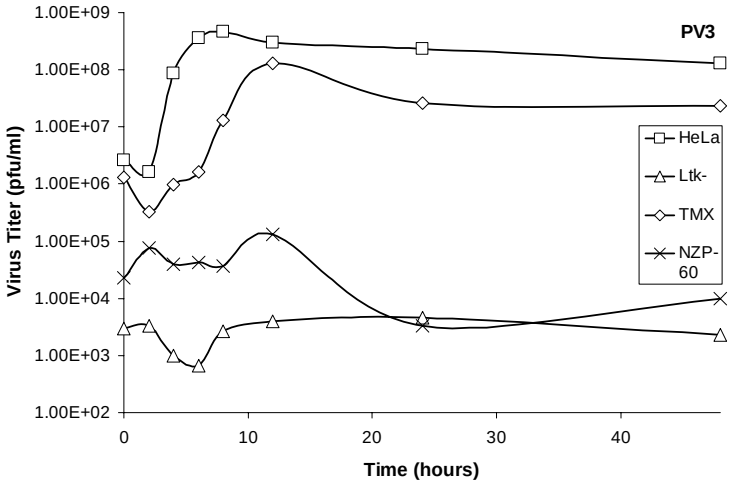
PV3
Virus Titer (pfu/ml)
1.00E+09
1.00E+08
1.00E+07
1.00E+06
1.00E+05
1.00E+04
1.00E+03
1.00E+02
0
10
20
30
40
Time (hours)
HeLa
Ltk-
TMX
NZP-60

FIG. 2

772

773

A

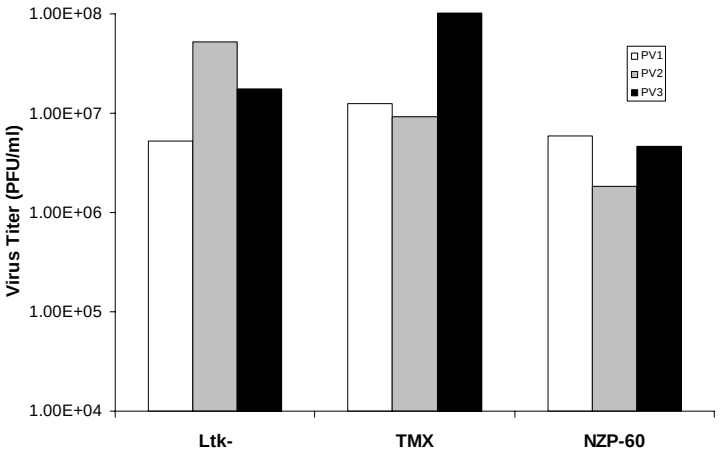

B

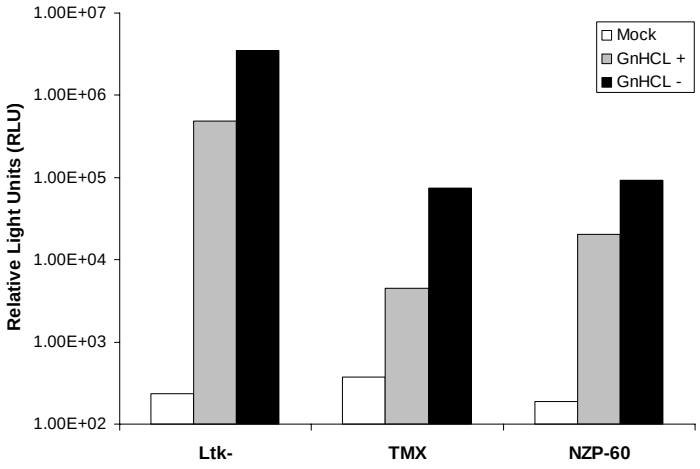

FIG. 3

774

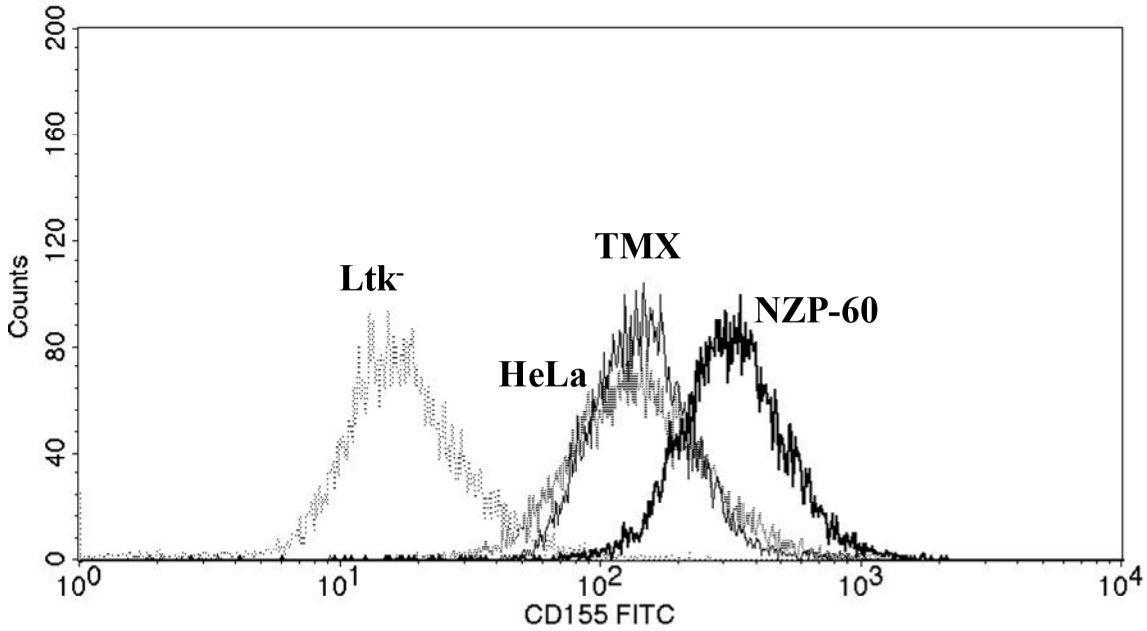

	Ltk-	HeLa	TMX	NZP-60
Mean Fluorescence*	27.92	155.92	159.07	332.71

*Mean fluorescence was determined by counting 10^6 cells.

177

FIG. 4

775

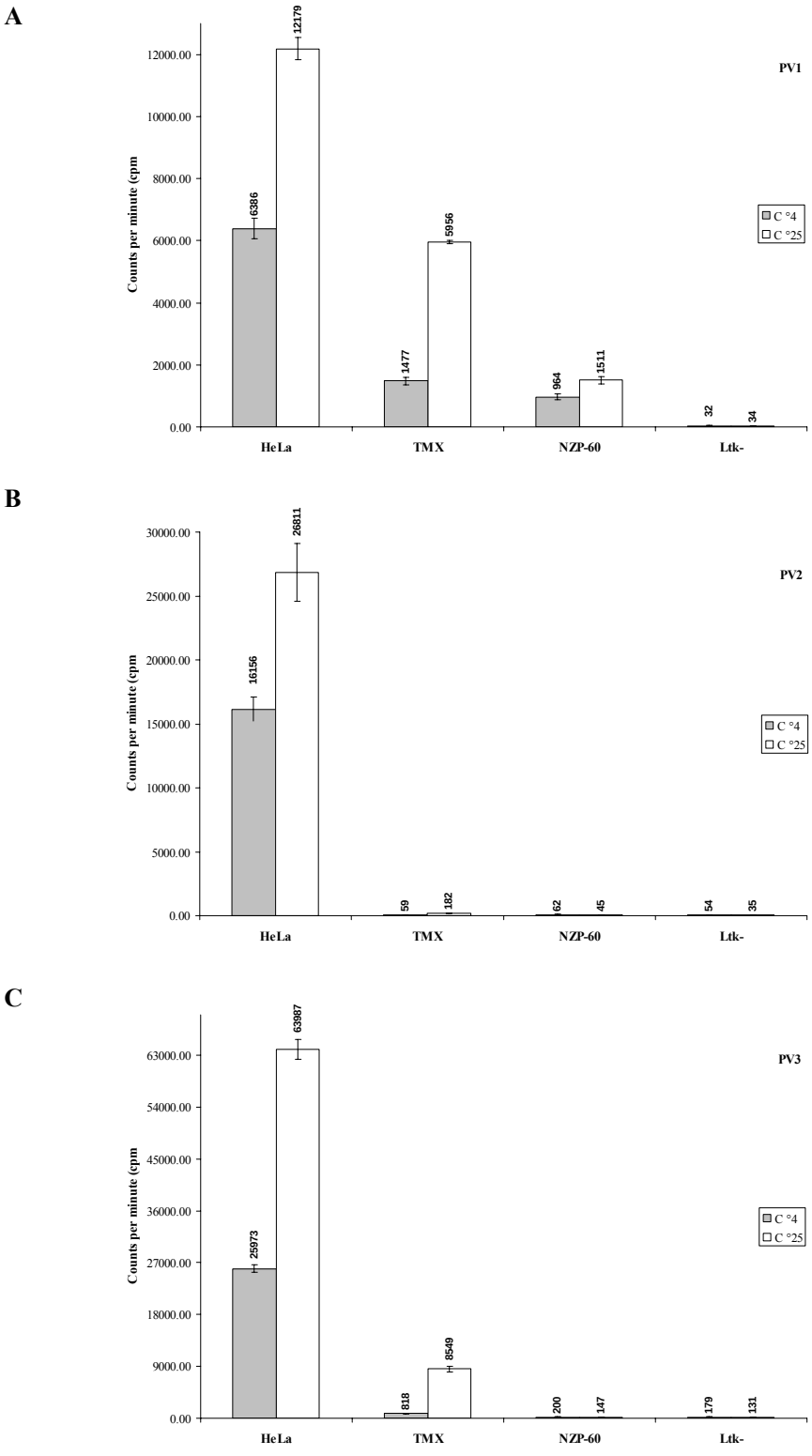
A
PV1
Counts per minute (cpm
12000.00
10000.00
8000.00
6000.00
4000.00
2000.00
0.00
6386
12179
1477
5956
964
1511
32
34
C °4
C °25
HeLa
TMX
NZP-60
Ltk-
B
PV2
Counts per minute (cpm
30000.00
25000.00
20000.00
15000.00
10000.00
5000.00
0.00
16156
26811
59
182
62
45
54
35
C °4
C °25
HeLa
TMX
NZP-60
Ltk-
C
PV3
Counts per minute (cpm
63000.00
54000.00
45000.00
36000.00
27000.00
18000.00
9000.00
0.00
25973
63987
818
8549
200
147
179
131
C °4
C °25
HeLa
TMX
NZP-60
Ltk-

776

FIG. 5

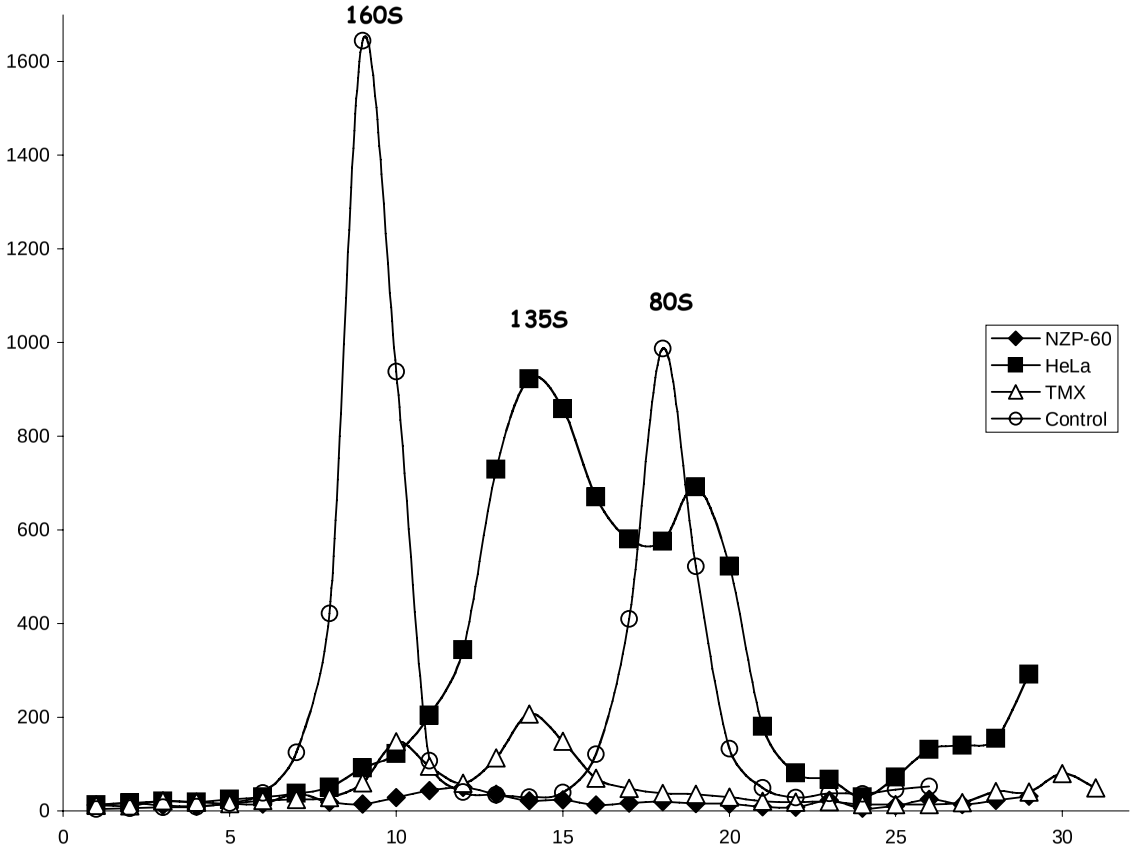
160S
135S
80S
NZP-60
HeLa
TMX
Control
0
200
400
600
800
1000
1200
1400
1600
0
5
10
15
20
25
30

FIG. 6

778

779

FIG. 7

780

781

782

A

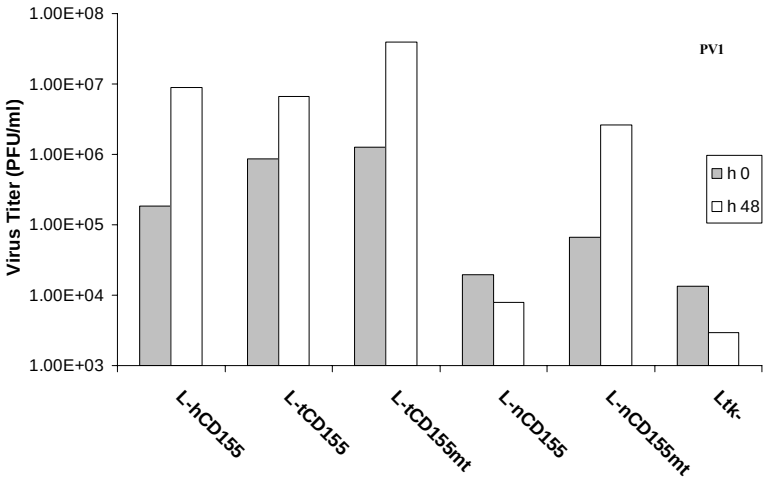

B

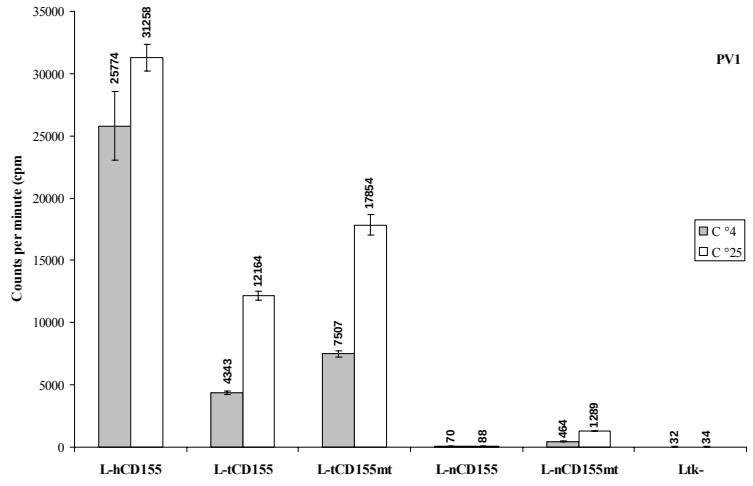

FIG. 8

783

Appendix B

Generation and analysis of a transgenic mouse expressing a modified CD155 receptor.

Hidemi Toyoda, Shaukat Khan, and Eckard Wimmer

(Manuscript in preparation)

Generation and analysis of a transgenic mouse expressing a modified CD155 receptor.

Hidemi Toyoda, Shaukat Khan, and Eckard Wimmer*

Department of Molecular Genetics and Microbiology, Stony Brook University, Stony Brook, N. Y. 11790

*Corresponding author. Mailing address: Department of Molecular Genetics and Microbiology, Life Science Building Room 213, Stony Brook University, Stony Brook, NY 11794-5222. Phone: (631) 632-8787. Fax: (631) 632-8891, Email: ewimmer@ms.sunysb.edu.

Word Number: 282 (Abstract), 4, 290 (Full text)

Skeletal muscle injury induces retrograde axonal transport of poliovirus (PV) and thereby facilitates viral invasion of the central nervous system and the progression of the spinal cord damage. Recently, it has been reported that the cytoplasmic domain of human poliovirus receptor (CD155) has binding affinity to Tctex-1, a cargo binding protein of the dynein motor complex. Efficient interaction of CD155 with Tctex-1 plays an important role in the retrograde transport of PV-containing vesicles along microtubules. To examine the mechanism of retrograde axonal PV transport, a new mouse model (ΔCD155tg mice) that is transgenic for modified CD155 was generated in which the interaction between Tctex-1 and CD155 was abolished. The transgene used was constructed by deleting six amino acid residues (SKCSRE), including the consensus sequence for Tctex-1 binding, within the juxtamembrane region of CD155. All of the CD155tg mice and ΔCD155tg mice, which had been inoculated into the gastrocnemius muscle with 1 x 10^6 plaque forming unit of PV1(M), showed symptoms of paralysis in the inoculated limbs within 48 hours after inoculation. The distribution profile of intramuscularly inoculated PV in various tissues of ΔCD155tg mice is similar to that in CD155tg mice. The appearance of initial paralysis after intramuscular inoculation was delayed by transection of sciatic nerve in ΔCD155tg mice. Furthermore, topical application of the antimicrotubule agent, vinblastine, to the sciatic nerve reduced the amount of virus transported from the gastrocnemius muscle to the spinal cord in ΔCD155tg mice. PV wasn't retrogradely transported in non-tg mice. The results suggest that PV is retrogradely transported along microtubules even in the absence of the Tctex-1 binding motif in the cytoplasmic domain of CD155 but CD155 expression is still required for retrograde axonal transport of PV.

Poliovirus (PV), known to be the causative agent of poliomyelitis, is a human enterovirus that belongs to the *Picornaviridae* family. PV infection is initiated by ingestion of virus followed by its primary multiplication in oropharyngeal and intestinal mucosa. Once extensive viral multiplication occurs in the tonsils and Peyer's patches of the small intestine, PV can enter the systemic circulation. Viremia is considered a prerequisite of the progression to poliomyelitis. One passage to the central nervous

system (CNS) is breaking through the blood brain barrier (BBB) (42). Along with this pathway of dissemination, retrograde axonal transport from neuromuscular junction to the neuron cell body has been reported in humans (27), monkeys (6), and PV-sensitive transgenic (tg) mice carrying the human PV receptor (hPVR/CD155) gene (15, 28, 30, 34). The probability of PV retrograde axonal transport into the spinal cord in infected individuals increases with muscle injury and it appears to be important in causing provocation poliomyelitis (15, 21). Using CD155tg mice, it has been suggested that PV inoculated into the gastrocnemius muscle is incorporated into the sciatic nerve and retrogradely transported through the axons as intact virion particles (30).

CD155 is a highly glycosylated 80 kDa type Ia single-pass transmembrane protein belonging to the Ig superfamily, and it is the only cell surface protein known so far to serve as a PV receptor. (3, 4, 17, 22). Alternative splicing of the CD155 primary transcript gives rise to 4 isoforms: CD155α and -δ, which are the membrane bound PV receptors, and CD155β and -γ, which lack the transmembrane domain, and thus are found as secreted protein (2, 17). Both CD155α and -δ, which differ only in the length of their cytoplasmic domain, are considered to play important roles in the early steps of infection such as binding of the virus to the cell surface, penetration of the cells, and uncoating of the virus. However, only the longer C-terminal tail of CD155α is serine phosphorylated (5); it carries a sorting signal that localizes it to the basolateral domain of polarized epithelial cells (29). CD155δ is sorted to both the basolateral and apical domains of polarized cells. We have reported that the cytoplasmic domain of CD155 associates strongly and specifically with Tctex-1, a light chain of the dynein motor complex, and that Tctex-1 interacts with an SKCSR motif in the juxtamembrane region of the cytoplasmic domain of CD155 (23). Considering the function of dynein as the major driving force for minus end-directed transport along microtubules, we suggested that the dynein motor drags PV, which has been captured at neuromuscular junctions into transport vesicles by CD155 and Tctex-1, to the neuron cell body along microtubules (23). Tissue culture cells of neuronal origin, which are more amenable to experimental manipulation, have been used to study responses to neurotropic signals. Using differentiated rat pheochromocytoma cells (PC12) transfected with expression vector for CD155α, Ohka et. al. demonstrated that vesicles composed of PV and CD155α

colocalized with Tctex-1 and vesicles containing PV and CD155α had retrograde motion (28). We have also studied retrograde axonal transport of PV in neurites of mouse neuroblastoma cells (Neuro-2a^{CD155}) expressing CD155α (unpublished data). Whereas these studies have yielded valuable information they are incomplete because they have been produced in tissue culture-induced processes (neurites).

In this study, we have focused on the mechanism of PV retrograde axonal transport based on the interaction between Tctex-1 and the cytoplasmic domain of CD155 in an animal model. We have therefore generated a novel mouse line (ΔCD155tg mice) transgenic for the modified human CD155 gene to prevent binding between CD155 and Tctex-1. The transgene used was constructed by deleting six amino acid residues (SKCSRE), including the consensus sequence for Tctex-1 binding, within the juxtamembrane region of CD155. Here, we describe that PV was retrogradely transported along microtubules in both CD155tg mice and ΔCD155tg mice, but not in non-tg mice. The results suggest that CD155 expression is required for PV retrograde axonal transport along microtubules, even if the Tctex-1 binding motif of CD155 is deleted.

Materials and Methods

Cells and viruses. The neurovirulent poliovirus type 1 (Mahoney) [PV1(M)] is the strain being used routinely in the laboratory (40). HeLa cells were maintained in Dulbecco modified Eagle medium (DMEM) supplemented with 5% fetal bovine serum (FBS) and used for plaque assay (31).

Construction of cosmids and DNA manipulation. The Tage4 (tumor-associated glycoprotein E4) promoter was kindly provided by Dr. Günter Bernhardt (32). The cosmid pTL-HC5, which contains the CD155 gene and the human promoter, was kindly provided by Dr. Akio Nomoto (17, 18). The 2.5 kb Tage4 promoter and 31 kb CD155 gene has been cloned into SuperCos 1 (Stratagene La Jolla, CA) and designated Tage4-CD155 (Fig. 1) (Khan et. al. manuscript in preparation). The cosmid, Tage4-CD155, was used to generate novel CD155tg mice under the control of the Tage4 promoter (Khan et. al. manuscript in preparation). To delete the 18 nucleotides including the Tctex-1 binding motif in Exon 6 of CD155 (Fig. 1A), two DNA fragment were amplified. The first DNA fragment was constructed by amplifying the 1.7kb sequence containing partial Exon 6 of the CD155 gene using primers 1 and 2. The second DNA fragment was constructed by

amplifying the 8.5kb sequence containing partial Exon 6 of the CD155 gene using primers 3 and 4. Then, these two PCR products were amplified using primers 5 and 6. After the amplification of the 10kb PCR product, the Tage4-ΔCD155 cosmid was generated according to the schematic shown in Fig 1B. Briefly, the Tage4-CD155 cosmid was treated with BspEI/NheI, the 10kb PCR product with BspEI/AatII and Tage4-CD155 cosmid with AatII/RsrII. The cut fragments were purified and ligated using the Rapid DNA Ligation kit (Roche). The ligated reaction was then packaged in lambda phages using Gigapack III XL Packaging Extract (Stratagene La Jolla, CA). *Escherichia coli* JM109 cells were infected with the phage particles carrying the cosmid clone of Tage4-ΔCD155 gene. Deletion and final constructs were verified through sequencing using the ABI Prism DNA Sequencing kit. Expression of functional ΔCD155 on the cell surface of mouse L cells transfected with the cosmid clone of Tage4-ΔCD155 gene was confirmed by an immunofluorescence study with an anti-CD155 monoclonal antibody, mAb 18 (1:2 hybridoma) (24).

Transgenic mice. The Tage4-ΔCD155 cosmid clone was linearized by cutting at *Not*I sites within the nucleotide sequence on the vector (Fig. 1B). The linearized DNA was introduced into the pronuclei of C57BL/6 mouse zygotes at the Cold Spring Harbor Laboratory as described previously (7). Mice were screened for the transgene by PCR to amplify 700 bp including exon 6 of CD155 with the primers 7 and 8. The PCR product was sequenced to verify the deletion of 18 nucleotides in exon 6 of the CD155 gene including the Tctex-1 binding motif (Fig. 1A). Novel tg mice expressing CD155 under the control of Tage4 promoter were used as control mice. All mice used were free from specific pathogens and were 6 weeks of age. All procedures involving experimental mice were conducted according to protocols approved by the institutional committees on animal welfare.

Detection of CD155 mRNA isoforms. For the detection of isoforms of CD155 mRNAs expressed in brain and spinal cord of the transgenic mice, cDNA was synthesized from 3 μg of the total RNA with oligo-dT for CD155α, β, and γ isoforms, or specific primer 9 for the CD155δ isoform in 20 μl reaction mixture. After the reverse transcription, the first PCR was performed with primers, 10 and 11 (CD155α, β, and γ isoforms), or 12 and 9 (CD155δ isoform). The second step of PCR was carried out using

2 μl of reaction mixture of the first step PCR and primers, 10 and 13 (CD155α, β, and γ isoforms), or 14 and 15 (CD155δ isoform).

Neurovirulence assays. Groups of CD155tg mice or ΔCD155tg mice (equal number of male and females) were inoculated with a given amount of PV1(M) ranging from 10^1 to 10^7 plaque-forming unit (pfu) (30 μl/mouse) intracerebrally, intramuscularly, intravenously or intraperitoneally. Mice were examined daily for 21 days post-inoculation for paralysis and/or death. The virus titer that induced death in 50% of the mice (LD_{50}) was calculated by the method of Reed and Muench (33).

Recovery of viruses from tissues. For determination of the titer of virus in the tissues, the mice inoculated with the viruses were anesthetized and whole blood was recovered from the right ventricle. Immediately, the mice were perfused with saline through the left ventricle, and the tissues of interest (spinal cord, brain and skeletal muscle) were removed from CD155tg mice or ΔCD155tg mice. Each sample was weighed, placed in 1 ml of minimal essential medium, and homogenized in a Dounce homogenizer (Wheaton). Each homogenate was serially diluted, and the amount of infectious particles per 10 mg of tissue was analyzed with a plaque assay.

Sciatic nerve transection and treatment with vinblastine. Right sciatic nerve transection was performed as described previously (15). For treatment with vinblastine, ΔCD155tg mice were anesthetized with an intraperitoneal injection of ketamine and xyladine. Then the right sciatic nerve along the thighbone was exposed. The sciatic nerve was surrounded with cotton soaked in 0.15 mM vinblastine (Sigma Chemical Co.) in PBS or PBS alone for 15 min (16, 28, 43). After the cotton was removed, the region was rinsed three times with PBS and the cutaneous defect was treated with three to five sutures with Prolene 0-5 (Ethicon). The next day, the mice were intramuscularly inoculated with 10^6 pfu of PV in the left or right calf with a Hamilton microsyringe. The spinal cords of these mice were collected 16 h after the inoculation. The amount of infectious particles in the spinal cords was determined by plaque assay.

Results

Transgenic mice carrying a modified CD155 gene. We have recently generated novel CD155tg mice under control of the Tage4 promoter (ICR-Tage4-CD155tg mice) (Khan et. al. manuscript in preparation). Tage4, discovered as a prominent cell surface

protein expressed in rat colon and rat mammary carcinoma cells, and a member of the CD155/nectin family, is recognized as the rodent homologue of CD155 (1, 9). The tissue distribution pattern of CD155 in these tg mice is similar to that of CD155 in humans, and they show symptoms of paralysis similar to those of human poliomyelitis with intracerebral, intramuscular, intravenous and intraperitoneal route of PV injection (Khan et. al. manuscript in preparation). In order to determine the influence of deletion of Tctex-1 binding site in the cytoplasmic domain of CD155, we generated tg mice that expressed modified CD155 under the transcriptional control of the Tage4 promoter. The construction procedure of a modified CD155 gene is described in Materials and Methods and is shown in Fig. 1. This modified CD155 gene doesn't contain the six N-terminal amino acids in the cytoplasmic domain of CD155, including the SKCSR motif for Tctex-1 binding (Fig.1A).

Two lines of tg mice derived from strain C57BL/6 have been established as described in Materials and Methods (B6-Tage4-ΔCD155tg-122 and B6-Tage4-ΔCD155tg-133). In order to obtain the same genetic background among strains, B6-Tage4-ΔCD155tg-133 mice were outcrossed with non-transgenic ICR mice and their F1 progenies were used as ΔCD155tg mice in the present study. ICR-Tage4-CD155tg mice were outcrossed with non-transgenic C57BL/6 mice and their F1 progenies were used as CD155tg mice in the present study.

CD155 expression in tg mice. We determined CD155 expression in the mice by two methods. First, PCR was carried out using primers 7 and 8 to confirm the presence of the transgene. The PCR product was sequenced to verify the deletion of 18 nucleotides in exon 6 of the CD155 gene including the Tctex-1 binding motif (data not shown). Secondly, we used RT-PCR to determine the type of CD155 mRNAs in the CD155tg mice and in the ΔCD155 mice. Three bands corresponding to mRNA species for CD155α, CD155β and CD155γ were observed in the PCR products from RNAs of spinal cord in CD155tg mice and in ΔCD155tg mice (Fig. 2A). PCR products of membrane-bound CD155 (CD155α and CD155δ) of ΔCD155tg mice migrate faster than those of CD155tg mice, because 18 nucleotides in exon 6 were deleted in ΔCD155tg mice (Fig. 2A and B). However, two bands corresponding to mRNA species for the secreted CD155s (CD155β and CD155γ) were detected at the same position in both ΔCD155tg mice and CD155tg

mice (Fig. 2A). The same results were observed when RNAs from the brain were used for RT-PCR (data not shown). The results strongly suggest that a similar multiple splicing occurs in ΔCD155tg mice as it does in CD155tg mice and provides four different CD155 mRNA isoforms.

Susceptibility of tg mice to poliovirus. PV1(M) was inoculated into transgenic mice by various routes. The CD155tg mice showed flaccid paralysis and died 2-14 days post inoculation by intracerebral, intramuscular, intravenous and intraperitoneal routes (Table 2). These are essentially the same phenomenon that is observed in PV-infected monkeys. By intracerebral route, the 50% lethal doses (LD_{50}) of the PV1(M) in the CD155tg mice and ΔCD155tg mice were $10^{1.9}$ and $10^{2.2}$ pfu, respectively (Table 2). More than 10^3 pfu of PV1(M) induced 100% mortality in both CD155tg mice and ΔCD155tg mice. By intravenous and intraperitoneal routes, disease progression and LD_{50} of the PV1(M) in CD155tg mice and ΔCD155tg mice were similar (Table 2). Disappointingly, ΔCD155tg mice are also susceptible to poliomyelitis following intramuscular inoculation of PV1(M) (Table 2). Paralysis was consistently seen initially in the leg that was inoculated.

Initial paralysis after intramuscular inoculation of poliovirus. All of the CD155tg mice and ΔCD155tg mice that had been inoculated with $1x10^6$ pfu of PV1(M) showed a flaccid paralysis in the inoculated limbs within 48 h post infection and died within 96 h post infection (Fig. 3). To confirm the involvement of the sciatic nerve in development of the initial paralysis, the sciatic nerve of ΔCD155tg mice was transected before intramuscular inoculation of the virus. Right sciatic nerve transections were performed in such a manner as to minimize muscle trauma interfering with the experiment, as described previously (15). Sham-operated mice were subjected to the identical procedure, only the nerve transection itself was left out. Seven days after surgery, all mice were inoculated intramuscularly with $1x10^6$ pfu of PV1(M) into right gastrocnemius muscle. As shown in Fig. 3, none of ΔCD155tg mice with sciatic nerve transection showed paralysis at 48 h post inoculation via the intramuscular route. Therefore, the paralysis observed at 48 h post inoculation was due to the effect of virus carried by retrograde axonal transport system through the sciatic nerve. Furthermore, the ΔCD155tg mice that were intravenously inoculated with $1x10^6$ pfu of PV1(M) were not paralyzed at 48 h post

246 inoculation (data not shown). The data indicate that virus leaking from the inoculation
247 site to the blood stream scarcely affected the initial paralysis.

248 **Virus distribution after intramuscular inoculation.** To examine whether
249 expression of ΔCD155 contribute to the virus delivery and growth after intramuscular
250 inoculation, we measured virus titers in samples of the muscle, spinal cord, brain and
251 plasma prepared at various times after intramuscular inoculation of $1x10^6$ pfu of PV1(M)
252 (Fig. 4). In the muscle, $1x10^3$ to $1x10^4$ pfu of the virus in 10 mg tissue was detected in
253 both CD155tg mice and ΔCD155tg mice continuously at 4 – 48 h post infection (Fig. 4
254 A). The data suggested that PV1(M) replicated in the muscle, albeit inefficiently. A
255 significant amount of virus was detected at 16 h post infection in the spinal cord; by 48 h
256 post infection, when the tg mice showed the initial signs of paralysis in the inoculated
257 limbs, 1-4 $x10^6$ pfu of the virus in 10 mg tissue was detected (Fig. 4 B). Thus, virus
258 growth in the spinal cord seemed to correlate with the expression of clinical symptoms in
259 both CD155tg mice and ΔCD155tg mice. Virus was not detected at significant levels in
260 brain until 36 h post infection and virus titer in the brain reached 5-9 $x10^4$ pfu in 10 mg
261 tissue at 48 h post infection (Fig. 4C). After intramuscular inoculation with PV1(M),
262 there is a gradual decline in circulating virus in both CD155tg mice and ΔCD155tg mice
263 (Fig. 4D).

264 **Role of ΔCD155 expression for retrograde axonal transport.** It was previously
265 suggested that PV spreads from muscle to spinal cord through nerve pathways after
266 intramuscular inoculation and the expression of CD155 plays an important role in viral
267 spread by this route (34). To examine whether the expression of ΔCD155 also plays an
268 important role in retrograde axonal transport, tissue distribution of PV1(M) in ΔCD155tg
269 mice or non-tg mice with or without sciatic nerve transection was carried out 16 h after
270 the intramuscular inoculation (Fig.5). The right sciatic nerve of ΔCD155tg mice or non-tg
271 mice was transected or sham-operated, and the mice were inoculated with $1x10^6$ pfu of
272 PV1(M) into right gastrocnemius muscle seven days after sciatic nerve transection. In
273 the spinal cords of the sham-operated ΔCD155tg mice inoculated with virus, 1- $4x10^3$ pfu
274 / 10 mg tissue was detected (Fig. 5 lane 1). On the other hand, in the spinal cords of
275 sciatic nerve-transected ΔCD155tg mice inoculated with virus, only 2- 20 pfu / 10 mg

tissue of the virus was detected (Fig. 5 lane 2). When non-tg mice with sham-operation or sciatic nerve transection were inoculated with virus, 10- 80 pfu / 10 mg tissue of the virus was detected in the spinal cord (Fig. 5 lane 3 and 4). These results indicate that retrograde axonal transport of PV is dependent on ΔCD155 expression, even if its Tctex-1 binding motif in cytoplasmic domain was deleted. Furthermore, when ΔCD155tg mice or non-tg mice were intravenously inoculated with $1x10^6$ pfu of PV1(M), 3- 80 pfu / 10 mg tissue or 20-30 pfu / 10 mg tissue of the virus was detected in the spinal cord at 16 h post inoculation, respectively (Fig. 5 lane 5 and 6). In a similar experiment, the virus in spinal cord of non-tg mice after intramuscular or intravenous inoculation was completely cleared by 48 h post inoculation (data not shown). The data indicate that virus leaking from the intramuscular inoculation site to the blood stream was distributed in the spinal cord via the blood brain barrier, and its virus titers were 2- 80 pfu / 10 mg tissue. Our findings are compatible with the results that specific distributions of poliovirus to the brain tissues after intravenous inoculations are not due to specific expression of CD155 on the brain capillary (42).

Microtubule dependency of the retrograde axonal transport of PV in ΔCD155tg mice. It is known that the retrograde axonal transport of PV is associated with microtubules (28). To investigate whether microtubules are involved in the transport of PV in ΔCD155tg mice, Vinblastine, known as an inhibitor of tubulin polymerization and used to inhibit axonal transport *in vivo*, was used to treat the sciatic nerve (8, 12, 28, 41, 43). The right sciatic nerve of ΔCD155tg mice was treated with vinblastine in PBS. As a control, PBS without vinblastine was used. One day after the treatment, the mice were inoculated with $1x10^6$ pfu of PV1(M) into the left or right gastrocnemius muscle. Tissue samples of the spinal cord were prepared at 16 h post inoculation and virus titers in the spinal cord were measured (Fig. 6). In the spinal cords of the PBS-treated mice inoculated with virus in the same (right) side, 1- $3x10^3$ pfu of virus was detected (Fig. 6 lane 1). When the mice treated with vinblastine were inoculated with virus in the opposite (left) side, 0.9- $3x10^3$ pfu of the virus was detected in the spinal cord (Fig. 6 lane 2). On the other hand, in the spinal cords of the mice treated with vinblastine and inoculated with virus in the same (right) side, only 8- 40 pfu was detected (Fig. 6 lane 3). These results indicate that topical vinblastine treatment greatly reduced the efficiency of the

axonal transport of PV through the sciatic nerve, suggesting that microtubules are part of the transport system in ΔCD155tg mice as well as CD155tg mice.

Discussion

Skeletal muscle injury, if concurrent with PV infection, is known to increase the risk of neurological complications in human, nonhuman primates and CD155tg mice (6, 15, 38). These circumstantial reports as well as experimental evidence suggested that retrograde axonal transport is responsible for PV invasion of the CNS after intramuscular administration of virus (34). It has been reported that the cytoplasmic domain of CD155 directly interact with Tctex-1 and efficient interaction between Tctex-1 and cytoplasmic domain is important for retrograde axonal transport of PV (23, 28). Using the yeast two-hybrid system, it was also observed that the deletion of the consensus sequence for Tctex-1 binding in the cytoplasmic domain of CD155 abrogates the interaction with Tctex-1 (28). In this study, to determine how the deletion of the Tctex-1 binding motif of CD155 affects the retrograde axonal transport and pathogenesis of PV, we generated ΔCD155tg mice and compared the clinical symptoms in two different mice (CD155tg mice and ΔCD155tg mice). Surprisingly, the clinical symptoms caused by intramuscularly inoculated PV were essentially the same between CD155tg mice and ΔCD155tg mice. Furthermore, retrograde axonal transport of PV along microtubules occurred in ΔCD155tg mice as well as CD155tg mice. Since ΔCD155 mice carry 44 amino acids in the cytoplasmic domain of ΔCD155α and 19 amino acids in that of ΔCD155δ, a reduced affinity of these truncated CD155 isoforms for Tctex-1 might be enough for these molecules to be transported retrogradely. Although the SKCSR motif in the cytoplasmic domain of CD155 contributes to the direct interaction with Tctex-1, it may not be the only determinant for Tctex-1 binding *in vivo*.

Even if the cytoplasmic domain of ΔCD155 doesn't have direct affinity for Tctex-1, it is possible that the retrograde transport of ΔCD155-containing vesicles is rescued by other molecules on the surfaces of endosomes. We previously demonstrated *cis* colocalization of CD155 and $\alpha_v\beta_3$ integrin on transfected mouse fibroblasts and their close association, possibly in a multiprotein adhesion complex (24). Numerous viruses have usurped integrins for cell invasion, because integrins are expressed on a wide variety cells throughout the body. Moreover, integrin ligation by microbial pathogens

elicits potent signaling responses that promote cytoskeletal reorganization and/or cell entry (37). Recently, it was suggested that human herpesvirus 8 (HHV-8; also called Kaposi's sarcoma-associated herpesvirus) utilizes the $\alpha_3\beta_1$ integrin as one of its cellular receptors, and modulates the cytoskeletal network consisting of microtubules and microfilaments in integrin-associated phosphatidylinositol 3-kinase (PI-3K)- and Rho GTPase-dependent manner (25, 36). Microtubules are vital for the nuclear trafficking of internalized HHV-8 (26). It is interesting to note that HHV-8 manipulates the host cell signaling pathways to promote the nuclear trafficking and to establish a successful infection. The modulation of microtubules dynamics by the PV-induced signaling pathway may rescue an inefficient interaction of ΔCD155 with Tctex-1 for the efficient retrograde transport of PV.

It is possible that the surfaces of PV-containing vesicles carry other molecules that have affinity for motor molecules for retrograde transport. Accessory and adaptor proteins are presumed to play an important role for both anterograde and retrograde transport, and the diverse functions of cytoplasmic dynein may require a different set of associated proteins (35, 39). The recently identified BPAG1 (bullous pemphigoid antigen 1) isoform, BPAG1n4, was shown to play an important role in retrograde transport in sensory neuron (19). Interestingly, an analysis of its amino acid sequence reveals that BPAG1n4 has no transmembrane region, suggesting that the association of BPAG1n4 with vesicles must be mediated through an unidentified membrane acceptor (20). Such an accessory protein is retrolinkin, a membrane protein, which functions as a receptor for BPAG1n4 to anchor the dynein/dynactin motor complex to endosomal cargoes (20). Soluble CD155 isoforms (CD155β and CD155γ) exist in human serum and cerebrospinal fluid, and are functional in terms of their interaction with PV (2). It is attractive to speculate that the complex containing soluble CD155 isoforms and PV is tethered to the dynein/dynactin motor complex by an unidentified membrane protein.

The other neurotropic viruses like herpesvirus, rabies virus, and pseudorabies virus also utilize neuronal retrograde transport to invade the CNS. Incoming herpes simplex virus type 1 (HSV-1) capsids associate with cytoplasmic dynein and dynactin, and their transport to the nucleus is dynein dependent (10). Until recently, it was not known which viral proteins were involved during retrograde HSV transport. The HSV-1 capsid protein

pUL35 was shown to colocalize with microtubules and Tctex-1, and move towards the cell nucleus (11). In case of pseudorabies virus, three capsid-associated tegument proteins pUL36, pUL37 and pUS3 have been shown to be prime candidates for viral proteins that interact with cellular motor proteins for transport (14). Recently, it was shown by using affinity chromatography that PV directly interacts with dynein for its retrograde axonal transport (13). Despite this finding, direct interaction between PV and Tctex-1 is unlikely to play significant roles during retrograde transport of PV *in vivo*, because PV is incorporated into vesicles at the nerve terminals in a CD155 dependent manner and the vesicles containing PV are transported retrogradely as a complex (28). However, further broader investigations are required to establish how and which viral proteins of PV are directly involved in binding of the dynein complex.

Deletion of the SKCSR motif in the cytoplasmic region of CD155 is not enough to impair the retrograde axonal transport of PV in animal model, even if ΔCD155 abrogates the interaction with Tctex-1 in the yeast two-hybrid system (28). The extraordinary length of axons and unique features of neurons may require a more complex system to meet the nuclear transport challenges that are far beyond those of non-neuronal cells. Our findings pertaining to ΔCD155 may contribute to a better understanding of relations between poliomyelitis and retrograde axonal transport of PV. The next challenge will be to understand how the interactions of PV-containing endocytic vesicles with dynactin/dynin and cytoskeletons facilitate retrograde axonal transport in an animal model.

Acknowledgements

We thank Dr. Akio Nomoto for the cosmid pTL-HC5 and Dr. Günter Bernhardt for the plasmid containing Tage4 promoter. This work was supported by NIAID Grants AI39485, AI15122 to Eckard Wimmer. Hidemi Toyoda was the recipient of a scholarship from Pediatric Oncology Research Foundation (Japan).

References

1. **Baury, B., R. J. Geraghty, D. Masson, P. Lustenberger, P. G. Spear, and M. G. Denis.** 2001. Organization of the rat Tage4 gene and herpesvirus entry activity of the encoded protein. Gene **265:**185-94.

2. **Baury, B., D. Masson, B. M. McDermott, Jr., A. Jarry, H. M. Blottiere, P. Blanchardie, C. L. Laboisse, P. Lustenberger, V. R. Racaniello, and M. G. Denis.** 2003. Identification of secreted CD155 isoforms. Biochem Biophys Res Commun **309:**175-82.

3. **Bernhardt, G., J. A. Bibb, J. Bradley, and E. Wimmer.** 1994. Molecular characterization of the cellular receptor for poliovirus. Virology **199:**105-13.

4. **Bibb, J. A., G. Bernhardt, and E. Wimmer.** 1994. Cleavage site of the poliovirus receptor signal sequence. J Gen Virol **75 (Pt 8):**1875-81.

5. **Bibb, J. A., G. Bernhardt, and E. Wimmer.** 1994. The human poliovirus receptor alpha is a serine phosphoprotein. J Virol **68:**6111-5.

6. **Bodian, D.** 1954. Viremia in experimental poliomyelitis. II. Viremia and the mechanism of the provoking effect of injections or trauma. Am J Hyg **60:**358-70.

7. **Brinster, R. L., H. Y. Chen, M. E. Trumbauer, M. K. Yagle, and R. D. Palmiter.** 1985. Factors affecting the efficiency of introducing foreign DNA into mice by microinjecting eggs. Proc Natl Acad Sci U S A **82:**4438-42.

8. **Bulenga, G., and T. Heaney.** 1978. Post-exposure local treatment of mice infected with rabies with two axonal flow inhibitors, colchicine and vinblastine. J Gen Virol **39:**381-5.

9. **Chadeneau, C., B. LeMoullac, and M. G. Denis.** 1994. A novel member of the immunoglobulin gene superfamily expressed in rat carcinoma cell lines. J Biol Chem **269:**15601-5.

10. **Dohner, K., A. Wolfstein, U. Prank, C. Echeverri, D. Dujardin, R. Vallee, and B. Sodeik.** 2002. Function of dynein and dynactin in herpes simplex virus capsid transport. Mol Biol Cell **13:**2795-809.

11. **Douglas, M. W., R. J. Diefenbach, F. L. Homa, M. Miranda-Saksena, F. J. Rixon, V. Vittone, K. Byth, and A. L. Cunningham.** 2004. Herpes simplex virus type 1 capsid protein VP26 interacts with dynein light chains RP3 and Tctex1 and plays a role in retrograde cellular transport. J Biol Chem **279:**28522-30.

12. **Fitzgerald, M., C. J. Woolf, S. J. Gibson, and P. S. Mallaburn.** 1984. Alterations in the structure, function, and chemistry of C fibers following local application of vinblastine to the sciatic nerve of the rat. J Neurosci **4:**430-41.
13. **Gonzalez Duran, E., R. M. del Angel, and J. S. Salas Benito.** 2007. In vitro interaction of poliovirus with cytoplasmic dynein. Intervirology **50:**214-8.
14. **Granzow, H., B. G. Klupp, and T. C. Mettenleiter.** 2005. Entry of pseudorabies virus: an immunogold-labeling study. J Virol **79:**3200-5.
15. **Gromeier, M., and E. Wimmer.** 1998. Mechanism of injury-provoked poliomyelitis. J Virol **72:**5056-60.
16. **Kashiba, H., E. Senba, Y. Kawai, Y. Ueda, and M. Tohyama.** 1992. Axonal blockade induces the expression of vasoactive intestinal polypeptide and galanin in rat dorsal root ganglion neurons. Brain Res **577:**19-28.
17. **Koike, S., H. Horie, I. Ise, A. Okitsu, M. Yoshida, N. Iizuka, K. Takeuchi, T. Takegami, and A. Nomoto.** 1990. The poliovirus receptor protein is produced both as membrane-bound and secreted forms. Embo J **9:**3217-24.
18. **Koike, S., C. Taya, T. Kurata, S. Abe, I. Ise, H. Yonekawa, and A. Nomoto.** 1991. Transgenic mice susceptible to poliovirus. Proc Natl Acad Sci U S A **88:**951-5.
19. **Liu, J. J., J. Ding, A. S. Kowal, T. Nardine, E. Allen, J. D. Delcroix, C. Wu, W. Mobley, E. Fuchs, and Y. Yang.** 2003. BPAG1n4 is essential for retrograde axonal transport in sensory neurons. J Cell Biol **163:**223-9.
20. **Liu, J. J., J. Ding, C. Wu, P. Bhagavatula, B. Cui, S. Chu, W. C. Mobley, and Y. Yang.** 2007. Retrolinkin, a membrane protein, plays an important role in retrograde axonal transport. Proc Natl Acad Sci U S A **104:**2223-8.
21. **McCloskey, B. P.** 1999. The relation of prophylactic inoculations to the onset of poliomyelitis. 1950. Rev Med Virol **9:**219-26.
22. **Mendelsohn, C. L., E. Wimmer, and V. R. Racaniello.** 1989. Cellular receptor for poliovirus: molecular cloning, nucleotide sequence, and expression of a new member of the immunoglobulin superfamily. Cell **56:**855-65.

23. **Mueller, S., X. Cao, R. Welker, and E. Wimmer.** 2002. Interaction of the poliovirus receptor CD155 with the dynein light chain Tctex-1 and its implication for poliovirus pathogenesis. J Biol Chem **277:**7897-904.

24. **Mueller, S., and E. Wimmer.** 2003. Recruitment of nectin-3 to cell-cell junctions through trans-heterophilic interaction with CD155, a vitronectin and poliovirus receptor that localizes to alpha(v)beta3 integrin-containing membrane microdomains. J Biol Chem **278:**31251-60.

25. **Naranatt, P. P., S. M. Akula, C. A. Zien, H. H. Krishnan, and B. Chandran.** 2003. Kaposi's sarcoma-associated herpesvirus induces the phosphatidylinositol 3-kinase-PKC-zeta-MEK-ERK signaling pathway in target cells early during infection: implications for infectivity. J Virol **77:**1524-39.

26. **Naranatt, P. P., H. H. Krishnan, M. S. Smith, and B. Chandran.** 2005. Kaposi's sarcoma-associated herpesvirus modulates microtubule dynamics via RhoA-GTP-diaphanous 2 signaling and utilizes the dynein motors to deliver its DNA to the nucleus. J Virol **79:**1191-206.

27. **Nathanson, N., and A. D. Langmuir.** 1963. The Cutter Incident. Poliomyelitis Following Formaldehyde- Inactivated Poliovirus Vaccination in the United States During the Spring of 1955. Ii. Relationship of Poliomyelitis to Cutter Vaccine. Am J Hyg **78:**29-60.

28. **Ohka, S., N. Matsuda, K. Tohyama, T. Oda, M. Morikawa, S. Kuge, and A. Nomoto.** 2004. Receptor (CD155)-dependent endocytosis of poliovirus and retrograde axonal transport of the endosome. J Virol **78:**7186-98.

29. **Ohka, S., H. Ohno, K. Tohyama, and A. Nomoto.** 2001. Basolateral sorting of human poliovirus receptor alpha involves an interaction with the mu1B subunit of the clathrin adaptor complex in polarized epithelial cells. Biochem Biophys Res Commun **287:**941-8.

30. **Ohka, S., W. X. Yang, E. Terada, K. Iwasaki, and A. Nomoto.** 1998. Retrograde transport of intact poliovirus through the axon via the fast transport system. Virology **250:**67-75.

31. **Pincus, S. E., D. C. Diamond, E. A. Emini, and E. Wimmer.** 1986. Guanidine-selected mutants of poliovirus: mapping of point mutations to polypeptide 2C. J Virol **57:**638-46.

32. **Ravens, I., S. Seth, R. Forster, and G. Bernhardt.** 2003. Characterization and identification of Tage4 as the murine orthologue of human poliovirus receptor/CD155. Biochem Biophys Res Commun **312:**1364-71.

33. **Reed, L. J., and H. Muench.** 1938. A simple method of estimating fifty per cent endpoint. Am. J. Hyg. **27:**493-497.

34. **Ren, R., and V. R. Racaniello.** 1992. Poliovirus spreads from muscle to the central nervous system by neural pathways. J Infect Dis **166:**747-52.

35. **Schroer, T. A.** 2004. Dynactin. Annu Rev Cell Dev Biol **20:**759-79.

36. **Sharma-Walia, N., P. P. Naranatt, H. H. Krishnan, L. Zeng, and B. Chandran.** 2004. Kaposi's sarcoma-associated herpesvirus/human herpesvirus 8 envelope glycoprotein gB induces the integrin-dependent focal adhesion kinase-Src-phosphatidylinositol 3-kinase-rho GTPase signal pathways and cytoskeletal rearrangements. J Virol **78:**4207-23.

37. **Stewart, P. L., and G. R. Nemerow.** 2007. Cell integrins: commonly used receptors for diverse viral pathogens. Trends Microbiol **15:**500-7.

38. **Strebel, P. M., N. Ion-Nedelcu, A. L. Baughman, R. W. Sutter, and S. L. Cochi.** 1995. Intramuscular injections within 30 days of immunization with oral poliovirus vaccine--a risk factor for vaccine-associated paralytic poliomyelitis. N Engl J Med **332:**500-6.

39. **Vale, R. D.** 2003. The molecular motor toolbox for intracellular transport. Cell **112:**467-80.

40. **van der Werf, S., J. Bradley, E. Wimmer, F. W. Studier, and J. J. Dunn.** 1986. Synthesis of infectious poliovirus RNA by purified T7 RNA polymerase. Proc Natl Acad Sci U S A **83:**2330-4.

41. **White, D. M., K. Mansfield, and K. Kelleher.** 1996. Increased neurite outgrowth of cultured rat dorsal root ganglion cells following transection or inhibition of axonal transport of the sciatic nerve. Neurosci Lett **208:**93-6.

42. **Yang, W. X., T. Terasaki, K. Shiroki, S. Ohka, J. Aoki, S. Tanabe, T. Nomura, E. Terada, Y. Sugiyama, and A. Nomoto.** 1997. Efficient delivery of circulating poliovirus to the central nervous system independently of poliovirus receptor. Virology **229:**421-8.

43. **Zhuo, H., A. C. Lewin, E. T. Phillips, C. M. Sinclair, and C. J. Helke.** 1995. Inhibition of axoplasmic transport in the rat vagus nerve alters the numbers of neuropeptide and tyrosine hydroxylase messenger RNA-containing and immunoreactive visceral afferent neurons of the nodose ganglion. Neuroscience **66:**175-87.

Figure legends

Fig. 1. Nucleotide sequence alignment of exon 6 for CD155 and construction of cosmid ΔCD155. (A) Partial nucleotide sequence alignment of exon 6 for the CD155 gene is shown. Capital letters represent nucleotide sequences of exon 6 for CD155α, and small letters those of intron 6. Partial amino acid sequences of the transmembrane and cytoplasmic domains of CD155α are listed above. The transmembrane domain is indicated by a box. Deleted region is shown underlined. Numbers indicate the amino acid positions with respect to the CD155α protein sequence (17, 23). (B) Construction procedure of a cosmid carrying the Tage4 promoter and the deletion in the cytoplasmic domain of CD155 (ΔCD155).

Fig. 2. Expression of CD155 mRNAs in the spinal cord of transgenic mice. The expression of CD155 mRNAs were analyzed by RT-PCR (Materials and Methods). (A) Bands specific for mRNA isoforms for CD155α, CD155β and CD155γ are indicated. DNA marker (lane 1), CD155tg mice (lane 2) and ΔCD155tg mice (lane 3) (B) Bands specific for mRNA isoform for CD155δ is indicated. DNA marker (lane 1), CD155tg mice (lane 2) and ΔCD155tg mice (lane 3)

Fig. 3. Clinical course of symptoms in transgenic mice intramuscularly inoculated with PV1(M) with and without sciatic nerve transection. Transgenic mice of three experiment groups were treated with intramuscular injections of $1x10^6$ pfu of PV1(M) into the right gastrocnemius muscle. All mice were observed for the appearance of neurological symptoms every 12 hours and clinically assessed according to the following scheme as described previously (15): 0, no symptoms; 1, general symptoms (ruffled fur and reduced

activity); 2, paraparesis; 3, paraplegia and/or involvement of upper extremities; 4, respiratory involvement; 5, death. The average clinical scores for eight mice are indicated. CD155tg mice with sham-operated (open square); ΔCD155tg mice with sham-operated (open circle); ΔCD155tg mice with sciatic nerve transection (closed circle).

Fig. 4. Distribution of PV1(M) in tissues of CD155tg mice or ΔCD155tg mice. Mice were sacrificed at the indicated time points following intramuscular virus administration. Virus titer in injected gastrocnemius muscle (A), spinal cords (B), brain (C) and plasma (D) of mice were measured. CD155tg mice (open bar); ΔCD155tg mice (closed bar).

Fig. 5. Distribution of PV1(M) in spinal cords of ΔCD155tg mice or non-tg mice. $1x10^6$ pfu of PV1(M) was inoculated intravenously (iv) or intramuscularly (im) (right gastrocnemius muscle) into ΔCD155tg mice or non-tg mice. Virus was then extracted from the spinal cord 16 h after the inoculation. Five to eight mice were used for each experiment.

Fig. 6. Effect of vinblastine on axonal transport. The right sciatic nerve of ΔCD155tg mice was treated with PBS with or without vinblastine, as described previously (28). The next day, virus was inoculated into the left (L) or right (R) gastrocnemius muscle. Spinal cords were isolated from the mice 16 h after the inoculation and amount of PV was measured by plaque assay. Four mice were used for each condition. +, present; -, absent.

Table 1. Oligonucleotides used for PCR

Primer	Sequence	
1	5’ ACACCCTGGACACCTAACTG 3’	(plus strand sequence)
2	5’ CCAAAGGACCCAATAGAAATAAATCCCGA 3’	(minus strand sequence)
3	5’ TTCTATTGGGTCCTTTGGCACTGTCATCT 3’	(plus strand sequence)
4	5’ GACAGCACAGATGGAGAACG 3’	(minus strand sequence)
5	5’ GGTATGGGAACTGACTTAGG 3’	(plus strand sequence)
6	5’ TAGGTCGGGGTGTGGTGTAT 3’	(minus strand sequence)
7	5’ CTTGTCTCTGCTTTTCGTTA 3’	(plus strand sequence)
8	5’ CAGCACAGAGCCCGTAGTAG 3’	(minus strand sequence)
9	5’ TTTTTTTTTTTTTTTTTTTTTTTCAATTA 3’	(minus strand sequence)
10	5’ TCCTGTGGACAAACCAATCAACAC 3’	(plus strand sequence)
11	5’ TGTGCCCTCTGTCTGTGGAT 3’	(minus strand sequence)
12	5’ GCGCCCAGCTCCTGATCCGT3’	(plus strand sequence)
13	5’ GAGGCGCTGGCATGCTCTGT3’	(minus strand sequence)
14	5’ CCTGTGGACAAACCAATCAA3’	(plus strand sequence)
15	5’ CGGCAGCTCTGGTGATGCTC 3’	(minus strand sequence)

Table 2. Neuropathogenicity of wild type poliovirus PV1(M) in CD155tg mice or ΔCD155tg mice

Route of inoculation	*LD_{50} (pfu) in CD155tg mice	LD_{50} (pfu) in ΔCD155tg mice
Intracerebral	$10^{1.9}$	$10^{2.2}$
Intramuscular	$10^{3.6}$	$10^{3.7}$
Intravenous	$10^{3.7}$	$10^{4.0}$
intraperitoneal	$10^{3.7}$	$10^{3.8}$

***Defined as the amount of virus that causes death in 50% of CD155tg mice or ΔCD155tg mice after various routes of inoculation.**

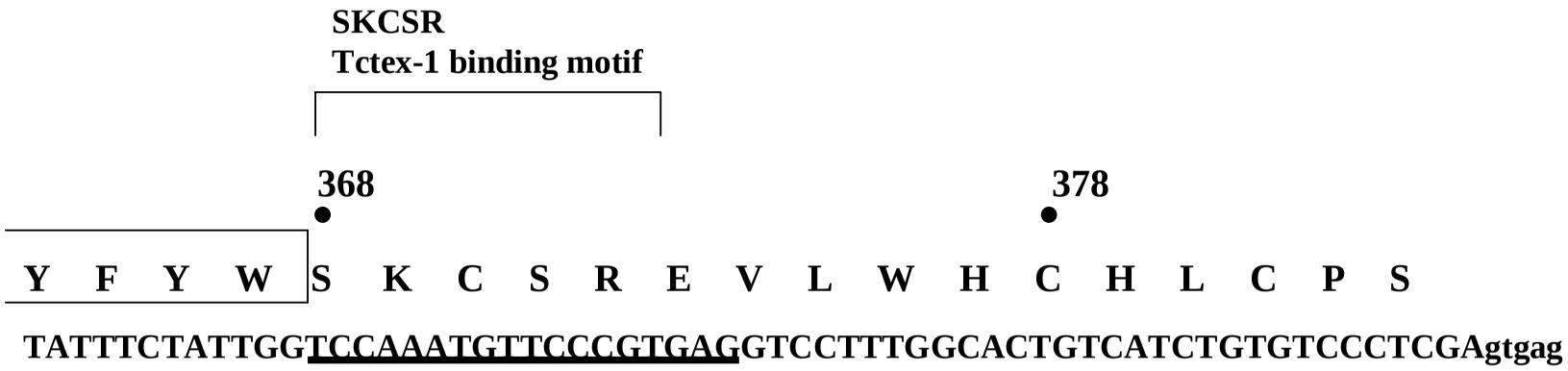

204

567

Fig. 1A

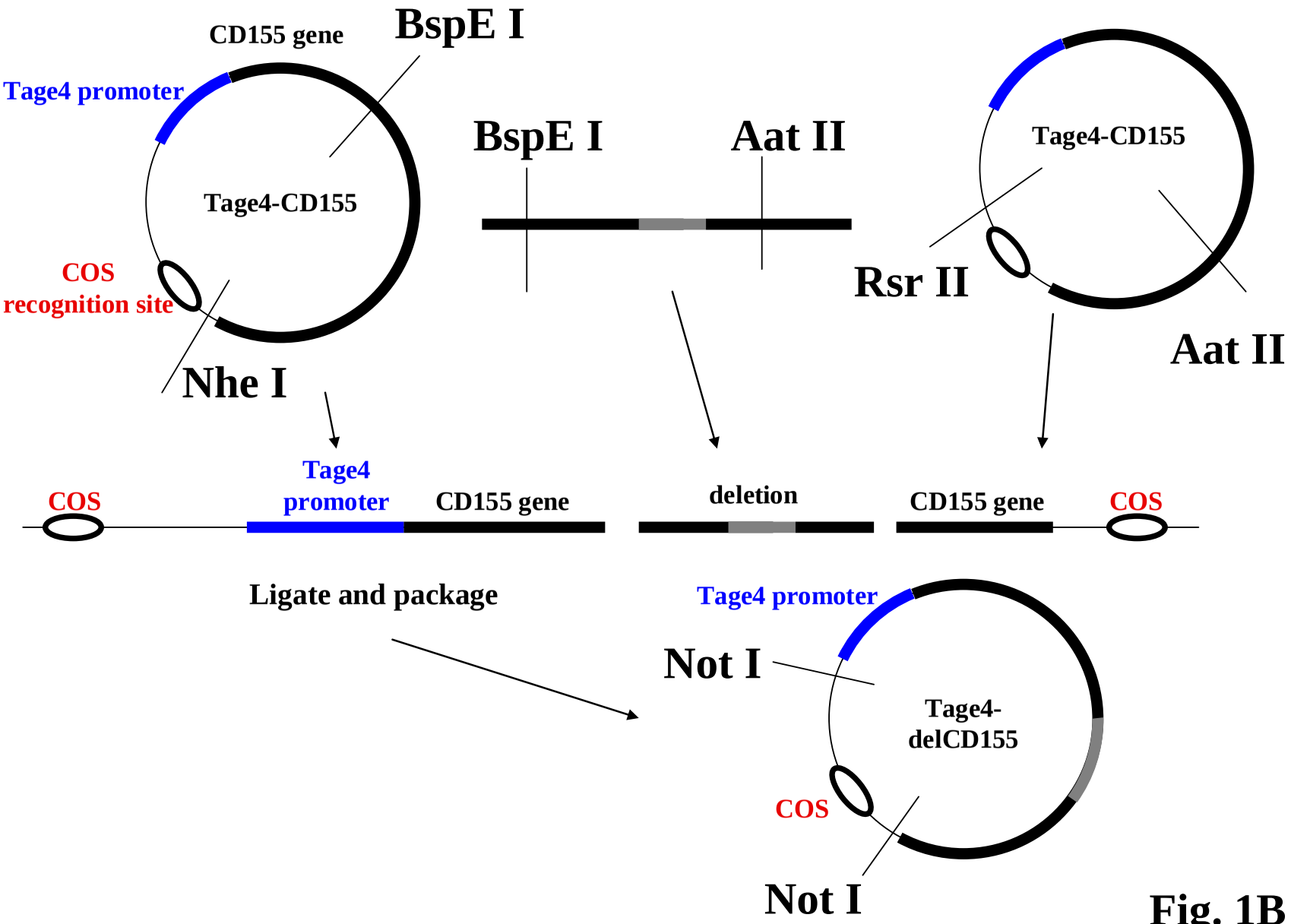

Fig. 1B

205

568

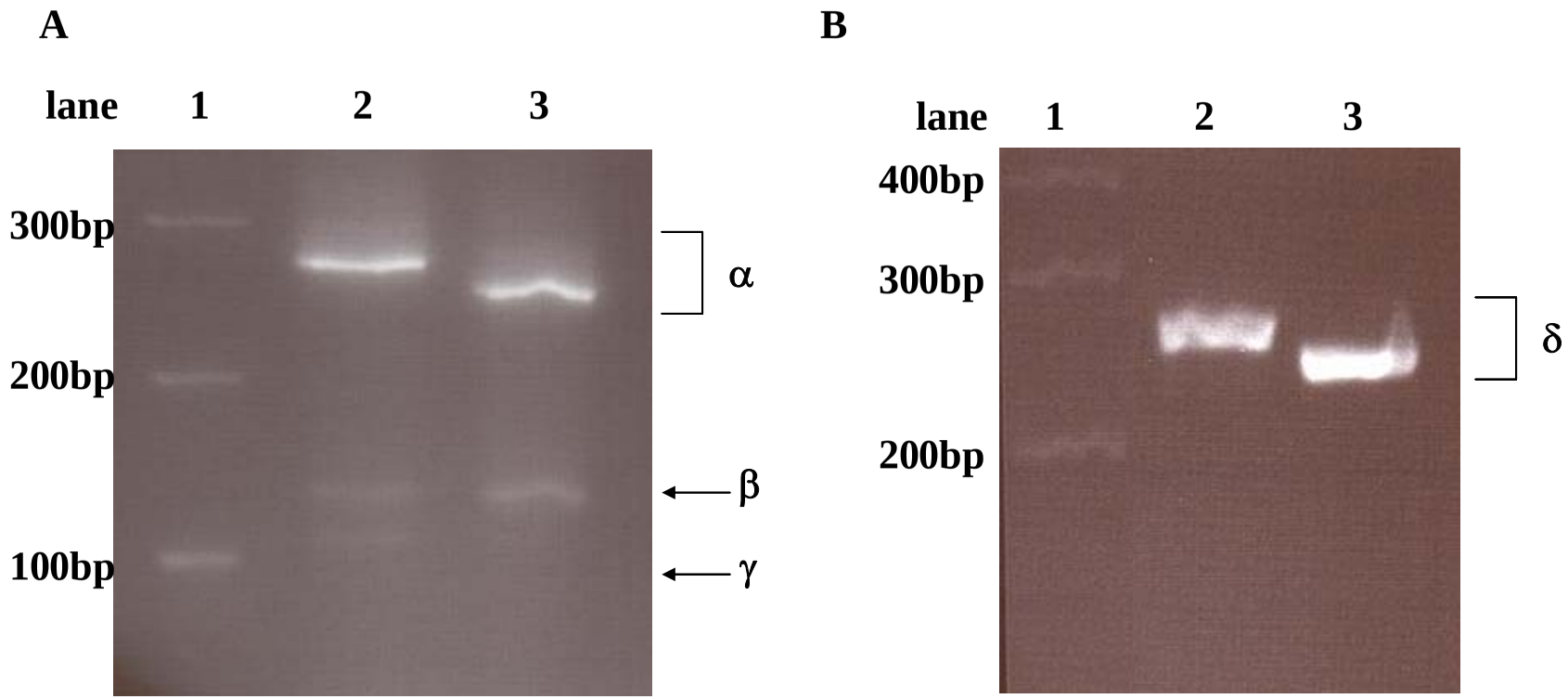
A
lane 1 2 3
300bp
200bp
100bp
α
β
γ
B
lane 1 2 3
400bp
300bp
200bp
δ

206

Fig. 2

569

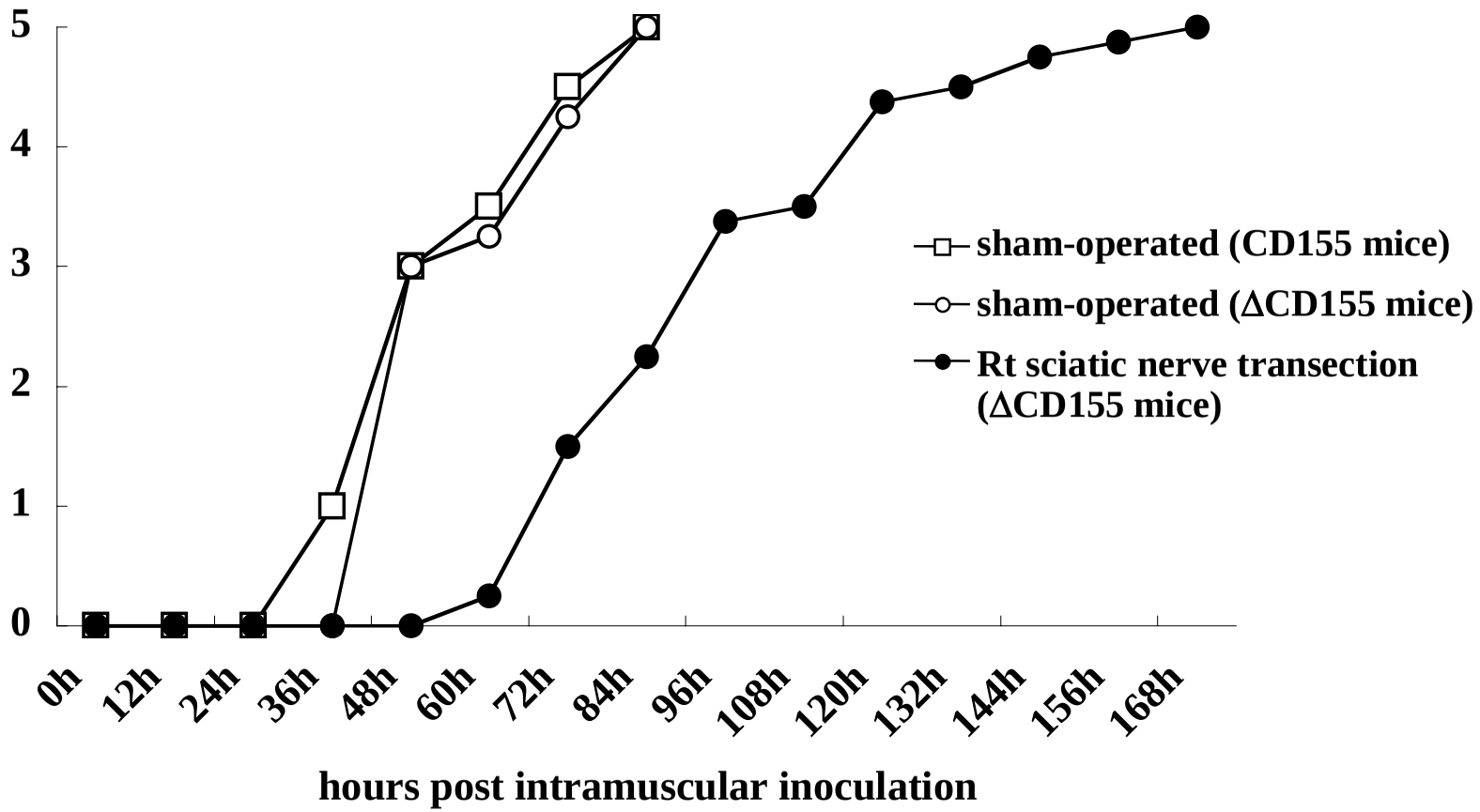
5
4
3
2
1
0
0h
12h
24h
36h
48h
60h
72h
84h
96h
108h
120h
132h
144h
156h
168h
hours post intramuscular inoculation
sham-operated (CD155 mice)
sham-operated (ΔCD155 mice)
Rt sciatic nerve transection (ΔCD155 mice)

207

Fig. 3

570

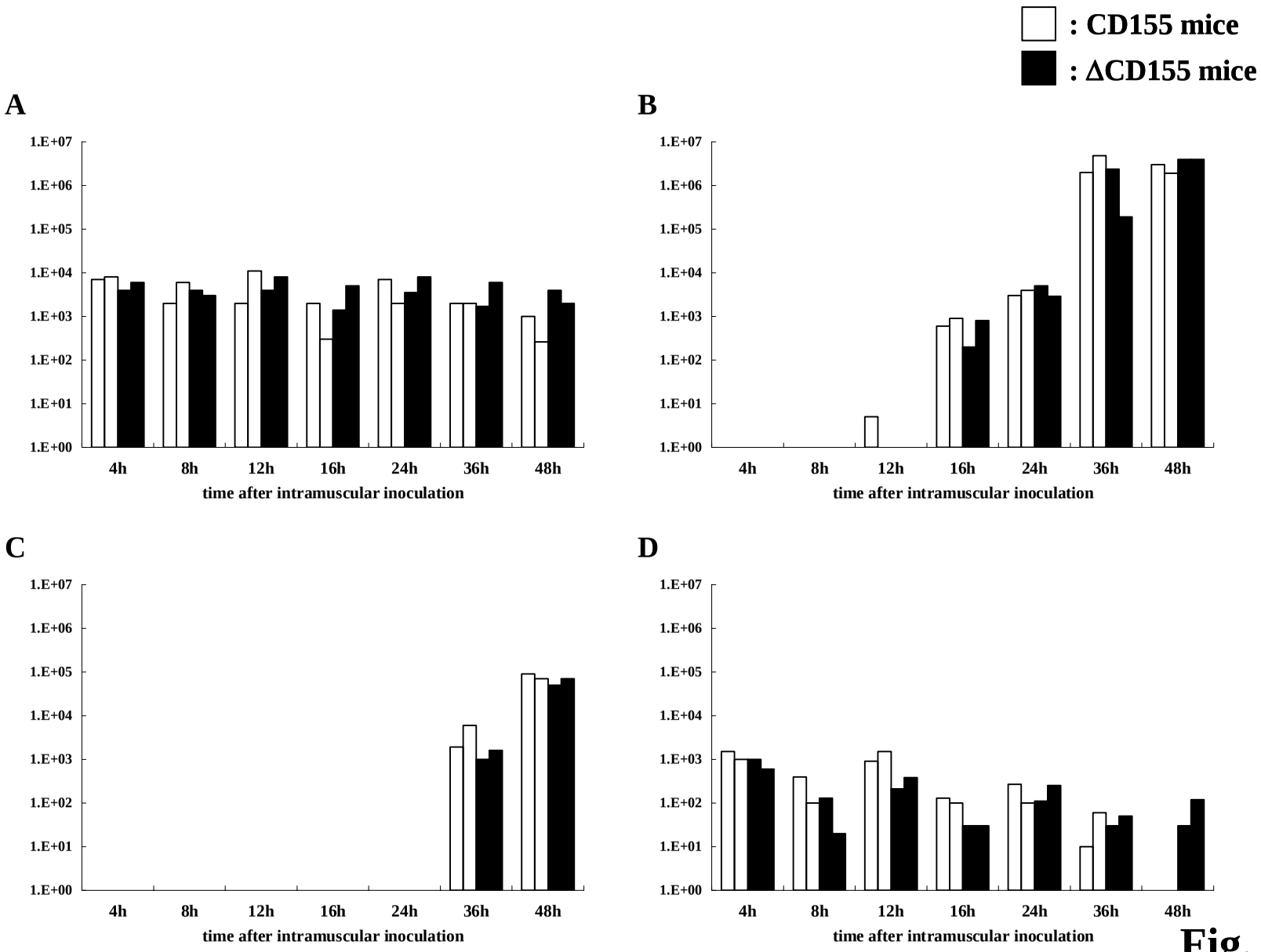
: CD155 mice
: ΔCD155 mice
A
B
C
D
1.E+07
1.E+06
1.E+05
1.E+04
1.E+03
1.E+02
1.E+01
1.E+00
4h
8h
12h
16h
24h
36h
48h
time after intramuscular inoculation

Fig. 4

208

571

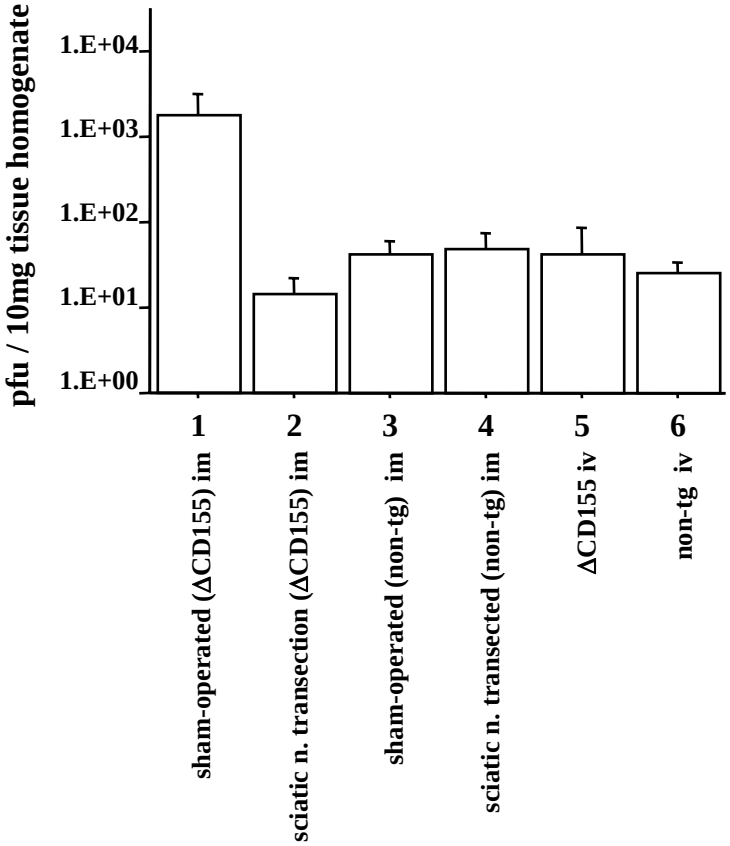
pfu / 10mg tissue homogenate
1.E+04
1.E+03
1.E+02
1.E+01
1.E+00
1
2
3
4
5
6
sham-operated (ΔCD155) im
sciatic n. transection (ΔCD155) im
sham-operated (non-tg) im
sciatic n. transected (non-tg) im
ΔCD155 iv
non-tg iv

Fig. 5

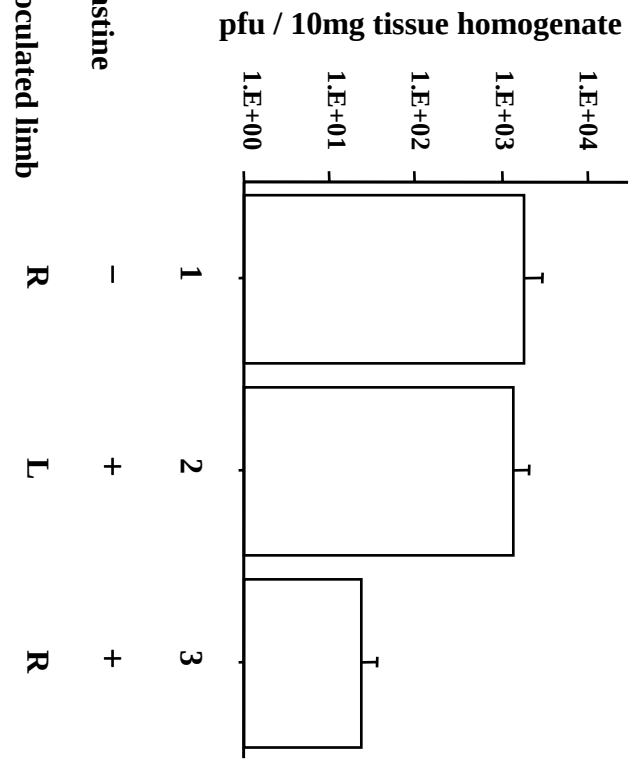
pfu / 10mg tissue homogenate
1.E+00
1.E+01
1.E+02
1.E+03
1.E+04
1
2
3
Vinblastine
–
+
+
PV-inoculated limb
R
L
R

Fig. 6